All-India Survey of Photovoltaic Module Reliability: 2016

National Centre for Photovoltaic Research and Education (NCPRE), IIT Bombay

&

National Institute of Solar Energy (NISE), Gurugram

March-May 2016

All-India Survey of Photovoltaic Module Reliability: 2016

Shashwata Chattopadhyay, Rajiv Dubey, Vivek Kuthanazhi,
Sachin Zachariah, Sonali Bhaduri, Chiranjibi Mahapatra,
Sugguna Rambabu, Firoz Ansari, Amey Chindarkar, Archana Sinha,
Hemant Kumar Singh, Narendra Shiradkar, Brij Mohan Arora,
Anil Kottantharayil, K. L. Narasimhan, Sanjeev Sabnis and Juzer Vasi

National Centre for Photovoltaic Research and Education
Indian Institute of Technology Bombay
Powai, Mumbai 400076, India

and

Birinchi Bora, Gopal Kumar, Yogesh Kumar Singh, Manander Bangar,
Mithilesh Kumar, Avinash Kumar Haldkar, Ramayan Singh,
Sahan Raghava, Manoj Morampudi, Gowri Ganesh, Rajesh Kumar and
O. S. Sastry

National Institute of Solar Energy
Gwalpahari, Gurugram, Haryana 122003, India

Survey conducted in March-May 2016

Rev. 2_25/01/2018

Contents

List of Appendices

Acknowledgements

The 2016 All-India Survey of Photovoltaic Module Reliability is the third in the series of such surveys conducted to assess the reliability and durability of photovoltaic (PV) modules in different parts of India. It was conducted between March and May 2016. The suggestion that such surveys be conducted came from a meeting in March 2013 of the "High Powered Task Force under JNNSM for Solar Photovoltaics," chaired by Mr. Gireesh Pradhan. As in the case of the previous surveys, the 2016 Survey was also conducted jointly by the National Centre for Photovoltaic Research and Education (NCPRE) at the Indian Institute of Technology Bombay (IITB) and the National Institute of Solar Energy (NISE).

NCPRE and NISE would like to thank the various participants in the 2016 survey at different levels (PV system owners, state Renewable Energy nodal agencies, private EPC contractors and local installers) who have helped us in multiple ways to bring the survey to fruition. Their names and organizations are not individually mentioned in order to preserve anonymity of the sites.

Thanks are due to many people at NCPRE and NISE who have helped in making the Survey possible. We thank Prof. B. G. Fernandes and Prof. Chetan Singh Solanki, Principal Investigators of NCPRE, and Dr. A. K. Tripathi, Director-General of NISE, for their support of the survey. We also thank Mrs. Smita Bhattacharjee, Dr. Diksha Makwani, Dr. K. Chalapathy, and Ms. Mallika Moolya of IIT Bombay for logistic and other support. We thank Mr. G. Yogeswara Rao, Mr. Devan Vasudevan and Mr. Ajeesh Alath for discussions and help in preparation of the report. We also thank Ms. Rashmi Singh, Ms. Supriya Rai and all staff of NISE for their co-operation and help during the survey. The team also wishes to thank Mr. Ajit Singh who made the arrangements for the vehicles for the cross-country travel, and the drivers Mr. Raj Kumar and Mr. Yadav, who drove the 18,000 plus kilometers safely in sometimes difficult terrain.

We are also thankful to several persons who have given advice and feedback on the Survey. Mr. Hemant Lamba gave the initial suggestion at the Task Force meeting which launched the surveys, and has continued to be actively involved over the years. Thanks are also due to Dr. S. P. Gonchaudhuri and Dr. B. Bhargava for their support and encouragement. We are also thankful to Dr. Sarah Kurtz, Dr. John Wohlgemuth, Dr. Lawrence Kazmerski, Dr. Dirk Jordan and Dr. Timothy Silverman of the National Renewable Energy Laboratory (NREL), USA, Dr. G. Tamizhmani of Arizona State University (ASU), and Dr. Rajeewa Arya, of Arya International and IIT Bombay, for their inputs.

Both NCPRE and NISE would like to thank the Ministry of New and Renewable Energy (MNRE), Government of India, for funding which enabled this survey to be undertaken. Part of the work at IIT Bombay was also funded by the Department of Science and Technology (DST), Government of India, through the project "Solar Energy Research Institute for India and the US" (SERIIUS). Thanks are also due to the Indo-US Science and Technology Forum (IUSSTF) which co-ordinated the SERIIUS project.

Executive Summary

The 2016 All-India PV Survey of Photovoltaic Module Reliability is the third in a series of such surveys conducted to assess the health, reliability and durability of photovoltaic (PV) modules put up in different parts of India. It was conducted between March and May 2016. The suggestion that such surveys be conducted arose at a meeting in March 2013 of the "High Powered Task Force under JNNSM for Solar Photovoltaics". As in the case with the 2013 and 2014 Surveys, the 2016 Survey was also conducted jointly by the National Centre for Photovoltaic Research and Education (NCPRE) at the Indian Institute of Technology Bombay (IITB) and the National Institute of Solar Energy (NISE).

The 2016 Survey was similar to the 2014 Survey, with a major difference: the number of large power plants surveyed was increased at the expense of small/medium plants. A total of 925 modules were inspected at 37 sites in all the 6 climatic zones of India. The age of the modules varied between 1 year to more than 25 years, and 6 different technology types were represented. The sites visited are shown in Fig. 1. The types of inspection undertaken in 2016 included: visual inspection, measurement of *I-V* characteristics under light and dark conditions, infra-red (IR) thermography under light and dark conditions, electroluminescence (EL) imaging, interconnect integrity test, insulation resistance test, and measurement of irradiance and ambient and module temperatures. We also performed a detailed analysis to ascertain the statistical significance of our data. Another important difference from the 2014 Survey was that we also calculated the Linear Degradation Rate for P_{max} (in %/year) in addition to the Overall Degradation Rate. We assume that there is a rapid initial degradation of 2% (for c-Si modules only) due to Light Induced Degradation (LID), followed by an almost linear fall in power; the Linear Degradation Rate refers to the latter (which discounts the initial LID), whereas the Overall Degradation Rate refers to the net rate including LID. This distinction is useful while comparing the performance of young and old modules.

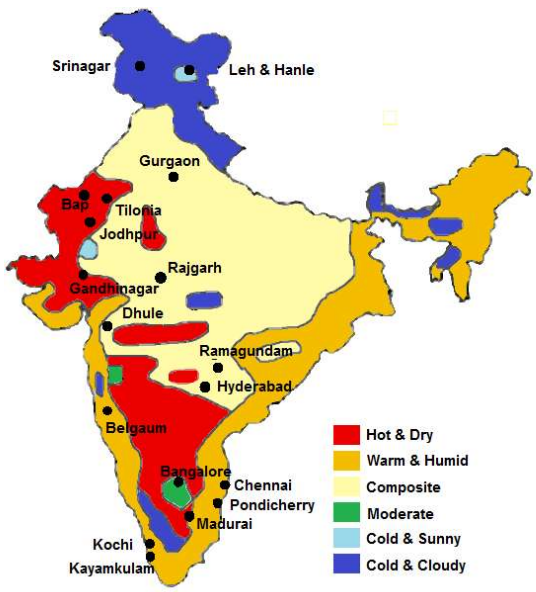

Fig. 1: Climatic zones of India and sites visited during the 2016 All-India Survey.

The distribution of the 925 modules surveyed in the 37 sites was as shown in Fig. 2. At each site, about 25 to 30 modules were typically taken up for the survey. Some modules (34 in number) showed Overall Degradation Rates of more than 5.12 %/year, and these modules, termed 'outliers', were not included in the main analysis as they appeared to suffer from serious quality problems and other extraneous issues, such as over-rating.

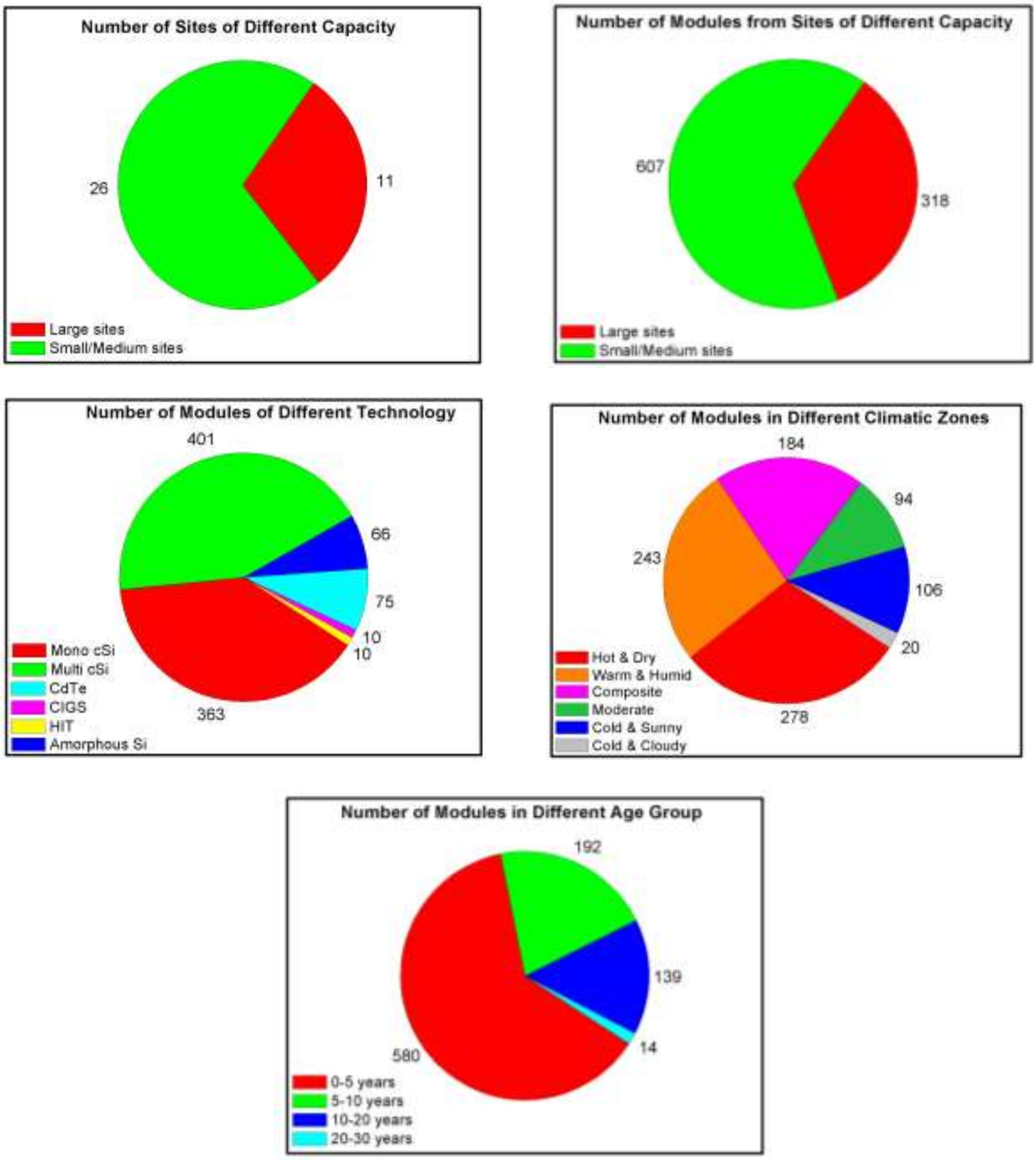

Fig. 2: Distribution of sites and modules in terms of installation size, technology used, climatic zone, and age. Large size refers to installations > 100 kW, and small/medium to installations < 100 kW.

One of the most significant observations of the survey was that there was a wide distribution in the performance of the modules. The histogram of the Overall Degradation Rate of the modules, that is, the rate at which the output power P_{max} decreases per year *without* discounting for LID, is shown in Fig. 3. It can be seen that the rates vary over a large range, from less than 0 %/year to more than 4 %/year, with the average at 1.55 %/year. (This average is lower than the 2.07 %/year seen in the 2014 Survey, mainly due to more large power plants included in 2016.) It can also be seen that some modules show *negative* rates; this is mainly due to under-rating and also light-soaking and spectral mismatch issues associated with *thin film modules*.

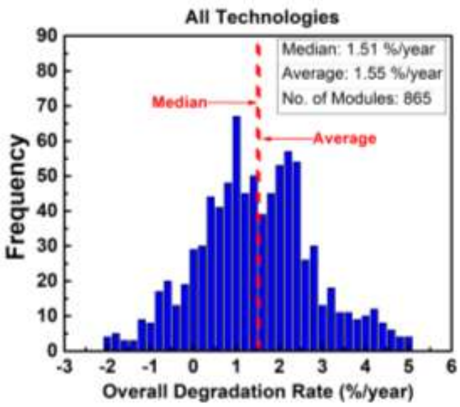

Fig. 3: Histogram of Overall P_{max} Degradation Rate (%/year) for all modules of all technologies.

As can be seen, many of the modules are performing well with low degradation rates, while others are not. To understand and analyze this wide variation, we have divided *only* the c-Si sites (which form the majority of sites and modules surveyed) into two categories: Group X sites and Group Y sites. The criterion for the division is that sites whose modules show an *average* Overall Degradation Rate of less than 2 %/year were considered to be 'good' sites, and labelled as Group X; and sites whose modules show an *average* Overall Degradation Rate of more than 2 %/year were considered to be 'problematic' sites, and labelled as Group Y. We emphasize that the 2% criterion is based on the *site* average, (since performance depends on both intrinsic module quality and installation procedures), and individual modules in Group X sites may show degradation rates of more than 2 %/year, just as individual modules in Group Y sites may show degradation rates of less than 2 %/year. Having made this distinction, we now plot the histogram for the Overall Degradation Rates for the c-Si modules. Fig. 4(a) shows the histogram for all 712 c-Si modules (called Group A), and Figs. 4(b) and 4(c) show the histograms for the modules in the Group X and Group Y sites respectively. It can be seen that the average for Group A is 1.90 %/year, which is rather high (the accepted international benchmark is between 0.6 to 1.0 %/year). It may be noted that 1.90 %/year is higher than the 1.55 %/year for all technologies, since thin films modules show lower rates, partly because of the point mentioned earlier. The modules in Group X ('good') sites do better at 1.22 %/year (but still higher than the benchmark), and, as expected, the modules in Group Y sites perform significantly worse.

Since the Overall Degradation Rate includes the 2% rapid LID drop for c-Si modules, we have also plotted histograms for the Linear Degradation Rates. These are shown in Figs. 5(a)-(c) for Group A, Group X and Group Y modules. (We will sometimes refer to modules in Group X sites as 'Group X modules', and similarly for Group Y). Naturally, these linear rates are improved, but still higher than the benchmark rates.

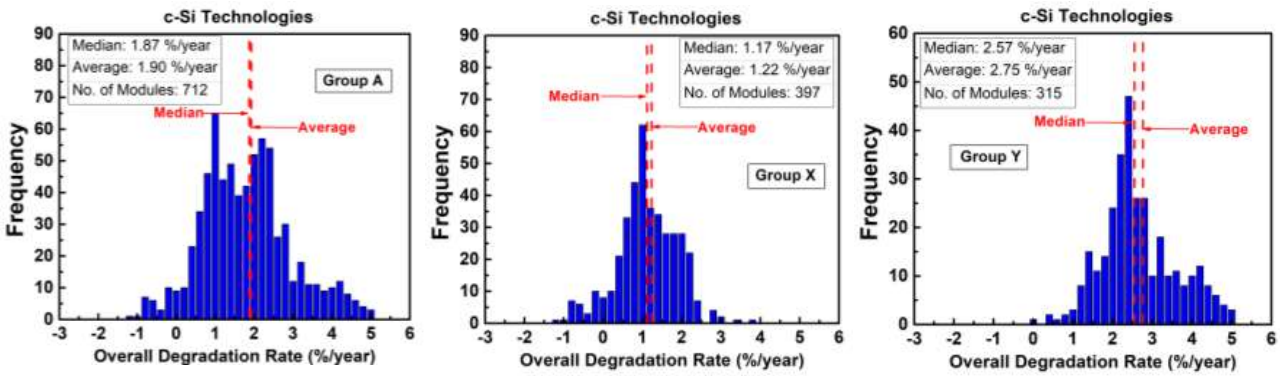

(a) (b) (c)

Fig. 4: Histogram of Overall P_{max} Degradation Rate (%/year) for c-Si (mono and multi) technologies only for (a) all modules (Group A) (b) modules in Group X sites (c) modules in Group Y sites.

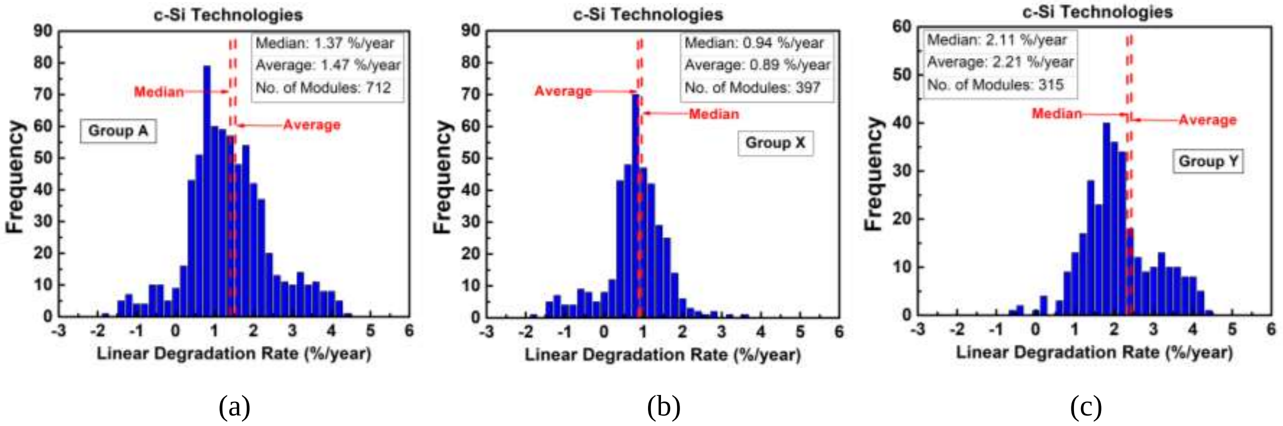

Fig. 5: Histogram of Linear P_{max} Degradation Rate (%/year) for c-Si (mono and multi) technologies only for (a) all modules (Group A) (b) modules in Group X sites (c) modules in Group Y sites.

The climatic variation is analyzed for modules falling in Group X. This is done since these are the 'good' sites, where extraneous effects are presumably not playing a role, and therefore the effect of climate is being correctly captured. While we have looked at the rates in all the 6 climatic zones, we find it is most instructive to separate these zones into two broad categories: *'Hot' zones* (comprising the Hot & Dry, Warm & Humid, and Composite zones), and *'Non-Hot' zones* (comprising Moderate, Cold & Sunny and Cold & Cloudy zones). The Linear Degradation Rates for Group X c-Si modules in the Hot and Non-Hot zones is shown in Fig. 6 (the open and filled symbols respectively represent young (<5 year) and old (>5 year) modules. It is clear that modules in the Hot zones degrade distinctly faster. This is a cause for concern since many of the solar installations in India will come up in Hot zones (which also have plentiful sunshine). Our detailed visual, IR and EL analysis indicates that the main reasons for modules to degrade faster in Hot zones is that the encapsulant (EVA) discolors faster, there is more metal and interconnect corrosion, and there are more interconnect breakages in the Hot zones.

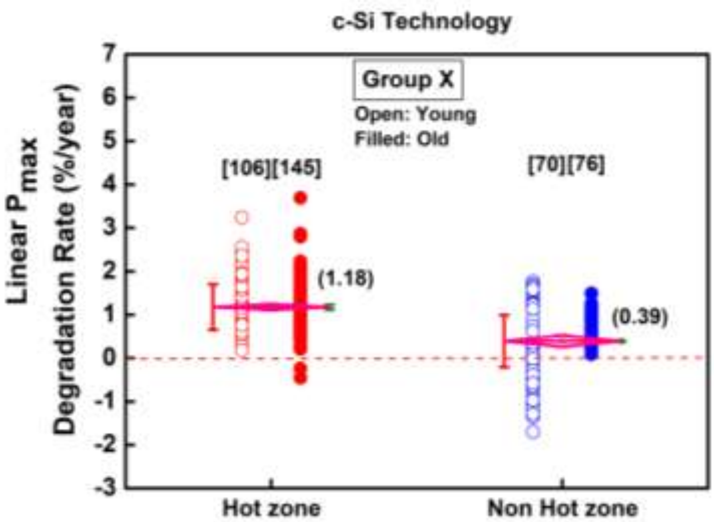

Fig. 6: Comparison of the Linear Degradation Rate of P_{max} for Group X modules in Hot and Non-Hot climatic zones. The open and filled symbols respectively represent young (<5 year) and old (>5 year) modules. The numbers on top represent the total number of modules in that zone and age group, and the horizontal red bar is the average degradation rate in that zone. Error bars due to nameplate and measurement error are also shown.

The histograms shown in Figs. 4 and 5 refer to all the 712 c-Si modules which have been analyzed. To see how the large power plants in Group X perform, we have looked at the breakup of Linear Degradation Rates in terms of *size* of the installation. This is shown in Fig. 7(a). It is comforting to note that modules in large (>100 kW) sites perform better than modules in small/medium sites. However, it is illuminating to do a more fine-grained analysis. Figure 7(b) shows the degradation rates for a subset of Group X modules in Hot climates, and Fig. 7(c) shows how the modules in large Group X sites separate out in terms of young and old sites. As can be seen, even among the large sites, in Hot zones the rate is 1.12 %/year, and more worrisome, for young large sites in Hot zones it is 1.43 %/year. These findings reinforce the observation that Hot climates enhance degradation, and also show that young sites are performing worse than old sites. This indicates that the quality of the modules themselves or the installation practices being adopted in recent years are inadequate. Also, the possibility that some of the young modules are over-rated cannot be ruled out. The latter point is especially true for modules in Group Y sites, though the corresponding data is not shown here.

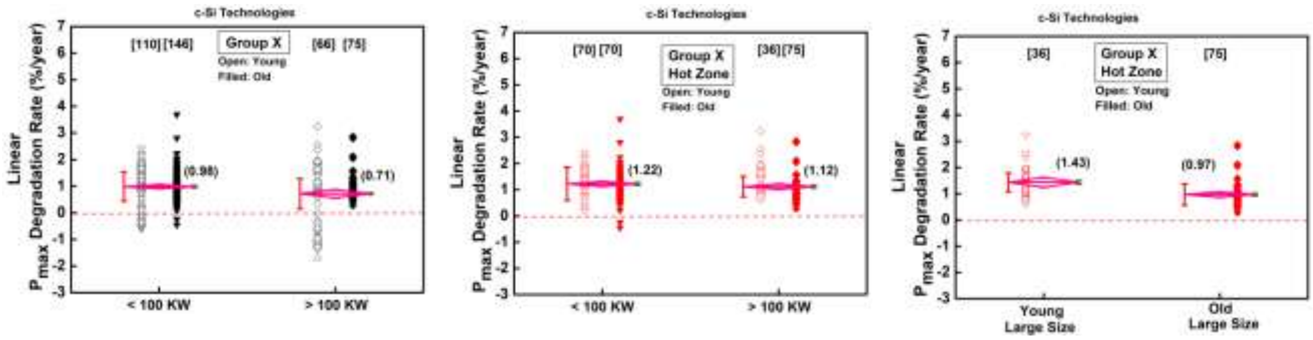

(a) (b) (c)

Fig. 7: (a) Effect of installation size on Linear P_{max} Degradation Rate for Group X modules (b) in Hot zones only and (c) the >100 kW sites in Hot zones separated for clarity into Young and Old sites.

The problem of young modules as compared to old modules emerges clearly in Fig. 8 which shows the age-wise histograms for *all* c-Si modules (Group A). The young c-Si modules have an average Linear Degradation Rate of 1.68 %/year, and the many modules with rates > 3 %/year hint at the possibility of unethical over-rating. For the young modules, the main contributor for P_{max} degradation is the fill factor (*FF*) which is often related to poor quality and cracks (and may also be indicative of over-rating), whereas for the old modules, it is short circuit current (I_{sc}) degradation, symptomatic of encapsulant discoloration.

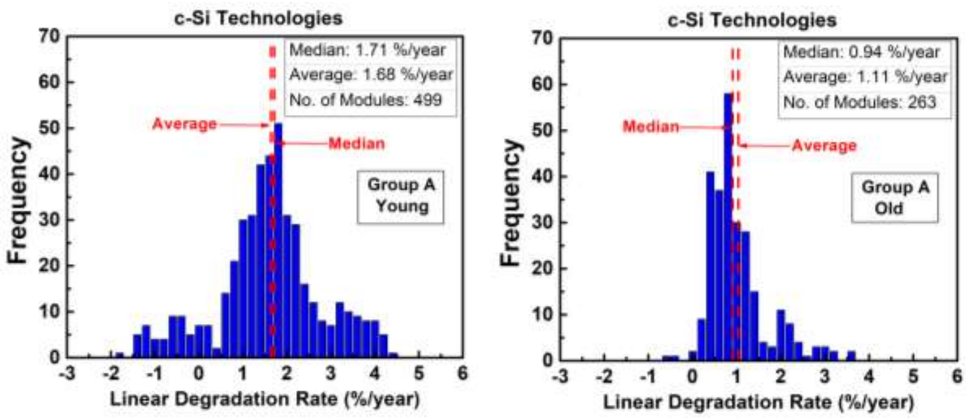

Fig. 8: Histograms of Linear P_{max} Degradation Rates for Young and Old Group A (all c-Si) modules.

Another observation which calls for serious consideration relates to the relative performance of roof-mounted versus ground-mounted modules. To make a fair comparison, roof-(rack)-mounted and ground-mounted c-Si modules of only the small/medium size (<100 kW) were compared, and these showed Linear Degradation Rates of 2.02 %/year and 0.99 %/year respectively. The higher rate for roof-mounted modules is correlated with more cracks in the cells seen on rooftops, indicating poor quality of modules and/or improper installation.

This means special attention is needed for the design and deployment of PV systems for India's 40 GW rooftop target.

We performed a detailed study of the visual degradation seen in modules, using an enhanced NREL visual checklist. Some of the key results are as follows. Encapsulant discoloration (yellowing or browning), shown in Fig. 9(a), occurs in all climatic zones, but at a faster rate in Hot zones. Though discoloration is generally seen in older modules, we have seen discoloration also in young Group Y modules, indicating poor quality, and this is one of the reasons for the poor performance of Group Y modules. Delamination (Fig. 9(b)) is seen to occur most frequently in Warm & Humid climates, and again is more widespread among Group Y modules. Snail trails, shown in Fig. 9(c), are usually associated with cracks in the cells, and are seen mainly in Hot climates. Further, many young modules (especially in Group Y sites) show snail trails. Metallization discoloration or staining (Fig. 9(d)) is seen in all climatic zones, but the severity is higher in Hot zones. Metal discoloration/staining can be due to corrosion or improper soldering. Many young modules, especially in Group Y sites, also show metal discoloration, indicating poor soldering quality. Backsheet degradation, including chalking and cracking, has been seen in both old and young modules. 40% of the young modules display backsheet problems, indicating again issues with quality and/or installation in recent years.

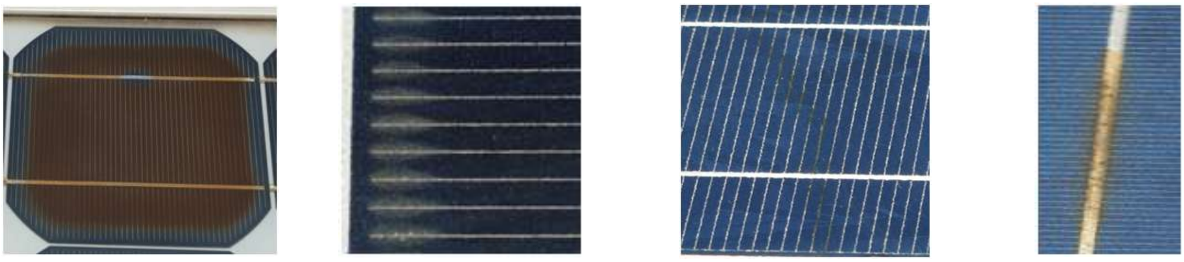

(a) (b) (c) (d)

Fig. 9: (a) Encapsulant browning (b) Delamination (c) Snail trails (d) Metallization discoloration.

We have correlated the visual defects with power degradation. Fig. 10 shows the correlation between power degradation and (a) encapsulant discoloration, (b) metal discoloration and (c) backsheet degradation. Note that in all cases, the y-axis shows the *total* percentage power loss suffered by the module since installation, and not the annual power degradation rate. It can be clearly seen that visible defects do indeed result in power loss.

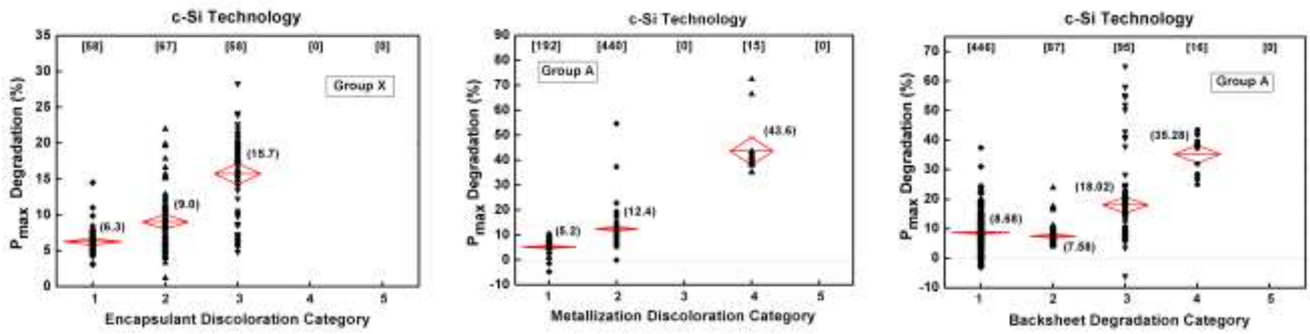

(a) (b) (c)

Fig. 10: Correlation of Total P_{max} degradation with (a) Encapsulation Discoloration Category, (b) Metallization Discoloration Category and (c) Backsheet Degradation Category. A higher Category number indicates more visible degradation. Group A refers to all c-Si modules.

Using a special low-light electroluminescence (EL) technique developed for the 2014 Survey, and a rugged lightweight DSLR based EL camera developed for the 2016 Survey, we have taken EL images of 202 modules during the survey. The EL images allow us to detect microcracks in the c-Si solar cells which cannot be seen with the naked eye, and help to ascertain the origin of snail trails, identify interconnect breakage and diode failure in short circuit, and indicate the presence of PID. Thus EL is a very powerful technique to identify problems in modules in the field. Fig. 11(a) shows an example of an EL image of a module in the Hot climate. Using EL, we have observed: (i) there are about 6 times more cracks in Group Y modules than Group X modules; (ii) there are about 50% more cracks in young modules compared to old modules; (iii) there are about 50% more cracks in rooftop modules compared to ground-mounted; and (iv) there are about 20% times more cracks in modules in small/medium installations compared to large installations. Power output decreases with number of cracks, as shown in Fig. 11(b). This data shows that microcracks are a major cause of poor performance in Group Y modules, and also contribute to the poorer performance of modules which are young, rooftop-mounted or in small installations. Prevalence of large number of cracks indicates low manufacturing quality, poor packaging/transport and/or improper/hasty installation.

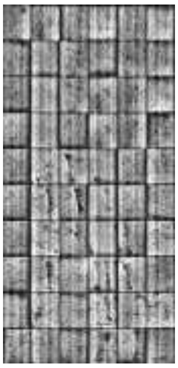

(a)

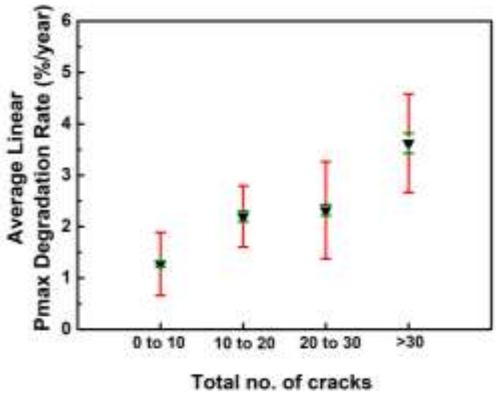

(b)

Fig. 11: (a) Field EL image of a module seen in Hot & Dry climate (b) Correlation of Linear P_{max} Degradation Rate with number of cracks in the module. The green and red bars indicate the instrument/STC translation error and nameplate error respectively.

We also used infra-red (IR) thermography, which shows the temperature distribution over the module. This is particularly useful for identifying hot spots, which can cause significant long-term degradation. The highest modal temperature seen during the Survey for a module operating under MPPT conditions was 67 °C, and highest hot cell temperature seen was 89 °C. We have defined a Thermal Mismatch Index (TMI), where a higher TMI indicates the possibility of hot spots. Fig. 12(a) shows a typical IR image and Fig 12(b) shows how the Total P_{max} Degradation is correlated with the presence of hot spots as measured by the TMI category.

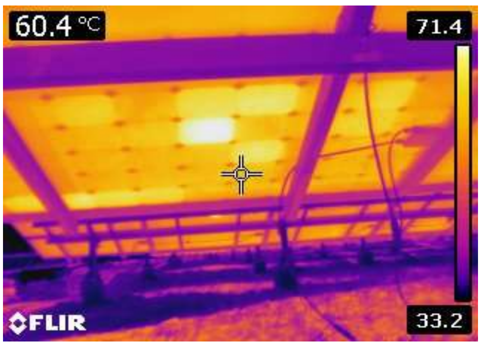

(a)

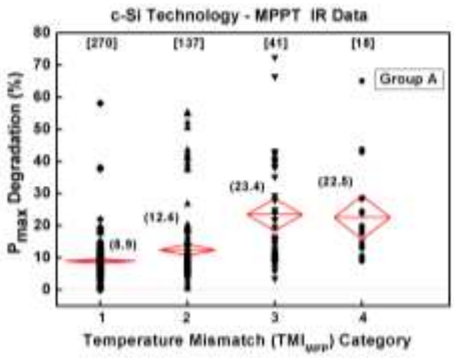

(b)

Fig. 12: (a) IR image of a module in Warm & Humid climate (b) correlation of Total P_{max} Degradation with Temperature Mismatch Index (TMI) category. Group A refers to all c-Si modules.

The 2016 Survey also undertook measurements of dark *I-V* characteristics, dark IR, insulation resistance and interconnect breakage occurrence. The dark *I-V* measurements yield the ideality factor *n* of the diode in the forward bias region. It was seen that *n*, which can be related to series resistance and/or cell quality, increases with age, and shows more degradation in Hot than Non-Hot climates. Further, increasing (worsening) values of *n* correlate well with power loss. The dry insulation resistance test showed that most modules (99%) pass the test, and all (100%) in the large-size category pass. The interconnect breakage (measured by a cell line tester and shown in Fig 13(a)) is most prevalent in the Hot & Dry zone, the reason most likely being thermal cycling caused by a large difference in the day and night temperature. The power degradation correlates well with the severity of interconnect breakage, as shown in Fig. 13(b).

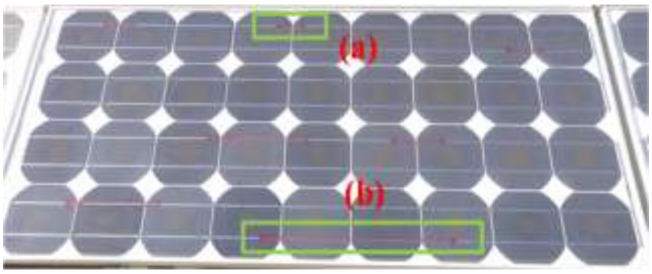

(a)

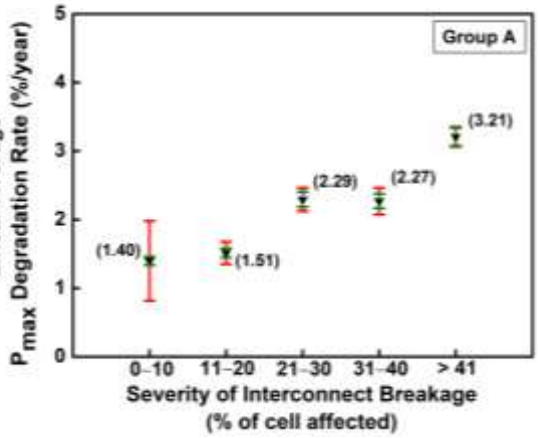

(b)

Fig. 13: (a) Module showing point (a) and line (b) breakage (b) power degradation rate versus severity of interconnect breakage.

An important question which arises is whether it is possible to identify the *risk* associated with various defects or degradation modes in different climatic zones. If so, it would be possible to check for those defects more regularly, and thus pre-empt both performance and safety failures. The method of assigning a Risk Priority Number (RPN) allows this to be done. The RPN depends on the severity of the defect (*S*), its frequency of occurrence (*O*), and how easily detectable (*D*) it is. RPN is defined as *S* x *O* x *D*. The RPN methodology has been used for analyzing the field data collected for the modules during the survey. One example of the results of the RPN analysis is presented in Fig. 14, which shows the Performance RPN versus failure modes for old modules in the Hot & Dry climatic zones (a higher RPN number indicate more risk). It can be seen that solder bond fatigue/failure has the highest RPN, which agrees with the observation noted earlier that interconnect breakage is seen most often in this climate.

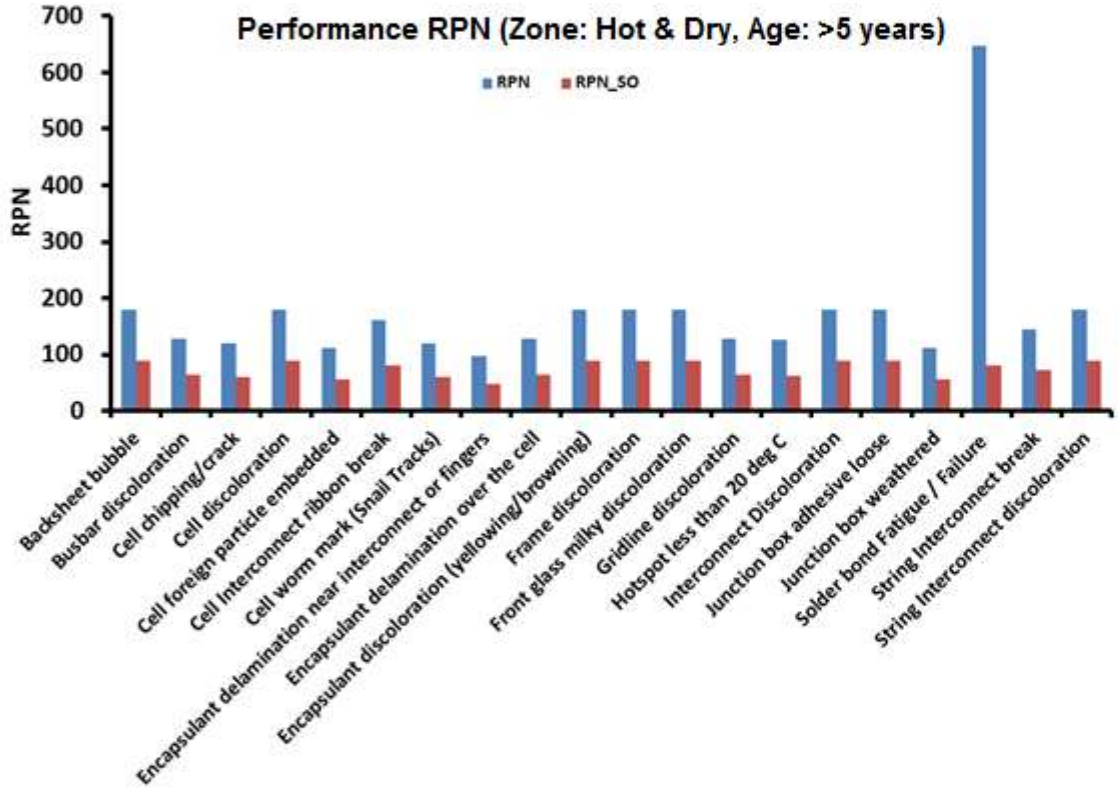

Fig. 14: Performance RPN for different failure modes for old modules (more than 5 year outdoor exposure) for Hot & Dry climate. RPN_SO designates a modified RPN calculation, where only Severity and Occurrence frequency are included (that is, ease of Detection is ignored).

In summary, a good picture of the durability and reliability of PV modules in the country has emerged from the 2016 All-India Survey. Broadly, the results agree with those of the previous 2014 Survey. One of the important observations is that there is wide variability in the quality and degradation rates. Many modules show excellent performance, but there are many others showing alarmingly high degradation rates. Crystalline-silicon modules show an average Linear Degradation Rate of 1.47 %/year; c-Si modules in Group X sites show reasonably good performance with an average Linear Degradation Rate of 0.89 %/year; but modules in Group Y sites show an average rate of 2.21 %/year, which is cause for concern. Large-size (>100 kW) Group X installations perform well (0.71 %/year), which is good news, but if one focuses on a subset of such installations which are young and in Hot zones, the degradation seen is 1.43 %/year. This highlights the problems being seen in recent installations, and also flags a warning for future installations, most of which will come up in Hot climates. Further, it is seen that roof-mounted systems perform worse than ground-mounted systems. This means that due consideration must be given to the long-term durability of small/medium roof-top systems. The modules in the underperforming Group Y sites suffer from material quality issues, including encapsulant and backsheet quality, as well as improper transport/installation procedures that show up as microcracks in the cells, scratches in the backsheet, etc, all of which cause a decrease in the module power. These problems have perhaps been caused by the aggressive pricing and deadlines associated with solar PV projects in recent years.

Based on the field observations, analysis and results, some high-level recommendations which can be made are the following:

- Due diligence should be exercised while selecting and procuring modules. This may include verifying the antecedents of the manufacturer, and independent checks on the quality of the module(s). Although most modules available in the market carry the IEC certification, it should be noted that the IEC certification is really a qualification of module design, and does not guarantee that the module will perform adequately through its intended life.

- Materials used in modules are important. EVA and backsheet particularly can be of different qualities, and should be specified by the manufacturer in the datasheet, and also in the tender for procurement.
- An independent audit of modules and installations by third party is strongly recommended. This may include detailed testing of randomly selected modules before as well as after shipment.
- Some cases of 'over-rating' of modules cannot be ruled out. This may be one of the reasons for high calculated degradation rates, especially for young modules. Owners and installers should be vigilant about this malpractice.
- Module manufacturers and installers should place more emphasis on proper packaging and handling of the modules during transportation since improper handling can induce cracks in the solar cells and lead to long-term degradation.
- Installation procedures and protocols are important, and standard procedures as recommended should be strictly followed.
- It is recommended that a random field-based electroluminescence (EL) testing be performed after receiving the modules at site and after installation to reveal micro-cracks which may have been caused during the transport and installation phases.
- It has been noted that the 'Hot' climates present a harsh operating environment for PV modules. An intensive study of degradation phenomena in Hot climates, which has not been emphasized sufficiently by the PV community so far, is needed. This is particularly important for India, where much of the 100 GW is expected to come up.
- The IEC certification protocols (eg. 61215), and the BIS standards, which are currently being updated, need to take into account the Hot climate phenomena, and to develop more aggressive test protocols going to higher temperatures.
- Modules and sites perform very well in the 'Cold & Sunny' climate of Ladakh. Power plants set up in this region will enjoy not only low degradation rates, but also excellent irradiance.
- It is possible that some of the quality issues seen, especially in the young modules, are the result of very aggressive pricing and commissioning deadlines for PV plants in India in recent years.
- Given the reliability issues observed for small/medium rooftop installations, it would be prudent to reduce the 40 GW rooftop target, and instead enhance the ground-mounted capacity.

1. Introduction

1.1 Introduction to the Survey

India has set ambitious renewable energy generation targets under the Jawaharlal Nehru National Solar Mission (JNNSM) in an effort to avoid over-dependence on fossil fuels for electricity generation. The 22 GW solar energy target by 2022 under the JNNSM was revised in 2015 to 100 GW (40% of which is to come from roof-mounted projects and rest from ground-mounted large scale solar power plants), which would require rapid growth in solar installations throughout the country in the coming years. This target is part of the overall goal to achieve 175 GW of non-fossil fuel energy by 2020, and resonates well with India’s COP-21 obligation in Paris to have 40% of its electricity generated by renewables by 2030. The success of the National Solar Mission in de-carbonizing the power generation sector will depend not just on meeting the 100 GW installation target but also on the satisfactory long-term performance of the photovoltaic systems, which are likely to constitute the major chunk of the solar installations. The expected lifetime of solar PV in the field is 25 years. Considering the lack of information with regard to the long-term performance of PV systems of various technologies in different climatic conditions of India, the High Powered Task Force of MNRE had in March 2013 requested the National Centre for Photovoltaic Research and Education (NCPRE), at the Indian Institute of Technology Bombay (IITB) to survey the performance of PV systems installed in the country. NCPRE requested the National Institute of Solar Energy (NISE) to partner in conducting the survey, keeping in view the wide experience which NISE (formerly Solar Energy Centre) had in monitoring PV system performance. Accordingly, a joint team was formed which surveyed 63 ‘visually degraded’ PV modules spread across the country in the summer of 2013 and submitted their report, *All India Survey of Photovoltaic Module Degradation: 2013* in early 2014 [1]. A more extensive survey encompassing 1148 modules in 51 sites spread over all six climatic zones of India was undertaken in October-November 2014, and the report *All India Survey of Photovoltaic Module Reliability: 2014* was submitted in early 2016 [2]. Both the surveys indicated that the PV modules were degrading at a faster rate in the Hot climates (Hot & Dry and Warm & Humid), where incidentally most of the utility-scale PV installations are expected to be concentrated. The primary cause behind the electrical degradation was the discoloration of the encapsulant and corrosion of the metallization, but many more important and interesting details were uncovered which have now been extensively documented [3-8]. Since the 2013 and 2014 surveys were highly successful and their results very revealing, it was decided that these surveys would be repeated biennially, thereby generating a consistent and exhaustive data base for India’s solar mission.

The 2016 All-India Survey was performed jointly by NCPRE and NISE during the early summer months (late March to early June). Since in 2016 many more utility-scale PV plants were operational compared to 2013 and 2014, the 2016 survey contained many more ‘large’ (>1 MW) sites than earlier. A total of 925 modules were surveyed from 37 different sites covering all six climatic zones of India. The field assessment included (as in the 2014 survey) a visual checklist, a detailed electrical characterization of the modules (illuminated *I-V*, dark *I-V*, insulation resistance test, interconnect breakage test, off-grid inverter performance test, electroluminescence imaging), thermal characterization (illuminated IR and dark IR), and measurement of the relevant weather and irradiance data. In addition, for the first time, an on-site measurement of the temperature coefficients of the modules was performed using a technique which had been specifically developed for the purpose [9].

The survey methodology and a review of some related literature are presented in the forthcoming sections of this chapter, including a brief discussion on the climatic zones of India. Chapter 2 deals with the survey statistics and some general information about the survey sites. Since the field data have been collected under various ambient conditions (different irradiance and module temperatures), it is necessary to convert all the data to standard test condition (STC) of 1000 W/m^2, 25 °C and AM1.5G solar spectrum for comparison and calculation of degradation rates. Chapter 3 deals with this conversion and assesses the errors associated with such conversions as well as due to other reasons. Chapters 4 to 7 deal with illuminated *I-V* analysis, analysis of dark *I-V*, dark IR and insulation resistance data, visual analysis and analysis of electroluminescence and infra-red thermography data. Risk Priority Number (RPN) is a recent concept in the field of photovoltaic system risk assessment, and the results are presented in Chapter 8. Finally, we present our concluding remarks in Chapter 9 with recommendations for the PV community.

Two important additions have been included in the analysis of the 2016 data. The first is that it was deemed necessary to include a rigorous statistical analysis of the data to ensure that despite the multiplicity of variables, the correct conclusions were being drawn; and the second was that it was felt desirable to include the rapid initial 'light-induced degradation' (LID) for panels, as the present survey included many young panels in recently-commissioned power plants. These points are discussed in some detail in Chapter 3.

1.2 Literature Review

A comprehensive review of the relevant literature has already been presented in the reports *All India Survey of Photovoltaic Module Degradation: 2013* [1] and *All India Survey of Photovoltaic Module Reliability: 2014* [2], and the reader is referred to these documents for relevant scientific literature. Here, we will only briefly mention some recent important publications which have appeared, and our review of the LID literature with the aim to obtain the most appropriate value for the rapid initial degradation.

Field surveys provide information about the performance degradation of photovoltaic modules in actual operating conditions. A recent publication by Jordan *et al*. [10] shows that the average degradation rate in hot climates is higher than those in cold climates. This has also been the experience in the All-India Surveys. They have reported that the average degradation rate of crystalline silicon modules is in the range of 0.8-0.9 %/year, while it is higher than 1% for HIT and thin film technologies. Other recent publications by Jordan *et al.* [11, 12] have reviewed the relevant literature on various degradation modes and indicated that encapsulant discoloration is the most common degradation mode, particularly in the older systems. Hot spots have also been identified as a matter of concern for the modules aged less than 10 years. Glass breakage and absorber layer delamination are the common problems in thin film modules.

There are various non-linearities involved in the degradation of PV modules, as discussed recently by Jordan *et al.* [12], which includes the rapid initial degradation observed in crystalline silicon modules upon exposure to sunlight, referred to as Light Induced Degradation (LID). Also, there are similar meta-stabilities in various thin film technologies, owing to which the power output decreases rapidly upon outdoor exposure (as in the case of the Staebler-Wronski effect in amorphous silicon modules [13, 14]) or even increase initially followed by long term degradation (for example, in CdTe modules [15, 16]). In case of CdTe, the performance enhancement due to light soaking effects can be up to 10%, and it shows a strong temperature dependence as well [17]. LID is commonly seen in crystalline silicon modules from almost all manufacturers, and the manufacturers usually incorporate this in their warranty documents, as a 2% to 3% initial rapid degradation in power output within the first year of operation [18-20]. It is primarily caused due to dissolved impurities like boron, iron, and oxygen in the silicon ingot, and hence the extent of LID depends on the quality of wafer and cell manufacturing processes [21]. Though LID varies from manufacturer to manufacturer, PVSyst software recommends a value of 2% LID for energy generation simulations [22], which we have also adopted in our present analysis. Table 1.1 gives the value of degradation in power, short circuit current, open circuit voltage and fill factor, in LID affected samples, compiled from the literature [21, 23-26]. In the works of Pingel *et al.* [21], and Sopori *et al.* [25], 40% of the degradation in power output is due to short circuit current (I_{sc}) degradation, another 40% due to open circuit voltage (V_{oc}) degradation, and the rest 20% is coming from fill factor (*FF)* degradation. Accordingly, for the purpose of our analysis, we have divided the 2% LID in power output into 0.8% for V_{oc}, 0.8% for I_{sc} and 0.4% for *FF*. Apart from LID, there are many other modes of degradation which are discussed in details in our previous survey reports [1, 2].

Table 1.1: Typical values of LID reported in literature

Cell Technology	**Typical Relative LID reported in Literature**				**Reference**
	P_{max}	V_{oc}	I_{sc}	***FF***	
Mono c-Si	3-4%	5-6%	2.5-3%	- 0.5%	[23]
	5%	NA	NA	NA	[24]
	2.8%	1.1%	1.1%	0.6%	[21]
	2.5%	1%	0.9%	0.5%	[25]
Multi c-Si	1%	NA	NA	NA	[24]
	2%	0.4%	0.9%	0.5%	[21]
	2.5%	0.7%	1.5%	-0.5%	[26]

1.3 Survey Methodology

The methods and protocols used in the field in the 2016 Survey were broadly similar to those used in 2014, with some differences. The protocol is repeated here for completeness. An extensive array of characterization tools was taken to the field for detailed inspection of the modules, as shown in Table 1.2.

The first activity on reaching the site was to collect dust samples from the top of a few modules for further analysis later in the laboratory. Then the modules were cleaned by pouring water from top, and wiped dry before starting any measurement. Before disconnecting the system for electrical *I-V* measurements, infrared (IR) thermography was performed with the system connected to load. Visual inspection, illuminated *I-V* and infrared (IR) thermography, measurement of temperature coefficient, interconnect failure test and insulation resistance test were performed in daylight. Electroluminescence imaging was performed on selected set of modules in the late afternoon, using a special daylight EL technique. It was followed by dark *I-V* and dark IR measurements. The methodology of the various tests is briefly explained below.

a) Visual Inspection

Visual inspection of the modules was done to record the physical degradation visible in various parts of the module. A visual inspection checklist, which is a slightly modified and enhanced version of the NREL Visual Inspection Checklist [27], was filled up. Images of the modules were taken using a high resolution camera for future reference. The high resolution images enable us to magnify the region of interest in the captured image, to get a better view of the defect zone. A sample Checklist sheet is given in Appendix A.

b) Current-voltage (I-V) Measurement under illumination

The current-voltage (*I-V*) characteristic is a major diagnostic tool for determining the electrical performance of a PV module [28]. Two sets of portable *I-V* tracers, which were cross-calibrated before starting the survey, were used in the survey, enabling us to collect data of multiple PV modules in parallel. Both the tracers had additional accessories for measurement of the Plane of Array (POA) global solar irradiance and module temperature. At least 5 sets of *I-V* readings were taken for each module, at intervals of about 1 minute. The ambient temperature and relative humidity were also recorded at the time of *I-V* measurement, which would aid in the spectral correction during STC translation of the field data [29], if required.

c) Infrared Thermography under Illumination

Infra-red (IR) images enable us to detect hot spots in the module which can degrade the module performance significantly [30]. IR images were taken from the backside of the module. One set of IR images were taken with the PV array connected to load (i.e. system under MPPT) and a second set of IR images were taken with the array disconnected, and the PV module short-circuited (individually). These images were taken only when the irradiance is above 700 W/m^2, so as to enable proper detection of hot spots.

d) Insulation Resistance Measurement

Insulation resistance is an important measure of the quality of insulating materials used in the module, like the encapsulant and backsheet [31]. Low values of insulation resistance can be a cause of concern with regard to the safety of the personnel handling such modules. The insulation resistance of the modules was checked in the field under both dry and wet conditions. The insulation resistance was measured between the shorted output terminals and the module frame.

e) Electroluminescence Imaging

Electroluminescence (EL) imaging of modules is an important diagnostic tool that provides information about the extent and nature of cracks and various other defects in the solar cells [32]. Two types of electroluminescence cameras, having silicon CCD and CMOS sensors, were used to capture the luminescence emitted by the selected PV module, when forward biased to carry the rated short circuit current using a DC power supply. One of the cameras was a low-cost standard DSLR camera suitably modified to take good EL images. An image difference technique, developed in-house at IIT Bombay specifically for such field surveys, was utilized to capture the EL images in the late afternoon hours, in low irradiance conditions in the field. This technique takes the difference of two images of the module captured by the camera – one taken with, and another without, forward biasing the module [33]. The EL images are later analyzed to find out what fraction of the short circuit current degradation is accounted for by the cracks and inactive areas in the module.

f) Dark I-V Measurement

The use of the illuminated and dark *I-V* characteristics of a PV module to determine the degradation modes has been explained in detail by Spataru *et al.* [28]. The dark *I-V* was taken by sweeping the applied terminal voltage from zero to the open circuit voltage of the respective module, using a programmable DC power supply (which was controlled by a custom-made MATLAB code running on a laptop).

g) Dark IR Measurement

Dark IR imaging was done in the evening hours by covering the selected module from the front. The module was forward biased at its rated short circuit current, and it was allowed to heat up for about 1 minute before taking the image using the infrared camera. The image was usually taken from the back side of the module, unless the installation structure prevented access to its back side. These dark IR images were later analyzed and compared with EL to assess whether dark IR can serve as a substitute for EL imaging in the field.

h) Interconnect Failure Test

Interconnect failure is one of the most common failure modes for PV modules installed in Hot & Dry climatic zones [34]. The Cell Line Checker from Togami Corporation is an innovative tool that can detect interconnect failures in PV modules [35]. It consists of 2 units – the transmitter (which is connected to the PV module output terminals) and the receiver (which is swept on the front side of the module over the interconnect ribbons). The receiver unit shows the health of the interconnect connections through flashes of LEDs on a scale of 0 to 10; with no flash meaning complete failure of the associated interconnect ribbon.

i) Measurement of Module Temperature Coefficient

One module at each site was cooled down to ambient temperature using water and then it was allowed to heat up through exposure to sunlight. Illuminated *I-V* measurements were performed on the module as it heated up to its operating temperature, and from these *I-V* curves the temperature coefficients for current and voltage were determined [9].

j) Use of Colorimeter to Measure extent of EVA Discoloration

Testronix TP110 colorimeter has been used to measure the colour of the solar cells. Measurements have been done at the edge and centre of the solar cells which can give an indication of how much the centre of the cell has browned in comparison to the edge.

Table 1.2: Equipment Specifications

Instrument	Make & Model No.	Specifications
I-V Tracer	Solmetric PVA-1000S	Voltage Range (& Accuracy) : 0-1000 V DC, (±0.5% ±0.25V) Current Range (& Accuracy) : 0-20 A DC, (±0.5% ±40mA) Irradiance Sensor Range & accuracy: 0-1500 W/m^2, (±2%)
Infrared Camera	FLIR E60	Temperature Range : -20 ^{o}C to 650 ^{o}C Thermal Sensitivity : <0.05 ^{o}C at 30 ^{o}C Detector Type (& size) : Uncooled Microbolometer, 320 x 240 Pixels
Electroluminescence Camera	Sensovation HR-830	No. of Pixels (& pixel size) : 3326 X 2504, (5.4 um x 5.4 um) Sensor cooling : Thermo-electric cooling to 50 ^{o}C below ambient
	Modified SONY camera	No. of Pixels (& pixel size) : 20.1MPixel Sensor Technology: CMOS
Cell Line Checker	Togami SPLC-A-Y1	Voltage range : 15V DC – 1000 V DC (Magnetic field mode), 0-1000V DC (Electric Field mode)
Insulation Resistance Tester	FLUKE 1550C	Insulation test voltage : 250 V / 500 V / 1000 V / 2500 V / 5000 V Leakage current measurement range : 1 nA – 2 mA
DC Power Supply	GWInstek PSW 160-14.4	Rated Output Voltage: 160 V dc Rated Output Current: 14.4 A dc
Digital camera	Nikon D3200	Effective Pixels : 24.2 Million Image sensor : 23.2 x 15.4 mm CMOS sensor
Colorimeter	Testronix TP110	Light Source: D65 Illumination/observation system: 8^{o} illumination angle/ diffuse viewing
Shading Analyzer	Solar Pathfinder	NA

1.4 Climatic Zones of India

The National Building Code of India [36] divides India into 5 climatic zones based on average annual temperature and humidity – Hot & Dry, Warm & Humid, Composite, Temperate and Cold. However, as argued in our 2014 report [2], it is better to use the six-zone classification system of Bansal and Minke [37], the criteria for which are described in Table 1.3.

Table 1.3: Climatic Zone Classification criteria as per Bansal and Minke [37]

Climate	Mean Monthly Temperature (°C)	Mean Relative Humidity (%)
Hot & Dry	>30	<55
Warm & Humid	>30	>55
Moderate	25 – 30	<75
Cold & Cloudy	<25	>55
Cold & Sunny	<25	<55
Composite	This applies when six months or more do not fall within any of above categories	

As per the six-zone classification, the coastal area of India (like Mumbai, Chennai and Kolkata) fall in the Warm & Humid zone, whereas the central parts of India (including the capital city of New Delhi) fall in Composite zone. Places in the central western part of India like Jaipur, Jodhpur, Jaisalmer and Gandhinagar lie in the Hot & Dry zone. Bangalore falls in the Moderate climatic zone. Sites in Ladakh fall in the Cold & Sunny climatic zone whereas sites in Jammu, Kashmir Valley and Himachal Pradesh experience Cold & Cloudy climate. The various climatic zones in India have been shown in Fig. 1.1, along with the sites where the 2016 survey has been conducted (in black dots). As evident from the figure, all the zones have been covered in this survey. The number of sites (refer to Table 1.4) is not quite evenly distributed, with many sites falling in the Warm & Humid and Composite zones, but nevertheless there are enough modules in all zones to gauge climatic variations. Further, it has been found (in 2014 and again in 2016) that many aspects of module degradation are similar between the 'Hot' zones, that is, Hot & Dry, Warm & Humid and Composite zones. Similarly, the cooler ('Non-Hot') climates, namely Moderate, Cold & Cloudy and Cold & Sunny zones also have similar kind of module degradation. Hence the six climatic zones will sometimes be classified into Hot and Non-Hot zones for the sake of analysis wherever found necessary.

Table 1.4: Survey site statistics

Climatic Zone	No. of Sites	No. of Modules
Warm & Humid	11	243
Hot & Dry	10	278
Composite	7	184
Moderate	4	94
Cold & Sunny	4	106
Cold & Cloudy	1	20

While the six-climate classification of Bansal and Minke is being used for the analysis of the survey data, we have provided some of the important climate-dependent analysis also in terms of the internationally accepted Koppen-Geiger climate classification system, in Appendix B.

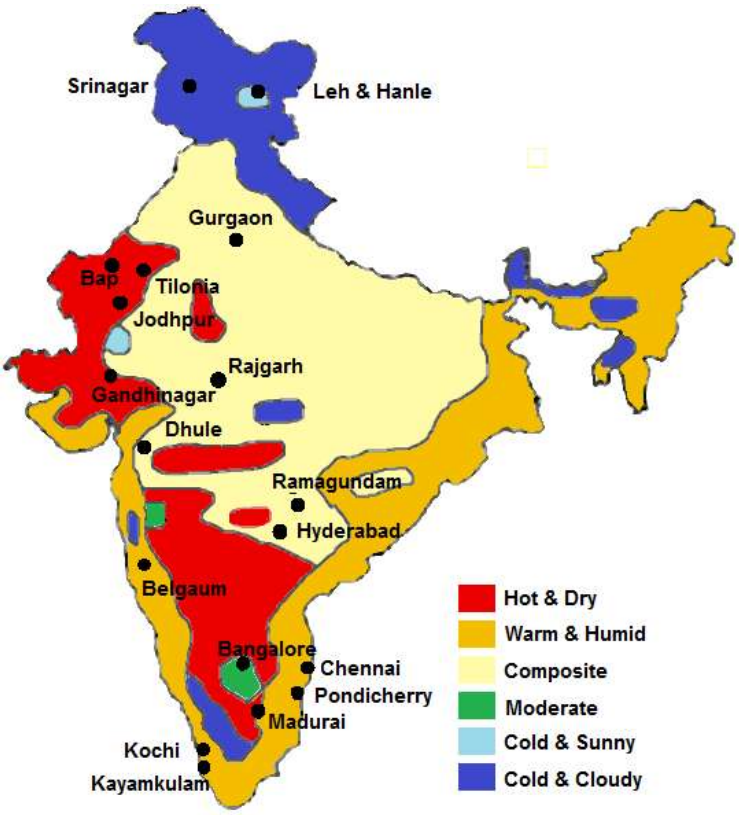

Fig. 1.1: Climatic Zones of India as per Bansal and Minke [37].

1.5 Summary

This chapter has given an overview of All-India Surveys of PV Module Degradation undertaken in 2013, 2014 and 2016, together with a brief review of some recent and relevant literature. The survey methodology, types of inspections and measurements undertaken, and the details of the equipment used in the field have been described. Since India experiences a variety of climatic conditions, from extremely hot climates in Rajasthan to cold climates in Ladakh, the six-zone climatic classification has been described. Before going into the analysis of the survey data, it is important to understand the distribution of the data, in terms of the age, technology and various other aspects. The following chapter discusses some of these vital statistics related to the survey.

2. Information on Modules Surveyed

2.1 Introduction

This chapter presents an overview of the diversity in the modules inspected during the 2016 Survey, in terms of the technology, climatic zone, power rating, age group, packaging material etc. A total of 925 modules were measured in the 6 different climatic zones of India, but these were not equally distributed among the various categories. However, each of the categories had a respectable representation in the survey, as will be clear from the data being presented here.

2.2 Statistics of Sites Surveyed

The survey team visited a total of 37 sites from Tamil Nadu to Ladakh, and from Rajasthan to Madhya Pradesh, covering all the climatic zones in India (Hot & Dry, Warm & Humid, Moderate, Composite, Cold & Cloudy and Cold & Sunny). Fig. 2.1 shows that most of the surveyed sites fall in the small/medium (having less than 100 kW installed capacity). Also 11 number of solar power plants were surveyed which fall in large category (installed capacity more than 100 kW). It should be noted that the percentage of large installations is higher in the 2016 survey compared to the 2014 survey (30% in 2016 versus 12% in 2014 survey). As evident from Fig. 2.2, 16 sites were rooftop installations, 21 sites were ground mounted system.

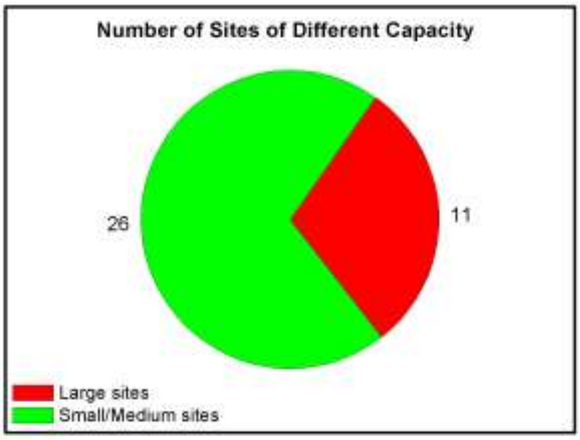

Fig. 2.1: Installed capacity (size) of the sites.

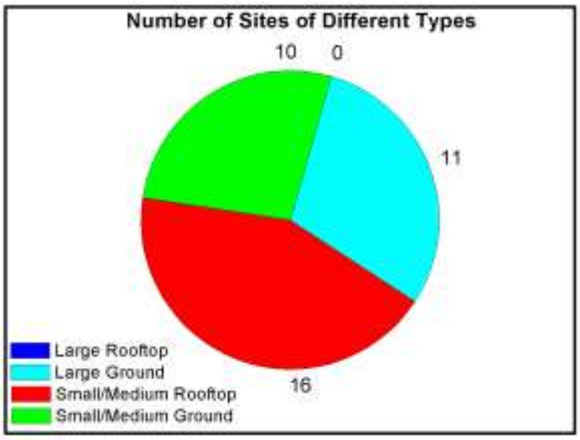

Fig. 2.2: Type of installation.

2.3 Statistics of Modules Inspected

The survey module details are summarized in Figures 2.3 through 2.10. Figure 2.3 shows the distribution of technology of the modules surveyed. Most of the modules inspected are crystalline silicon modules, about evenly distributed between the mono crystalline silicon (mono c-Si) and multi crystalline silicon (multi c-Si). Apart from crystalline silicon modules, we have good representation of amorphous silicon (a-Si) and cadmium telluride (CdTe), as well as a few CIGS and HIT. Figure 2.4 shows the histogram of the age of the modules, and it is seen that a majority of the modules (about 60%) fall in the young age group of 0 to 5 years, although we also have more than 345 modules in the older age categories. Figure 2.5 shows that the name-plate power ratings of the inspected modules mostly belong to the 200-300 Wp category. The maximum number of modules was surveyed in the Hot & Dry (H&D) zone, followed by the Warm & Humid (W & H) zone, but the other climatic zones were also well represented, as evident from Fig. 2.6. Figure 2.7 shows the biasing condition of the modules. Figure 2.8 shows the statistics with regard to the packaging materials used in the modules, at the front and back. A majority of the modules had glass cover on top (front) and polymer backsheet, as evident from Fig. 2.8. A few of the amorphous silicon modules had polymer on the front instead of glass and metal at the back. Almost all of the systems surveyed had either an inverter only (grid-tied systems), or inverter plus battery (refer to Fig. 2.9). In Fig. 2.10, we have provided statistics regarding the various characterization tests performed during the survey. The major characterization tests like current-voltage (*I-V*) characterization (in daylight), infrared (IR) thermography, visual inspection, insulation resistance and interconnect breakage test were performed on all inspected modules at each site. Further, based on these characterization tests, some of the modules were selected for further testing, and were subjected to dark current-voltage (dark *I-V*) characterization, dark IR thermography, and electroluminescence (EL) testing.

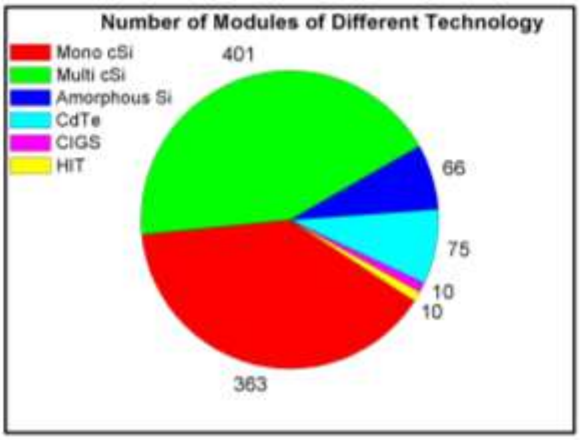

Fig. 2.3: Technology-wise distribution of inspected modules.

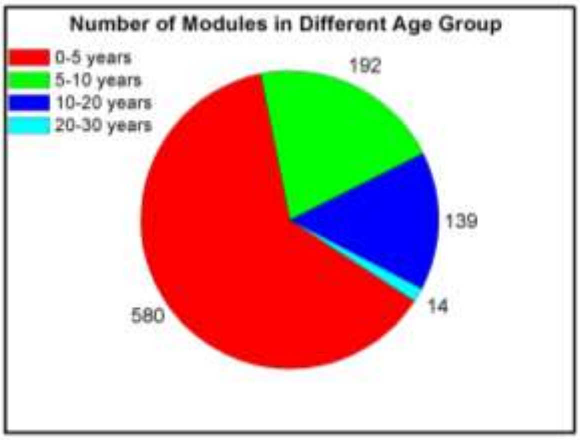

Fig. 2.4: Age-wise distribution of inspected modules.

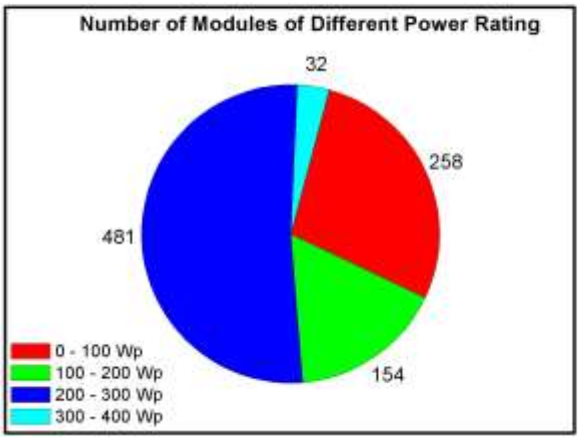

Fig. 2.5: Rated power distribution of inspected modules.

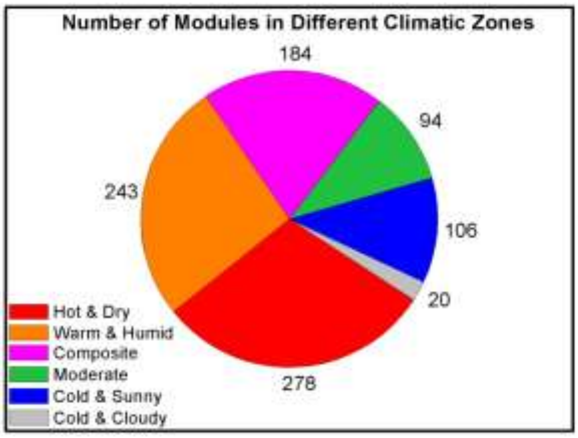

Fig. 2.6: Climatic zone-wise distribution of the modules.

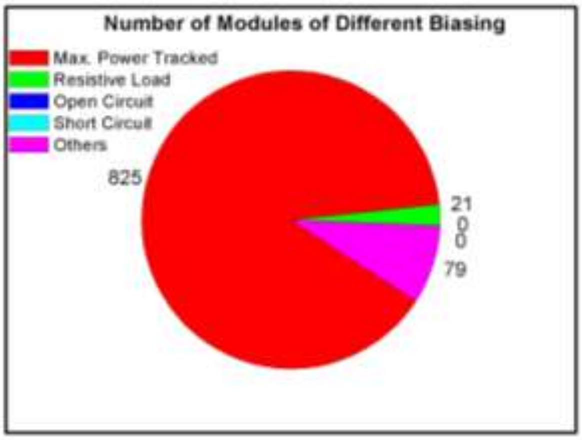

Fig. 2.7: Type of biasing of the inspected modules.

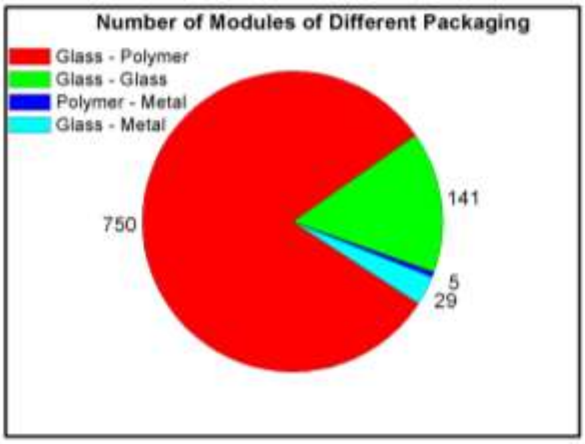

Fig. 2.8: Packaging material of inspected modules.

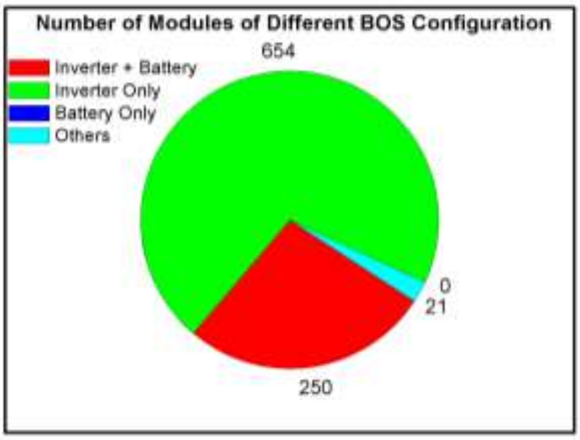

Fig. 2.9: Balance of system configuration.

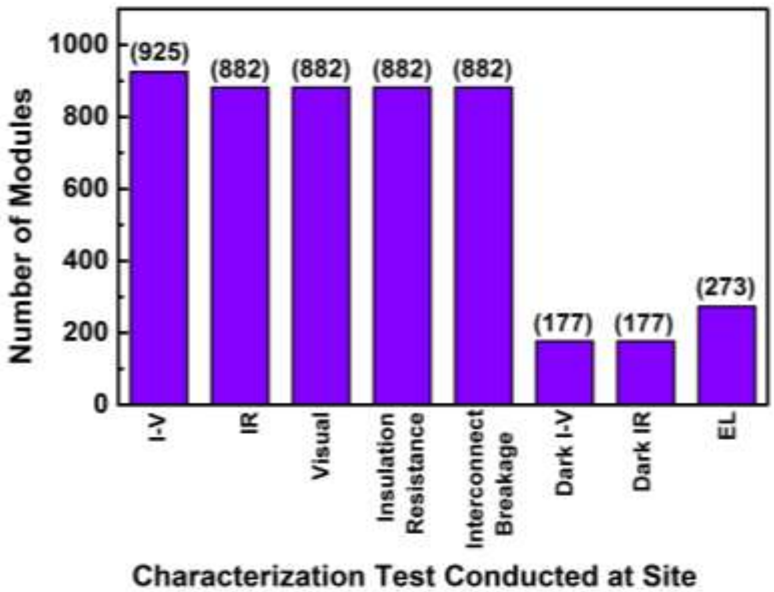

Fig. 2.10: Characterization tests conducted at the site.

2.4 Summary

This chapter gives the distribution of the surveyed modules in terms of various categories of site size, age, technology, climatic zone and other important aspects. It is seen that the 925 modules inspected during the 2016 Survey are quite well represented in most of these categories. In particular, we generally have large enough numbers (barring a few cases) to arrive at reasonable statistical analyses. The following chapters will deal with the analysis of the electrical performance of the inspected modules, and correlate them with the visual and non-visual defects observed in these modules.

3. Correction Procedures and Statistical Methods Applied to Survey Data

3.1 Introduction

During the survey, *I-V* data of the PV modules were measured at various conditions of module temperature and irradiance. In order to understand their performance it was necessary to translate the measured *I-V* data to a standard condition. The Standard Test Condition (STC) for PV modules has been defined by the International Electrotechnical Commission (IEC) as 1000 W/m^2 irradiance with AM 1.5G spectrum and 25 ºC module temperature. Further, IEC 60891 defines the standard correction procedure for translating measured *I-V* data between different irradiance and temperature values. We have utilized a modified version of IEC 60891 correction procedure 1 [38] for translating the *I-V* measured during the survey. In this chapter we discuss the correction procedure and the associated errors introduced due to the use of the modified version of IEC 60891 especially when translating from high temperature. We will also discuss the errors associated with the measurement itself and the uncertainty in maximum power rating of the module. For the 2016 Survey, we have introduced and used the 'Linear Degradation Rate', which discounts the rapid initial light-induced degradation (LID) seen in many modules and this definition is described in this chapter. Also, we present the data plotting format with different error bars. Finally, we will discuss the importance of using statistical methodology and, also, the results obtained through it.

3.2 IEC 60891 Correction Procedure

The IEC 60891 standard defines a procedure to translate the measured *I-V* characteristics of photovoltaic devices to standard test condition (STC) i.e. 1000 W/m^2 irradiance and 25 ºC module temperature. Correcting *I-V* data to STC condition helps in comparing the performance of different PV modules. Three different procedures have been defined in IEC 60891 for translating the measured *I-V* characteristics to other conditions of temperature and irradiance (such as STC). The first procedure involves two equations, one for correcting current and the other for voltage; therefore each point of the entire *I-V* curve is corrected. In case of large irradiance corrections (>20%) for better results the second correction procedure can be used, which involves an alternative algebraic method. In both these procedures, correction parameters must be determined prior to the correction; whereas the third correction procedure, which is an interpolation method, does not require any correction parameters. All three correction procedures have been comprehensively reviewed and presented in the report of the All India Survey of Photovoltaic Module Degradation 2013 [1], and elsewhere, and the interested reader is referred to it.

3.3 Correction Procedure Adopted for Survey Data

IEC 60891 correction procedure 1 was adopted for translating the *I-V* data to STC condition. It requires four correction parameters for translating the entire *I-V* curve. These are: α (temperature coefficient for current), β (temperature coefficient for voltage), R_s (internal series resistance of the test specimen) and k (curve correction factor). It is obviously better for high accuracy if all the four parameters are used; obtaining the values of R_s and k requires measurements of temperature and irradiance dependency of the current and voltage. We explore whether these can be neglected without much loss of accuracy.

3.3.1 Correction Procedure 1a

The value of R_s of a module is determined by using three *I-V* curves at constant temperature but different irradiances, whereas in order to determine the value of k, we need three *I-V* curves at constant irradiance but different temperatures. Since enough field data is often not available to determine the values of R_s and k**,** we have considered only two parameters i.e. α (temperature coefficient for current) and β (temperature coefficient for voltage) while keeping R_s and k equal to zero. Furthermore, we have used the values of temperature coefficient measured in the field (this is different from our previous surveys). The procedure of obtaining the temperature coefficients has been described in detail in [9]. We have used the nameplate values of I_{sc} and V_{oc} in order to convert the values of α (temperature coefficient for current) and β (temperature coefficient for voltage) from %/°C to A/°C and V/°C respectively. Therefore, the equations of Correction Procedure 1 will get modified as follows:

$$I_2 = I_1 + I_{sc} * \left(\frac{G_2}{G_1} - 1\right) + \alpha * (T_2 - T_1) \quad \text{.... (3.1)}$$

$$V_2 = V_1 + \beta(T_2 - T_1) \quad \text{.... (3.2)}$$

We have used above two equations for correcting the measured *I-V* curve to the STC condition. We call this procedure as Correction Procedure 1a. A MATLAB code was written in order to do this in an automated way.

In order to understand the level of accuracy of Correction Procedure 1a, we performed an exhaustive set of experiments which is described in detail in Appendix C.

3.3.2 Low Irradiance/High Temperature Correction

As per IEC 60891, translation procedures can be applied only for 20% variation in the irradiance, that is, the irradiance should lie between 800 W/m^{2}and 1200 W/m^2 for translation to STC. In order to achieve these conditions the 2016 Survey was planned in the summer season. However it led to a high module operating temperature during *I-V* measurements. In our case, almost all of the *I-V* data were taken at irradiance greater than 780 W/m^2. Module temperature was typically between 50 °C to 70 °C.

In order to determine the errors associated in translating the *I-V* data measured at high temperature to STC using Correction Procedure 1a, we had performed an exhaustive set of experiments as described in *All India Survey of PV Module Reliability 2014* [2]. The results of these experiments are reproduced in Table 3.1, which show the error associated with translation from a particular temperature & irradiance combination to STC. The shaded cells in the table indicate irradiance and temperature conditions not encountered during the survey. It can be noticed that we can indeed use Correction Procedure 1a for irradiances more than 700 W/m^2 and temperature less than 70 °C without exceeding an error limit of 4%.

Table 3.1: Error in P_{max} value at STC obtained by translating using Procedure 1a

ΔP_{max} (%)	Module Temperature (°C)									
Irradiance (W/m^2)	**25**	**30**	**35**	**40**	**45**	**50**	**55**	**60**	**65**	**70**
500	4.59	4.12	4.05	4.10	4.37	4.59	4.90	5.08	5.41	5.91
550	4.09	3.58	3.48	3.51	3.74	3.93	4.22	4.37	4.69	5.17
600	3.69	3.17	3.03	3.07	3.25	3.37	3.65	3.78	4.07	4.51
650	3.08	2.61	1.78	1.57	1.38	1.29	1.20	1.07	0.94	0.84
700	2.62	2.16	1.30	1.04	0.82	0.72	0.60	0.44	0.27	0.16
750	2.22	1.72	0.82	0.52	0.28	0.13	-0.01	-0.19	-0.39	-0.51
800	1.70	1.18	0.96	0.94	1.03	1.19	1.25	1.32	1.00	1.28
850	1.25	0.72	0.44	0.39	0.49	0.60	0.63	0.66	0.35	0.40
900	0.86	0.29	0.00	-0.07	-0.03	0.07	0.07	0.07	-0.29	-0.28
950	0.37	-0.37	-0.94	-1.24	-1.56	-1.67	-2.00	-2.47	-2.73	-2.90
1000	0.00	-0.60	-1.40	-1.75	-2.10	-2.24	-2.59	-3.08	-3.36	-3.58

3.3.3 Definition of Degradation Rate

In order to calculate the degradation rate, the initial performance data is needed. However, in most cases, the initial *I-V* curves were not available, so the performance data was computed based on the nameplate data. Since there is usually a tolerance on the name plate power rating, we have defined the Nominal Power rating as the name plate power plus average of the tolerance band. Most manufacturers of crystalline silicon modules provide for an initial rapid degradation in their modules (usually 2% - 3% in the first year of field exposure) which is mainly due to Light Induced Degradation (LID), followed by a linear power warranty. To accommodate this initial LID loss in the modules, we have assumed a 2% LID loss in power output from the Nominal Power, and named it as LID discounted power rating. LID loss in modules varies widely depending on the wafer quality and we have taken the 2% figure as an average, as described in detail in Section 1.2. A linear power degradation rate is calculated based on this LID discounted power rating, using the relation shown in Eqn. 3.3. Figure 3.1 shows graphically the calculation of Linear Degradation Rate for a 15-year old module. Suppose a module is rated at 100 W and has a tolerance of -0% to 5%. Then its Nominal Power will be 102.5 W; applying 2% LID on Nominal Power, we get 100.4 W and this is taken to be $P_{LID\_discounted}$. Then the 'Linear Degradation Rate' is calculated as follows:

$$Linear\ P_{max}\ Degradation\ Rate\ (\%/year) = \frac{(P_{LID\_discounted} - P_{Present}) * 100}{P_{LID\_discounted} * Age} \quad \text{... (3.3)}$$

It should be noted that the LID discounting for c-Si modules has been introduced for the first time in the 2016 survey. The reason is that it was felt that not accounting for this, and just using $P_{nominal}$ instead of $P_{LID,\ discounted}$ gives an unduly pessimistic value of degradation rate, especially for younger modules. However, this also means that we should not directly compare the degradation rates reported in this survey with those obtained from the 2013 and 2014 survey analysis where LID discounting was not done.

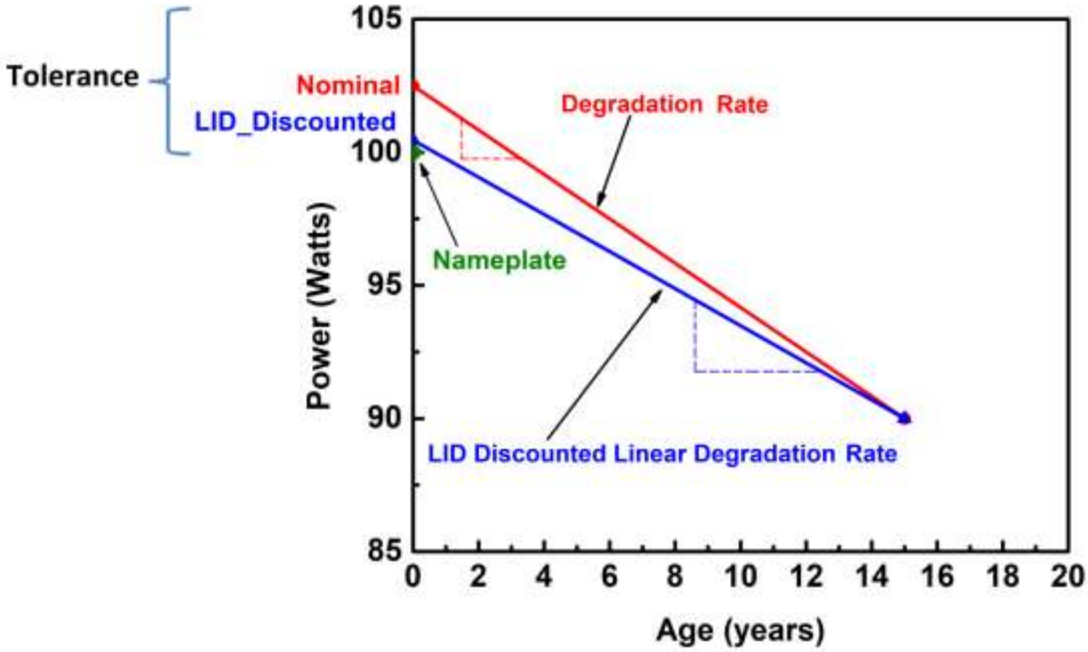

Fig. 3.1: Graphical representation of 'Linear Degradation Rate', and comparison with simple 'Degradation Rate'.

3.4 Uncertainty in the Linear Degradation Rate Calculation

The *I-V* parameters at STC are obtained from the field measurement followed by STC translation using Correction Procedure 1a. Therefore, any uncertainty in the electrical parameters at STC depends on the uncertainty introduced by the correction procedure plus the uncertainties or errors due to the measurement equipment.

3.4.1 <u>Uncertainties in Measurements</u>

Solmetric PVA-1000S portable *I-V* curve tracer was used as a measurement tool during the survey. It uses a K-type thermocouple as the temperature sensor, and a silicon photodiode as the irradiance sensor. The typical uncertainties of measured irradiance arise from stability, temperature coefficient, data acquisition and spectral mismatch. As per the manufacturer's datasheet, measurement uncertainty is ±2% for irradiance measurement, and ±2^{0}C for temperature measurement. The manufacturer datasheet specifies the maximum measurement uncertainty in both voltage and current as ±0.5%.

We have calculated the errors caused by the instrument on the *I-V* parameters at STC through a detailed error analysis, which is described in detail in *All India Survey of PV Module Reliability 2014* [2]. The result of the error analysis is presented in Table 3.2 and it can be seen that the maximum possible error caused by the instrument on the P_{max} value at STC is 4%.

Table 3.2: Error caused by the instrument on P_{max} at STC

ΔP_{max} (%)	**Module Temperature (°C)**									
Irradiance (W/m^2)	**25**	**30**	**35**	**40**	**45**	**50**	**55**	**60**	**65**	**70**
500	4.05	4.05	4.04	4.03	4.01	4.00	3.99	3.97	3.96	3.93
550	4.05	4.05	4.03	4.03	3.97	3.95	3.94	3.91	3.90	3.88
600	4.05	4.05	4.04	4.03	3.97	3.95	3.94	3.92	3.91	3.88
650	4.05	4.05	4.01	3.99	3.97	3.95	3.93	3.92	3.90	3.89
700	4.04	4.04	4.01	3.99	3.97	3.95	3.93	3.92	3.91	3.89
750	4.04	4.05	4.00	3.99	3.97	3.95	3.93	3.92	3.90	3.89
800	4.04	4.04	3.99	3.97	3.96	3.94	3.92	3.91	3.89	3.88
850	4.04	4.04	4.00	3.98	3.96	3.94	3.93	3.91	3.90	3.89
900	4.03	4.03	4.00	3.98	3.97	3.95	3.93	3.92	3.91	3.89
950	4.03	4.03	4.01	3.99	3.98	3.96	3.95	3.94	3.93	3.88
1000	4.03	4.03	4.00	3.99	3.98	3.96	3.95	3.94	3.93	3.92

3.4.2 Uncertainties in Power at STC

The uncertainty in the corrected P_{max} is the combination of uncertainties in the measurement of the *I-V* data, temperature and irradiance in the field, and also due to the uncertainties in the temperature coefficients which are used in the translation equations. Table 3.3 shows the worst case error in the corrected P_{max} will be around 6% for crystalline silicon modules, taking into account all the errors and uncertainties.

3.4.3 Uncertainties in Nameplate Data

The practical limitations of the field survey like ours, is that it is usually not feasible to get the initial performance data of the module when it was first installed, so the name plate data has to be used instead. Therefore, an additional uncertainty in the degradation rate is introduced by the tolerance band provided by the module manufacturers in the name plate power ratings of the modules (usually ±3% but also, in a few cases, –0% / +5%). Therefore the actual initial rating can have any value within the tolerance band. This has been described in more detailed in *All India Survey of PV Module Reliability 2014* [2].

Table 3.3: Total error caused by instrument and Correction Procedure 1a on P_{max} at STC

ΔP_{max} (%)	Module Temperature (°C)									
Irradiance (W/m^2)	**25**	**30**	**35**	**40**	**45**	**50**	**55**	**60**	**65**	**70**
500	8.64	8.17	8.09	8.13	8.38	8.59	8.89	9.05	9.37	10.44
550	8.14	7.63	7.51	7.54	7.71	7.88	8.16	8.28	8.59	9.05
600	7.74	7.22	7.07	7.1	7.22	7.32	7.59	7.7	7.98	8.39
650	7.13	6.66	5.96	5.73	5.63	5.64	5.63	5.3	5.12	4.83
700	6.66	6.2	5.48	5.25	5.12	5.1	5.06	4.83	4.52	4.18
750	6.27	5.77	5.02	4.76	4.6	4.55	4.5	4.12	3.89	3.54
800	5.74	5.22	4.95	4.91	4.99	5.13	5.22	5.33	5.54	5.83
850	5.3	4.76	4.44	4.43	4.52	4.7	4.77	4.86	5.06	5.33
900	4.92	4.32	4	3.93	4.03	4.16	4.21	4.28	4.45	4.68
950	4.43	3.66	3.99	4.13	4.33	4.67	4.73	5.05	5.35	5.56
1000	4.03	3.43	3.55	3.66	3.85	4.15	4.21	4.51	4.75	5.01

3.4.4 Uncertainties in Initial LID

As mentioned earlier, we have taken the initial rapid LID drop for crystalline modules to be 2%, but this may vary. This can give rise to additional error, which we have not quantified.

3.5 Graph Templates

Figures 3.2-3.4 show the template which will be followed for most of the graphs in this report (the values presented in these figures are indicative only). Fig. 3.2 shows the histogram; the two dashed red lines indicate the average and the median value of the data set. The boxed inset shows the value of average, median and the number of samples. Fig. 3.3 shows template for electrical parameter degradation rates plotted against various groups. The hollow symbols indicate Young modules (age less than 5 years) while the solid symbols indicate Old modules (age greater than 5 years). The mean of each group (value in parentheses) is shown by the read horizontal line, while the red diamond shows the 95% confidence interval. The number in square brackets above the data points represents the number of samples (modules). Also, the following errors will be marked for each group:

a) Error due to measurement and STC correction (on right side of the plotted data, in green)
b) Error due to uncertainty in name plate (on left side of the plotted data, in pink)

The cumulative probability distribution for the data points has also been shown on the right side of the figure. The cumulative probability refers to the probability that a random variable is less than or equal to a specified value. Not all symbols for the data points have been marked in the cumulative probability plot as it would impair the readability of the plot, although all data points have been incorporated. From this cumulative probability plot, one can easily understand the distribution of the data points. The data point at 50% probability is actually the median of the data set.

Graphs with single data point per group (see Fig. 3.4) will show the errors (a) and (b) as indicated above (i.e. error due to measurement and STC correction in green, and error due to uncertainty in name plate in pink), but there would be no mean value or confidence interval.

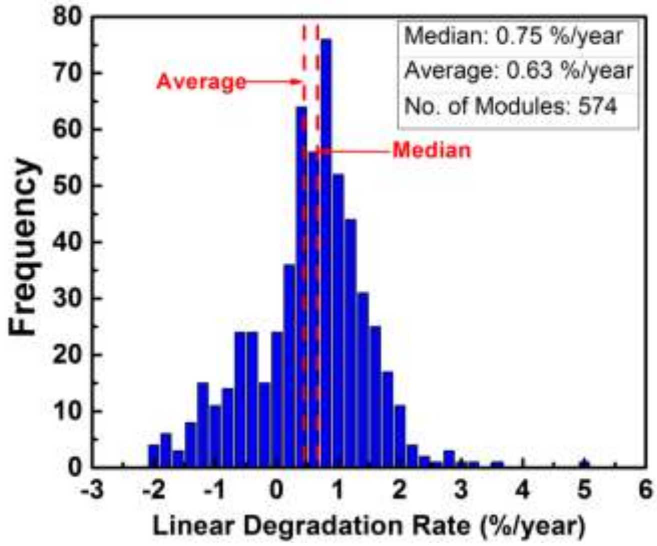

Fig. 3.2: Graph template showing histogram for group of data.

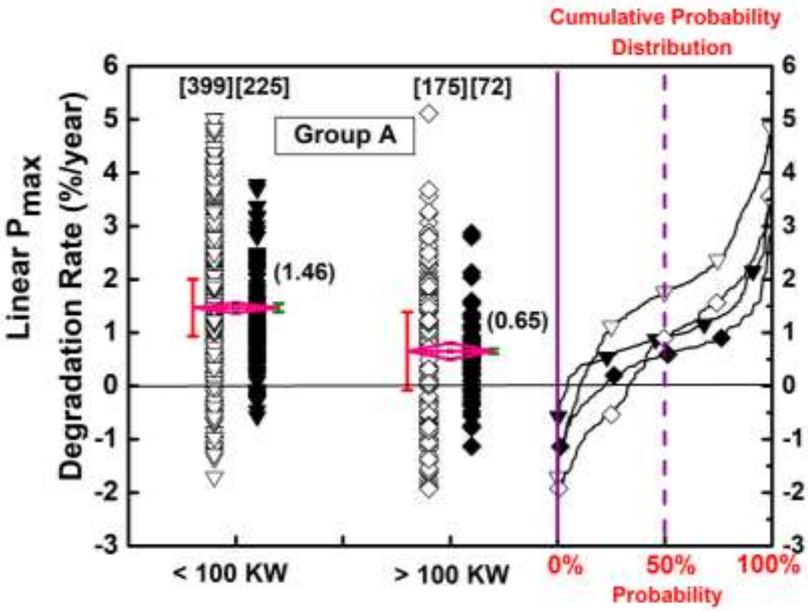

Fig. 3.3: Graph template showing various uncertainties and cumulative probability for group of data.

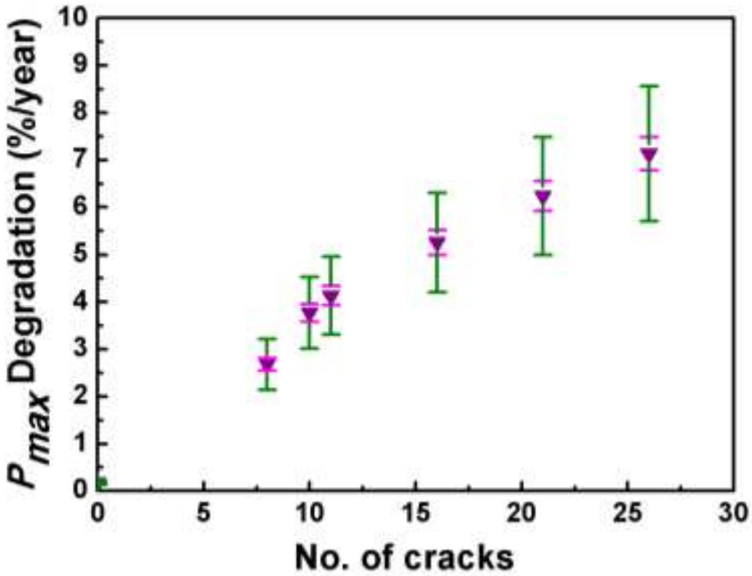

Fig. 3.4: Graph template showing various uncertainties for a single point data.

3.6 Statistical Analysis

3.6.1 Introduction

The modules in photovoltaic systems are often found to degrade differently even if they are made of the same materials. As a result, almost all studies concerning degradation rates exhibit high variability in data related to electrical performance measures. Hence it is necessary to perform rigorous statistical analysis of the data in order to find out whether perceived differences in central tendencies of the data sets are statistically significant or just artifacts of the data distribution. High variability in the P_{max} degradation rates, ranging from –2 %/year to as high as +5 %/year, has been observed for the surveyed modules and this aspect will be taken up for discussion in detail later in Chapter 4. In this section, we shall present the statistical methods employed for the analysis of the survey data and it is hoped that this would help the readers understand the statistical analysis presented in the forthcoming chapters.

The first step in statistical analysis is to remove outliers present in the data. The next subsection briefly outlines the procedure used in identifying outliers.

3.6.2 Definition of Outliers

Before doing any analysis on the data, it is important to identify and separate out the outliers from the data set. We have identified the outliers in the degradation rate data based on the inter-quartile range. The data points are arranged in ascending order, and then split into two halves, with the median included in both halves if the total number of sample points is odd. Then the lower fourth (lf) is the median of the lower half, while the upper fourth (uf) is the median of the upper half. A measure of the spread which is resistant to outliers is given by the difference between the upper fourth and lower fourth, which is referred to as the inter-quartile range. Any observation beyond 1.5 times of inter-quartile range from its nearest fourth is considered as an outlier. In our case, all data points above 5.12 %/year degradation rate are identified as outliers, as shown in Fig. 3.5. The subsequent analysis of the data is carried out after eliminating the outliers from the original data set.

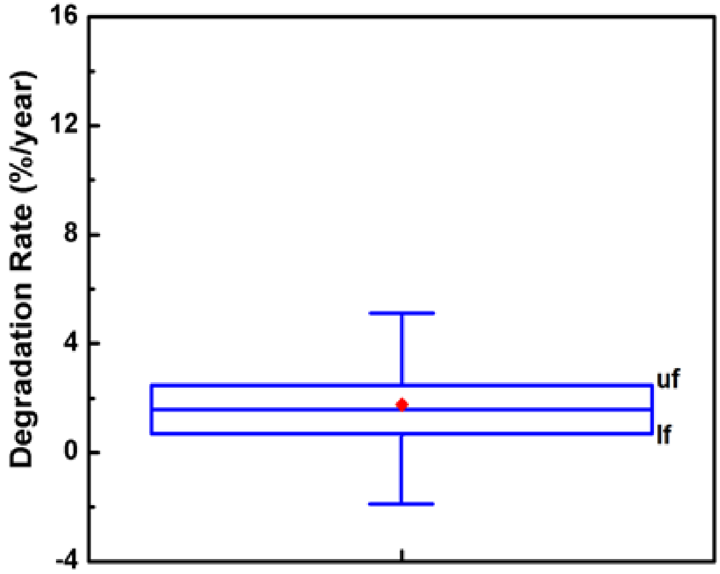

Fig. 3.5: Box plot for P_{max} degradation rates for c-Si modules in all sites (The red dot indicates the sample mean).

3.6.3 Choice of Mean versus Median

In order to arrive at meaningful conclusions, we need to present overall trends in the measurements from the huge set of data collected in our survey using suitable summary statistics. We have used sample mean over the sample median for the same purpose. In order to be consistent with the 2014 survey we have used the sample mean as an estimator of the central tendency. The justification for using mean has been described in detail in the *All India Survey of PV Module Reliability 2014* [2].

Apart from the mean of the data, and its spread, it is also important to understand the overall distribution of the data points. A tight distribution of the data points close to the mean value provides us higher confidence on the use of the mean to represent the data set, as opposed to the situation where the data points are distributed over broad range of values, far from the mean. Hence, we have provided the cumulative probability distribution plots in many cases so that one can get an idea about the overall distribution of the data points.

3.6.4 Procedure for finding Confidence Intervals

Since the measured P_{max} degradation rates do not follow the normal distribution, it is not possible to construct 100(1-α) % confidence intervals using percentile points of normal distribution. Hence, we have used the bootstrap method to construct the confidence intervals. This method involves drawing a large number of samples of size n with replacement from the original sample of size n. For each of the bootstrap samples, test statistics of interest (the average degradation rate in the present context) is computed. This, in turn, is used to determine the percentile points which are then used to obtain the requisite 100(1-α) % confidence interval for the unknown parameters. Fig. 3.6 shows the histogram of the bootstrap means and the 95% bootstrap confidence interval (CI) for the population mean of P_{max} degradation rates. For the data at hand, 95% bootstrap confidence interval turns out to be (1.15, 1.30). These computations are based on the sample size n = 925 and the number of bootstrap samples N = 10,000.

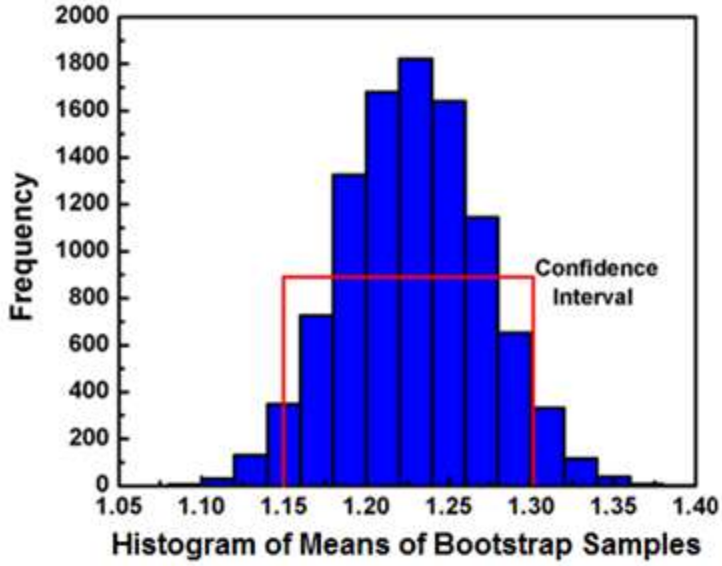

Fig. 3.6: Sampling distribution of P_{max} degradation means based on bootstrap samples.

3. 6.5 Methodology for Statistical Analysis

The modules in the field are influenced not only by the climatic conditions but also by various other factors like the mounting configuration and the quality of installation (which can vary depending on the system size). The PV modules can be grouped into various categories based on the following factors:

a) Climatic zone (Hot & Dry, Warm & Humid, Composite, Moderate, Cold & Sunny, Cold & Cloudy)
b) Age (a continuous variable)
c) Mounting configuration (ground (rack) mounted, rooftop (rack) mounted)
d) System size (small/medium, large)

The above factors are considered as the explanatory variables and the degradation rate is treated as a response variable. It is evident from Fig. 3.6 that the distribution of this response variable is non-normal, which has also been confirmed by formal analysis involving the use of the Shapiro-Wilk test.

Let Y = 1 if the P_{max} degradation rates of the module is greater than 1 %/year
= 0 if the P_{max} degradation rates of the module is less than or equal to 1 %/year

This figure of "1 %/year" is taken based on the internationally accepted power warranty provided by many module manufacturers (usually 20% degradation in power output in 25 years). In order to assess the impact of each of the afore-mentioned explanatory variables on this binary response random variable Y, the logistic regression model, which is a member of the generalized linear models, is considered for analysis. This model is given by:

$$g(EY) = \text{logit}[\pi(\underline{x})] = \log \frac{\pi(\underline{x})}{1-\pi(\underline{x})} = \alpha+\beta_1 x_1+\ldots+\beta_p x_p \qquad \ldots(3.4)$$

where,
EY denotes the expected value of response variable Y
g(EY) is a well-defined function of EY.
$\underline{x} = (x_1, x_2, \ldots, x_p)$ is a vector of p explanatory variables $x_1, x_2, \ldots, x_p$
α is the intercept,
β_i is the coefficient associated with i^{th} explanatory variable x_i, $(i = 1,2,\ldots,p)$
$\pi(\underline{x})$ = P[Y=1 for given $\underline{x}$] = P [the P_{max} degradation rate is greater than 1 %/year for given $\underline{x}$]

This model in Equation 3.4 yields two important expressions and they are:

(i) $\pi(\underline{x})$ = P[Y=1] = P [the P_{max} degradation rate is greater than 1 %/year under $\underline{x}$]

$$= \frac{\exp[\alpha+\beta_1 x_1+\cdots+\beta_p x_p]}{1+\exp[\alpha+\beta_1 x_1+\cdots+\beta_p x_p]} \quad \ldots (3.5)$$

and,

(ii) $\frac{\pi(x)}{1-\pi(\underline{x})}$ = the odds of the P_{max} degradation rate are greater than 1 %/year under $\underline{x}$

$$= \exp[\alpha+\beta_1 x_1+\cdots+\beta_p x_p] \quad \ldots (3.6)$$

The logistic regression has been performed on the degradation data with R software package and the p-values of the results are used to judge whether the explanatory variables are statistically significant or not. An explanatory variable x_i is considered to be statistically significant if the p-value corresponding to the estimator, of its unknown parameter, is less than 0.05. The use of the above model is illustrated below by considering data corresponding to (i) climate (6 levels), (ii) age (continuous variable), (iii) mounting (2 levels), and (iv) system size (2 levels) as the explanatory variables.

$$\log\frac{\pi(x)}{1-\pi(x)} = \alpha + \beta_1(\text{climate}_2) + \beta_2(\text{climate}_3) + \beta_3(\text{climate}_4) + \beta_4(\text{climate}_5) + \beta_5(\text{climate}_6) + \beta_6(\text{age}) + \beta_7(\text{mounting}) + \beta_8(\text{system size}) \quad \ldots (3.7)$$

where,
climate_2 = Hot & Dry
climate_3 = Moderate
climate_4 = Composite
climate_5 = Cold & Sunny
climate_6 = Cold & Cloudy
mounting = Ground mounted
system size = Large systems

It can be seen that for each of the categorical variables, the number of dummy variables that have been introduced in the regression model is equal to (number of levels of the variable – 1) and this essentially ensures that there is no redundancy in the levels of the given categorical variables. The parameter estimates obtained after fitting the above model to the degradation rate data are given in Table 3.4. The climate categories, like Hot & Dry, Moderate and Cold & Cloudy, for which p-values are greater than 0.05 do not have any significant effect on the degradation rates, while the Cold & Sunny climate condition seem to have significant effect. Also, the age of the system and system size appear to have insignificant effect on the degradation rates. In view of this, a revised logistic regression model consisting of two categories of the climate variable, namely Hot and Non-Hot, along with the other variables of the above model has been entertained in Chapter 4. The parameter estimates provide us a measure of the effect on the response variable, with negative estimates meaning the response variable (here, power degradation rate) reduces as the level of corresponding covariate increases. For example, the parameter estimate is negative for the mounting structure, so power degradation rate is lower for ground mounted systems (mounting level = 1) as compared to rooftop systems (mounting level = 0).

Table 3.4: Parameter estimates and p-values for six climatic zone model

Covariates	Estimates	p-value
Intercept	2.71410	3.22e-15
Climate Category 2 (Hot & Dry)	0.43965	0.07953
Climate Category 3 (Moderate)	1.12257	0.15015
Climate Category 4 (Composite)	0.76486	0.00706
Climate Category 5 (Cold &Cloudy)	-16.52064	0.97544
Climate Category 6 (Cold & Sunny)	-2.98704	1.05e-12
Age	-0.03544	0.11454
Mounting (=1 for ground mounted)	-2.61777	< 2e-16
System size (=1 for large system size)	-0.07216	0.77676

3.7 Summary

We have used the STC Correction Procedure 1a (a modified version of IEC 60891 Correction Procedure 1) to translate measured field data to STC, and estimated errors due to this procedure. We have also assessed various errors originating from measurement uncertainties. The measurement and STC translation procedures together have been assessed and total error in P_{max} degradation rate has been found to be within 6% for crystalline silicon modules measured above 800 W/m^2. A further error arises due to uncertainty in nameplate rating. We have defined the '*Linear Degradation Rate*' which considers the LID of the module in degradation rate calculations. We have also presented the significance of various statistical models used in the analysis. We have laid a lot of emphasis on the errors involved, as the degradation rates calculated and presented in succeeding chapters need to be appropriately qualified. Statistical analysis has been performed to ascertain whether the differences among various groups of data are significant or just random errors. Statistical analysis has shown that many of the climatic conditions of the six climatic zone classification do not have significant effect on the power degradation rates of PV modules, so the climatic zones have been combined into two categories - Hot and Non-Hot climates. In the following chapter the electrical degradation data is analyzed in detail and the results are verified through statistical analysis.

4. Analysis of Electrical Degradation

4.1 Introduction

There is presently a world-wide push for renewable energy as a consequence of which large utility-scale solar PV installations have increased significantly. It is important to accurately measure the power generation of the deployed modules and determine the average degradation rate per year which can help us to predict the performance over the long term. In this chapter we shall present the degradation rate analysis for the surveyed modules.

The field-measured *I-V* data of the modules is translated to standard test conditions (STC) using Procedure 1a of IEC 60891, as explained in Chapter 3. The extrapolated STC *I-V* data of the module enable us to compare its present-day performance with its initial performance at the time of installation, and thus calculate the Overall Degradation Rate (%/year) of the output power (P_{max}) and other important electrical parameters like short-circuit current (I_{sc}), open circuit voltage (V_{oc}) and fill factor (*FF*). For those modules whose initial performance data was unavailable we have used the 'Nominal' values of the electrical parameters (average of the higher and lower end nameplate values, as defined in Chapter 3). The outliers have been removed from the initial dataset using statistical techniques and then the data of the remaining modules has been analyzed. LID discounting has been done on the Nominal value for crystalline silicon modules to arrive at the Linear Degradation Rate as explained in the previous chapter. A 2% LID discounting has been done for power rating, split up as 0.8% discounting for I_{sc} and V_{oc}, and 0.4% for *FF*. It may be noted that the 2% LID figure has been arrived at after a literature survey (detailed in Chapter 3). It is applicable for Aluminium BSF based crystalline silicon modules, and not for PERC modules which may suffer much higher LID depending on the cell manufacturing process. The thin film modules also show different types of instability when exposed to sunlight, owing to which the power output may increase over the initial value, as in case of CdTe [17], or decrease as in case of amorphous silicon [14]. The light soaking effects can cause up to 10% increase in power output of CdTe modules with respect to the initial value (depending on the ambient temperature) [17]. Also, since silicon photodiode based sensor was used for the irradiance measurement during *I-V* characterization, the spectral mismatch of the thin film modules also comes into picture and can introduce some error in the irradiance measurement. However, the light soaking effects are much greater than the spectral mismatch effects and it is difficult to quantify the extent (or even sign) of the light soaking effect in the inspected modules. So, the *I-V* data of the thin film modules has been presented after irradiance and module temperature corrections but *without considering any spectral mismatch or light soaking effects*.

Unlike the previous survey of 2014, in the 2016 survey all modules were measured above 700 W/m^2, so there is no rejection of data due to low irradiance. Similar to the 2014 survey data, the 2016 data also shows a wide variance in the degradation rate, so we have again separated out the surveyed sites (but only for c-Si sites) into two different categories – Group X and Group Y – based on the average degradation rate of the site in order to draw meaningful conclusions from the analysis.

In this chapter, we present the degradation of the electrical parameters (P_{max}, I_{sc}, V_{oc}, *and FF*) with respect to climate, technology, age group and X/Y group. The modules have been segregated into young (installed in/after 2011 so age is less than or equal to 5 years) and old (installed before 2011 so age is more than 5 years) categories to understand the difference in the degradation rates of the recent installations via-à-vis the older ones. The P_{max} degradation rate with respect to the system size is also presented in order to capture the difference in performance for large plants (more than 100 kW) and medium-to-small installations (less than

100 kW). The template used for the graphs has been explained in Chapter 3 and the reader can refer to Section 3.5 to clearly understand the information conveyed in the figures presented here. Statistical analysis of the data has been presented in order to check whether the results of the electrical degradation analysis are statistically significant or not. Finally, the degradation of the modules/sites which were repeats (in 2014 and 2016 surveys) has been compared in the last section.

4.2 Overall P_{max} Performance and Classification of c-Si Sites into Group X and Group Y

A total of 925 modules have been inspected during the survey, out of which the *I-V* of 26 modules could not be translated to STC due to fault in temperature measurements. Out of the remaining 899 modules, 34 modules showed high P_{max} degradation rates above 5.12 %/year, and these have been considered as "outliers' (based on statistical analysis discussed in Chapter 3). Their performance is discussed separately in Appendix G. The histogram of the remaining 865 modules having Overall P_{max} Degradation Rate within 5.12 %/year is shown in Fig. 4.1. The Overall Degradation Rate and the Linear Degradation Rate are both shown in the figure. From Fig. 4.1(a), we can see that the average (mean) value of the Overall P_{max} Degradation Rate of these modules is 1.55 %/year with a median value of 1.51 %/year. The Overall P_{max} Degradation Rate of the 2016 survey is less than the Overall P_{max} Degradation Rate of survey 2014 (2.07 %/year) and the reason for this is probably the inclusion of more large power plants. The average Linear Degradation Rate is 1.2 %/year. As the initial rapid degradation (LID) of the c-Si modules is already taken care of, this is still higher than the normal warranty conditions (20% degradation in 25 years implying a Linear Degradation Rate in P_{max} of less than 0.8 %/year). It can be seen that there is a wide variability in the degradation rates. Based on these observations, we can conclude that the quality of the modules and/or installation procedures vary widely, as also reported in the 2014 survey report.

It can be seen from Fig. 4.1 that there are many modules which have a *negative* degradation rate. It turns out that many of these are thin-film (mainly CdTe) modules. This is probably due to the spectral mismatch and light-soaking effects described earlier, and also perhaps due to conservative under-rating. We have therefore plotted the histograms for c-Si modules only, which constitute the majority of modules (refer to Fig. 4.2). Group A in the figure refers to 'All' c-Si modules. It is seen that the c-Si modules continue to show a wide variance (in contrast, the thin-film modules are rather tightly distributed). Also, the average value is now 1.90 %/year and 1.47 %/year for Overall and Linear Degradation Rates for the c-Si modules, both of which are quite high, and cause for concern. Of course, some of the c-Si modules are performing quite well, whereas others are not: there are some 'good' sites and some 'problematic' sites. Following the procedure adopted for the 2014 Survey, we have divided the c-Si *sites* into Group X ('good') sites, where the average Overall Degradation Rate is < 2 %/year; and Group Y ('problematic') sites, where the average Overall Degradation Rates is > 2 %/year. Probably, the Group X sites have used better quality modules and/or correct installation procedures than the Group Y sites. Note that this division of Group A into Group X and Group Y sites has been done only for c-Si, since they constitute the majority, do not suffer from uncertainties of thin-film, and represent the present mainstream technology. As explained previously for the 2014 survey analysis, it would be prudent to concentrate only on the 'good' Group X sites when trying to understand the influence of the climatic zone on the performance of the modules, so as to avoid any extraneous factor. Equally important, an analysis of the Group Y sites will reveal the deficiencies which cause rapid degradation. The separation of the sites into Group X and Group Y has been undertaken with these objectives in mind. It should be noted that for all further analysis, the Linear P_{max} Degradation Rate will be used and the Overall P_{max} Degradation Rate will be provided for a few cases (to enable the reader to compare with the 2014 survey analysis if needed).

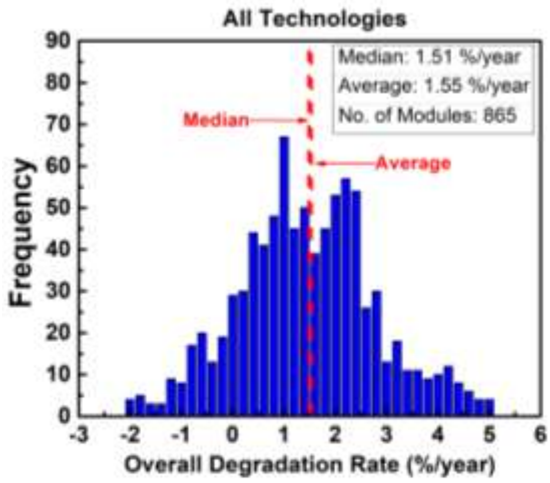

(a)

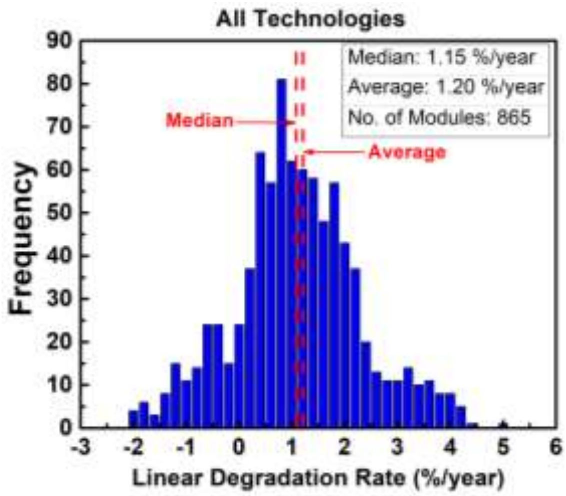

(b)

Fig. 4.1: (a) Histogram of Overall P_{max} Degradation Rate of survey data, and (b) Histogram of Linear P_{max} Degradation Rate.

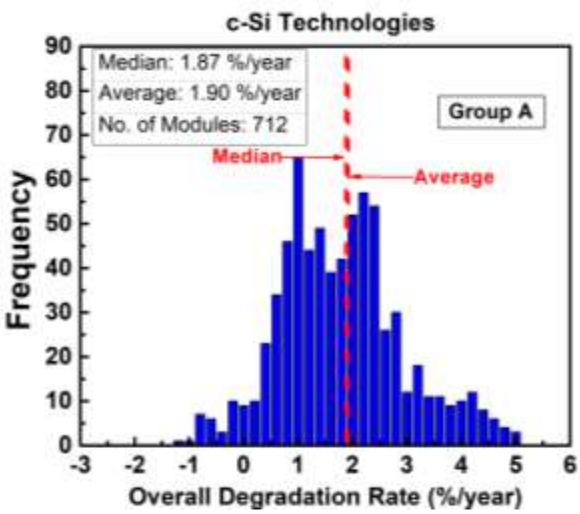

(a)

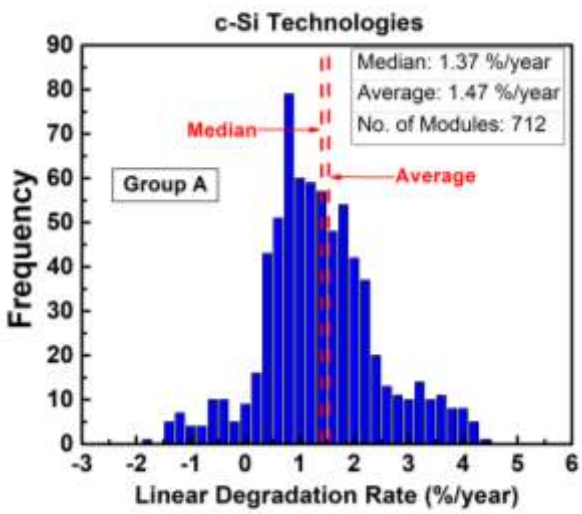

(b)

Fig. 4.2: (a) Histogram of Group A Overall P_{max} Degradation Rate of crystalline silicon modules, and (b) Histogram of Group A Linear P_{max} Degradation Rate of crystalline silicon modules.

Figure 4.3 shows the data for each manufacturer of c-Si modules and c-Si site. To preserve the anonymity of the manufacturers, their names have been coded as A through V (shown along x-axis in the figure) and the different sites of each of these manufacturers have been indicated using numbers (1,2,3, etc.), which is mentioned at the top of the figure. Further, the data is colour coded to represent the different climatic zones. Also, the age of the modules has been shown in the figure, with open symbols indicating young modules (age less than or equal to 5 years) and closed symbols representing old modules (age greater than 5 years). It can be seen that there is a wide variability at most of the sites having crystalline silicon modules, with only a few showing a tight distribution. Further the average degradation rate (indicated by the red horizontal bar) varies a lot from site to site. Hence, the sites with crystalline silicon modules are grouped into 2 categories – Group X (*sites* with average value of Overall Degradation Rate less than equal to 2 %/year) and Group Y (*sites* with average value of Overall Degradation Rate above 2 %/year). For this categorization, we have used the Overall Degradation Rate instead of the Linear Degradation Rate, in order to maintain compatibility with the 2014 survey analysis. Also, the demarcation value of 2 %/year has been chosen to be the same as in 2014 for the same reason.

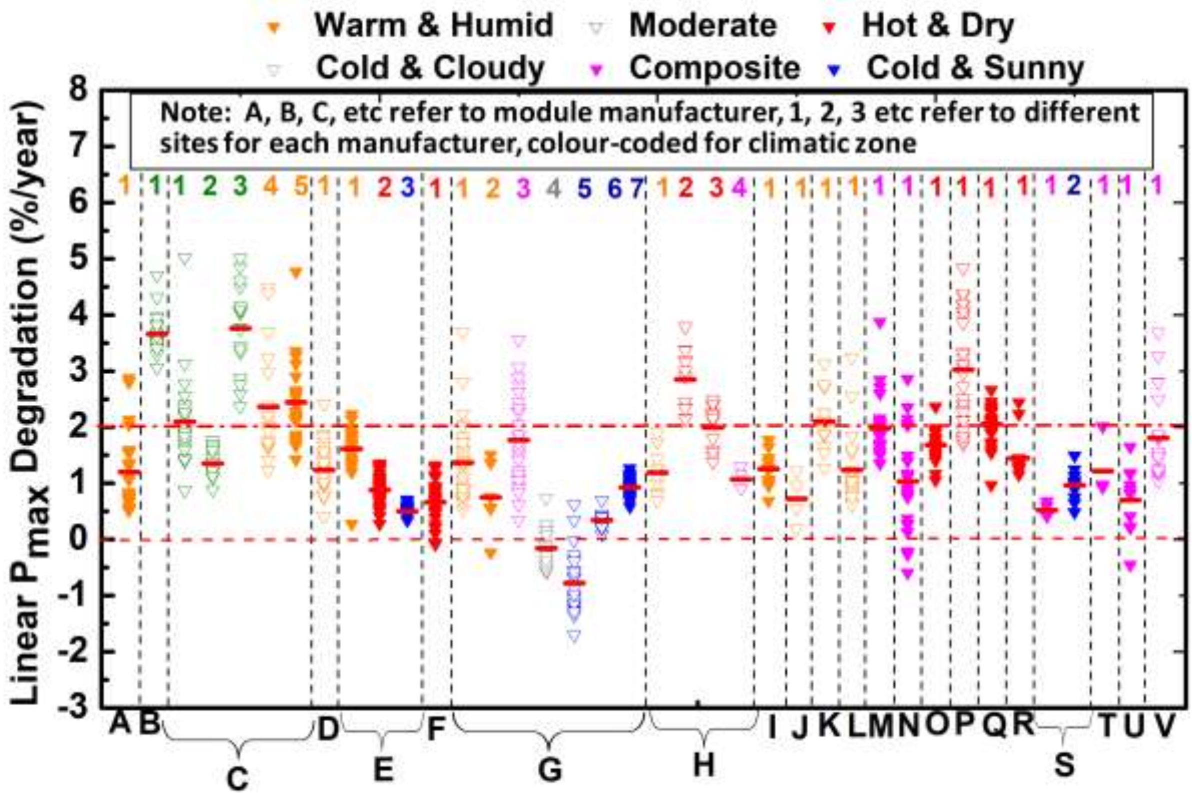

Fig. 4.3: Manufacturer wise and site wise P_{max} degradation rates, incorporating climatic zone data.

The histograms of Overall Power Degradation Rate and Linear Power Degradation Rate, for crystalline silicon modules belonging to Group X and Group Y sites are shown in Fig. 4.4 and 4.5. In Fig. 4.4(a), we can see that the average Overall Degradation Rate is 1.22 %/year, which is a higher value than the value promised in warranty contracts. Also, almost 90% of the modules in Group X have Overall Degradation Rate below 2 %/year. A total of 397 modules fall in Group X sites, which represents 40% of all the surveyed modules, and 45% of the 865 modules taken for detailed electrical analysis after discarding outliers. On the other hand, Fig. 4.4(b) shows the histogram of the Overall Power Degradation Rate for sites in Group Y, where we can see that the average degradation rate is about 2.75 %/year with almost 30% of the modules showing degradation rate above 3 %/year. The histograms of the Linear Degradation Rates shown in Fig. 4.5 also lead us to similar conclusions (though the absolute values have come down due to LID discounting). For the Group X sites, the average Linear Degradation Rate is 0.89 %/year, which, though still high, is acceptable. However, the average degradation rate even after LID discounting for the Group Y sites (comprising 45% of Group A modules) is 2.21 %/year which is a matter of concern. The Group Y sites show poor performance, which may be due to material quality issues, poor manufacturing processes, poor transportation and/or handling, or other causes such as over-rating of modules. Inaccurate rating of modules may result from poorly calibrated measurements in the PV module manufacturing facilities. Furthermore, deliberate over-rating of modules also cannot be ruled out, since some unethical manufacturers may be aware that for some shipments, on-site testing is unlikely. As mentioned before, the climatic zone influence is later checked only for the Group X sites, and not for Group Y sites, in order to avoid any extraneous factors like manufacturing quality and installation procedures from influencing our conclusions. We have done technology and age variation analysis for both Group X as well as Group A modules (Group A is the super set comprising of both Group X and Group Y), in addition to the thin film modules. In subsequent chapters, we shall analyze the Group A modules, or Group-wise modules as deemed appropriate.

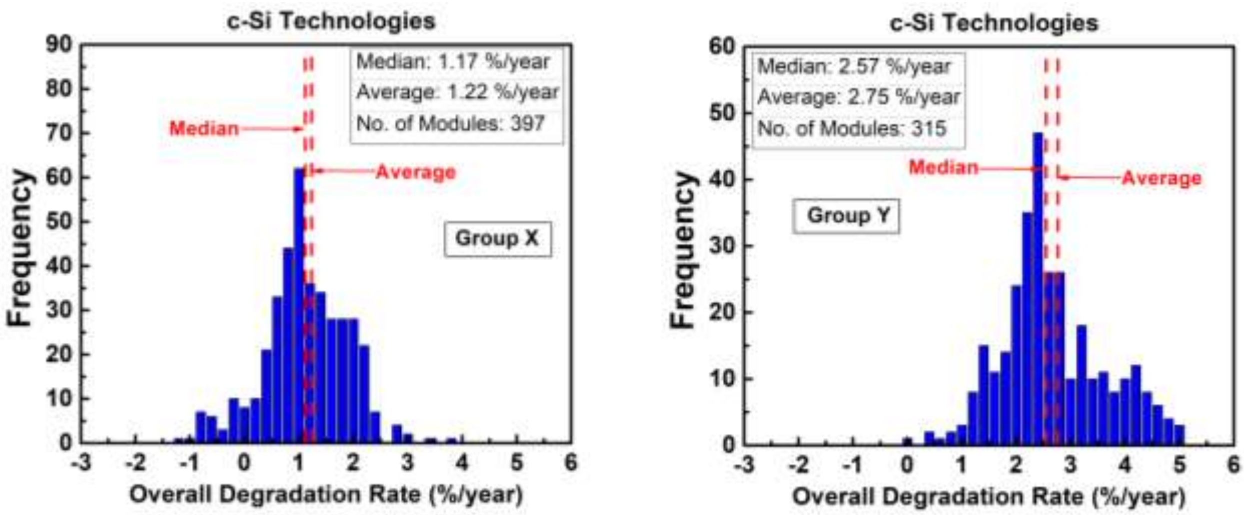

(a) (b)

Fig. 4.4: Histogram of Overall P_{max} Degradation rate of (a) Group X modules and (b) Group Y modules.

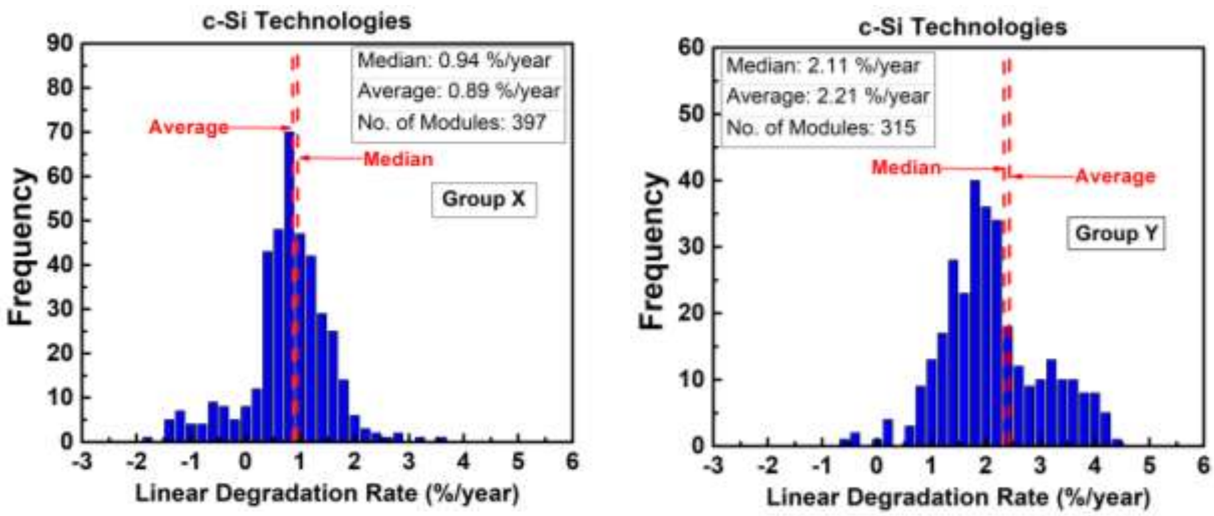

(a) (b)

Fig. 4.5: Histogram of Linear P_{max} Degradation Rate of (a) Group X modules and (b) Group Y modules.

4.3 Climatic Zone Variation

Climate plays a major role in the performance degradation of the PV modules [10], so we shall first discuss the degradation rates of *I-V* parameters with respect to the climatic zone. We will focus on the climatic variation analysis for Group X modules. Bansal and Minke [37] have divided India into six climatic zones. We shall initially present the performance data with respect to the six-zone classification system, and then also show the data as per the internationally accepted Koppen-Geiger classification system. The six climatic zones have been colour coded for the ease of understanding, using orange for Warm & Humid, red for Hot & Dry, green for Composite, magenta for Moderate, blue for Cold & Sunny and grey for Cold & Cloudy. Also, as in the 2014 survey data analysis, we shall present some of the data by clubbing the climatic zones into Hot zone (Warm & Humid, Hot & Dry and Composite zones) and 'Non-Hot' zone (Cold & Sunny, Cold & Cloudy and

Moderate zones) to highlight the effect of hot climates. In addition to the P_{max} degradation rate, we also present the various other *I-V* parameter degradation rates as a function of climate zone.

We have used the mean (average) to represent our data set which is shown by a red horizontal line in all the figures of this chapter. The error due to measurement and STC correction has been shown using green bar on right side and the error due to uncertainty in name plate has been shown using pink bar on left side of the datasets. The red diamond represents the 95% confidence interval. The total number of data points (modules) is indicated inside the square bracket at the top of the respective category. Inverted triangle symbols have been used for data representing Indian climatic zones, diamonds for the international classification and circles for the Hot and Non-Hot zones. Hollow symbols have been used for modules whose age is less than or equal to 5 years and solid symbols for age more than 5 years.

4.3.1 Influence of Climate on P_{max} Degradation

The Linear Power Degradation Rate of the Group X modules with respect to the six-zone climatic classification system has been shown in Fig. 4.6. It is seen that the average Linear Degradation in power is highest in Warm & Humid climate (neglecting the 20 modules from the Moderate climate as the number of samples is too low) and least in Cold climate, which is consistent with the 2014 survey results. It needs to be remembered here, that the power degradation rates mentioned in this plot are arrived at after discounting for LID so the numbers are lower than those reported in 2014 survey results. Also, the 2016 data show lower overall degradation compared with 2014 because of the inclusion of more large sites. The reason for the highest degradation rates in the Warm & Humid zone may be that discoloration, delamination and corrosion in interconnects are accelerated at higher temperatures and humidity. It can be seen that the P_{max} degradation rate variation is tight for the Group X modules, and this lends confidence to our assertion that climatic variations are well captured for Group X. Some of the young modules have a negative Linear Degradation Rate, which may be due to over-discounting of LID, under-rating of the nameplate, and/or error due to STC translation.

The power degradation rate of the Group X modules with respect to Hot and Non-Hot zones is plotted in Fig. 4.7. In this plot, the cumulative probability distribution is also shown so that the reader can understand the nature of the distribution. In the cumulative plot, the points on the 50% probability line represent the median values. We can see that modules deployed in the Hot zones are degrading at a faster rate than the modules in the Non-Hot zones. Looking at the cumulative plot, one can say that the young modules in Hot zone have the highest degradation, followed by the Old modules in the Hot and Non-Hot zones, and the least degradation is seen in the young modules in Non-hot zone. Figure 4.8 shows the Linear Power Degradation Rate of the Group X modules with respect to Koppen-Geiger climate classification system. We can see that modules in Tropical climates followed by Arid hot climate show high value of Linear P_{max} Degradation Rate which again confirms that the modules in the hot climates are degrading at a faster rate. In our survey, only thin film modules were inspected in the Arid desert climate so the graph shows no samples for this zone.

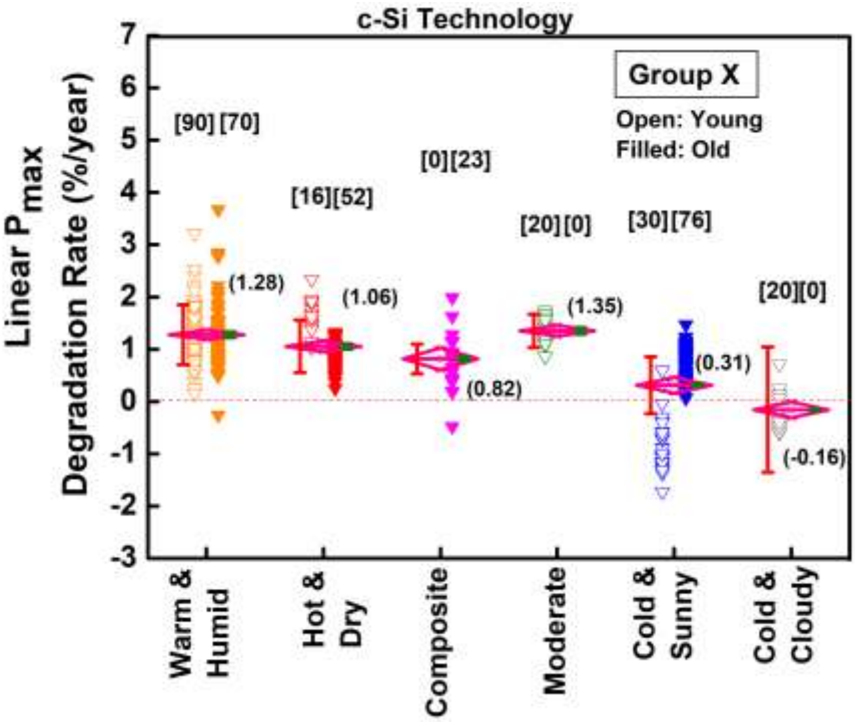

Fig. 4.6: Comparison of Linear P_{max} Degradation Rate with respect to six-zone classification system for Group X modules.

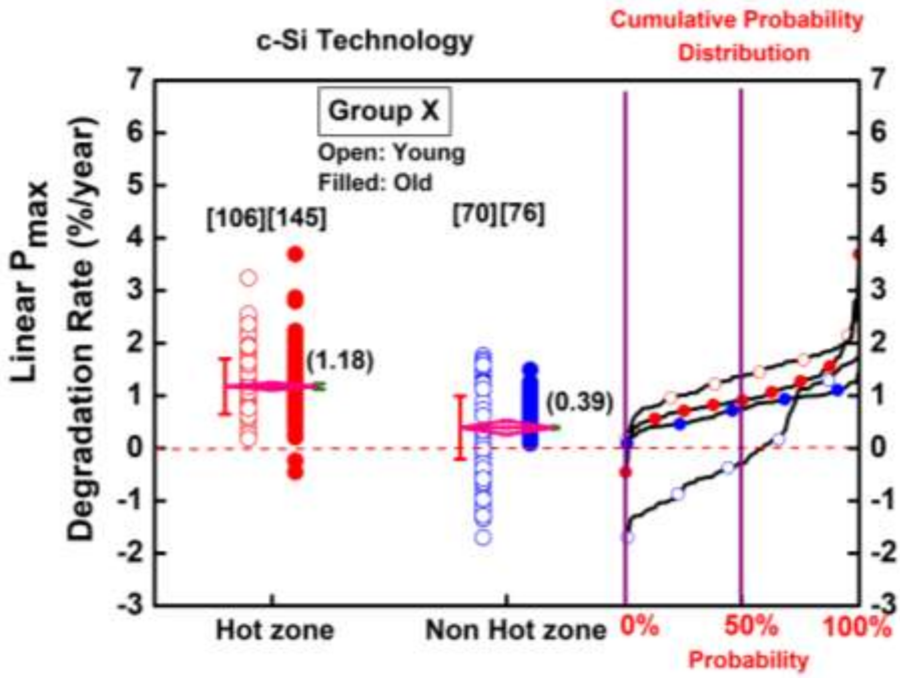

Fig. 4.7: Comparison of Linear P_{max} Degradation Rate with respect to Hot and Non-Hot zone for Group X modules.

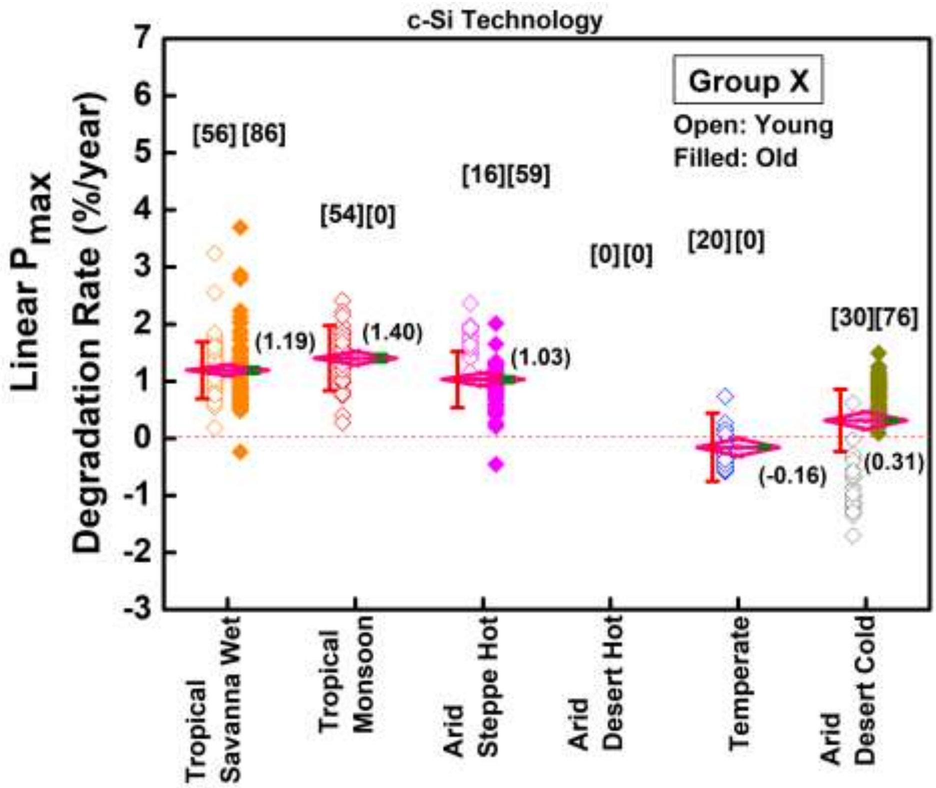

Fig. 4.8: Comparison of Linear P_{max} Degradation Rate with respect to Koppen-Geiger climate classification for Group X modules.

4.3.2 Influence of Climate on *I-V* Parameters (I_{sc}, V_{oc} and *FF*)

The climatic-zone-wise distribution of Linear Degradation Rates for the various *I-V* parameters (P_{max}, I_{sc}, V_{oc} and *FF*) for Group X modules is shown in Fig. 4.9. For most climate zones *FF* degradation is the largest contributor to P_{max} degradation, though for the Hot & Dry and Composite zones, the I_{sc} degradation rate is also significant. The reason for the high *FF* degradation is probably due to cell to cell mismatch in the module caused by cracks as evident from the snail tracks and EL images (explained in more detail in Chapters 6 and 7 respectively). The higher I_{sc} degradation is probably due to the high temperature in these climates (especially Hot & Dry), leading to increased encapsulant browning which reduces the light transmission to the solar cells (refer also to Chapter 6 where I_{sc} degradation and encapsulant browning are correlated).

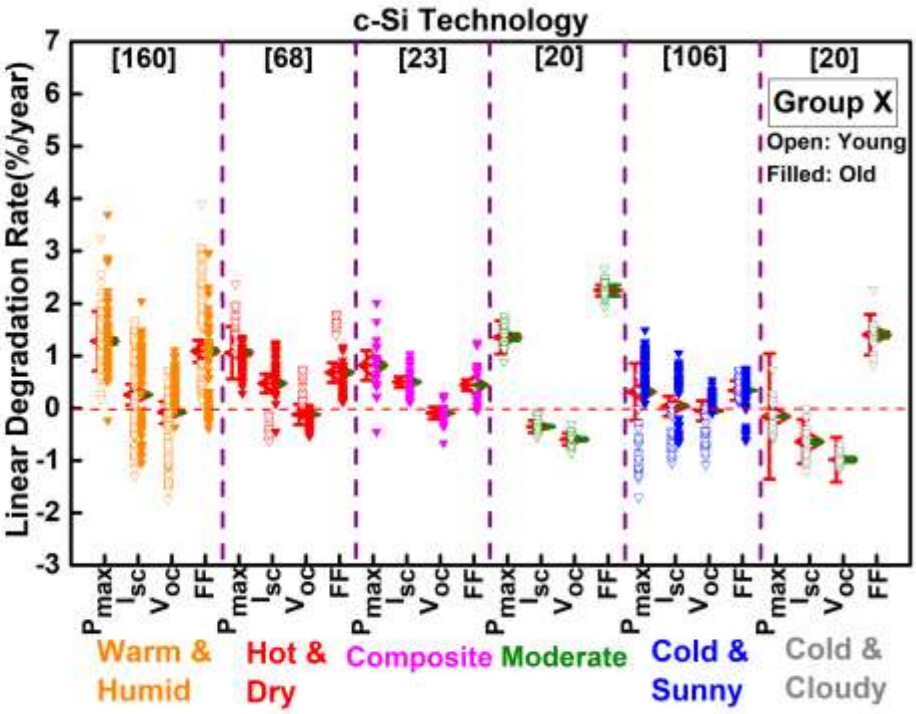

Fig. 4.9: *I-V* parameter degradation distribution with respect to six-zone classification system for Group X modules.

4.4 Technology Based Variation

4.4.1 Influence of Technology on P_{max} Degradation

Figure 4.10 shows the Linear P_{max} Degradation Rate (%/year) for Group X c-Si and thin film modules. From the figure we can see that multi-crystalline silicon modules are degrading at a faster rate than mono-crystalline silicon modules. Among the thin-film modules, CdTe modules are degrading the least. Both CdTe and a-Si modules are degrading at a much lower rate as compared to the crystalline silicon modules. It should be kept in mind that the CdTe and a-Si modules are usually under-rated (as a standard practice) to take care of the stabilization effects. Further, these modules are usually from internationally well-known manufacturers who have strict control over their production (and sometimes installation) quality. On the other hand, there are many c-Si module manufacturers, some of whom are new to module manufacturing. Hence, it is not unreasonable to find that the average degradation rates of the thin film modules are lower than that of the crystalline silicon modules. There are insufficient samples for CIGS and HIT, so we will not comment on these technologies. Figure 4.11 shows the Linear P_{max} Degradation per year for Group A c-Si and thin film modules. It may be noted here that we have not used colours in these plots since the technologies are not differentiated by climatic zone.

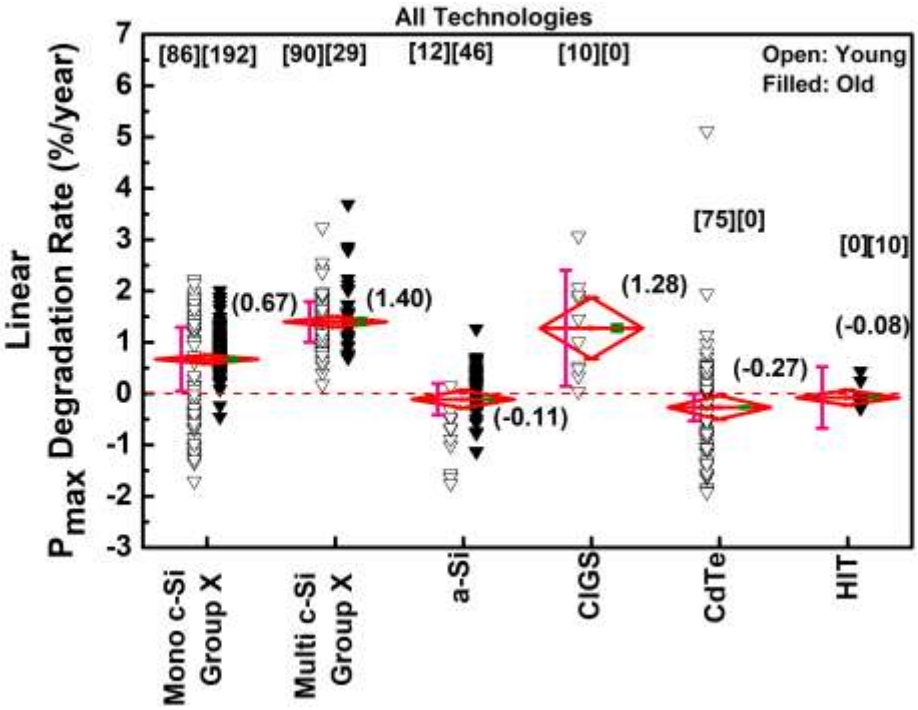

Fig. 4.10: Linear P_{max} Degradation per year for modules of different technologies (for c-Si, only Group X modules are considered).

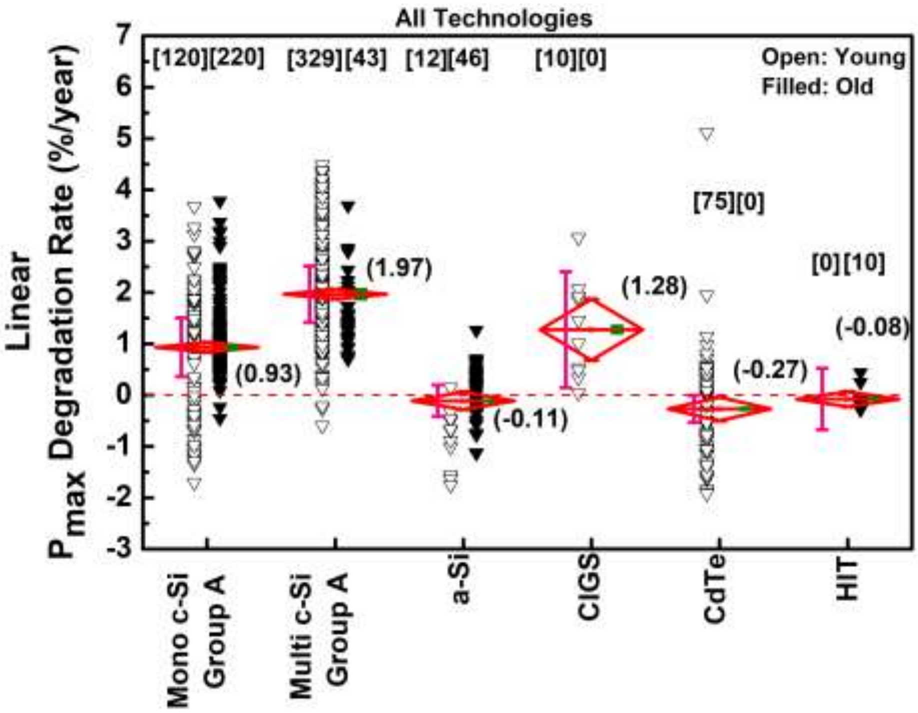

Fig. 4.11: Linear P_{max} Degradation per year for modules of different technologies (all (Group A) c-Si modules are considered).

4.4.2 Influence of Technology on *I-V* Parameters (I_{sc}, V_{oc} & *FF*)

The degradation in the power output is caused by degradation in one or more of the electrical parameters. Figure 4.12 shows the Linear P_{max}, I_{sc}, V_{oc} and *FF* degradation rates for Group X c-Si and thin-film category modules. From the figure it is quite evident that for crystalline silicon modules P_{max} degradation is mainly due to degradation in *FF*, followed by I_{sc}. On the other hand, for the thin film modules, P_{max} degradation is mostly associated with the degradation in V_{oc} followed by the *FF*. Figure 4.13 shows the Linear P_{max}, I_{sc}, V_{oc} and *FF* degradation for Group A c-Si and thin-film modules, which yields similar conclusions.

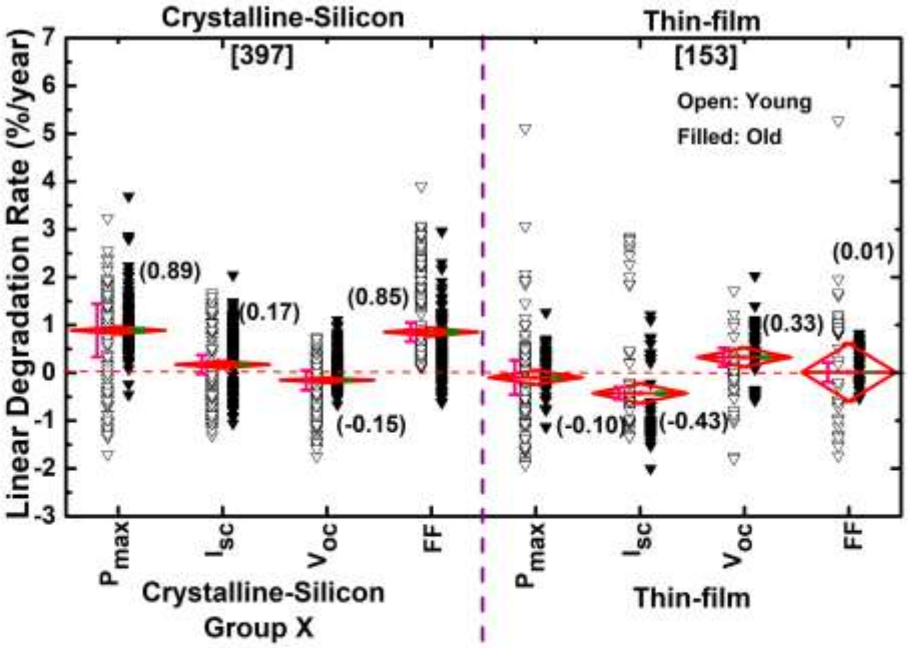

Fig. 4.12: Linear P_{max}, I_{sc}, V_{oc} and *FF* degradation for Group X c-Si and thin-film modules.

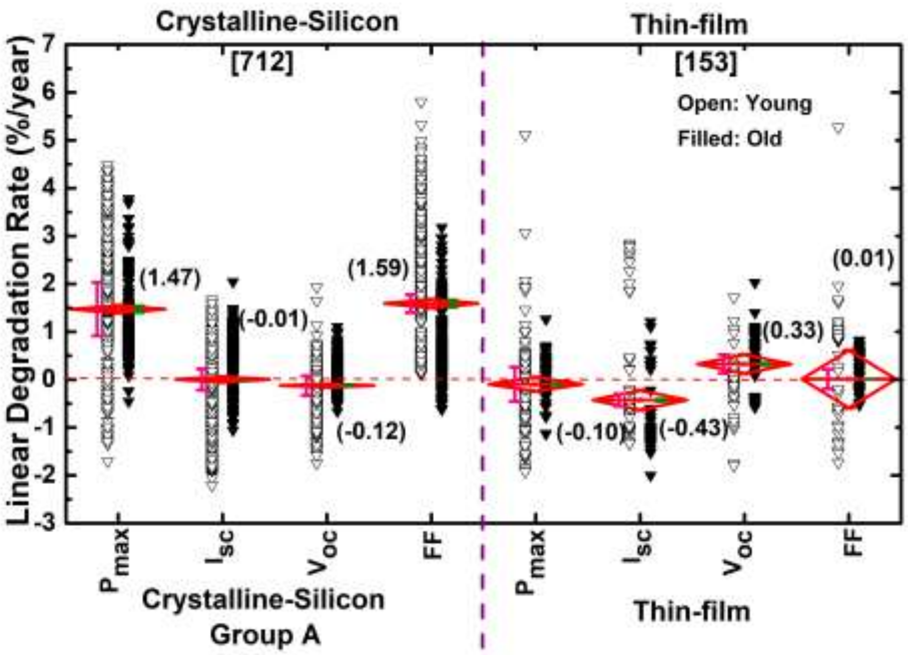

Fig. 4.13: Linear P_{max}, I_{sc}, V_{oc} and *FF* Degradation for Group A c-Si and thin-film modules.

4.5 Age Based Variation

We have separated out the modules into young (installed in/after 2011, so age ≤ 5 years) and old (installed before 2011, so age > 5 years) categories in order to ascertain the effect of age on the P_{max} degradation rate (% per year). We have confined this analysis of age variation only to crystalline silicon modules, as we had very few thin film modules in the old age category. Figure 4.14 shows the histograms of Linear P_{max} Degradation of young and old c-Si modules in Group A. We can see that the average Linear Degradation Rate of the young modules is much greater (1.68 %/year) than that of the old modules (1.11 %/year), and also the spread of the degradation rates is much wider in young modules as compared to old modules.

Figure 4.15 shows the effect of module age on the degradation of the *I-V* parameters of the crystalline silicon modules only from Group X sites. From the figure we can say that these young modules from Group X sites are degrading marginally *slower* than the old modules. Also, it is seen from the figure that the degradation in power for young modules is entirely due to degradation in fill factor (*FF*). However, for the old modules, the degradation in P_{max} is due to degradation in both I_{sc} and *FF*. This seems to point to the fact that old modules degrade mainly due to encapsulant browning (which reduces I_{sc}), cell cracks and corrosion (both of which reduce the *FF*), whereas young modules degrade due to decrease in *FF*, possibly caused by cracks generated during installation (this is discussed in more detail in Chapter 7).

Figure 4.16 shows the effect of age on the degradation of the *I-V* parameters of Group Y crystalline silicon modules. Here, in clear contrast to the observation for Group X modules, the degradation in P_{max} is higher for young modules. This may be indicative of over-rating, if we speculate that this unethical behavior is more prevalent in recent times. Also, inaccurate rating of modules can be the result of poorly calibrated measurements in the module manufacturing facilities. Again we can notice that degradation in power for young modules is mainly due to fill factor (*FF*), whereas for old modules, degradation is due to both I_{sc} and *FF*. The *FF* degradation can be ascribed to cracks caused by poor installation. The *FF* degradation rate is much higher in Group Y as compared to Group X young modules, which indicates that the problem of cracks is more severe in Group Y modules as compared to Group X modules (this is confirmed by EL analysis as described in Chapter 7).

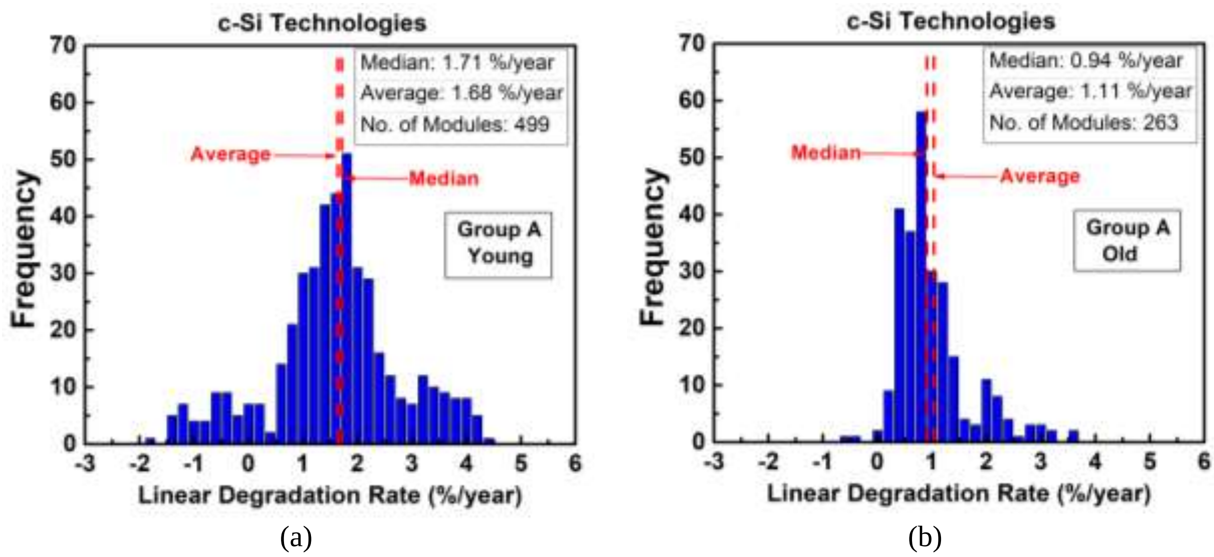

Fig. 4.14: Histogram of Linear Degradation Rates of c-Si modules in Group A, for (a) young modules, and (b) old modules.

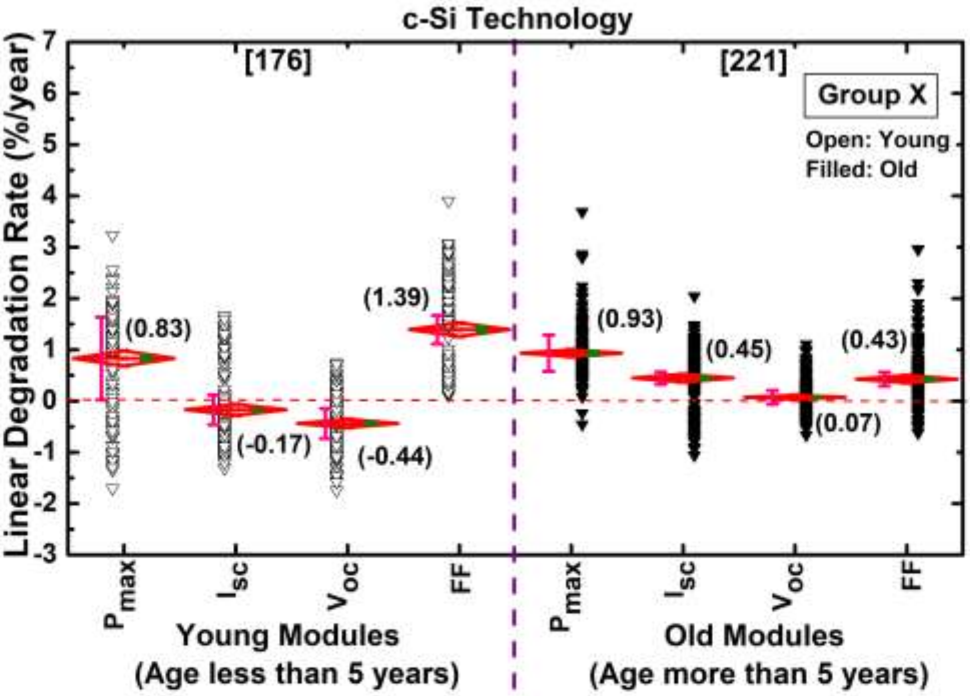

Fig. 4.15: Linear P_{max}, I_{sc}, V_{oc} and *FF* Degradation for young and old crystalline silicon modules in Group X.

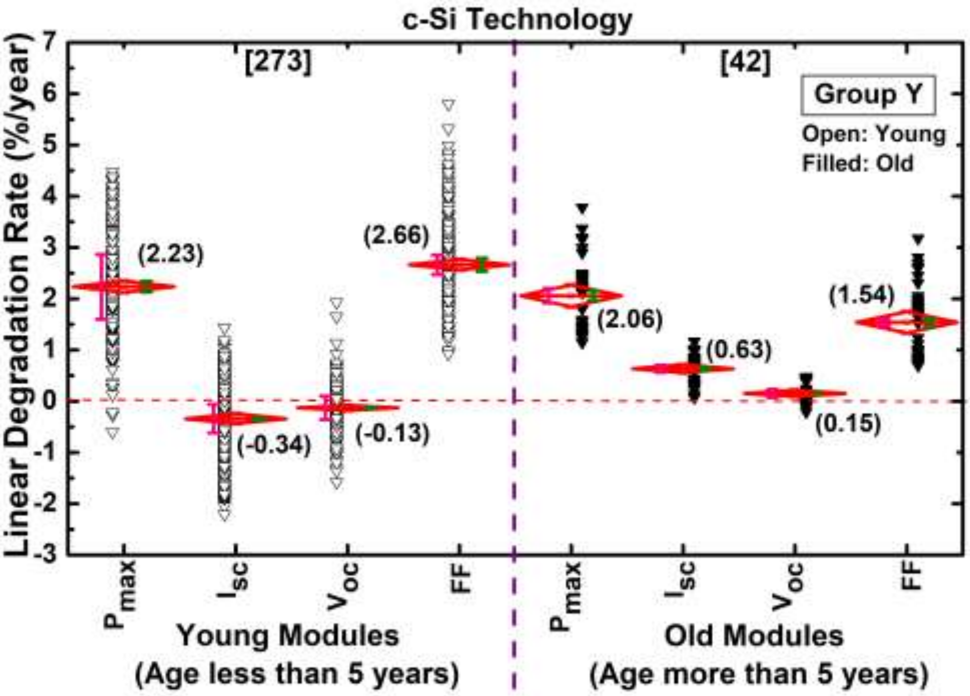

Fig. 4.16: Linear P_{max}, I_{sc}, V_{oc} and *FF* Degradation for young and old crystalline silicon modules in Group Y.

4.6 System Size and Installation Based Variation

We have separated out the sites surveyed into two categories based on the size of the installation – small/medium size (less than or equal to 100 kW) and large size (greater than 100 kW capacity). In order to maintain consistency with the 2014 survey analysis, we have chosen 100 kW as the demarcation. The reason for choosing 100 kW as a demarcation can also be justified from Fig 4.17, which shows the average Linear P_{max} Degradation Rate for different Group A sites with respect to respective system size. Also, we can see from Fig. 4.17 that the site-wise average Linear P_{max} Degradation Rate is concentrated on the either side of 100 kW line.

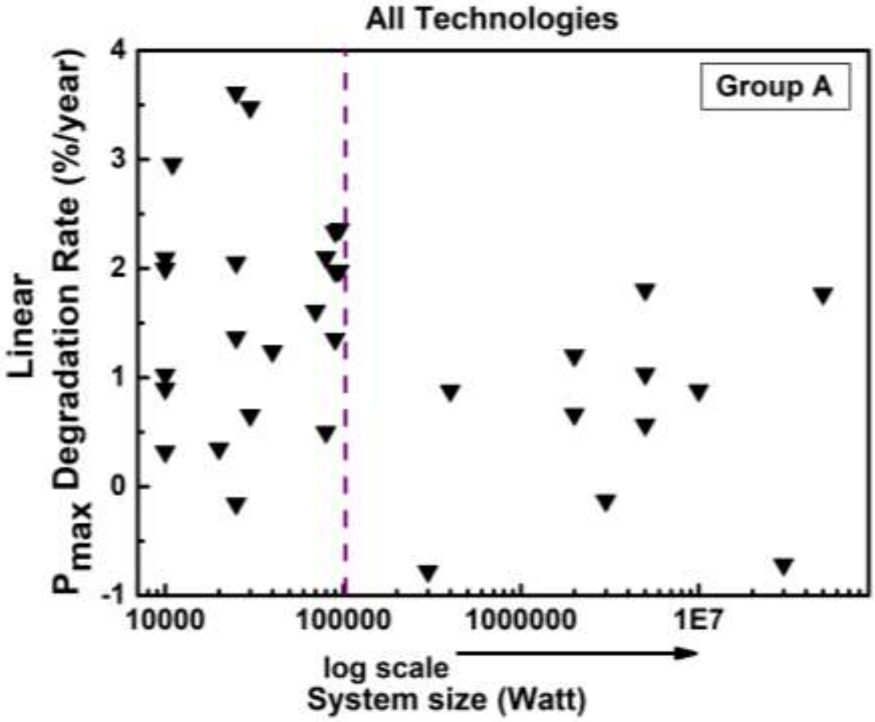

Fig. 4.17: Average Linear P_{max} Degradation rate of Group A sites with respect to system size.

Figure 4.18 shows the Linear P_{max} Degradation Rate for these categories, for Group A, while Fig. 4.19 shows the corresponding data for Group X only. We can clearly see from the figures that modules installed in large PV systems (including MW scale power plants) are degrading at a much lower rate than the modules in the smaller installations. The cumulative probability plots given on the right side of the figures show that the data distributions are different from each other (so the differences are statistically significant). This important result informs us that large commercial and utility scale installations (even in Group A) are performing better (0.99 %/year) than smaller installations, but also flags a warning about poor performance of small and medium sites (1.68 %/year). However, if we only look at installations in the Hot zone, the large sites in Group A have an average degradation rate of 1.28 %/year (refer Fig. 4.20) which is quite high. Even for the Group X modules, the average degradation rate for large installations in Hot zones is high at 1.12 %/year as shown in Fig. 4.21. Segregating the sites into young and old, as done in Figs. 4.22 and 4.23, clearly shows that the young large power plants are degrading at a significantly higher rate than the old power plants in the Hot zone. Since most of the large installations are going to come in the Hot zone, this data indicates that large power plant installers also need to be cautious about the quality of the panels and installation procedures. The difference we see between young and old modules appears to indicate that such caution has not been adequately exercised in the newer sites.

We have also tried to capture the effect of roof-mounted and ground-mounted installation on the Linear P_{max} Degradation Rate. (Note that most 'roof-mounted' are actually rack mounted installations deployed on flat roofs.) Figure 4.24 shows the Linear P_{max} Degradation Rate for roof and ground mounted modules for Group A sites. From the figure it is seen that ground-mounted modules are degrading at a lower rate than the roof-mounted panels for the small size category (we do not have any roof-mounted large installation in our survey). This is not unexpected, and may be due to the module quality and installation related issues in the smaller rooftop sites (our data in Chapter 7 rules out the conjecture that roof-rack-mounted sites run hotter). Figure 4.25 shows the corresponding plot for Group X modules, and we can see a similar trend.

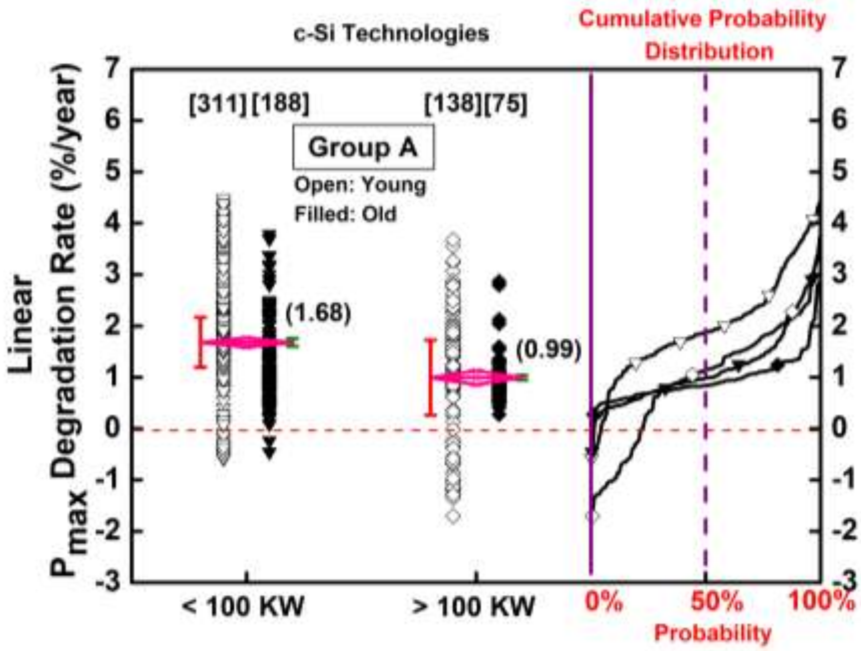

Fig. 4.18: Effect of system size on Linear P_{max} Degradation for Group A modules. .

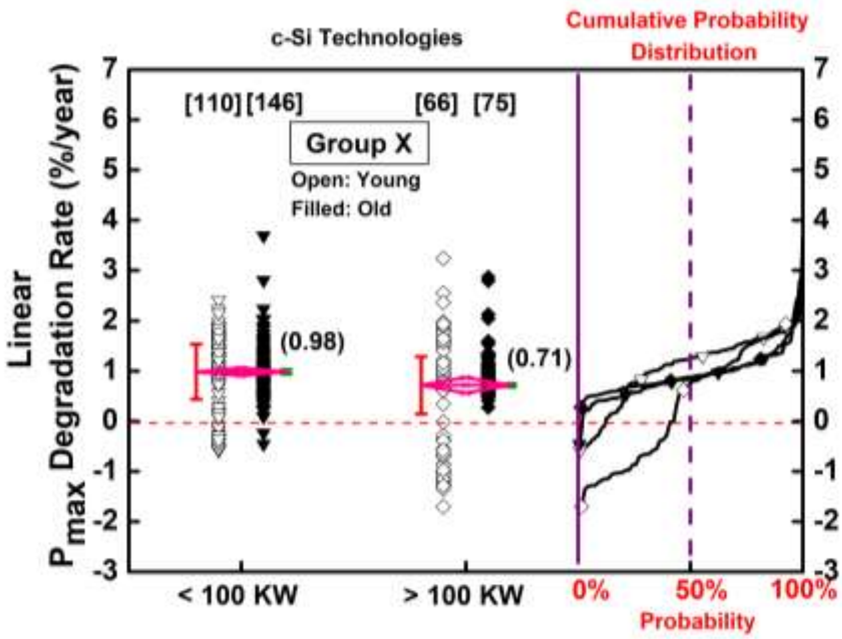

Fig. 4.19: Effect of system size on Linear P_{max} Degradation for Group X modules.

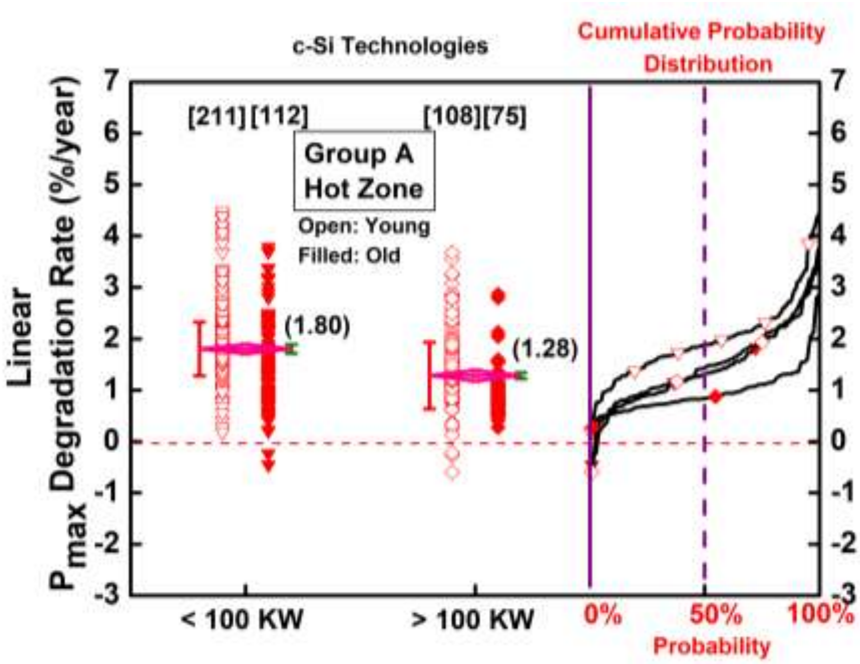

Fig. 4.20: Effect of system size on Linear P_{max} Degradation for Group A modules in Hot zones.

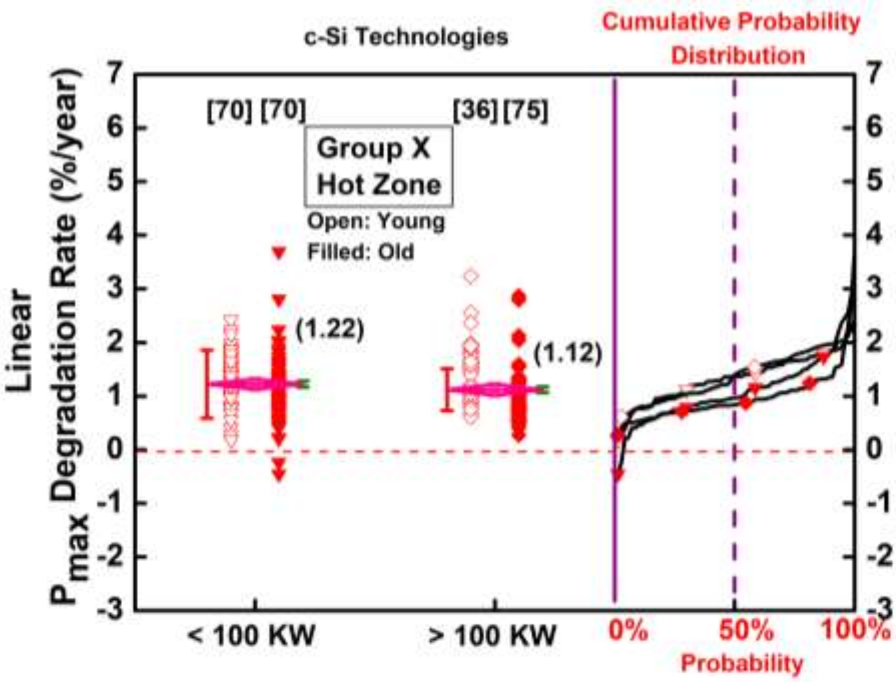

Fig. 4.21: Effect of system size on Linear P_{max} Degradation for Group X modules in Hot zone.

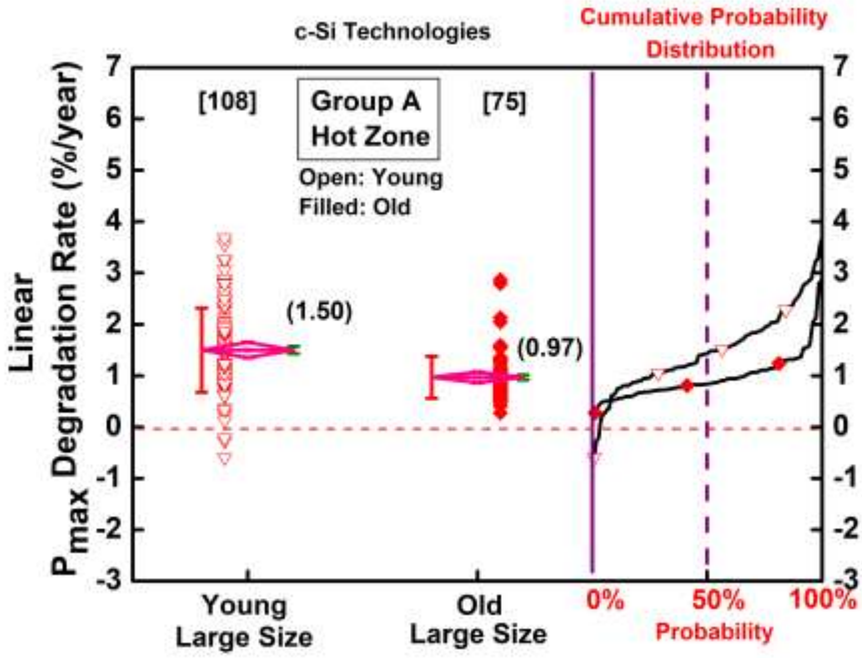

Fig. 4.22: Linear P_{max} Degradation for young and old crystalline silicon modules in Group A for Large size system in Hot zone.

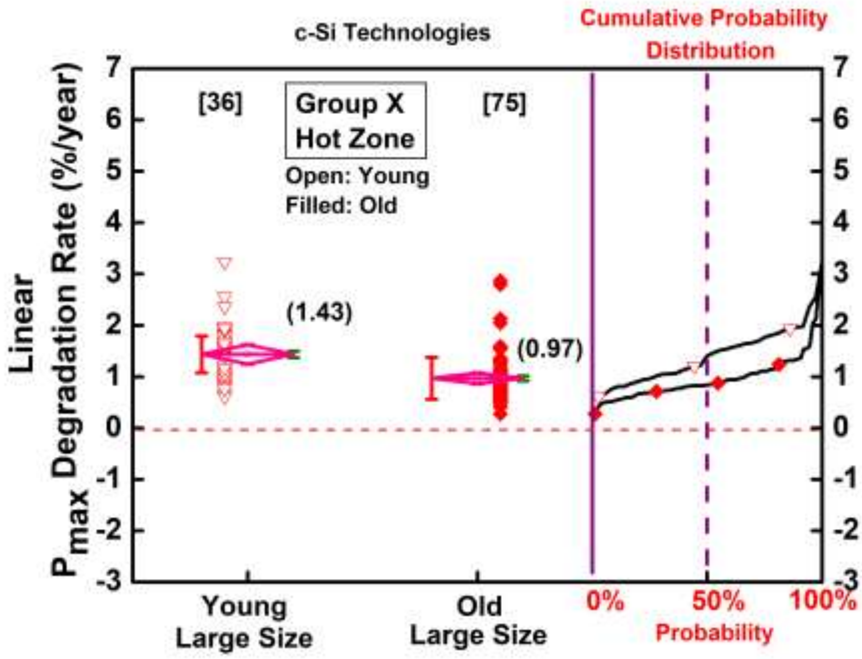

Fig. 4.23: Linear P_{max} Degradation for young and old crystalline silicon modules in Group X for Large size system in Hot zone.

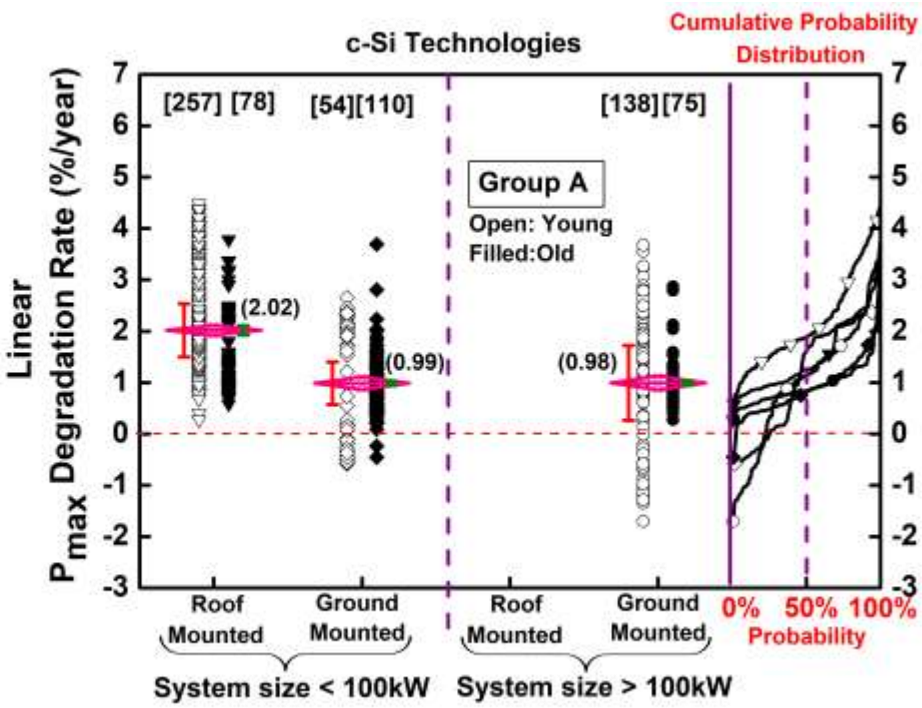

Fig. 4.24: Effect of installation type on Linear P_{max} Degradation for Group A modules.

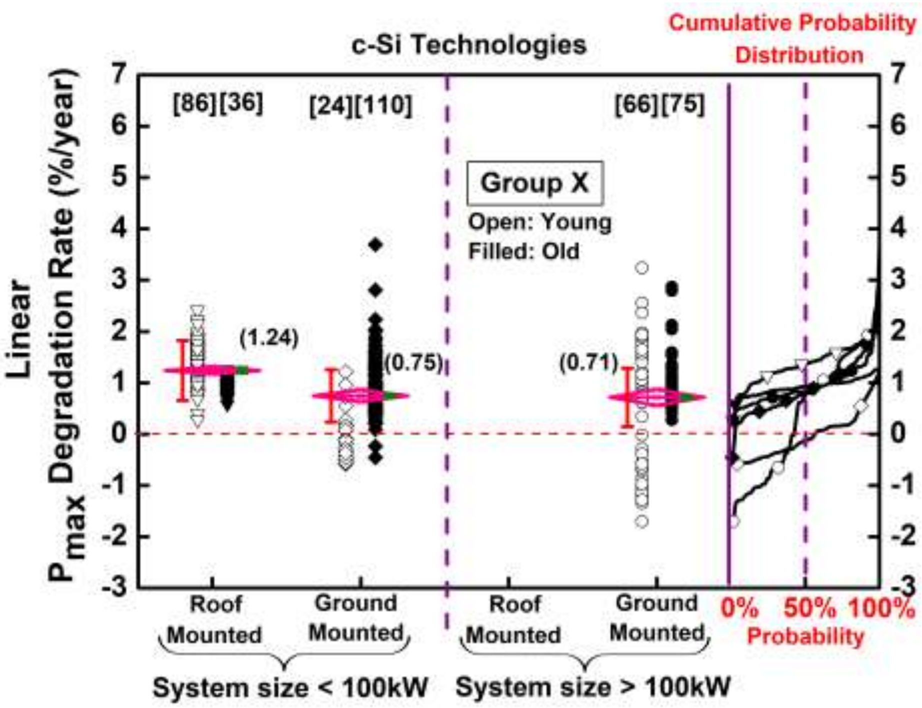

Fig. 4.25: Effect of installation type on Linear P_{max} Degradation for Group X modules.

From the foregoing analysis, the following overall picture emerges for c-Si modules. Large installations, especially the Group X sites, are performing reasonably well, but if we look at a subset of these in the Hot zones, we see a relatively high degradation rate. Further, the newer sites perform worse than the older sites. These conclusions indicate fairly clearly that (a) hot climates accelerate degradation and (b) adequate care has not been taken in module quality and/or installation in recent years.

4.7 Study of Potential Induced Degradation

The high degradation rates observed in the Group Y sites raises concern about the possibility of potential induced degradation (PID) at these sites. PID has recently been one of the major concerns of PV power plant owners since the power output of PID affected modules drops down drastically within a short period of field exposure [39]. PID always affects the modules that operate at a negative voltage with respect to ground (for modules made from p-type wafers), and this means that a distinct signature of PID is the higher degradation at the negative end of the string, which gradually reduces towards the positive end [39]. During the survey, the position of the modules in the string with respect to the negative terminal of the inverter was noted down in order to ascertain whether the module degradation rate has any correlation to the position in the string. Fig. 4.26 shows the Linear P_{max} Degradation Rates with respect to the position of the modules in the string for some of the PV power plant sites surveyed. The data does not show much evidence of PID in the modules inspected during the survey. However, at one of the sites, EL images of some of the modules have shown degradation of the cells at the edges of the modules (which is a signature of PID) and these modules have degradation rate greater than 5.12 %/year so these modules are discussed in Appendix G "Analysis of Outliers".

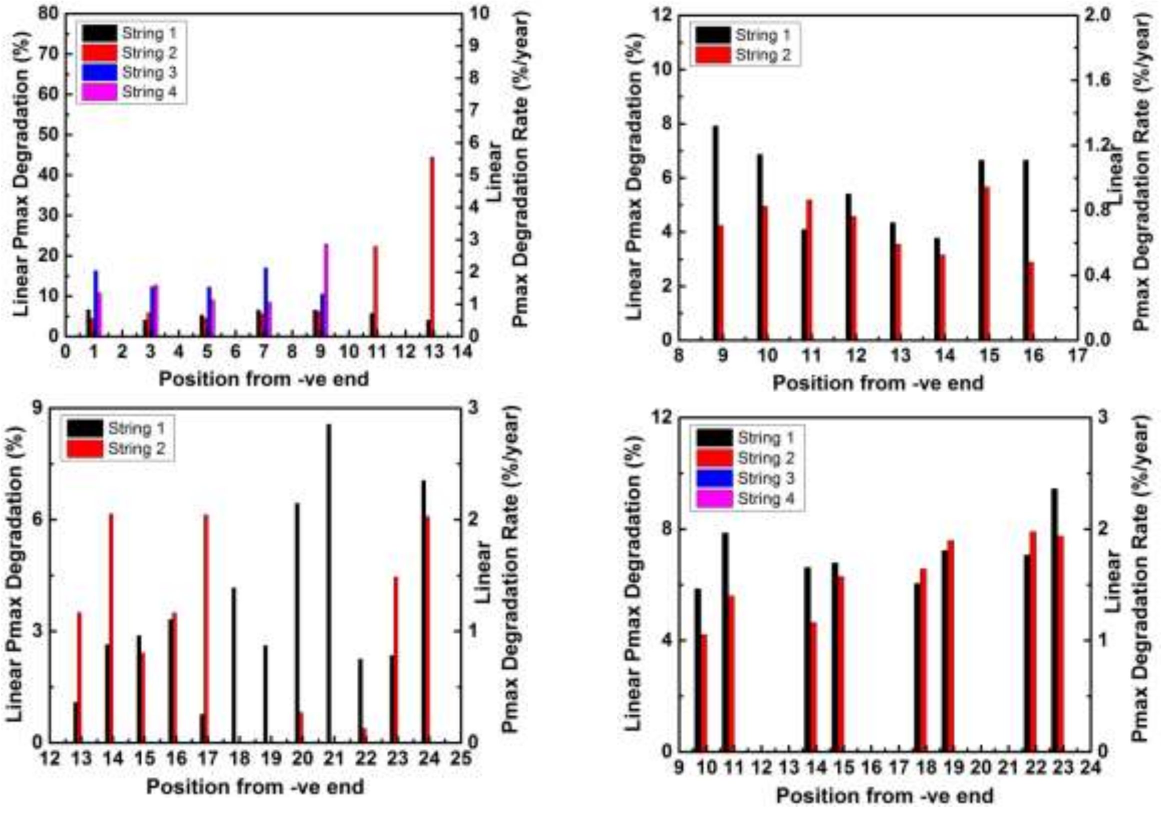

Fig. 4.26: Linear P_{max} Degradation Rates with respect to the position of the modules in the string for some of the inspected PV power plants.

4.8 Statistical Analysis

4.8.1 Nature of Degradation Rate Distribution

The histogram of Linear P_{max} Degradation for the crystalline silicon modules does not follow any standard distribution. However, by virtue of the Central Limit Theorem, the asymptotic distribution of the average Linear Degradation Rate per site turns out to be a normal distribution. Also, by virtue of extreme value theory, the limiting distribution of the maximum Linear Degradation Rate per site is found to be the Gumbel distribution (shown in Fig. 4.27), with estimated value of the location parameter = 2.043 and scale parameter = 1.218. Based on this information it is possible to compute the probability of various events of interest and use properties of the underlying probability distribution, albeit approximate, to draw inferences about physical characteristics of the phenomenon under consideration. For example, the probability of maximum Linear Degradation Rate of any module at a particular site exceeding 1 %/year is calculated to be 0.905, while the probability exceeding 2 %/year is 0.645. It should be noted that this is the *maximum* rate at the site, and most of the modules will degrade at a lower rate.

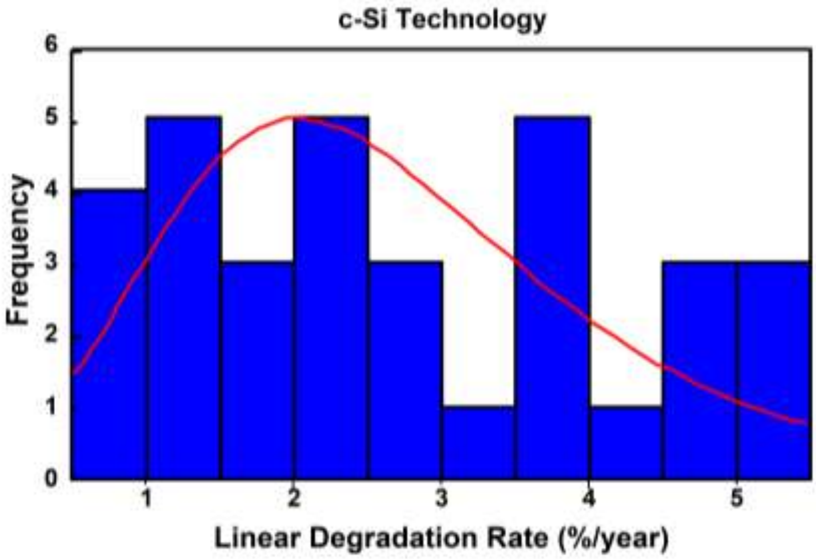

Fig. 4.27: Histogram for maximum Linear P_{max} Degradation Rates for a module at any site with Gumbel curve over histogram.

4.8.2 Determination of Statistical Significance

Since there are multiple factors at any site that can influence the module degradation rates, it is important to check the statistical significance of the results obtained from the analyses in the preceding sections. For this purpose, statistical regression has been performed using the logistic regression model as explained in Section 3.6.This is considered as Model I (refer to Eq. 4.1).

$$\log \frac{\pi(x)}{1-\pi(x)} = \alpha + \beta_1(\text{climate}_2) + \beta_2(\text{climate}_3) + \beta_3(\text{climate}_4) + \beta_4(\text{climate}_5) + \beta_5(\text{climate}_6) + \beta_6(\text{age}) + \beta_7(\text{mounting}) + \beta_8(\text{system size}) \quad \ldots (4.1)$$

where,
climate_2 = Hot & Dry
climate_3 = Moderate
climate_4 = Composite
climate_5 = Cold & Sunny
climate_6 = Cold & Cloudy
mounting = Ground mounted
system size = Large systems

All six climatic zones have been initially considered for this analysis, but the results have shown that some of the climatic zones are not statistically significant as the p-value is greater than 0.05 (refer to Table 4.1).

Table 4.1: Parameter Estimates and p-values for two climatic zone model

Covariates	Estimates	p-value
Intercept	2.71410	3.22e-15
Climate Category 2 (Hot & Dry)	0.43965	0.07953
Climate Category 3 (Moderate)	1.12257	0.15015
Climate Category 4 (Composite)	0.76486	0.00706
Climate Category 5 (Cold &Cloudy)	-16.52064	0.97544
Climate Category 6 (Cold & Sunny)	-2.98704	1.05e-12
Age	-0.03544	0.11454
Mounting (=1 for ground mounted)	-2.61777	< 2e-16
System size (=1 for large system size)	-0.07216	0.77676

Hence, the six-climate model is better replaced with a two-climate (Hot and Non-Hot) model. Such a model has been developed, with the following factors as explanatory variables:

a) Climatic (a categorical variable with two categories – 'Hot' and 'Non-Hot')
b) Age (a continuous variable)
c) Mounting type (a categorical variable with two-rooftop and ground mounting- categories)
d) System size (a categorical variable with two-large and small- categories)

The two-climate model (referred to as Model II) has the following formulation:

$$\log\frac{\pi(\underset{\sim}{x})}{1-\pi(\underset{\sim}{x})} = \alpha + \beta_1(\text{age}) + \beta_2(\text{mounting}) + \beta_3(\text{system size}) + \beta_4(\text{zone}) \qquad \ldots (4.2)$$

where,
climate_1 (climate_2) = Hot (Non-Hot)
mounting_1 (mounting_2) = rooftop (ground)
system size_1 (system size_2)= large (small)
and $\underset{\sim}{x}$ is a four-dimensional column vector with its elements being one level of each of the categorical explanatory variables (climate, mounting, system size) and a continuous variable, age.

Table 4.2 shows the parameter estimates obtained after fitting the above model to the degradation rate data. As the system size explanatory variable turns out to be statistically insignificant (p-value = 0.665 > 0.05), Model II is refitted by dropping this explanatory variable and the resulting model is denoted as Model III. The information about its parameter estimates is summarized in Table 4.3. It is evident from the information in this table that each of the explanatory variables mentioned below are statistically significant (p-value < 0.05) and affects the probability of P_{max} degradation rates for the module being greater than 1 %/year.

a) Climatic zone (a categorical variable with two categories – Hot and Non-Hot)
b) Age (a continuous variable)
c) Mounting type (a categorical variable with two-rooftop and ground mounting- categories)

Table 4.2: Parameter Estimates and p-values for two-climatic zone model (Model II)

Covariates	Estimates of Parameters	p-value
Intercept	1.88387	2.39e-12
Age	-0.10685	3.32e-09
Mounting (ground mounted)	-3.42402	< 2e-16
System size (large system size)	-0.10387	0.665
Zone	2.41870	1.04e-15

Table 4.3: Parameter Estimates and p-values for revised two-climatic zone model (Model III)

Covariates	Estimates of Parameters	p-value
Intercept	1.86730	1.86e-12
Age	-0.10440	1.10e-09
Mounting (ground mounted)	-3.44135	< 2e-16
Zone	2.38193	< 2e-16

The parameter estimate is negative for age, which means that the older modules have a lower degradation rate. Similarly, in view of the negative parameter estimate for mounting type, modules in the ground mounted systems have lower probability of degradation rate exceeding 1 %/year as compared to modules in rooftop systems. The sign of the parameters estimate corresponding to zone variables is positive implying that the modules in Hot zone area have higher degradation rates than those in Non-Hot zones.

To understand the impact of type of mounting (ground versus rooftop), the above model is re-formulated separately for the roof mounted and ground mounted systems. Table 4.4 shows the odds and probabilities for power degradation greater than 1 %/year for modules installed in different mounting configurations and climatic zones. The odds of module P_{max} degradation rate greater than 1 %/year are lowest for ground mounted systems in Non-Hot zone, and highest for roof mounted systems in Hot zone. In the Hot zone, the chances of power degradation greater than 1 %/year are significantly higher in roof mounted modules than in ground mounted modules.

Table 4.4: Effect of mounting type and climatic zone

Covariates	Odds for age=1 $[\pi(x)/(1-\pi(x))]$	Probability for age=1 $[\pi(x)]$	Odds for age=5 $[\pi(x)/(1-\pi(x))]$	Probability for age=5 $[\pi(x)]$
GM* systems in Hot Zone	2.02080	0.66896	1.33097	0.57099
GM* systems in Non-Hot Zone	0.18666	0.15730	0.12294	0.10948
RM* systems in Hot Zone	63.10767	0.98440	41.56514	0.97650
RM* systems in Non-Hot Zone	5.82936	0.85357	3.83944	0.79336
* GM=Ground Mounted, RM=Roof Mounted				

4.9 Three Point Data Analysis for Repeat Sites

Figure 4.28 shows the performance of the modules installed at sites which were repeated in 2014 and 2016 survey. Each plot (a) to (j) represents a site which was repeatedly measured in 2014 and 2016 surveys. The average power (after STC translation) of the modules inspected at the site is shown along with the translation/measurement error (green bar). In most cases, the average power is monotonically decreasing except for one site (refer Fig. 4.28(j)). The slope of the red line joining the 3 points on the plots represents the degradation rate. In most cases, this slope is larger between the nameplate and the 2014 measurement as compared to the slope between 2014 and 2016 measurements, which indicate the influence of the Light Induced Degradation in the initial years of field exposure.

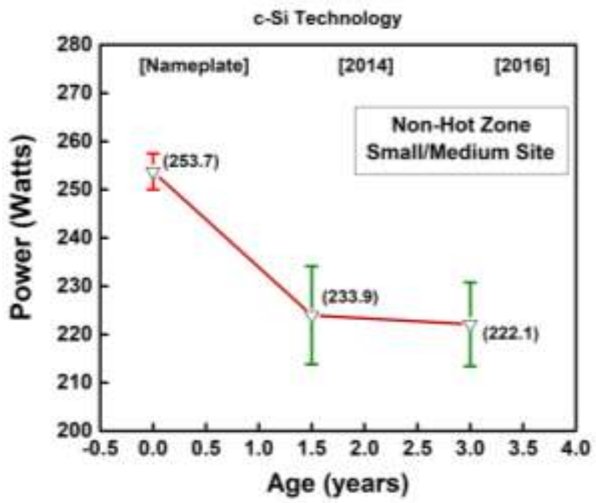

(a)

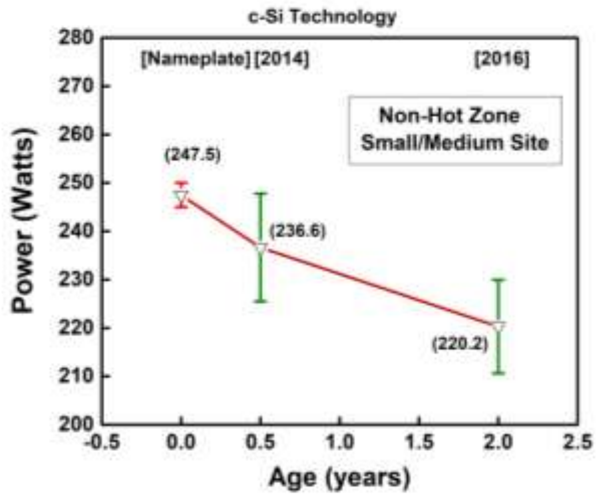

(b)

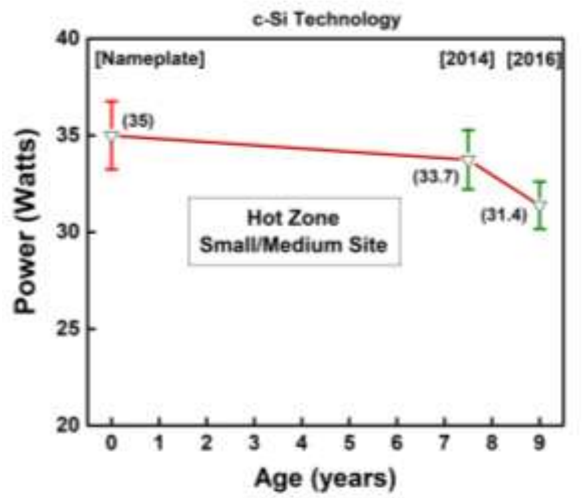

(c)

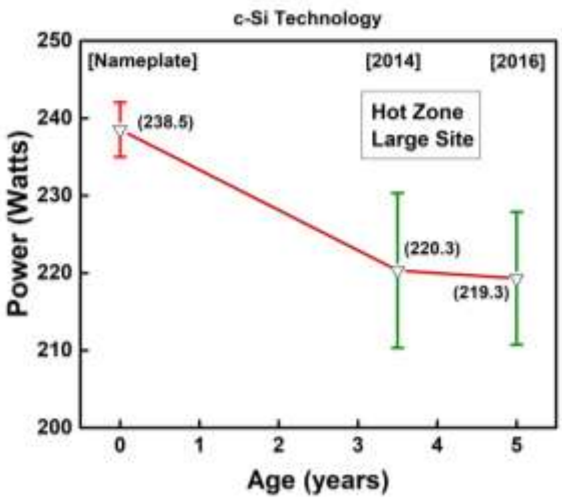

(d)

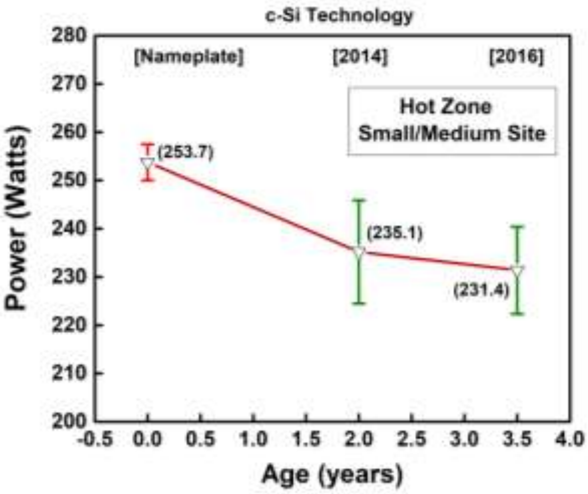

(e)

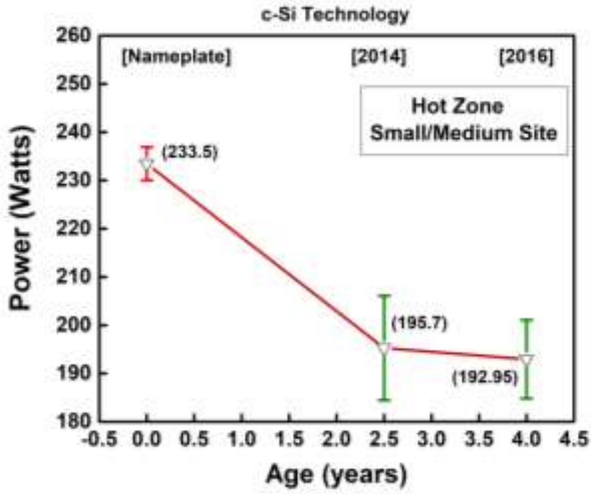

(f)

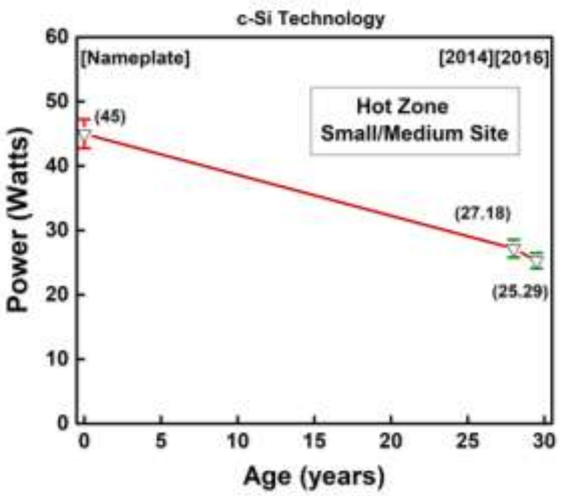

(g)

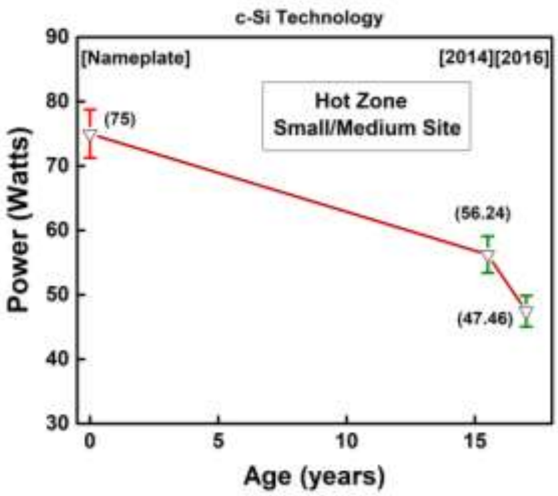

(h)

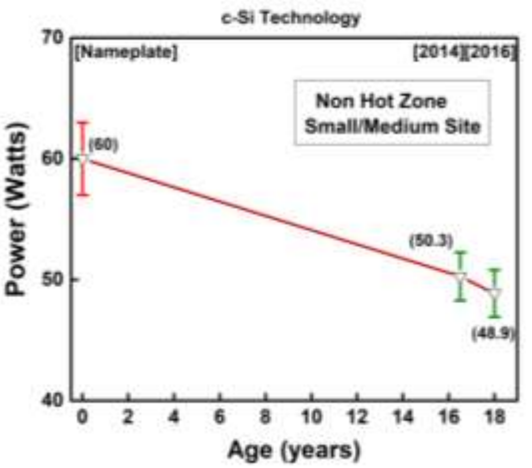

(i)

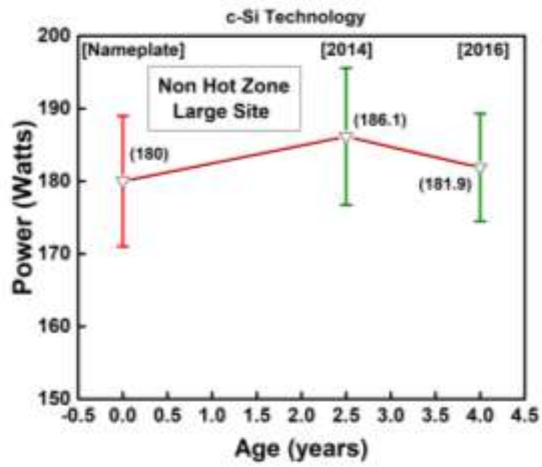

(j)

Fig. 4.28: Performance of the modules installed at 10 sites (a) through (j) which were repeated in 2014 and 2016 survey.

Table 4.5 provides the average degradation rates of the repeat sites calculated by 4 different procedures:

a) LID discounted degradation rate based on 2016 survey measurements
b) Overall Degradation Rate based on 2016 survey measurements
c) Overall Degradation Rate based on 2014 survey measurements
d) Overall Degradation Rate based on difference in power output between 2014 and 2016 measurements

It can be seen that the degradation rates given in the second, third and fourth columns of the table are mostly quite close to each other, but differ significantly from the values given in the last column (calculated based on repeat measurements in 2014 and 2016). The average degradation rate of these sites based on repeat measurements is 3.04 %/year, whereas the average value of the LID discounted degradation rate as per 2016 measurements is 2.43 %/year. In some of the sites, the degradation rate between 2014 and 2016 are very high, which may be due to the error in translation and measurement. Also, it is important to note that the 2014 survey was conducted in Sept-Nov (early winter) while the 2016 survey was conducted in March-May (early summer).

Table 4.5: Degradation rates of repeat sites

Site No. (as per 2016 survey)	LID Discounted P_{max} (%/year) rate for modules measured in 2016	Overall P_{max} (%/year) rate for modules measured in 2016	Overall P_{max} (%/year) rate for modules measured in 2014	Overall P_{max} (%/year) rate between 2014 & 2016
2	3.99	4.75	4.43	0.55
5	5.05	6.17	2.30	4.60
12	1.03	1.28	0.41	4.66
17	1.32	1.75	1.65	0.31
18	2.14	2.76	2.26	1.08
22	4.64	5.25	4.89	0.79
26	2.52	2.64	2.22	4.63
27	3.23	3.41	1.96	10.41
37	1.13	1.27	1.08	1.86
34	-0.76	-0.26	-0.83	1.52
Average of above sites	2.43	2.90	2.04	3.04

4.10 Summary

From the electrical degradation analysis we can draw the following conclusions:

- There is a lot of variability in performance of crystalline silicon modules. Almost half of the surveyed c-Si modules (Group X) are performing reasonably well, while the rest of the modules (falling in Group Y) are not. Some sites show excellent performance, whereas some show grave problems. These observations point to issues regarding module quality and/or installation procedures.
- Modules in Hot zones (Hot & Dry, Warm & Humid and Composite) show higher degradation rates than the modules in Non-Hot zones (Moderate, Cold & Cloudy and Cold & Sunny). This warrants more attention to understanding the hot climate degradation modes, as well as accelerated testing and appropriate certification for these climates.
- In Group X, young modules (age <5 years) show a slightly lower degradation rate than old modules (age >5 years). However, if modules from Group A (‘All’ – Group X plus Group Y) are considered, young modules show a higher degradation rate than old modules. This indicates that young modules seem to have problems regarding quality of modules, installation, and/or possible over-rating.

- In old crystalline silicon modules the main contributor to the P_{max} degradation is I_{sc} followed by *FF*, whereas in the case of young crystalline silicon modules the main contributor to the P_{max} degradation is *FF* degradation. The fact that young modules show a higher degradation rate mainly due to FF degradation indicates the possibility of deliberate over-rating of the power of the module.
- Modules installed in large systems (size more than 100 kW) are degrading at a much lower rate (~1 %/year average Linear Degradation Rate for Group A) than modules installed in small systems of size less than 100 kW. All large systems fall in the 'good' Group X category. However, the modules from the large sites in only the Hot zone haves an average Linear P_{max} Degradation Rate of 1.28 %/year which is much higher than the linear warranty. Also the young large systems are degrading at a higher rate than the old large systems in Hot zones. Hence, installers need to be cautious about the quality of materials and installation practices.
- Roof mounted modules suffer from a higher degradation rate as compared to ground mounted modules. This needs special attention as 40 GW of India's 100 GW target are planned to be installed on rooftops.
- The power degradation rate for the surveyed c-Si modules does not follow any known statistical distribution, but the maximum degradation rates at the sites follow the Gumbel distribution. Statistical analysis of the data confirms that the module degradation rates in the different climates of Hot are similar, and hence it is recommended that for analysis of photovoltaic degradation, only two climatic zones be considered – Hot and Non-Hot. Statistical analysis has shown that while the influence of the climate, type of mounting and age are significant, the size of installation surprisingly does not have any significant effect on the power degradation rate.

5. Analysis of Dark *I-V*, Insulation Resistance and Interconnect Breakage Data

5.1 Introduction

Dark *I-V* is a commonly used characterization tool for assessment of degradation in the semiconductor devices (solar cell). It provides information regarding into the quality of the solar cell including the contacts, series and shunt resistance. High insulation resistance is an important safety criterion for PV modules, particularly in high voltage systems like PV power plants. Interconnect breakage test helps in identifying discontinuity in the cell or string interconnects which may be caused by corrosion or thermal fatigue in the module.

In this chapter, we will present the analysis of the dark *I-V* data, in terms of degradation in the overall ideality factor of the solar cell, with respect to age and climatic zone. We shall also correlate the Linear P_{max} Degradation with degradation of the overall ideality factor. We will then present the analysis of the insulation resistance with respect to Group X and Group Y modules and also with respect to small/medium and large systems. Finally we present the correlation of series resistance and Linear P_{max} degradation with the number and extent of interconnect breakage in the PV modules.

5.2 Analysis of Dark *I-V* Data

Dark *I-V* characterization was done in the field by covering the module by with a black cloth and then sweeping the voltage from zero to the open circuit voltage and measuring the output current. The dark *I-V* of the module thus obtained was converted into the dark *I-V* of an equivalent solar cell by dividing the voltage (at each *I-V* data point) by the number of cells in the module [28]. Figure 5.1 graphically demonstrates the concept of dark *I-V* of the equivalent cell. The advantage of applying this technique is that it enables us to directly use the one diode model to obtain the dark *I-V* parameters such as ideality factor (n) and reverse leakage current (J_o) [40]. Since the ideality factor calculated is influenced by whole *I-V* curve, we refer to it as the 'Overall ideality factor'. This technique to obtain the dark *I-V* parameters has been described in detail and discussed separately in Appendix G.

5.2.1 Correlation of Overall Ideality Factor with Age

The Overall ideality factor n of the equivalent cell is calculated at the maximum power point. Figure 5.2 shows the variation in Overall ideality factor with age. From the plot, we can see that the Overall ideality factor n increases with increase in age of the module. This indicates that the solar cell itself, and not only the packaging material of the PV modules, degrade over the years. This increase in Overall ideality factor n is a reasonable expectation because as the age of the diode increases, its characteristics degrade (for, example due to increased leakage) and hence its Overall ideality factor increases. However in Fig 5.3a shows that the series resistance for those modules increases with age and Overall ideality factor n has an increasing trend with the series resistance (as shown in Fig. 5. 3b). This indicates that the Overall ideality factor may be degrading partly due to increased series resistance. The increase in the series resistance is due to corrosion in metallization. The correlation between the series resistance and the corrosion is shown in Chapter 6 in more detail.

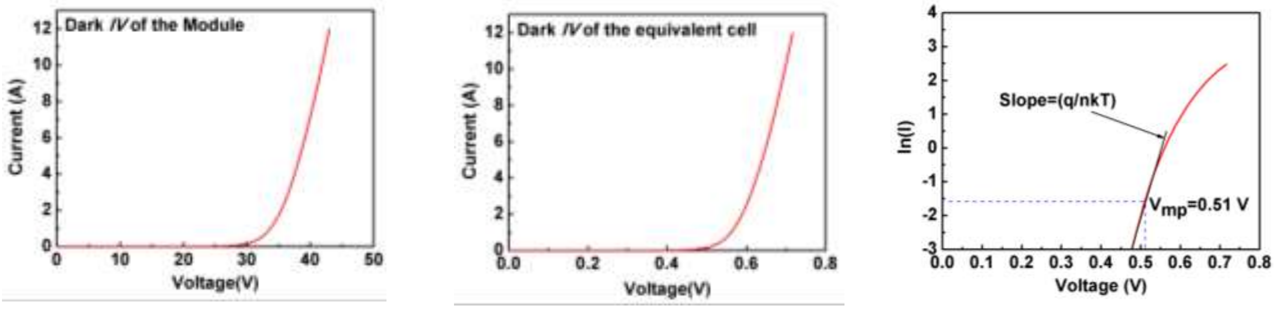

(a) (b) (c)

Fig. 5.1: (a) Measured dark *I-V* of the module and, (b) dark *I-V* of the equivalent cell obtained by dividing the module *I-V* voltages by number of cells (here 60), (c) *ln(I)* vs. voltage plot, showing also the tangent at V_{mp}, from which *n* can be found.

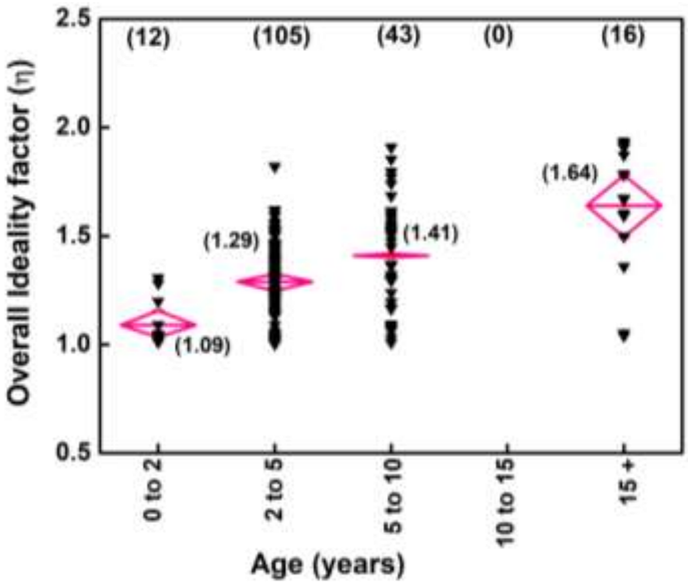

Fig. 5.2: Correlation of Overall ideality factor *n* with age. The red diamond represents the 95% confidence interval.

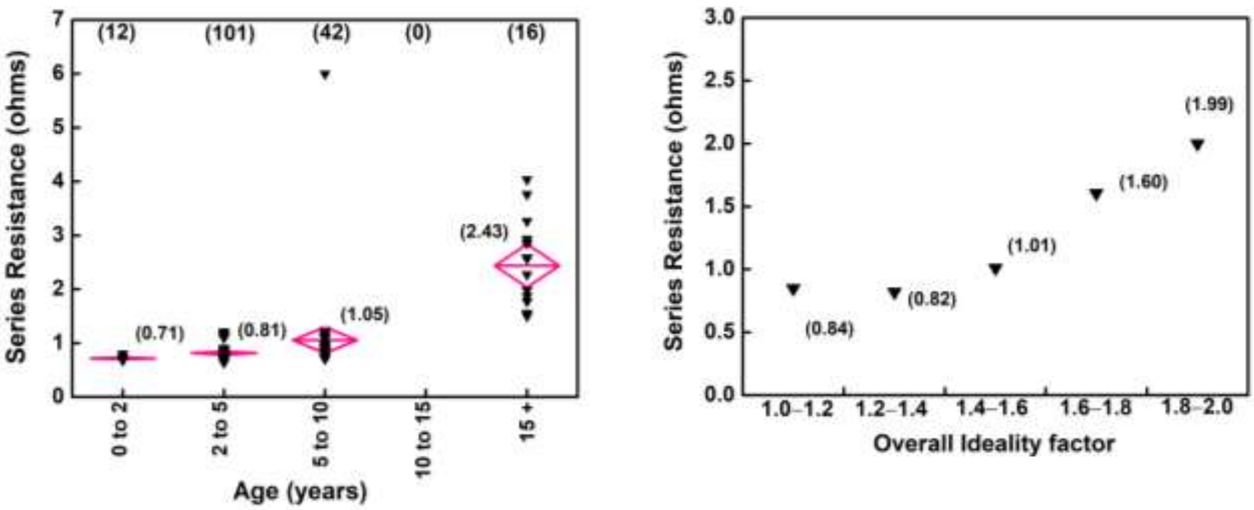

(a) (b)

Fig. 5.3: Correlation of (a) series resistance with age and (b) series resistance with Overall ideality factor. The red diamond represents the 95% confidence interval.

5.2.2 Variation of Overall Ideality Factor with Climate

Figure 5.4 shows the age-averaged Overall ideality factor variation with respect to Hot and Non-Hot Zones. It is seen from the figure that the modules in the Hot zones have a slightly higher value of *n* as compared to modules in Non-Hot zones. Possible reason for this may be the higher operating temperature and/or humidity of the PV modules, which may accelerate degradation. The high value of Overall ideality factor causes decrease in the value of the *FF* and eventually results in the degradation in P_{max} [41]. Hence we can say that in Hot zones the P_{max} degradation is not only due to degradation in packaging materials, but also a small contribution due to the degradation in the solar cell. However, it should be noted that our data set for *n* is small, so reaching a definitive conclusion for climatic zone variation is difficult.

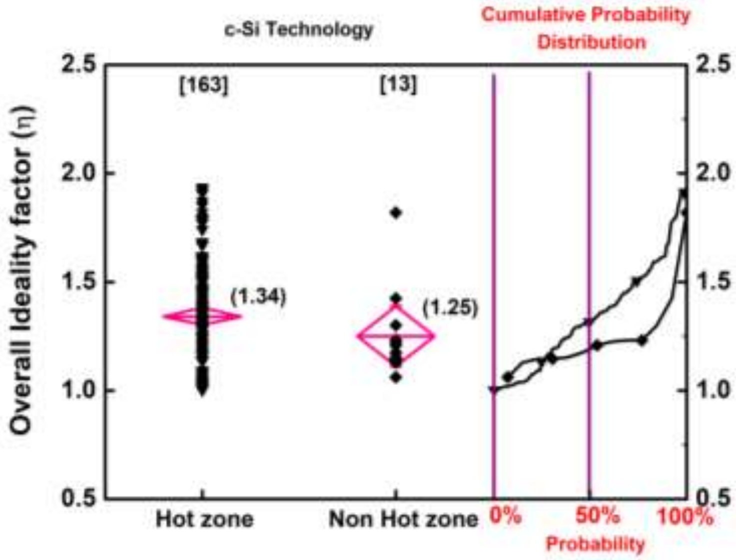

Fig. 5.4: Correlation of Overall ideality factor with respect to Hot and Non-Hot zones. The Overall ideality factor is averaged over all ages.

5.2.3 Correlation of Overall Ideality Factor with Linear P_{max} Degradation

Figure 5.5 shows the correlation between the Overall ideality factor *n* and the (total) percentage Linear P_{max} Degradation Rate for Group A modules. An increase in *n* causes a decrease in the *FF* value which finally decreases the power output of the module. Hence it clearly correlates the power output of the module with the quality of the semiconductor device. Note that in Fig. 5.5, the total power degradation is plotted, not the annual degradation rate.

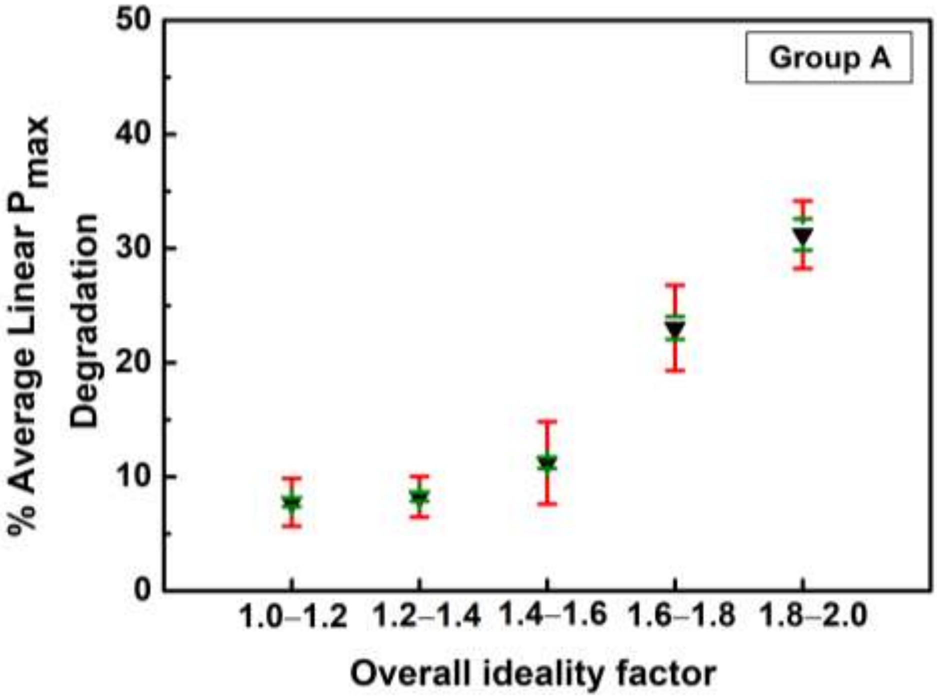

Fig. 5.5: Correlation of Overall ideality factor n with the percentage Linear P_{max} degradation.

5.3 Analysis of Insulation Resistance Data

Insulation resistance of the PV modules was measured by using a Fluke Insulation Tester. The output terminals of the module were shorted and connected to the positive terminal of the instrument, while the negative terminal of the instrument was connected to the frame of the module. The dry insulation resistance was measured in this manner. For the 'wet' insulation resistance, the top glass of the module was fully covered by a wet cloth. This procedure of our 'wet' insulation test differs from the IEC prescribed method which is used for indoor testing and certification of modules. In the IEC 61215 test procedure, the wet insulation resistance is measured by submerging the module in water. Since our 'wet' insulation resistance measurement in the field is not as per the IEC procedure, the interpretation of the data will not be comparable to the IEC standard, but is presented here because of importance in terms of safety.

5.3.1 Analysis of Dry Insulation Resistance

As per the IEC 61215 standard, the criterion for passing the dry or wet insulation test is that the product of insulation resistance and area of the module be more than 40 MΩ m^2 (for module area more than 0.1 m^2). From Fig. 5.6(a), we can say that 99.5% of the surveyed modules in all the categories (All, Group X and Group Y) have passed the dry insulation test. Also, from Fig. 5.6(b) we notice that 99.5% of both the young and old modules have passed the dry insulation resistance test in all the categories (All, Group X and Group Y).

5.3.2 Analysis of 'Wet' Insulation Resistance

For the analysis of our 'wet' insulation resistance test, which is less stringent as compared to the IEC 61215 test method, we have considered the pass-fail criteria as mentioned in IEC standard (same as for the dry insulation resistance test mentioned above). Figure 5.7 shows the results for our 'wet' insulation resistance test for the surveyed modules. Overall 23% of the surveyed modules have failed in our test, and the percentage of failed modules is significantly higher in Group Y as compared to Group X. This is a major safety concern, considering that the modules are mainly manually cleaned in India using water, during daylight hours when the system voltages are high.

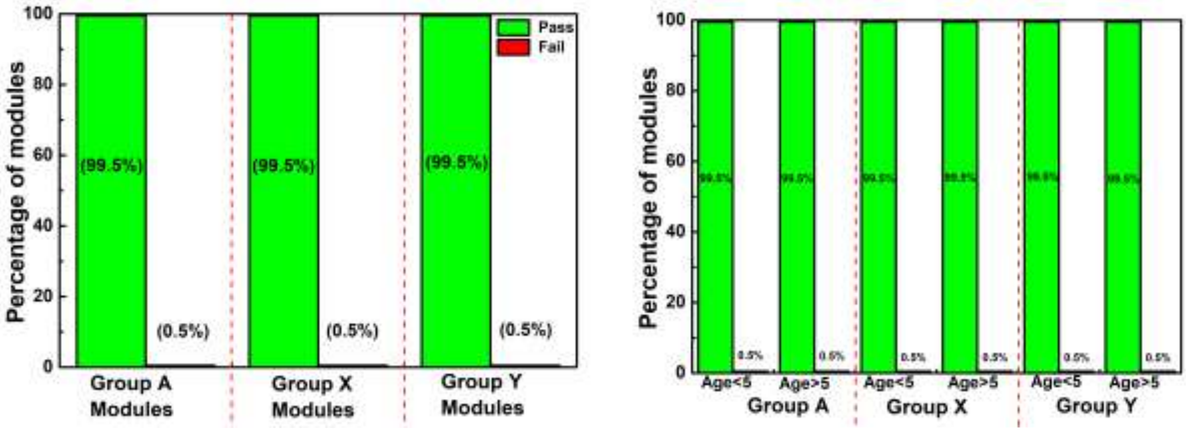

(a) (b)

Fig. 5.6: (a) Percentage of modules passed or failed in the dry insulation resistance test for different groups – Group A, Group X, and Group Y, and (b) percentage of modules passed or failed in dry insulation resistance test for 'All', Group X, and Group Y modules for young and old category.

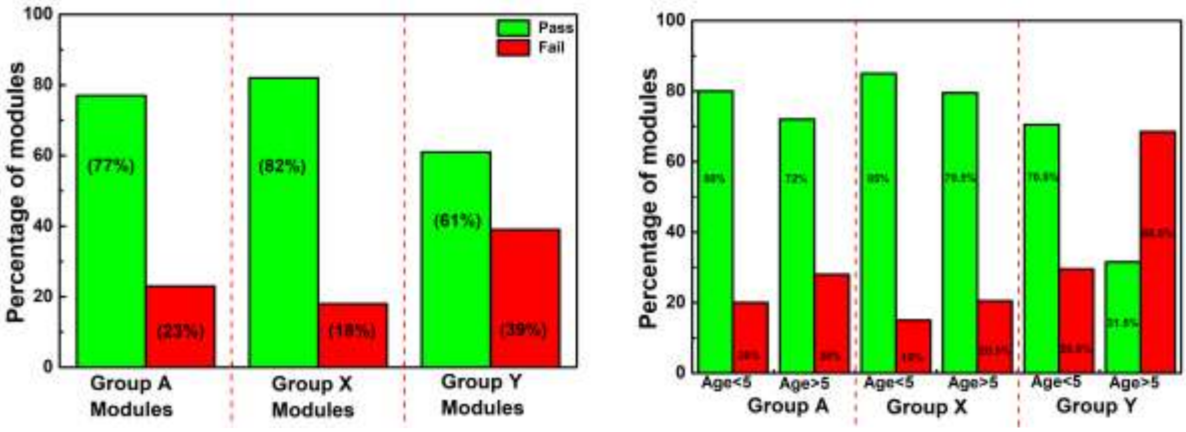

(a) (b)

Fig. 5.7: (a) Percentage of modules passed or failed in the 'wet' insulation resistance test for different groups – Group A, Group X, and Group Y, and (b) percentage of modules passed or failed in 'wet' insulation resistance test for Group A, Group X, and Group Y modules for young and old category.

5.3.3 <u>Analysis of Insulation Resistance with respect to System Size</u>

Figure 5.8 shows the percentage of modules passed or failed in the dry insulation resistance test for small/medium systems (system size less than 100 kW) and large systems (system size more than 100 kW). It is evident that the modules in large installations are slightly performing better than small/medium installations, and 100% of the modules in the large installations have passed the dry installation test. This is very good with respect to the safety in the large size PV system. Figure 5.9 shows the percentage of modules passed or failed in our 'wet' insulation resistance test for small/medium systems (system size less than 100 kW) and large systems (system size more than 100 kW). It is evident that a significantly higher percentage of modules from small/medium installations have failed in our 'wet' insulation resistance test as compared to the large installations. Since 30% of the surveyed modules in the small/medium sites have failed the test, it is a matter of concern from safety point of view.

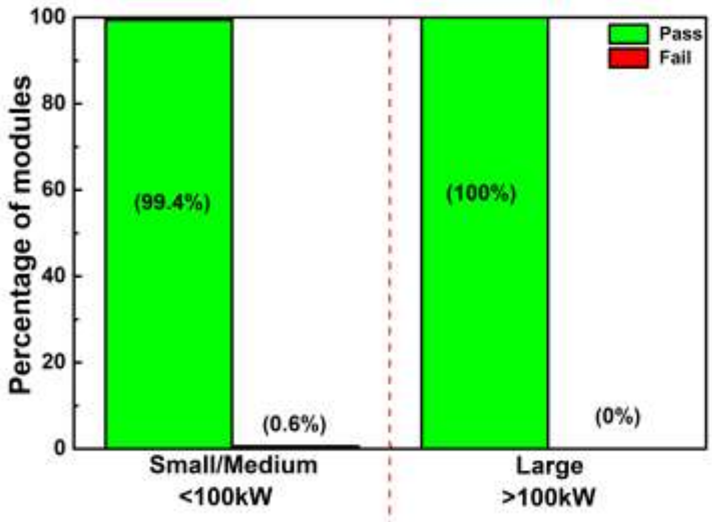

Fig. 5.8: Percentage of module passed or failed dry insulation resistance test for small/medium and large installation.

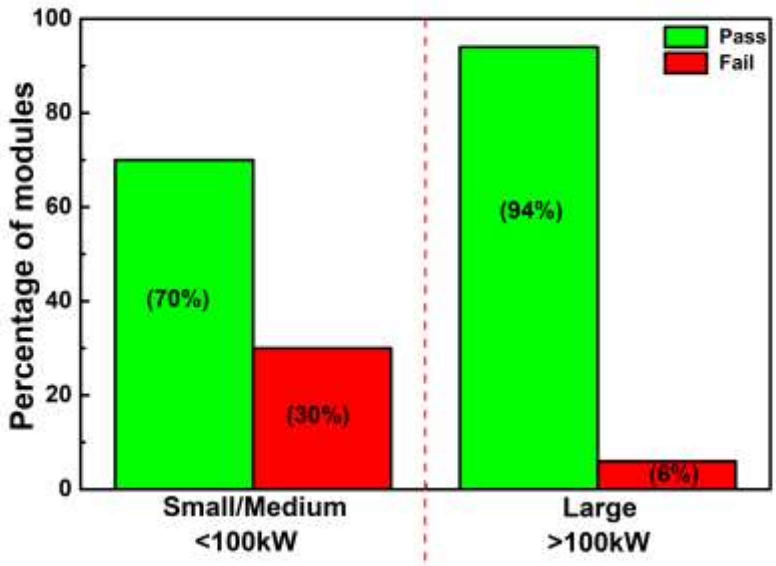

Fig. 5.9: Percentage of module passed or failed the 'wet' insulation resistance test for small/medium and large installation.

5.3.4 Correlation of Linear P_{max} Degradation with Insulation Resistance

Figure 5.10 shows that the Linear P_{max} Degradation Rate (%/year) increases with decrease in dry insulation resistance for Group A modules. This clearly indicates the correlation of the output power degradation of the PV modules with the material quality. Also, poor insulation resistance may result in safety related issues.

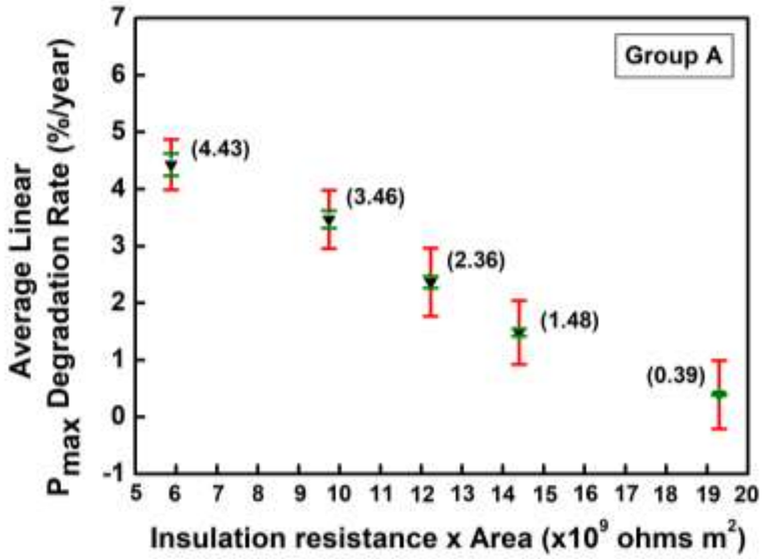

Fig. 5.10: Correlation of P_{max} degradation rate (%/year) with insulation resistance for Group A modules.

5.4 Analysis of Interconnect Breakage Data

Interconnects provide electrical connection between the cells and conduct the electrical power to the external load from the cells in the PV module. Usually there are 2 or 3 interconnects in each cell, which provide necessary redundancy in case of breakage in any part of the interconnect. However, if there is a breakage even in one interconnect, the whole cell's current would have to be conducted by the other interconnects in the cell, leading to current crowding, which increases the series resistance of the module, thereby degrading the fill factor and the power output. The Togami Cell Line Checker was used to test the interconnect breakage in the PV modules during the survey. The point where the interconnect breakage was obtained was marked with a red marker pen on the module. If the breakage is at a single point, it is termed as point breakage, and if it continues over a length of the busbar it is termed as line breakage. Figure 5.11 shows some examples of point breakage and line breakage. Severity in interconnect breakage is defined as the ratio of number of cells affected by the interconnect breakage to the total number of cells in the module.

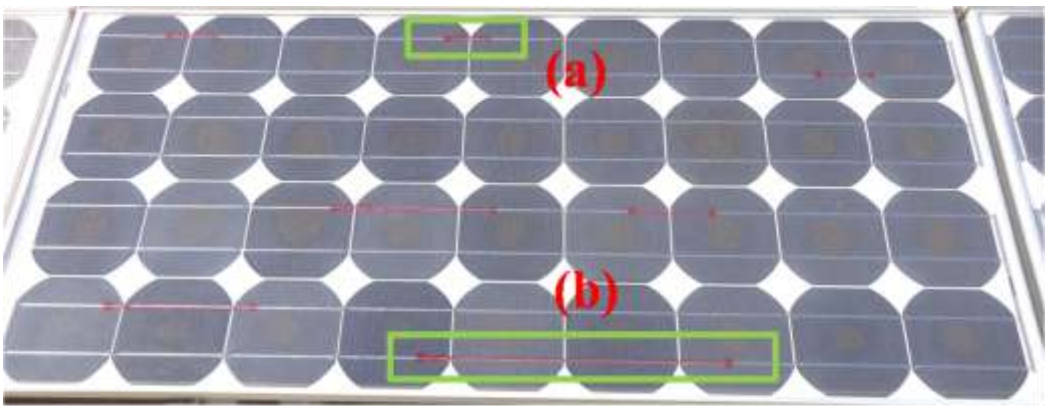

Fig. 5.11: (a) Point breakage and, (b) line breakage.

5.4.1 Analysis of Interconnect Breakage with respect to Climatic Zone

Table 5.1 shows the percentage of modules affected by interconnect breakage in different climatic zone in all age categories. This table has been colour coded for ease of understanding, where green is used for low values (percentage of affected modules is less than 33%), orange for medium values (affected modules between 33% to 66%) and red for high values (more than 66% modules affected). From the table we can see that modules in Hot & Dry zone are affected the most as compared to the other climatic zones. The reason for high interconnect failure in this climatic zone is likely to be due to thermal cycling because of change in the day and night temperature [34]. Also, the percentage of modules affected by interconnect failure in old modules is relatively high in the Warm & Humid climatic zone. Corrosion of interconnect could be the probable reason for this. From this table we can conclude that the percentage of modules having interconnect breakages is more in Hot zones as compared to the Non-Hot zones.

Table 5.1: Percentage of modules affected by interconnect breakage in different climatic zones and age groups

Percentage of Modules Affected					
	0-5	**5-10**	**10-20**	**20+**	**All Ages**
Hot and Dry	4% (57)	6% (52)	68% (28)	36% (14)	19% (151)
Warm and Humid	4% (100)	7% (84)	30% (30)	NA	9% (214)
Composite	0% (132)	15% (132)	33% (19)	NA	5% (164)
Moderate	0% (80)	NA	NA	NA	0% (80)
Cold & Sunny	0% (30)	NA	13% (76)	NA	10% (106)
CW	0% (20)	NA	NA	NA	0% (20)

5.4.2 Correlation of Interconnect Breakage with Series Resistance

The series resistance of the module is calculated by taking the inverse of slope of the lighted *I-V* curve near the open circuit voltage point (where current is nearly zero). Figure 5.12 shows the correlation of series resistance with the severity of the interconnect breakage. It can be clearly seen that as the severity of the interconnect breakage increases, the series resistance (expectedly) also increases which reduces the *FF* and consequently decreases the P_{max}. In Section 5.4.1, we have seen that percentage of modules having interconnect breakage is more in Hot zones, so this is one more reason why modules in Hot zones have higher degradation rates as compared to the Non-Hot zones.

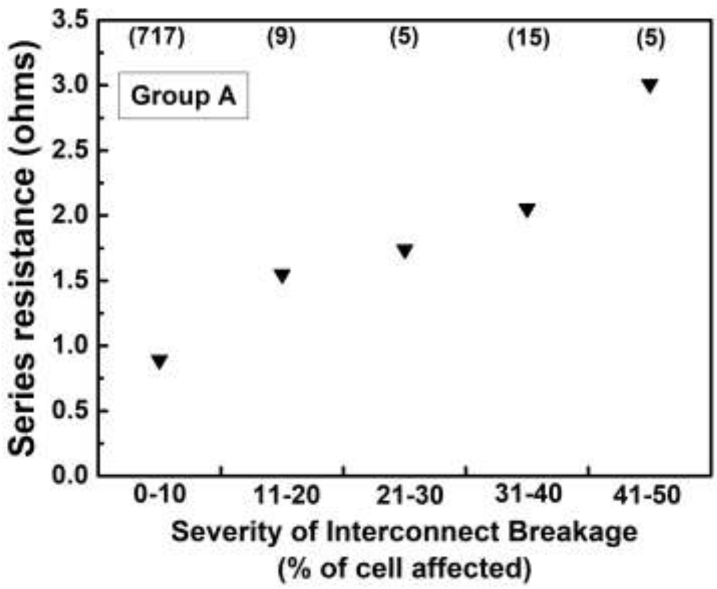

Fig. 5.12: Correlation of average value of series resistance with severity of interconnect breakage (numbers on top represent the number of modules in each category).

5.4.3 Correlation of Interconnect Breakage with Linear P_{max} Degradation

Figure 5.13 shows the correlation of Linear P_{max} Degradation Rate (%/year) with severity of interconnect breakage for Group A modules. It can be clearly seen that the output power degradation rate increases with the increase in the severity of interconnect breakage.

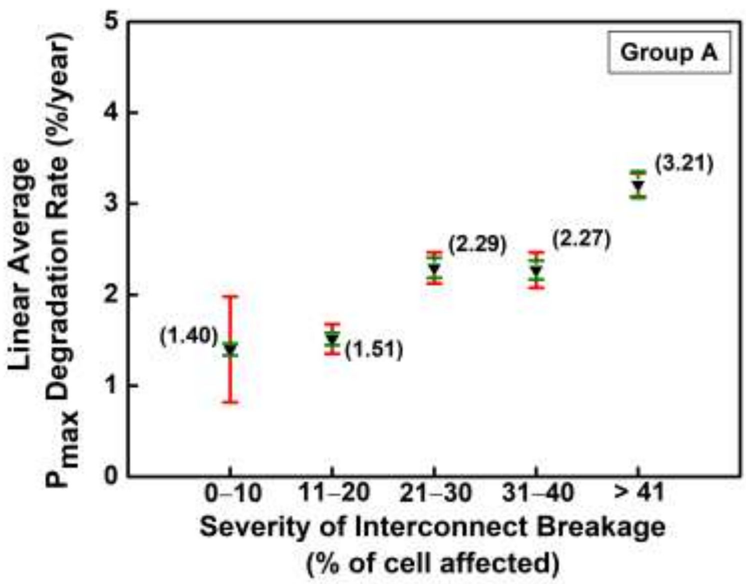

Fig. 5.13: Correlation of Linear P_{max} Degradation Rate (%/year) with severity of interconnect breakage for Group A modules.

5.5 Summary

From the analysis of the dark *I-V*, insulation resistance and interconnect breakage data, we can reach the following conclusions:

- The Overall ideality factor of the module increases with the increase in the age of the module. This shows that the quality of the cells does degrade as the age of the module. It could be due increase in series resistance.

- The Overall ideality factor n is slightly higher in the Hot zones as compared to the Non-Hot and it has good correlation to the percentage power degradation.

- Analysis of insulation resistance shows that more than 99% of the modules have passed the dry insulation resistance test. Also, 100% modules installed in the large system category have passed the dry insulation test which shows that large power plants are doing well with respect to the safety the PV system. Also, P_{max} degradation increases with decrease in the measured value of the insulation resistance.

- Modules in the Hot zones have shown larger percentage of interconnect failure as compared to the Non-Hot zones. Also the series resistance of the module increases with the increase in the severity of the interconnect failure which eventually reduces the power output of the module.

6. Analysis of Visual Degradation

6.1 Introduction

Many of the degradation modes of PV modules show visible signs which make it easy to identify them. These visible degradation modes serve as early indicators of impending loss in electrical power output. Also, visual degradation analysis helps in identifying the root cause of the electrical degradation. During the All India survey, we have inspected the modules with the help of a slightly modified version of the NREL visual inspection checklist [27], which is attached in Appendix A. In the following sub-sections, the various degradation modes observed during the survey are analyzed based on technology, age, climatic zone and size of installation, and shown separately for crystalline silicon modules and thin film modules. The data will be presented first for Group A modules (which includes Group X and Group Y), and then separately for Group X and Group Y, in order to bring out the differences. The data presented in the tables are colour coded for ease of understanding. For all tables showing percentage of affected modules, green colour shall indicate 'nil' value (0% affected), yellow shall indicate low values (below 33%), orange medium values (33% - 66%), and red shall indicate high values (greater than 66% affected) of the corresponding visual degradation.

6.2 Visual Degradation Observed in Crystalline Silicon Modules

Various components of PV modules degrade upon exposure to the outdoor environment. The UV content of the incident solar radiation, the high operating temperatures and the outdoor humidity levels (with intermittent rainfall) all affect the PV modules in different ways. The major degradation modes observed for crystalline silicon modules are discussed in the following sections.

6.2.1 Influence of Climatic Zone and Age Group on Visual Degradation Modes

a) Discoloration of Encapsulant

Discoloration (browning) of encapsulant is one of the most common causes behind reduction in short-circuit current (I_{sc}) and consequently power output (P_{max}) of field-aged PV modules. The composition of the encapsulant has undergone several changes in the evolution of the PV module, in order to improve its long term durability. Ethyl Vinyl Acetate (EVA) is the most commonly used encapsulant due to its favourable properties and low cost, but it is sensitive to photo-thermal degradation and has to be mixed with the proper additives to prevent untimely discoloration [43]. In our field survey, discoloration has been observed even in some of the Young modules (aged less than 5 years), as indicated in Fig. 6.1 and Table 6.1. In this table, each cell provides the percentage of modules affected in the respective climatic zone and age group, followed by the number of samples (in brackets). The values are colour-coded as described above. Categories without any module samples are indicated by "NA". Table 6.1 shows that among the Young modules, discoloration is most commonly seen in the Hot & Dry climate with no observed cases in the Non-Hot climates (Moderate, Cold & Cloudy and Cold & Sunny). However, after 10 years of exposure, most of the modules show discoloration even in the Non-Hot climates. The data for glass-glass crystalline silicon modules is not shown in this table, as such modules were found only at one site in the survey, and interestingly these modules did not show significant discoloration even after 27 years of operation. This leads us to suspect that either the encapsulant used may not have been EVA, but some other high grade alternative, or the Cerium content of the front glass may be very high, which could prevent UV rays from passing into the module, thereby preventing discoloration of the encapsulant [43].

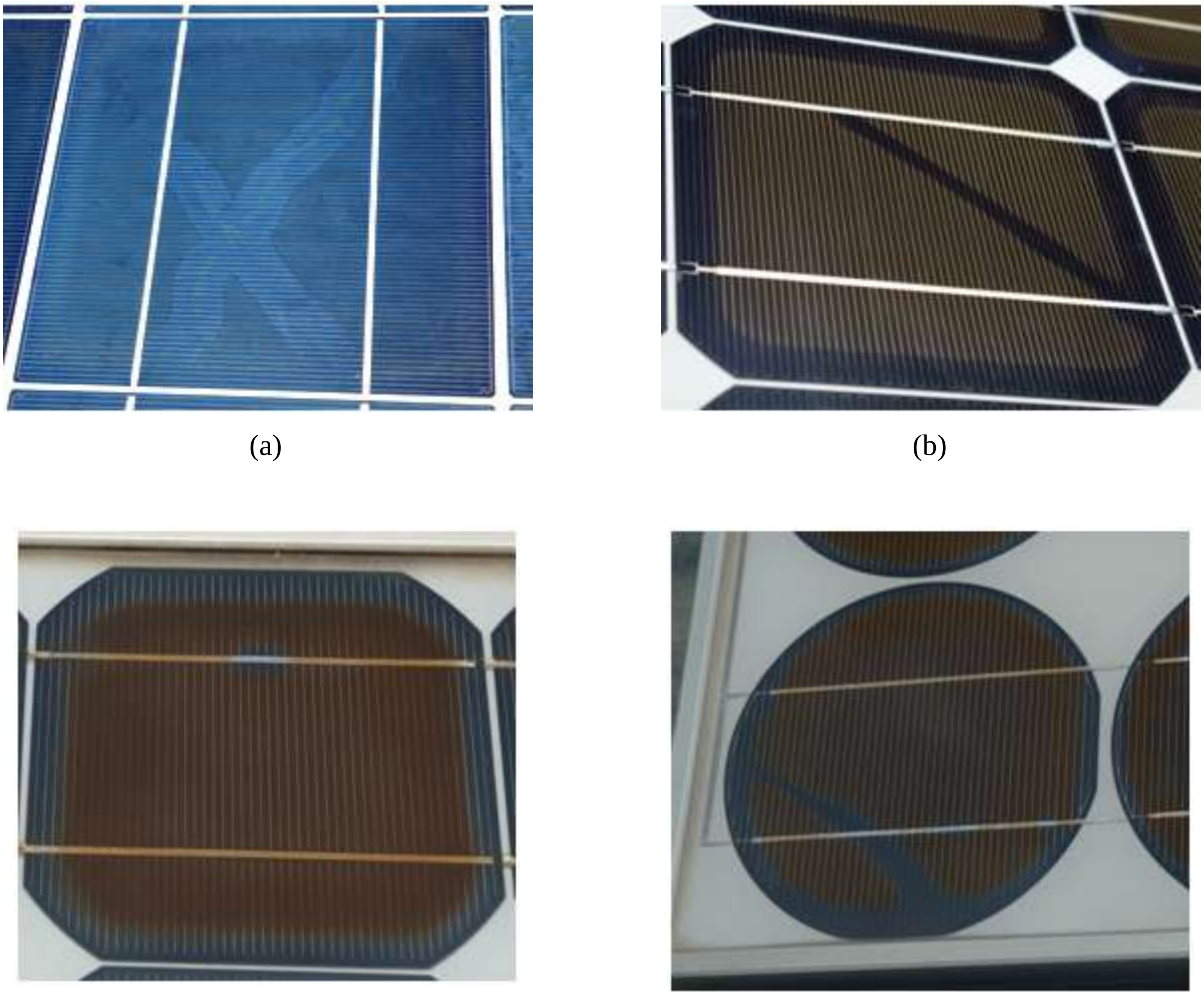

(a) (b) (c) (d)

Fig. 6.1: Examples of encapsulant discoloration observed during the survey – (a) discoloration in a 3 year old module in Hot & Dry zone (with photo-bleaching effect along crack in centre of cell), (b) discoloration in a 8 year old module in Warm & Humid zone (with snail track formation along crack), (c) discoloration in a 18 year old module in Warm & Humid zone (with crack induced photo-bleaching near the busbar), and (d) discoloration in a 18 year old module in Cold & Sunny climate (with crack induced photo-bleaching).

In Chapter 4, it has been shown that there are some "good" sites (having average Overall P_{max} Degradation Rate less than 2 %/year, referred to as Group X) and some "not-so-good" sites (having Overall P_{max} Degradation Rate greater than 2 %/year, referred to as Group Y). We have analyzed the visual degradation separately for the two Groups, as this may give pointers to why some modules are performing better than others. Table 6.2 compares the percentage of modules affected by encapsulant discoloration in Group X with Group Y for all six different climates. The last row of this table shows the comparison of the two groups by combining the data for all categories for which samples exist for both Groups X and Y (highlighted with blue shade), and it seems that there is not much difference between the two groups. However, when we look at the data by combining the climates into Hot and Non-Hot zones (shown in Fig. 6.3), we can clearly see that higher percentage of modules are affected by encapsulant discoloration in Group Y as compared to Group X, in the Hot zone. This implies that the encapsulant material quality is poorer in the Group Y modules. Also, the early onset of discoloration in the young modules in Hot zone raises concern about the material quality used in newer modules.

Table 6.1: Percentage of c-Si modules in Group A affected by encapsulant discoloration in different climatic zones and age groups (number of samples is given in brackets).

Climatic Zone	0 - 5 yrs old	5 - 10 yrs old	10 - 20 yrs old	20+ yrs old
Hot & Dry	35% (63)	39% (41)	100% (30)	NA*
Warm & Humid	2% (138)	77% (66)	100% (4)	NA
Composite	0% (99)	0% (14)	52% (25)	NA
Moderate	0% (80)	NA	NA	NA
Cold & Sunny	0% (25)	NA	61% (76)	NA
Cold & Cloudy	0% (20)	NA	NA	NA
*Excluding glass-glass modules from one particular manufacturer which have shown almost no discoloration even after 28 years in the field in Hot & Dry zone.				

Table 6.2: Comparison of Groups X and Y for discoloration in different climatic zones and age groups (number of samples is given in brackets).

Climatic Zone	Age Groups			
	0-5 Years	**5-10 Years**	**10-20 Years**	**20+ Years**
Hot & Dry	X: NA Y: 35% (63)	X:39% (41) Y: NA	X: NA Y: 100% (30)	X: NA Y: NA*
Warm & Humid	X: 4% (85) Y: 0% (53)	X: 77% (66) Y: NA	X: 100% (4) Y: NA	X: NA Y: NA
Composite	X: 0% (30) Y:0% (69)	X: 0% (14) Y: NA	X: 27% (15) Y: NA	X: NA Y: NA
Moderate	X: 0% (20) Y:0% (60)	X: NA Y: NA	X: NA Y: NA	X: NA Y: NA
Cold & Sunny	X: 0% (25) Y: NA	X: NA Y: NA	X: 61% (76) Y: NA	X: NA Y: NA
Cold & Cloudy	X: 0% (20) Y: NA	X: NA Y: NA	X: NA Y: NA	X: NA Y: NA
All Climates (comparative)	X: 2% (135) Y: 0% (182)	Comparison not possible	Comparison not possible	Comparison not possible
*Excluding glass-glass modules from one particular manufacturer which have shown almost no discoloration even after 28 years in the field in Hot & Dry zone.				

Table 6.3: Comparison of Group X and Group Y for discoloration in Hot and Non-Hot climates

Climatic Zone	Group	0 - 5 yrs old	5 - 10 yrs old	10 - 20 yrs old	20+ yrs old
Hot Zone	Group X	3% (115)	55% (121)	42% (19)	NA
	Group Y	12% (185)	NA	100% (30)	NA*
Non-Hot Zone	Group X	0% (65)	NA	61% (76)	NA
	Group Y	0% (60)	NA	NA	NA
*Excluding glass-glass modules from one particular manufacturer which have shown almost no discoloration even after 28 years in the field in Hot & Dry zone.					

It is necessary to quantify the severity of visual degradation in order to look for correlations with the electrical degradation. During the survey, it has been observed that discoloration is usually seen in all the cells of the affected modules, but some of the cells may show slightly larger discolored area or intensity (like the cells having nameplate or junction box at the back usually show slightly higher discoloration). There is some subjectivity involved in this visual estimation process, and it is possible that different persons will arrive at different estimations of the degree and area of discoloration for the same module. Hence the process of determining the Discoloration Index has been automated through in-house software, which reads the colour of each pixel of the photographs of modules, and computes the average extent of yellowness in the module, which is referred to as the "Pseudo Yellowness Index" (PYI) [44]. Since the edges of the solar cells usually are photo-bleached, leaving the initial blue colour intact, this is used as the reference colour to identify the change in the colour of the modules due to field exposure and a Discoloration Index (DI) is defined, as indicated below. The detailed procedure for determination of the discoloration index is explained elsewhere [44].

$$DI = \frac{PYI_{present} - PYI_{initial}}{PYI_{range}} \qquad \dots (6.1)$$

where,
$PYI_{present}$ = present value of Pseudo Yellowness Index
$PYI_{initial}$ = initial value of Pseudo Yellowness Index
PYI_{range} = difference in PYI between the worst possible browning and the initial (blue) colour.

Examples of the discoloration Index for some sample images are shown in Fig. 6.2, which proves that this technique is able to differentiate between various levels of discoloration in solar cells. The severity data has been color-coded for ease of understanding, as per Table 6.4 which also indicates the severity category from Low to High. The average discoloration severity category for Group X modules in different age groups and climatic zones is given in Table 6.5. The total number of sample modules in Table 6.5 is lower than the total in Group X, as the discoloration index could be computed only for modules which do not show high colour difference between grains in the crystalline silicon solar cells. We have previously discussed that the climatic zone influences will be analyzed for Group X modules (and not Group Y, since the Group Y modules are degrading at much higher rate than Group X modules, which may be due to manufacturing and/or installation issues). From Table 6.5, in "0-5 years" age group, it is clear that the severity of the various zones is in the order: Warm & Humid > Composite > Moderate. Similarly from "5-10 years" age group, the severity order is Hot & Dry > Warm & Humid > Composite. The highest average discoloration is seen in modules aged more than 10 years. In Table 6.6, young Group X modules have comparatively higher discoloration severity than Group Y modules in Hot zone but the trend is reversed in the Non-Hot zone so we cannot come to any definite conclusion from this table.

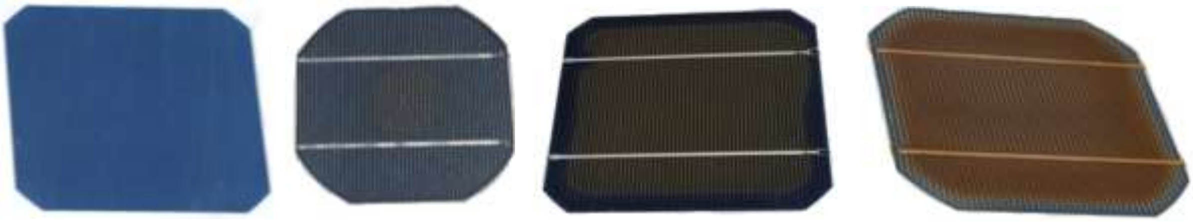

(a) DI = 0.005 (b) DI = 0.106 (c) DI = 0.383 (d) DI = 0.549

Fig. 6.2: Examples of Discoloration Index for different extent of encapsulant browning.

Table 6.4: Discoloration Severity Category

Discoloration Index	0 – 0.05	0.05 – 0.25	0.25 – 0.5	0.5 – 0.75	0.75 – 1
Discoloration Category	Nil	Low	Medium	High	Very High

Table 6.5: Average severity of discoloration (Discoloration Index) in Group X modules in different climatic zones and age groups (number of samples is given in brackets).

Climatic Zone	**0 - 5 yrs old**	**5 - 10 yrs old**	**10 - 20 yrs old**	**20+ yrs old**
Hot & Dry	NA	0.145 (40)	NA	NA
Warm & Humid	0.061 (47)	0.088 (37)	0.364 (4)	NA
Composite	0.038 (27)	0.040 (4)	NA	NA
Moderate	0.023 (20)	NA	NA	NA
Cold & Sunny	NA	NA	0.345 (46)	NA
Cold & Cloudy	NA	NA	NA	NA
Climatic zone with the highest average	Warm & Humid	Hot & Dry	Warm & Humid	-
NOTE: Some modules with multi crystalline silicon cells having high contrast between grains could not be processed by the image processing software.				

Table 6.6: Average severity of discoloration in Group X and Group Y modules in Hot and Non-Hot zones

Climatic Zone	**Group**	**0 - 5 yrs old**	**5 - 10 yrs old**	**10 - 20 yrs old**	**20+ yrs old**
Hot Zone	**Group X**	0.053 (74)	0.114 (81)	0.364 (4)	NA (0)*
	Group Y	0.032 (184)	NA (0)	0.131 (30)	NA (0)
Non-Hot Zone	**Group X**	0.035 (65)	NA (0)	0.345 (46)	NA (0)
	Group Y	0.051 (50)	NA (0)	NA (0)	NA (0)

Table 6.7 shows that in the young age category, large installations (size greater than 100 kW) show average severity almost similar to small/medium installations. In modules aged “5-10 years” in Hot zone, higher

severity is observed in large installations as compared to small/medium installations. In the "10-20 years" age group, the average discoloration in Non-Hot climate is higher than that in "Hot" climate (the modules belong to different manufacturers and so the bill of material may not be identical). It should also be noted that many modules manufactured in 1990s used cerium oxide glass, which blocks the UV rays and hence prevent/reduce the discoloration of the encapsulant, which might be the reason in this case.

Table 6.7: Average extent of discoloration in Group A modules for small/medium and large installations in the Hot and Non-Hot climatic zones (number of samples is given in brackets).

Size of Installation	Climatic Zone	Age Groups			
		0-5 Years	5-10 Years	10-20 Years	20+ Years
Small/ Medium	Hot	0.038 (187)	0.115 (17)	0.161 (42)	NA (0)
	Non-Hot	0.041 (126)	NA (0)	0.345 (46)	NA (0)
Large	Hot	0.034 (83)	0.112 (65)	NA (0)	NA (0)
	Non-Hot	0.04 (25)	NA (0)	NA (0)	NA (0)

Based on the above, we can conclude that the Hot zones are the harshest climates for the encapsulant (as per Fig. 6.5). The order of harshness seems to be Hot & Dry > Warm & Humid > Composite > Moderate > Cold zone. Higher percentage of modules is affected by discoloration in Group Y as compared to Group X, which points towards the use of poor quality materials in Group Y modules. Severity of discoloration is higher in Group X as compared to Group Y, which indicates that discoloration is not the main culprit responsible for the higher degradation observed in Group Y modules.

b) Front-side Delamination

Delamination on the front-side occurs due to loss of adhesion between the encapsulant and glass or between the encapsulant and solar cell. As a consequence, there is an increase in reflection losses from the affected area and the current generation gets reduced. In the 2016 survey, front-side delamination has mostly been seen in the form of bubbles along snail tracks (refer Fig. 6.3). Also, at one site, all modules showed delamination along the gridlines as shown in Fig. 6.3(b).

Table 6.8 provides the statistics of front-side delamination in all (Group A) surveyed c-Si modules. In this survey, significant delamination (covering more than 10% of the cell area in affected cells) has only been observed in some 28 year old glass-glass modules located in Hot & Dry climate. The glass-glass construction of the modules prevents escape of the vapors that may evolve during degradation of the encapsulant, and this trapped vapor can lead to delamination and bubble formation. At other sites, mostly small bubbles have been observed along snail tracks (which are also associated with cell cracks). Also, delamination along the fingers of the solar cells has been observed in all surveyed modules at a 7 year old site in Hot & Dry zone, as shown in Fig. 6.3(c).

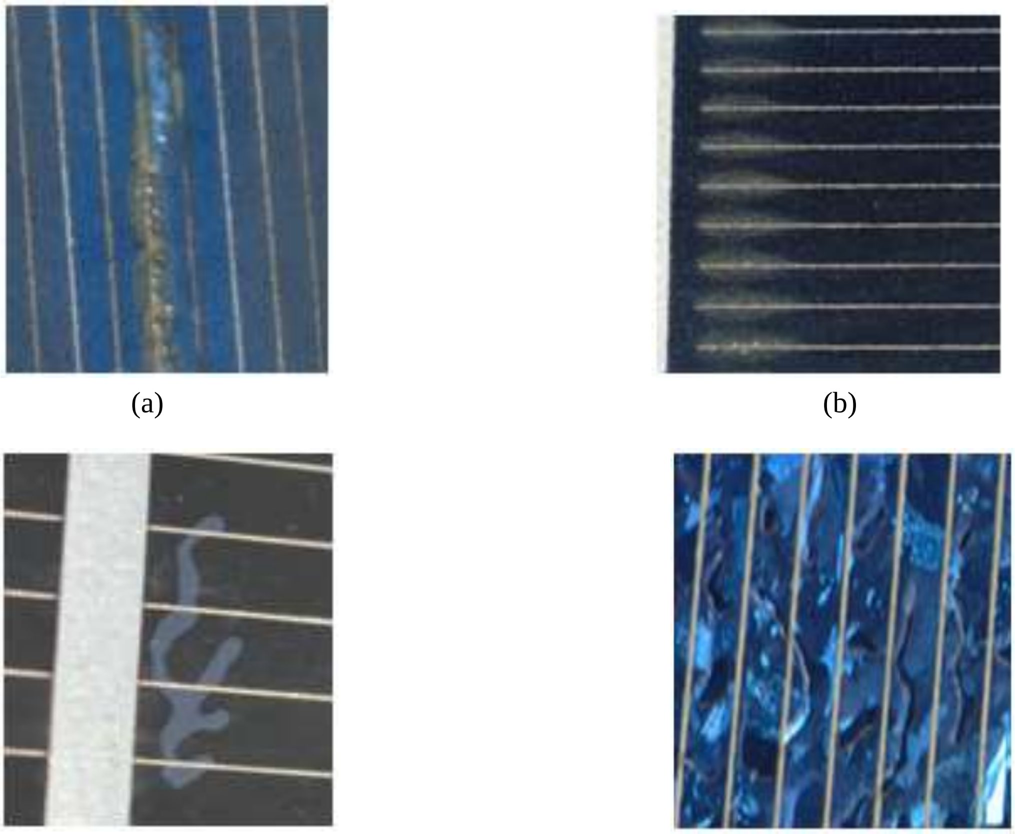

(a) (b) (c) (d)

Fig. 6.3: Examples of delamination observed during the survey – (a) along snail track, (b) along fingers at cell edge, (c) near the busbar, and (d) on top of whole cell in an old glass-glass module.

Table 6.8: Percentage of Group A modules affected by delamination in different climatic zones and age groups (number of samples is given in brackets).

Climatic Zone	0 - 5 yrs old	5 - 10 yrs old	10 - 20 yrs old	20+ yrs old
Hot & Dry	3% (63)	44% (41)	0% (30)	78% (14)*
Warm & Humid	1% (138)	49% (66)	100% (4)	NA (0)
Composite	23% (99)	21% (14)	7% (15)	NA (0)
Moderate	0% (80)	NA (0)	NA (0)	NA (0)
Cold & Sunny	0% (25)	NA (0)	0% (76)	NA (0)
Cold & Cloudy	0% (20)	NA (0)	NA (0)	NA (0)
* Glass-glass modules, which have been in field for 28 years.				

Tables 6.9 and 6.10 compare the delamination (bubble) statistics for Groups X and Y. It is evident that the delamination is restricted to the Hot climates. The comparison of the statistics for Group X and Group Y shows that Group Y modules are more affected by the bubble formation as compared to the Group X modules.

This is not unexpected since the bubbles are mostly occurring along the snail tracks, which are in fact more prevalent in group Y modules than in Group X modules (discussed in detail in the next section).

Table 6.9: Comparison of Groups X and Y for delamination in different climatic zones and age groups (number of samples is given in brackets).

Climatic Zone	Age Groups			
	0-5 Years	**5-10 Years**	**10-20 Years**	**20+ Years**
Hot & Dry	X: NA (0) Y: 3% (63)	X: 44% (41) Y: NA (0)	X: NA Y: 0% (30)	X: NA Y: 79% (14)
Warm & Humid	X: 1% (85) Y: 0% (53)	X: 49% (66) Y: NA (0)	X: 100% (4) Y: NA (0)	X: NA Y: NA
Composite	X: 10% (30) Y: 29% (69)	X: 21% (14) Y: NA (0)	X: 7% (15) Y: NA (0)	X: NA Y: NA
Moderate	X: 0% (20) Y: 0% (60)	X: NA Y: NA	X: NA Y: NA	X: NA Y: NA
Cold & Sunny	X: 0% (25) Y: NA (0)	X: NA Y: NA	X: 0% (76) Y: NA (0)	X: NA Y: NA
Cold & Cloudy	X:0% (20) Y: NA (0)	X: NA Y: NA	X: NA Y: NA	X: NA Y: NA
All Climates (comparative)	X: 3% (135) **Y: 11% (182)**	Comparison not possible	Comparison not possible	Comparison not possible

Table 6.10: Comparison of Group X and Group Y for delamination in Hot and Non-Hot climatic zones

Climatic Zone	Group	0 - 5 yrs old	5 - 10 yrs old	10 - 20 yrs old	20+ yrs old
Hot Zone	**Group X**	3% (115)	44% (121)	26% (19)	NA
	Group Y	12% (185)	NA	0% (30)	79% (14)
Non-Hot Zone	**Group X**	0% (65)	NA	0% (76)	NA
	Group Y	0% (60)	NA	NA	NA

Further analysis of the severity of delamination has not been done, since significant delamination (covering more than 5% cell area) has rarely been observed in the 2016 survey, and in most cases, delamination (bubbles) has been found associated with snail tracks. However, in the previous survey in 2014, significant delamination was observed in some very old modules in the Warm & Humid and the Hot & Dry zones (module age was more than 20 years). Delamination has not been observed in the Cold zone in any of the surveys. From the 2016 survey, it is seen that higher percentage of Group Y modules are affected as compared to Group X (but this may be mainly due to the association with the snail tracks).

c) Snail Tracks and Visible Cracks

Cracks in the solar cells can lead to different effects in the encapsulant. In the old modules having discoloration, cracks in the cells allow oxygen to pass through to the discolored encapsulant at the top of the cells, and this oxygen then bleaches the discoloration in the presence of sunlight [43]. On the other hand, in many of the newer modules, moisture and other gases are able to migrate through the cracks in the cells and cause Snail track formation on top of the cells [45]. Also, the spacing between the cells can serve as a pathway for moisture penetration up to the metallization on top of cells, and in some cases this leads to framing type snail tracks which occur along the edges of the cells. Examples of the two types of snail tracks are shown in Fig. 6.4. In the survey, we have found good correlation between the cell cracks and non-framing type snail tracks. Fig. 6.5 shows some examples of cracks (observed in EL images) and snail tracks (observed visually), in same modules. The snail tracks are found to be associated with cracks in the solar cells. Both snail tracks (non-framing type) and photo-bleaching effects of the encapsulant serve as visual indications of cracks in the cells. It is important to note that while the EL image also shows the area affected by the crack, snail tracks only delineate the crack's location but do not provide any indication about the severity of the crack (in terms of actual area affected by the crack). In this section, we shall first present the statistics related only to the snail tracks and then the overall statistics for visible indications of cracks (which includes both snail tracks and photo-bleaching). It is important to note that the cracks in the solar cells may not always lead to a visible sign (in terms of snail tracks or photo-bleaching) and Electroluminescence (EL) imaging is the only way to check for such cracks (discussed in more detail in Chapter 7).

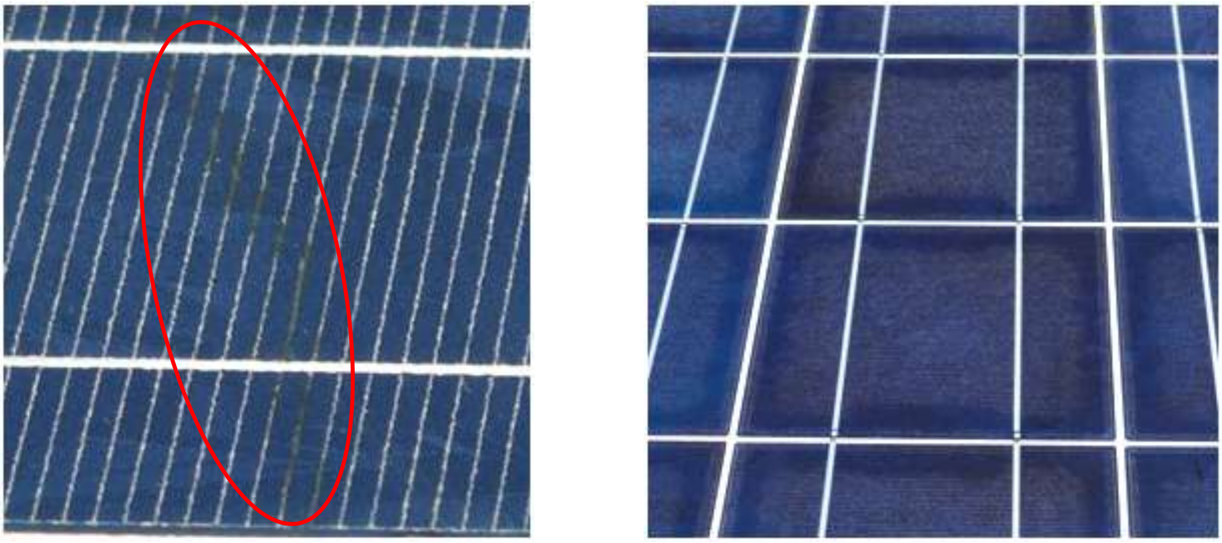

(a) (b)

Fig. 6.4: Snail Tracks observed during the survey – (a) snail track in a young module in Hot & Dry zone, and (b) framing type snail track in a young module in Warm & Humid zone.

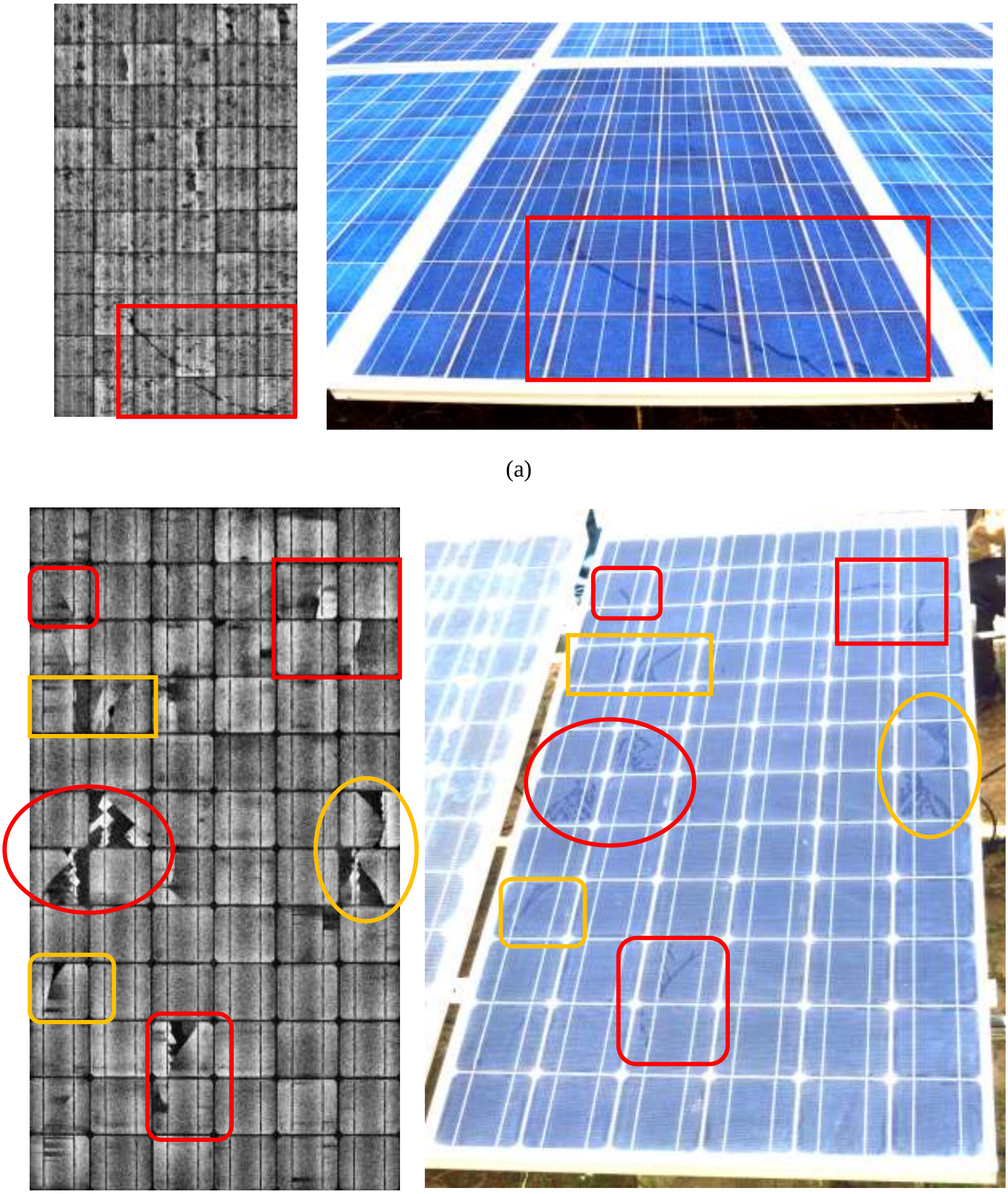

(a)

(b)

Fig. 6.5: Examples of cracks (shown in EL images on left side) and snail tracks (shown in digitally enhanced contrast-adjusted photographs on right side) observed during the survey.

<u>Non-framing type Snail Tracks</u>

The statistics of the non-framing Snail tracks (generally associated with cracks in solar cells) is presented in Table 6.11. Snail tracks are predominantly seen in the modules less than 10 years in age, and their frequency is higher in the Young modules in Composite and Moderate climatic zones. Snail tracks have not been seen in the colder climates (Cold & Sunny and Cold & Cloudy).

Table 6.11: Percentage of modules affected by Snail tracks (non-framing type) in Group A, in different climatic zones and age groups (number of samples is given in brackets).

Climatic Zone	Age Group			
	0 - 5 yrs old	5 - 10 yrs old	10 - 20 yrs old	20+ yrs old
Hot & Dry	17% (63)	2% (41)	0% (30)	0% (14)
Warm & Humid	5% (138)	24% (66)	0% (4)	NA
Composite	61% (99)	0% (14)	0% (15)	NA
Moderate	30% (80)	NA	NA	NA
Cold & Sunny	0% (25)	NA	0% (76)	NA
Cold & Cloudy	0% (20)	NA	NA	NA

The statistics of snail track affected modules in Group X and Group Y categories have been compared in Tables 6.12 and 6.13. Overall, in both Hot and Non-Hot climates, Group Y modules are more affected by snail tracks as compared to Group X modules. Comparing Group X modules in Hot and Non-Hot climates, it is found that modules in Hot zone are more prone to snail tracks, and within the Hot zone, highest percentage of modules affected has been found in the Composite zone.

Table 6.12: Comparison of Groups X and Y for snail tracks in different climatic zones and age groups (number of samples is given in brackets).

Climatic Zone	Age Group			
	0 - 5 yrs old	5 - 10 yrs old	10 - 20 yrs old	20+ yrs old
Hot & Dry	X: NA Y: 17% (63)	X: 2% (41) Y: NA	X: NA Y: 0% (30)	X: NA Y: 0% (14)
Warm & Humid	**X: 8% (85)** Y: 0% (53)	X: 24% (66) Y: NA	X: 0% (4) Y: NA	NA
Composite	X: 53% (30) **Y: 69% (69)**	X: 0% (14) Y: NA	X: 0% (15) Y: NA	NA
Moderate	X: 0% (20) **Y: 40% (60)**	NA	NA	NA
Cold & Sunny	X: 0% (25) Y: NA	NA	X: 0% (76) Y: NA	NA
Cold & Cloudy	X: 0% (20) Y: NA	NA	NA	NA
All Climates (comparative)	X: 17% (135) **Y: 39% (182)**	Comparison not possible	Comparison not possible	Comparison not possible

Table 6.13: Percentage of modules affected by snail tracks in Hot and Non-Hot zones

Climatic Zone	Group	0 - 5 yrs old	5 - 10 yrs old	10 - 20 yrs old	20+ yrs old
Hot Zone	Group X	20% (115)	14% (121)	0% (19)	NA
	Group Y	30% (185)	NA	NA	0% (14)
Non-Hot Zone	Group X	0% (65)	NA	0% (76)	NA
	Group Y	40% (60)	NA	NA	NA

The percentage of cells affected by snail trails in a module has been considered as the criterion for determining severity of snail trails, and the modules may be categorized as shown in Table 6.14. The average severity levels of snail tracks for the various climatic zones and age groups have been given in Table 6.15. The highest severity levels are seen in Composite, Warm & humid and Moderate climates. Tables 6.16 and 6.17 show that the average snail track severity is much higher in Group Y modules than in Group X modules.

Table 6.14: Snail track severity category

Cells affected by Snail Trail (%)	0%	0 – 1%	1% - 10%	10% - 50%	>50%
Snail Track Severity Category	Nil	Low	Medium	High	Very High

Table 6.15: Average severity of snail tracks in Group A

Climatic Zone	Age Group			
	0 - 5 yrs old	5 - 10 yrs old	10 - 20 yrs old	20+ yrs old
Hot & Dry	1.1 (63)	0.5 (41)	0.0 (30)	0.0 (14)
Warm & Humid	0.2 (138)	4.7 (66)	0.0 (4)	NA
Composite	6.0 (99)	0.0 (14)	0.0 (15)	NA
Moderate	3.0 (80)	NA	NA	NA
Cold & Sunny	0.0 (25)	NA	0.0 (76)	NA
Cold & Cloudy	0.0 (20)	NA	NA	NA
Climatic zone with the highest average	Composite	Warm & Humid	-	-

Table 6.16: Average severity of snail tracks in Group X and Group Y

Climatic Zone	Age Group			
	0 - 5 yrs old	**5 - 10 yrs old**	**10 - 20 yrs old**	**20+ yrs old**
Hot & Dry	X: NA Y: 1.1 (63)	X: 0.5 (41) Y: NA	X: NA Y: 0.0 (30)	X: NA Y: 0.0 (14)
Warm & Humid	**X: 0.3 (85)** Y: 0.0 (53)	X: 4.7 (66) Y: NA	X: 0.0 (4) Y: NA	NA
Composite	X: 2.0 (30) **Y: 8.4 (69)**	X: 0.0 (14) Y: NA	X: 0.0 (15) Y: NA	NA
Moderate	X: 0.0 (20) **Y: 3.9 (60)**	NA	NA	NA
Cold & Sunny	X: 0.0 (25) Y: NA	NA	X: 0.0 (76) Y: NA	NA
Cold & Cloudy	X: 0.0 (20) Y: NA	NA	NA	NA
All Climates (comparative)	X: 0.6 (135) **Y: 4.5 (182)**	Comparison not possible	Comparison not possible	Comparison not possible

Table 6.17: Average severity of snail tracks in Group X and Group Y modules in Hot and Non-Hot zones

Climatic Zone	Group	Age Group			
		0 - 5 yrs old	**5 - 10 yrs old**	**10 - 20 yrs old**	**20+ yrs old**
Hot Zone	**Group X**	0.8 (115)	2.7 (121)	0.0 (19)	NA (0)
	Group Y	3.3 (185)	NA (0)	0.0 (30)	0.0 (14)
Non-Hot Zone	**Group X**	0.0 (65)	NA (0)	0.0 (76)	NA (0)
	Group Y	3.9 (60)	NA (0)	NA (0)	NA (0)

The average severity of snail tracks in small/medium and large installations in Group A have been compared in Table 6.18. Large installations are mostly the MW scale power plants. The highest average severity is seen in the Large installations in Hot zones. Also, interestingly, the younger modules show a greater propensity to snail tracks. It may be noted that snail track formation not only depends on the cracks in the cells, but also the combination of silver paste, backsheet and encapsulating material used in module manufacturing, so there may be cracks in the modules even though snail tracks are not formed. So, while presence of snail track indicates presence of cracked cell, the reverse is not true.

Table 6.18: Average severity of snail tracks in Group A modules for small/medium and large installations in the Hot and Non-Hot climatic zones (number of samples is given in brackets).

Size of Installation	Climatic Zone	Age Groups			
		0-5 Years	5-10 Years	10-20 Years	20+ Years
Small/ Medium	Hot	0.4 (195)	0.0 (56)	0.0 (49)	0.0 (14)
	Non-Hot	2.4 (100)	NA (0)	0.0 (76)	NA (0)
Large	Hot	5.9 (105)	5.1 (65)	NA (0)	NA (0)
	Non-Hot	0.0 (25)	NA (0)	NA (0)	NA (0)

Based on the above discussion, we may conclude that non-framing type snail tracks are more common in Group Y as compared to Group X, and the average severity is also higher in Group Y. Large installations seem to have higher severity of snail tracks as compared to small/medium installations. It should be noted here that snail tracks are formed due to cracks, but also the other materials play a major role [46], so one should be careful that fewer (or no) snail tracks do not necessarily mean fewer (or no) cell cracks.

Framing type Snail tracks

Framing type snail tracks occur along the edges of the solar cells, and are not associated with cracks. The statistics for such snail tracks for the various climatic zones and age categories are presented in Table 6.19, and the climatic zones have been combined into Hot and Non-Hot in Table 6.20. Framing has been observed in the modules less than 10 years old, in all zones except the Cold zones. Group Y sites have higher percentage of affected modules as compared to Group X sites. The average severity (% of cells affected per module) has been presented in Tables 6.21 and 6.22. Group Y modules have higher severity of framing type snail tracks as compared to the Group X modules, in both Hot and Non-Hot climates. Also, the average severity for both Group X and Group Y are higher in Hot zone as compared to Non-Hot zone.

We can conclude that snail tracks (and cracks accompanying them) can be one of the reasons for the poorer performance of Group Y modules, as well as higher degradation in Hot zones.

Table 6.19: Percentage of modules affected by framing type snail tracks in Group A

Climatic Zone	0 - 5 yrs old	5 - 10 yrs old	10 - 20 yrs old	20+ yrs old
Hot & Dry	0% (63)	39% (41)	0% (30)	0% (14)
Warm & Humid	4% (138)	0% (68)	0% (7)	NA
Composite	21% (99)	0% (14)	0% (15)	NA
Moderate	3% (80)	NA	NA	NA
Cold & Sunny	0% (25)	NA	0% (76)	NA
Cold & Cloudy	0% (20)	NA	NA	NA
All Zones	**8.2% (546)**		0% (139)	

Table 6.20: Percentage of modules with framing type snail tracks in Group X and Group Y modules in Hot and Non-Hot zones

Climatic Zone	Group	0 - 5 yrs old	5 - 10 yrs old	10 - 20 yrs old	20+ yrs old
Hot Zone	Group X	5% (115)	13% (121)	0% (19)	NA (0)
	Group Y	11% (185)	NA (0)	0% (30)	0% (14)
Non-Hot Zone	Group X	0% (65)	NA (0)	0% (76)	NA (0)
	Group Y	3% (60)	NA (0)	NA (0)	NA (0)

Table 6.21: Average severity of framing type snail tracks in Group X and Group Y modules

Climatic Zone	Age Group			
	0 - 5 yrs old	5 - 10 yrs old	10 - 20 yrs old	20+ yrs old
Hot & Dry	X: NA Y: 6.3 (63)	X: 39.0 (41) Y: NA	X: NA Y: 0.0 (30)	X: NA Y: 0.0 (14)
Warm & Humid	X: 7.1 (85) Y: 0.0 (53)	X: 0.0 (66) Y: NA	X: 0.0 (4) Y: NA	NA
Composite	X: 3.3 (30) Y: 31.3 (69)	X: 0.0 (14) Y: NA	X: 0.0 (15) Y: NA	NA
Moderate	X: 0.0 (20) Y: 3.3 (60)	NA	NA	NA
Cold & Sunny	X: 0.0 (25) Y: NA	NA	X: 0.0 (76) Y: NA	NA
Cold & Cloudy	X: 0.0 (20) Y: NA	NA	NA	NA
All Climates (comparative)	X: 5.2 (135) **Y: 12.9 (182)**	Comparison not possible	Comparison not possible	Comparison not possible

Table 6.22: Average severity of framing type snail tracks in Group X and Group Y modules in Hot and Non-Hot zones

Climatic Zone	Group	Age Group			
		0 - 5 yrs old	5 - 10 yrs old	10 - 20 yrs old	20+ yrs old
Hot Zone	Group X	6.1 (115)	13.2 (121)	0 (19)	NA
	Group Y	13.0 (185)	NA	0 (30)	0 (14)
Non-Hot Zone	Group X	0 (65)	NA	0 (76)	NA
	Group Y	3.3 (60)	NA	NA	NA

Visible Cracks (Non-framing type Snail tracks and Photo-bleaching)

As discussed earlier, snail tracks in young modules and photo-bleaching effects in the old modules can serve as visual indications of cracks, and in some cases the cracks in solar cells are wide enough to be visible without sophisticated tools, as shown in Fig. 6.6(a). Modules showing visible cracks in the solar cells, or indication of cracks in terms of snail tracks and photo-bleaching, have been identified and their statistics is shown in Table 6.23. Cracks in the modules less than 10 years in age are mostly identified through the snail tracks, while for those more than 10 years old, cracks are mostly identified through photo-bleaching effect on discolored encapsulant. It can be seen that 31% of the modules installed in the last decade show visible signs of cracks compared to 29% of the modules older than 10 years, considering modules under Group A. However, if we consider all c-Si modules including the outliers, then the difference becomes significant (31% for modules aged less than 10 years have visible cracks as compared to 24% of modules aged more than 10 years). This suggests that cracks are more prevalent in the recent installations as compared to the older systems (but it's only a hint and no conclusion can be reached based on this data alone, since cracks may not always lead to visible signs).

(a) (b) (c)

Fig. 6.6: (a) Crack in the solar cell visible with naked eye, (b) Crack made visible by snail track, and (c) Crack made visible by photo-bleaching of discolored encapsulant.

Table 6.23: Percentage of modules with visible indications of cracks (snail tracks and photo-bleaching) in Group A

Climatic Zone	Age Group			
	0 - 5 yrs old	**5 - 10 yrs old**	**10 - 20 yrs old**	**20+ yrs old**
Hot & Dry	29% (63)	22% (41)	0% (30)	0% (14)
Warm & Humid	9% (138)	58% (66)	50% (4)	NA
Composite	61% (99)	29% (14)	0% (15)	NA
Moderate	31% (80)	NA	NA	NA
Cold & Sunny	0% (25)	NA	39% (76)	NA
Cold & Cloudy	0% (20)	NA	NA	NA
All Zones	31% (546)		29% (139)	

As done in the case of snail tracks, the severity of visible cracks in a module is determined based on the percentage of affected cells per module. The average severity of all the modules inspected in the various climatic zones and age groups is shown in Table 6.24. This table is color coded for the ease of interpretation, and the coding scheme is same as shown in Table 6.14. It can be seen that the modules in "5-10 years" age group in Warm & Humid zone have the highest severity, followed by the "Young" modules in Composite, Moderate and Hot & Dry zones. It can be seen that the severity levels are generally lower in the more than 10 years old modules as compared to the newer modules, which raises concern about the cracks being induced in the modules during the transportation or installation. Also, the cells in the modules have been made thinner in recent years to reduce the cell and module costs, and this may be another reason for the excessive cracks being seen in the newer modules.

Table 6.24: Average severity of visible cracks (including snail tracks and photo-bleaching) in Group A

Climatic Zone	Age Group			
	0 - 5 yrs old	5 - 10 yrs old	10 - 20 yrs old	20+ yrs old
Hot & Dry	2.7 (63)	1.6 (41)	0.0 (30)	0.0 (14)
Warm & Humid	0.6 (138)	**23.6 (66)**	3.5 (4)	NA
Composite	6.0 (99)	3.6 (14)	0.0 (15)	NA
Moderate	3.0 (80)	NA	NA	NA
Cold & Sunny	0.0 (25)	NA	2.8 (76)	NA
Cold & Cloudy	0.0 (20)	NA	NA	NA
Climatic zone with the highest average	Composite	Warm & Humid	Warm & Humid	-

Table 6.25 shows the severity of visible cracks (including snail tracks and photo-bleaching), for group X and group Y modules in the Hot and Non-Hot zones. Among the Young modules, average severity of visible cracks is higher in group Y as compared to group X sites. Comparing the severity in the group X modules in "10-20 years" age group, it is found that the severity is higher in Non-Hot zone as compared to Hot zone, but no conclusion can be made as sample size is quite low in the Hot zone.

Table 6.25: Average severity of visible cracks (including snail tracks and photo-bleaching) in Group X and Group Y modules in Hot and Non-Hot zones

Climatic Zone	Group	Age Group			
		0 - 5 yrs old	5 - 10 yrs old	10 - 20 yrs old	20+ yrs old
Hot Zone	**Group X**	1.3 (115)	13.8 (121)	0.7 (19)	NA (0)
	Group Y	3.9 (185)	NA (0)	0.0 (30)	0.0 (14)
Non-Hot Zone	**Group X**	0.0 (65)	NA (0)	2.8 (76)	NA (0)
	Group Y	4.0 (60)	NA (0)	NA (0)	NA (0)

The severity of visible cracks in small/medium and large installations is presented in Table 6.26. The highest severity is seen in the small/medium installations in Hot zone. Among the young modules, "Large" installations are having higher severity than the small/medium sites. Detailed analysis of the large installation sites has shown that close to 66% of the modules are affected by snail tracks, which is a cause for concern.

Table 6.26: Average severity of visible cracks (including snail tracks and photo-bleaching) in Group A modules for small/medium and large installations in the Hot and Non-Hot climatic zones (number of samples is given in brackets).

Size of Installation	Climatic Zone	Age Groups			
		0-5 Years	5-10 Years	10-20 Years	20+ Years
Small/ Medium	Hot	0.9 (195)	23.1 (56)	0.3 (49)	0.0 (14)
	Non-Hot	2.4 (100)	NA (0)	2.8 (76)	NA (0)
Large	Hot	6.5 (105)	5.8 (65)	NA (0)	NA (0)
	Non-Hot	0.0 (25)	NA (0)	NA (0)	NA (0)

In conclusion it can be said that snail tracks (and visible cracks) are seen more in group Y modules as compared to group X modules, and is one of the distinguishing factors between the two groups. Highest severity of visible cracks is seen in small/medium installations in the Hot zone, though significant snail track severity is also seen in the large installations, and this calls for improvement in the installation practices in order to prevent crack formation.

d) Discoloration on Metallization

The function of the metallization in the solar panels – gridlines, busbars and interconnect ribbons – is to conduct the current generated in the solar cells to the terminal box. Metallization discoloration can occur due to corrosion and sometimes due to improper manufacturing processes. Some examples of metallization discoloration are shown in Fig. 6.7. The statistics for metallization discoloration (including interconnects and output terminals inside junction box) for the different age groups and climatic zones is shown in Table 6.27. The discoloration of metallization in the young modules (0 – 5 years age category) is predominantly due to non-corrosion issues (like discoloration due to solder flux etc.) whereas in the older modules, corrosion is the predominant reason behind such discoloration. As evident from the table, many young modules in the hot climates have discoloration issues that hint at poor manufacturing practices. Most of the panels aged more than 10 years have suffered from corrosion, irrespective of the climatic zone. Tables 6.28 and 6.29 show the statistics for Group X and Group Y, and it can be seen that percentage of modules affected is higher in Group Y than in Group X.

Table 6.27: Percentage of modules in Group A affected by discoloration on metallization in different climatic zones and age groups (number of samples is given in brackets).

Climatic Zone	Age Groups				Total
	0-5 Years	5-10 Years	10-20 Years	20-30 Years	
Hot & Dry	100% (63)	39% (41)	100% (30)	100% (14)	83% (148)
Warm & Humid	64% (138)	98% (66)	100% (4)	NA	76% (208)
Composite	29% (99)	29% (14)	100% (15)	NA	38% (128)
Moderate	95% (80)	NA	NA	NA	95% (80)
Cold & Sunny	0% (25)	NA	100% (76)	NA	75% (101)
Cold & Cloudy	0% (20)	NA	NA	NA	0% (20)

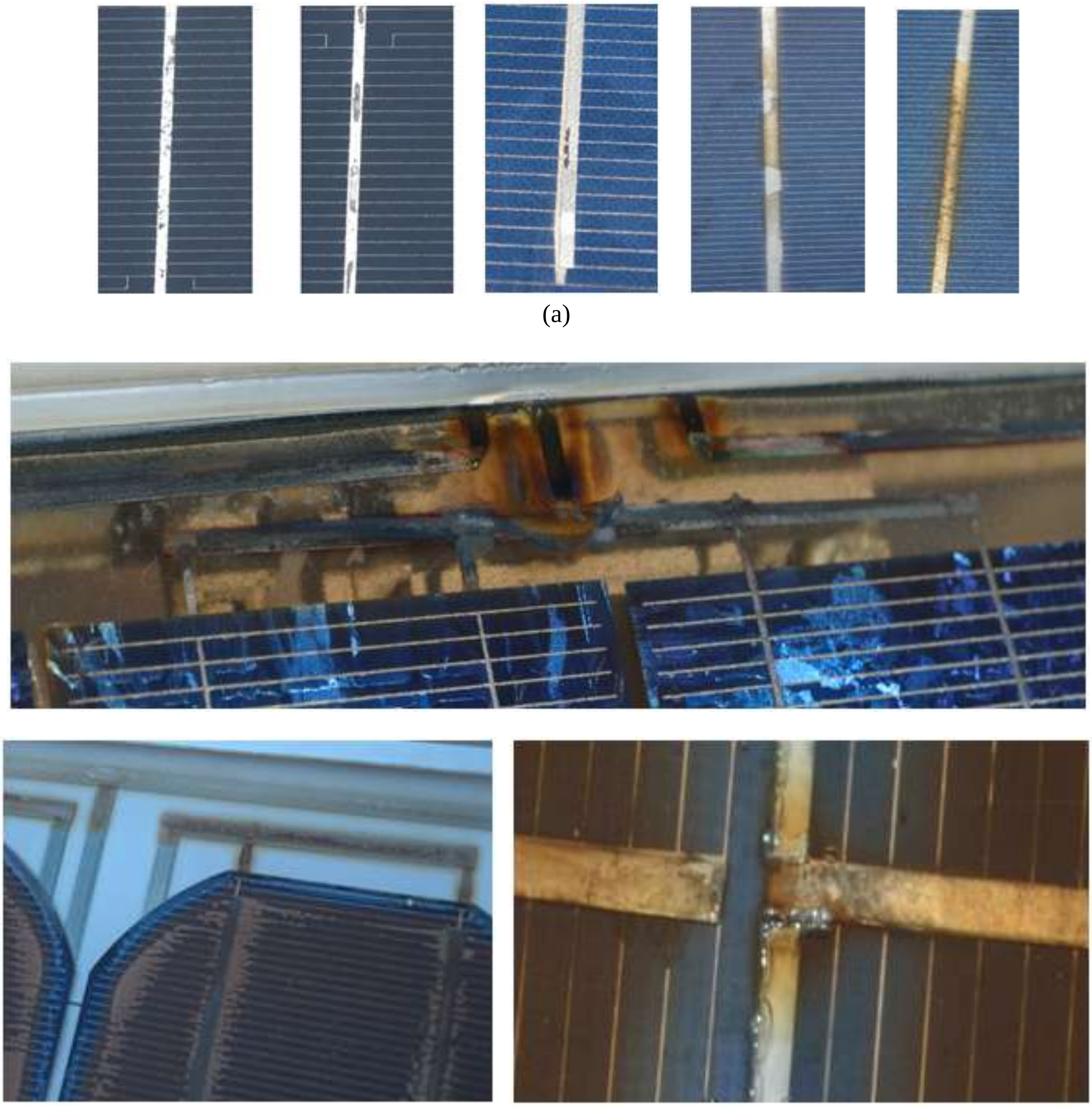

(a)

(b)

Fig. 6.7: Metallization discoloration on interconnect ribbons observed during the survey – (a) discoloration patterns in cell interconnects observed in young modules, and (b) corrosion in interconnect ribbons observed in old modules.

Table 6.28: Comparison of Groups X and Y for discoloration of metallization in different climatic zones and age groups (number of samples is given in brackets).

Climatic Zone	Age Groups			
	0-5 Years	**5-10 Years**	**10-20 Years**	**20+ Years**
Hot & Dry	X: NA Y: 100% (63)	X: 39% (41) Y: NA	X: NA Y: 100% (30)	X: NA Y: 100% (14)
Warm & Humid	X: 60% (85) Y: 72% (53)	X: 98% (66) Y: NA	X: 100% (4) Y: NA	NA
Composite	X: 0% (30) Y: 42% (69)	X: 29% (14) Y: NA	X: 100% (15) Y: NA	NA
Moderate	X: 100% (20) Y: 93% (60)	NA	NA	NA
Cold & Sunny	X: 0% (25) Y: NA	NA	X: 100% (76) Y: NA	NA
Cold & Cloudy	X: 0% (20) Y: NA	NA	NA	NA
All Climates (comparative)	X: 53% (135) **Y: 68% (182)**	Comparison not possible	Comparison not possible	Comparison not possible

Table 6.29: Percentage of modules with metallization discoloration in Group X and Group Y (shown for Hot and Non-Hot zone separately)

Climatic Zone	Group	0 - 5 yrs old	5 - 10 yrs old	10 - 20 yrs old	20+ yrs old
Hot Zone	**Group X**	44% (115)	70% (121)	100% (19)	NA
	Group Y	70% (185)	NA	100% (30)	100% (14)
Non-Hot Zone	**Group X**	31% (65)	NA	100% (76)	NA
	Group Y	93% (60)	NA	NA	NA

The extent of metallization discoloration has been estimated from the visual images of the modules in terms of the Metallization Discoloration Index (MDI) [2]. The discoloration in different metallic current-carrying components of the module like fingers, busbars and interconnects have been summed up by using the following formula. The output terminals have also been included in the calculation of the Metallization Discoloration Index (MDI), as it would affect the overall resistance to the current flow.

$$\text{MDI} = \frac{\sum_{i=1}^{n}(\text{degree of discoloration of ith component x affected area category of the component})}{\text{Maximum possible value of the numerator i.e. } 2\text{x}5\text{x}n} \quad ...(6.2)$$

where, degree of discoloration = 0 (no discoloration),

= 1 (for light discoloration),

= 2 (for dark discoloration)

Affected area category is determined based on the percentage area of the module's metallization affected by discoloration, as given in following table.

Table 6.30: Affected area category for metallization discoloration

Affected area	0 – 5%	5 – 25%	25 – 50%	50 – 75%	75-100%
Area Category	1	2	3	4	5

The index *i* indicates a visible metallization component like fingers, busbars, interconnects and output terminals. Its value can vary from 1 to the total number of visible metallization components (denoted by *n*). For example, for the standard c-Si modules available in the market, *i* =1 will represent the fingers, *i* = 2 will represent the busbars and cell interconnects, *i* =3 will represent the string interconnects, *i* = 4 will represent the output terminals, and in such a case *n* is equal to 4. The value of *n* can vary depending on the module design, like in some modules, string interconnects are not visible externally, so total number of visible metallization components *n* becomes 3. Further in some module designs, there may be no visible metallization at all, in which case this method cannot be applied.

Based on the above index, the modules have been grouped into 5 categories as shown in Table 6.31. The metallization discoloration data for Group X modules is shown in Table 6.32. The MDI values are low in the young modules, since the discoloration is mostly related to yellow or black spots on cell interconnects (refer Fig. 6.6a). The highest MDI values are seen in the Warm & Humid zone, both for “5-10 years” and “10-20 years” categories. Further, for the “10-20 years” age group, discoloration of metallization (which is mainly due to corrosion in these old modules) is more severe in the Warm & Humid and Composite zones as compared to the Cold & Sunny climate. Table 6.33 compares the average MDI values for Group X and Group Y sites. The highest metallization discoloration has been found in 27 year old modules from Hot zone, which fall in Group Y category. These modules have glass-glass construction, and were located in Hot & Dry climate. Hence we can rule out moisture as being responsible for corrosion, but instead the decomposition products of the encapsulant might have played a major role in the corrosion (since these products could not escape due to the glass at both front and backside of the module). In the “10-20 Years” age group, Group X modules have higher average MDI value as compared to Group Y modules, but in the young modules, there is not much difference between Group X and Group Y. Based on this it can be said that metallization discoloration does not appear to be a factor in causing the higher degradation rates observed in Group Y modules.

Table 6.31: Metallization discoloration category based on MDI

Metallization Discoloration Index	0	0 – 0.25	0.25 – 0.5	0.5 – 0.75	0.75 - 1
Metallization Discoloration Category	Nil	Low	Medium	High	Very High

Table 6.32: Average extent of discoloration in metallization in Group X modules in different climatic zones and age groups (number of samples is given in brackets).

Climatic Zone	Age Group			
	0-5 Years	5-10 Years	10-20 Years	20+ Years
Hot & Dry	NA	0.04 (41)	NA	NA
Warm & Humid	0.03 (85)	0.13 (66)	0.36 (4)	NA
Composite	0.00 (30)	0.03 (4)	0.30 (15)	NA
Moderate	0.06 (20)	NA	NA	NA
Cold & Sunny	0.00 (25)	NA	0.18 (76)	NA
Cold & Cloudy	0.00 (20)	NA	NA	NA
Climatic zone with highest index value	Moderate	Warm & Humid	Warm & Humid	NA

Table 6.33: Average extent of discoloration in metallization in Group X and Group Y (shown for Hot and Non-Hot zone separately)

Climate	Group	Age Groups			
		0-5 Years	5-10 Years	10-20 Years	20+ Years
Hot	**Group X**	0.02 (115)	0.09 (121)	0.31 (19)	NA
	Group Y	0.03 (185)	NA	0.17 (30)	0.74 (14)
Non-Hot	**Group X**	0.02 (65)	NA	0.18 (76)	NA
	Group Y	0.04 (60)	NA	NA	NA

Table 6.34 gives the average severity of metallization discoloration for the modules in small/medium and large installations, and it can be seen that small installations have slightly higher degradation index as compared to large installations.

Table 6.34: Average extent of discoloration in metallization in Group A modules for small/medium and large installations in the Hot and Non-Hot climatic zones and various age groups (number of samples is given in brackets).

Size of Installation	Climatic Zone	Age Groups			
		0-5 Years	5-10 Years	10-20 Years	20+ Years
Small/ Medium	**Hot**	0.03 (195)	0.17 (46)	0.22 (49)	0.74 (14)
	Non-Hot	0.04 (100)	NA	0.18 (76)	NA
Large	**Hot**	0.02 (105)	0.04 (65)	NA	NA
	Non-Hot	0.0 (25)	NA	NA	NA

In conclusion, it can be said that the Hot zone is more harsh than the Non-Hot zone from the metallization discoloration perspective. Percentage of affected modules is higher in Group Y as compared to Group X. Small/medium installations have a higher average severity as compared to large installations, which points at the difference in material quality used in these installations.

e) Backsheet Degradation

The backsheet performs the function of providing electrical insulation and minimizing moisture ingress into the module. Unlike the other outer components of the module (front glass and aluminum frame), the backsheet is very vulnerable to mishandling, resulting in scratches. Other defects include de-adhesion (which causes bubbles and delamination), cracking, chalking etc. which are shown in Fig. 6.8.

(a)

(b)

(c)

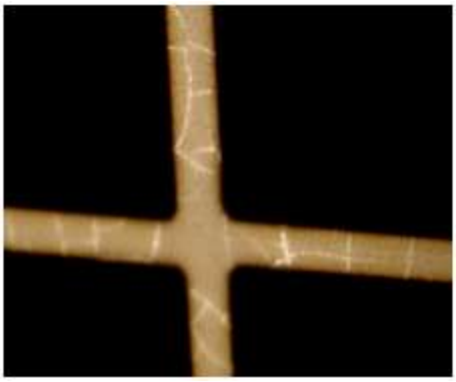

(d)

Fig. 6.8: Backsheet degradation observed during the survey – (a) Chalking, (b) scratch and delamination, (c) cracks in outer layer of backsheet, (d) cracks observed outside the edges of the solar cells.

Table 6.35 provides the statistics of modules with backsheet damage (includes chalking, discoloration, bubbles, scratches and cracking) observed during the survey. There is considerable degradation of the backsheet in all climates. More than 30% of the young modules show problems of the backsheet, which indicates use of poor quality materials in these modules and/or improper handling and installation practices. Table 6.36 shows the comparison of modules in Groups X and Y, and there does not seem to be significant difference between the two groups (based on comparative analysis shown in bottom of the Table, for which only those categories are compared which has samples from both Group X and Group Y). Similar conclusions can also be drawn from Table 6.37, which combines the climatic zones into Hot and Non-Hot.

Table 6.35: Percentage of Group A modules affected by degradation of backsheet in different climatic zones and age groups (number of samples is given in brackets).

Climatic Zone	Age Groups			
	0-5 Years	5-10 Years	10-20 Years	20-30 Years
Hot & Dry	6% (63)	56% (41)	100% (30)	NA
Warm & Humid	36% (138)	15% (66)	100% (4)	NA
Composite	20% (99)	29% (14)	67% (15)	NA
Moderate	56% (80)	NA	NA	NA
Cold & Sunny	24% (25)	NA	100% (76)	NA
Cold & Cloudy	65% (20)	NA	NA	NA

Table 6.36: Comparison of Groups X and Y for backsheet degradation in different climatic zones and age groups (number of samples is given in brackets).

Climatic Zone	Age Groups			
	0-5 Years	5-10 Years	10-20 Years	20+ Years
Hot & Dry	X: NA Y: 6% (63)	X: 56% (41) Y: NA	X: NA Y: 100% (30)	NA
Warm & Humid	X: 35% (85) Y: 37% (53)	X: 15% (66) Y: NA	X: 100% (4) Y: NA	NA
Composite	X: 10% (30) Y: 25% (69)	X: 29% (14) Y: NA	X: 67% (15) Y: NA	NA
Moderate	X: 100% (20) Y: 42% (60)	NA	NA	NA
Cold & Sunny	X: 24% (25) Y: NA	NA	X: 100% (76) Y: NA	NA
Cold & Cloudy	X: 65% (20) Y: NA	NA	NA	NA
All Climates (comparative)	X: 39% (135) Y: 34% (182)	Comparison not possible	Comparison not possible	Comparison not possible

Table 6.37: Percentage of modules with backsheet degradation in Group X and Group Y (shown for Hot and Non-Hot zone separately)

Climatic Zone	Group	0 - 5 yrs old	5 - 10 yrs old	10 - 20 yrs old	20+ yrs old
Hot Zone	Group X	29% (115)	31% (121)	74% (19)	NA
	Group Y	22% (185)	NA	100% (30)	100% (14)
Non-Hot Zone	Group X	60% (65)	NA	100% (76)	NA
	Group Y	42% (60)	NA	NA	NA

For quantifying the extent of backsheet degradation of a module, a Backsheet Degradation Index (BDI) has been developed based on the affected module area, which can be calculated as follows:

$$\text{Backsheet Degradation Index} = \frac{\text{severity of chalking} + \text{severity of burns} + \text{severity of bubbles} + \text{severity of cracks}}{\text{Maximum value of numerator}} \quad \ldots (6.3)$$

Where, severity of chalking = 2.5 for slight chalking,
= 5 for excessive chalking

The severity of burns, bubbles and cracks is decided based on the affected module area as follows:

Table 6.38: Severity category for backsheet defects

Affected area	0-5%	5-25%	25 – 50%	50 – 75%	>75%
Severity Category	1	2	3	4	5

The maximum value of the numerator is 20, and the BDI can vary in the range of 0 to 1. Based on this backsheet degradation index, the modules have been binned into 5 categories as mentioned below.

Table 6.39: Degradation category for backsheet

Backsheet Degradation Index	0	0 – 0.1	0.1 – 0.25	0.25 – 0.5	>0.5
Backsheet Degradation Category	Nil	Low	Medium	High	Very High

Table 6.40 gives the average backsheet degradation index for different age groups and climatic zones, for Group X sites. It is evident that the Hot zones are more severe for the backsheet as compared to the Non-Hot zone, which is not unexpected. In the young modules in Warm & Humid climate, bubbles have been observed in all modules at one site while at another site, there were minor crack lines along cell edges. Also, crack lines were observed in some of the young modules in Moderate climate. Burn marks were observed in a young module in the Composite climate. Among the old modules, chalking was observed in all climates, and additionally bubbles and burn marks were observed in the Warm & Humid climate.

Table 6.40: Average extent of backsheet degradation in Group X modules in different climatic zones and age groups (number of samples is given in brackets).

Climatic Zone	**Age Groups**			
	0-5 Years	**5-10 Years**	**10-20 Years**	**20+ Years**
Hot & Dry	NA	0.01 (41)	NA	NA
Warm & Humid	0.03 (85)	0.01 (66)	0.24 (4)	NA
Composite	0.00 (30)	0 (14)	0.04 (15)	NA
Moderate	0.05 (20)	NA	NA	NA
Cold & Sunny	0 (25)	NA	0.13 (76)	NA
Cold & Cloudy	0 (20)	NA	NA	NA

Table 6.41 shows the BDI values by combining the climatic zones into Hot and Non-Hot. We can see that there does not seem to be any significant difference between the Group X and Group Y modules in young age (0-5 years old), but the Group Y modules in the '10-20 years' category in Hot zone are showing significantly higher degradation index compared to Group X modules. These Group Y modules suffer from both chalking and bubbles. This seems to indicate that the use of poor quality backsheets would affect the performance of the modules in the long run (and not so much in the short term). For the '10-20 years' old modules in Group X, the BDI is higher in Non-Hot zone as compared to the Hot zone, which may be due to the higher UV radiation in the Cold & Sunny sites which are at very high altitudes (Leh is about 3500 m above sea level, and UV radiation increases by 10% for every 1000 m increase in altitude). Some of the young modules are showing degradation in the backsheet within 5 years of outdoor exposure, which may cause degradation in the module's performance in the long run and is not a good sign for the long term reliability of the modules.

Table 6.41: Average extent of backsheet degradation in Group X and Group Y modules in Hot and Non-Hot climatic zones for different age groups (number of samples is given in brackets).

Climate	Group	Age Groups			
		0-5 Years	5-10 Years	10-20 Years	20+ Years
Hot	Group X	0.02 (115)	0.01 (121)	0.08 (19)	NA
	Group Y	0.00 (185)	NA	0.23 (30)	NA
Non-Hot	Group X	0.02 (65)	NA	0.13 (76)	NA
	Group Y	0.02 (60)	NA	NA	NA

Table 6.42 gives the average BDI values for the modules in small/medium and large installations, and it seems that the average BDI values are similar in each age group. The highest BDI is found for the small/medium installations in the '10-20 Years' age group in Hot zone, but we do not have any comparative data for the large installations in this age category.

Table 6.42: Average extent of backsheet degradation in Group A modules for small/medium and large installations in the Hot and Non-Hot climatic zones and various age groups (number of samples is given in brackets).

Size of Installation	Climatic Zone	Age Groups			
		0-5 Years	5-10 Years	10-20 Years	20+ Years
Small/ Medium	Hot	0.01 (194)	0.00 (56)	0.17 (49)	NA
	Non-Hot	0.02 (100)	NA	0.13 (76)	NA
Large	Hot	0.01 (105)	0.01 (65)	NA	NA
	Non-Hot	0.00 (25)	NA	NA	NA

Based on the above discussion we conclude that backsheet degradation is comparable in the young modules in Group X and Group Y, but in the old modules, the severity is higher for Group Y as compared to Group X. There is no difference between the average severities in the small/medium and large installations. Since backsheet degradation is a safety concern, it is important to use proper materials that can resist degradation in outdoor environment, and can provide the necessary levels of safety for the entire service life of the installation.

f) *Glass Degradation*

The front glass performs the role of protecting the solar cells from environmental factors like humidity and dust, while allowing the solar radiation to pass to the cells unhindered. The deposition of dust and the use of hard water in cleaning the modules can lead to haziness in the glass (which can reduce the transmission of light to the cells). Also, improper handling can lead to scratches, chips and cracks (shattering) in the front glass, as shown in Fig. 6.9. Table 6.43 gives the statistics for the various degradation modes of front glass observed in the survey. Haziness is the most prevalent problem observed in the front glass of crystalline silicon modules, occurring mostly at the bottom edge of the module.

(a) Haziness in glass observed in old modules

(b) Brown and white spots on front glass

(c) Scratch on glass

(d) Shattered glass

Fig. 6.9: Glass degradation observed during the survey.

Table 6.43: Statistics of crystalline silicon modules affected by damage in front glass

Type of damage	Percentage of modules affected	Additional Comments
Haziness in Glass	81%	No significant difference between Groups X and Y
Scratches in Glass	7.5%	No significant difference between Groups X and Y
White Spots on Glass (paint marks)	6.7%	Higher percentage of modules affected in Group X (9.6%) as compared to Group Y (3.2%)
Brown Spots on Glass	6.2%	Higher percentage of modules affected in Group Y (8.8%) as compared to Group X (3.6%)
Glass cracked/shattered	0%	-

g) *Frame Degradation*

The frame provides mechanical strength to the module, helps in keeping the various parts of the laminate together and also prevents moisture ingress through the edges of the module. Improper handling of the modules during installation and environmental stresses like heat and humidity can have an adverse impact on the frame, some examples of which are shown in Fig. 6.10. Table 6.42 shows the statistics of frame degradation observed during the 2016 survey, and it is evident that scratches on the frame are the most prevalent damage, indicating that the installation practices are not proper at many sites. Almost 11% of the young modules show scratches in the frame as compared to about 7% in the old modules. Also, frame grounding has been done in only 29% cases (31% in large installations versus 28% in small/medium sites), which means that a vast majority of modules pose a safety risk (if touched) particularly during the monsoons.

(a) Algae growth (b) Corrosion (c) Scratches (d) Joint separation

Fig. 6.10: Degradation of frame observed during the survey.

Table 6.44: Statistics of frame damage observed in the survey

Type of damage	Percentage of modules affected	Additional Comments
Scratches	9.4%	Percentage of young modules affected by scratches (10.8%) is slightly higher than the old modules (7%).
Corrosion	1.5%	Not seen in young modules
Bent	0.1%	Not seen in young modules
Joints separated	0.8%	Not seen in young modules
Cracking	0%	Not seen in young modules

h) *Junction Box Degradation*

The junction box provides protection to the output terminals of the PV module from the outside environment. Damage to the junction box will cause degradation in the output terminals, particularly corrosion due to humidity ingress, and this in turn will increase the series resistance and decrease the power output of the PV module. Some examples of Junction Box damage are given in Fig. 6.11, and Table 6.45 shows the statistics.

Fig. 6.11: Examples of damaged junction boxes observed during the survey in old modules.

Table 6.45: Statistics of junction box degradation observed in the survey

Type of damage	Percentage of modules affected	Additional Comments
Weathered, physically unsound or cracked	11.3%	Percentage of modules affected in Group Y (14.8%) is much higher than the modules affected in Group X (7.5%).
Poor sealing	14%	Percentage of modules affected in Group Y (15.5%) is higher than the modules affected in Group X (11.9%).
Lid missing, loose or cracked	3.1%	Not prevalent in young modules
Discoloration of output terminals (including tarnish and corrosion)	41%	Major corrosion is seen in only 5.7% cases (predominantly in the old modules).

6.2.2 Correlation of Visual Degradation with Electrical Performance Degradation

In this section, we correlate the visual defects observed with degradation in electrical performance, which was described in Chapter 4.

a) Encapsulant Discoloration

The primary effect of encapsulant discoloration is the reduction in the transmission of light to the underlying solar cells, which causes a reduction in the short circuit current and the power output. In order to check the effect of discoloration on these electrical parameters, the PV modules have been segregated into 5 categories based on the discoloration index, as per Table 6.44.

Table 6.46: Categorization based on discoloration index

Discoloration Index	0 – 0.05	0.05 – 0.25	0.25 – 0.5	0.5 – 0.75	0.75 – 1
Discoloration Category	1	2	3	4	5

Figure 6.12 shows the effect of encapsulant discoloration on short circuit current degradation, for modules from both Group X and Group Y sites. The modules with snail tracks and other visible signs of cracks have been removed from the dataset for this comparison, since the cracks may influence the short circuit current loss (this is analyzed separately). In these plots, the average degradation values are indicated using the red horizontal lines (and the top and bottom edges of the red diamond indicate the 95% confidence interval). The cumulative probability distribution is also shown on the right side of the scatter plot. It may be noted that there are no Group X modules in discoloration categories 4 and 5, and no Group Y modules in discoloration categories 3 to 5. In many cases, mostly in the young modules, the I_{sc} degradation has been found to be negative (which may be due to the uncertainty in the name plate data and also the uncertainty introduced by STC translation procedures which are discussed in detail in Chapter 3). It is interesting to note that the worst browning in the modules in Group X has caused close to 15% drop in I_{sc} (in 18 years of field exposure which means a degradation rate of ca. 0.83 %/year). The average I_{sc} degradation in Group Y is slightly higher than Group X (comparing discoloration category 2). For Group X modules, the average degradation values follow an almost linear trend. Considering category 1 as "light discoloration", and category 2 as "dark discoloration", it can be seen that the average I_{sc} degradation for dark discoloration is approximately twice that of the value for light discoloration (which is in agreement with the assumption used in 2014 survey analysis).

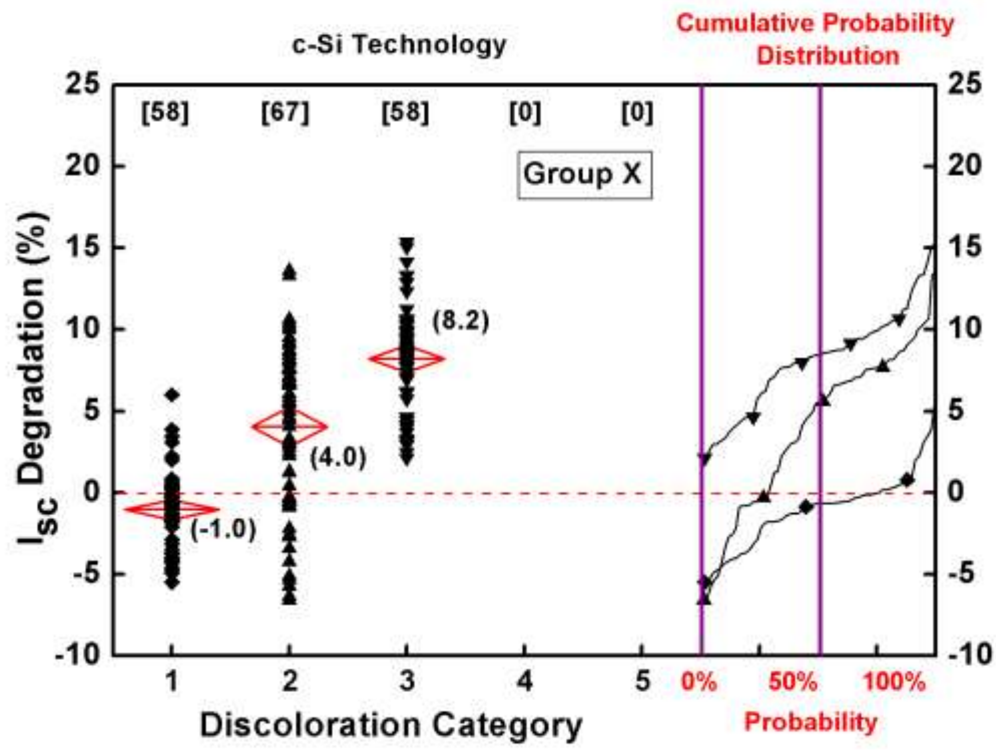

(a)

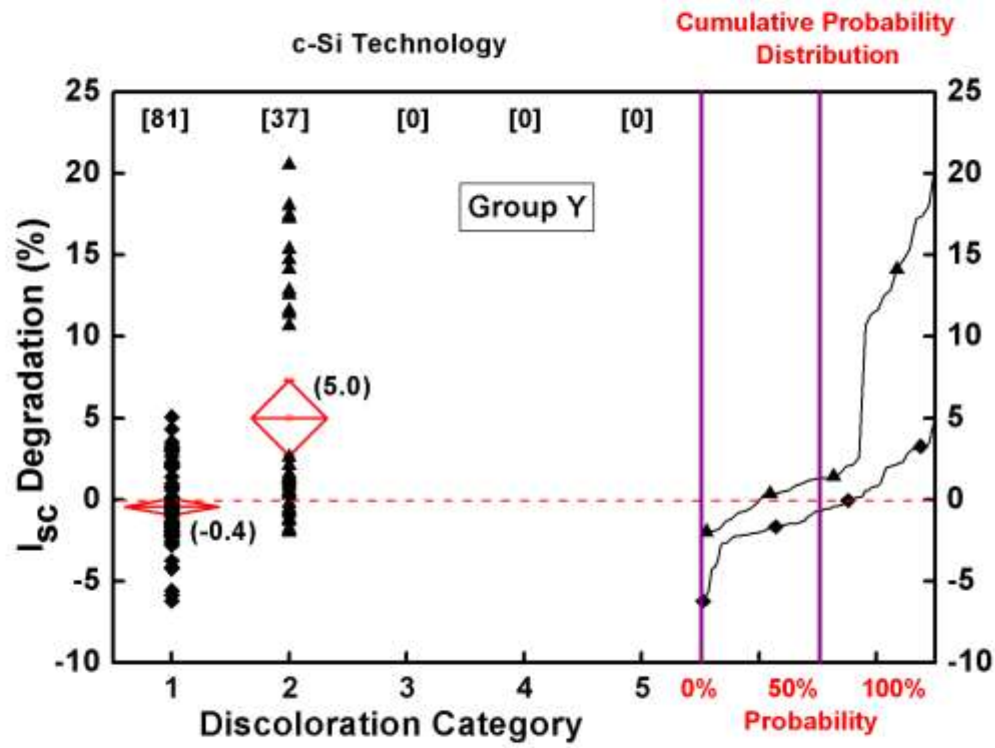

(b)

Fig. 6.12: Plot of short circuit current degradation versus severity of discoloration for (a) Group X modules, and (b) Group Y modules.

In Fig. 6.13, the total electrical degradation (% and not %/year) is plotted against the same discoloration categories. Almost linear trends are seen for V_{oc} and P_{max} degradation. In case of *FF* degradation, some of the young modules with almost no discoloration (category 1) show very high *FF* degradation which causes a departure from linear trend. It should also be noted that these modules have also suffered other degradations (particularly corrosion of metallization in the old modules, which reduces the fill factor and hence the power output). The worst discolored modules have suffered about 24% degradation in P_{max} in 18 years of field exposure, so the average Linear Degradation Rate for these modules is 1.2 %/year (after discounting 2% LID).

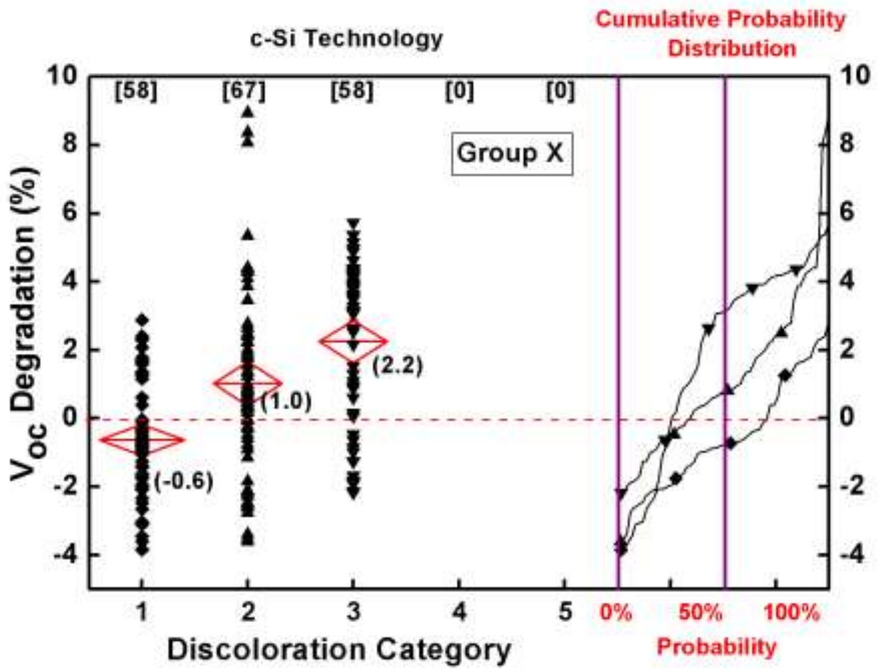

(a)

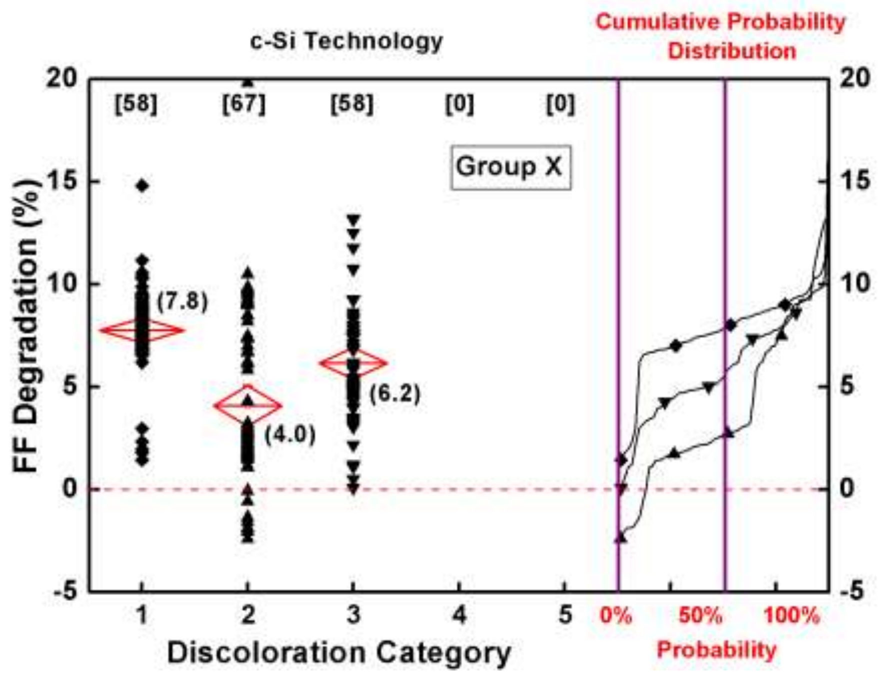

(b)

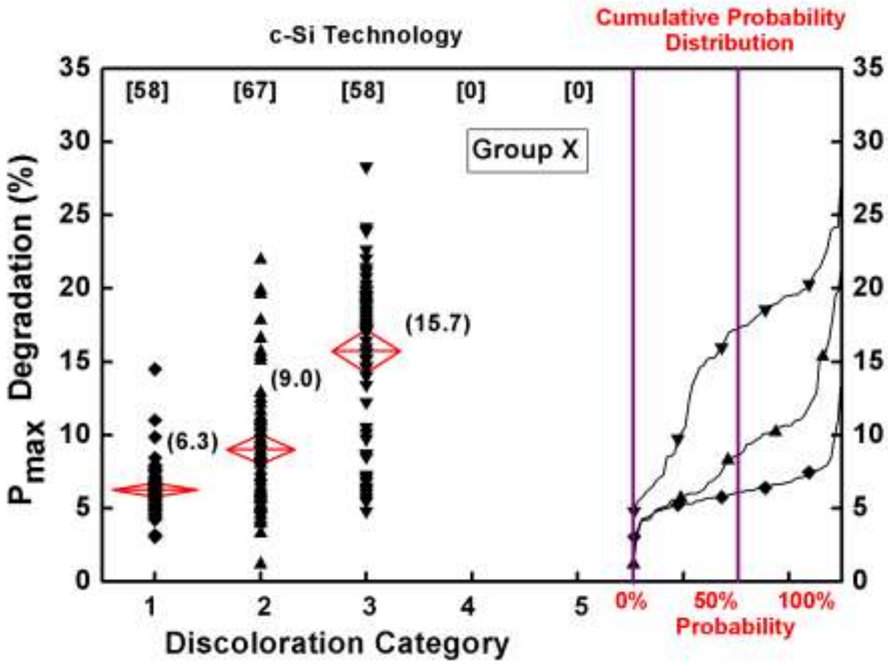

(c)

Fig. 6.13: Plot of electrical degradation versus extent of discoloration (Discoloration category) for Group X modules - (a) V_{oc} degradation (%), (b) *FF* degradation (%), and (c) P_{max} degradation (%).

b) Metallization Discoloration

Discoloration of metallization in modules is usually caused by corrosion in the older modules. This results in an increase in the series resistance of the modules. Fig. 6.14 shows the plot of the normalized series resistance versus the metallization discoloration category for modules of Group X and Group Y. Normalization of the series resistance has been done by dividing it with the number of cells in the module, so that modules of different sizes (ratings) can be compared. It can be seen that the normalized series resistance per cell increases with increase in the extent of metallization discoloration thereby indicating a positive correlation between the two (as expected from theory). The degradation in electrical parameters for different MDI categories have been plotted for Group A in Fig. 6.15. The rising trend is visible for all electrical parameters. The Mann-Whitney-Wilcoxon test has confirmed that all the categories in the electrical degradation plots for Group A are statistically different distributions.

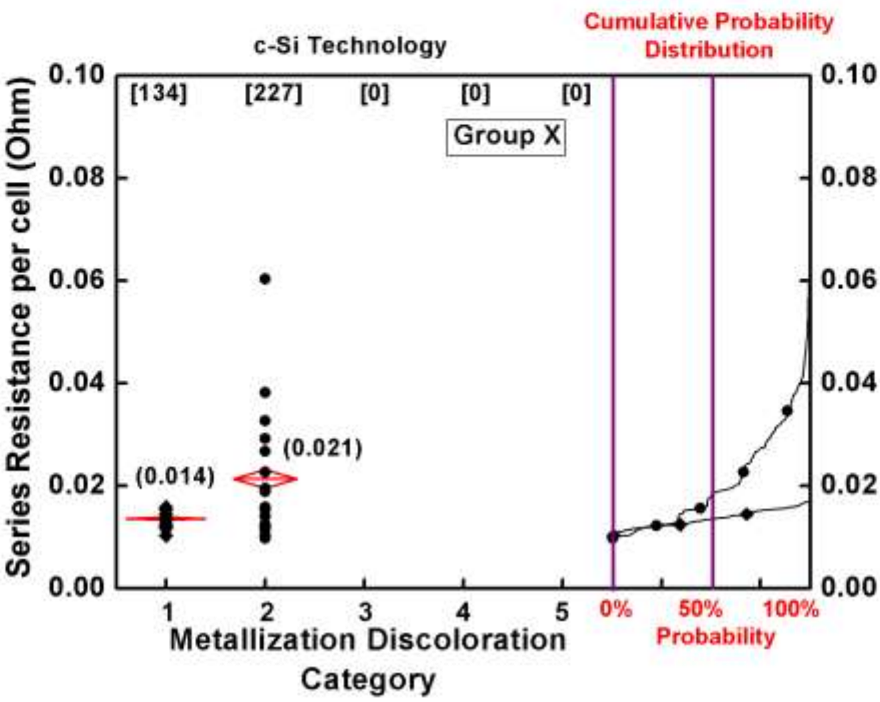

(a)

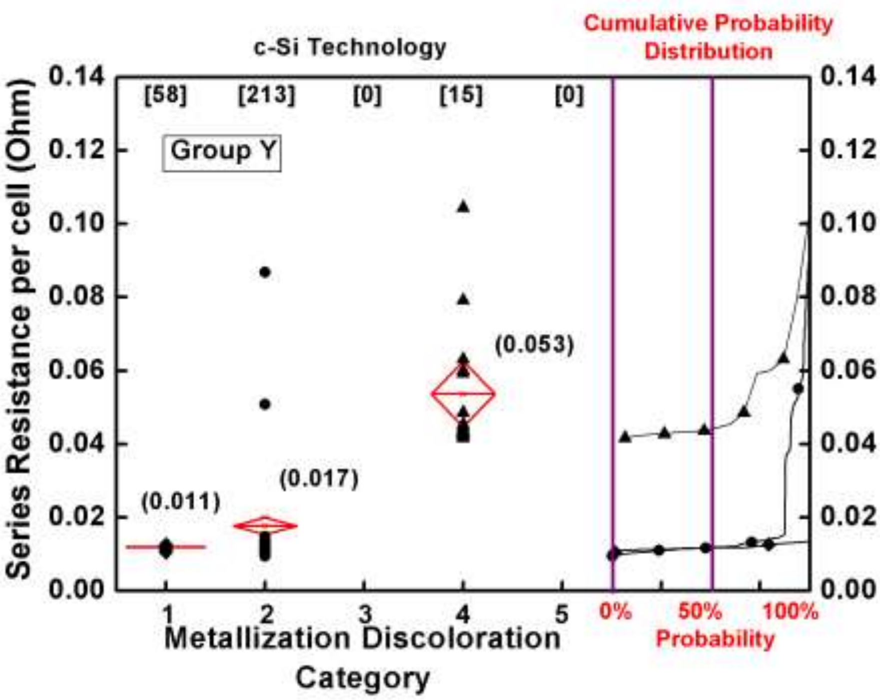

(b)

Fig. 6.14: Plot of series resistance per cell versus severity of metallization discoloration (MDI category), for (a) Group X modules, and (b) Group Y modules.

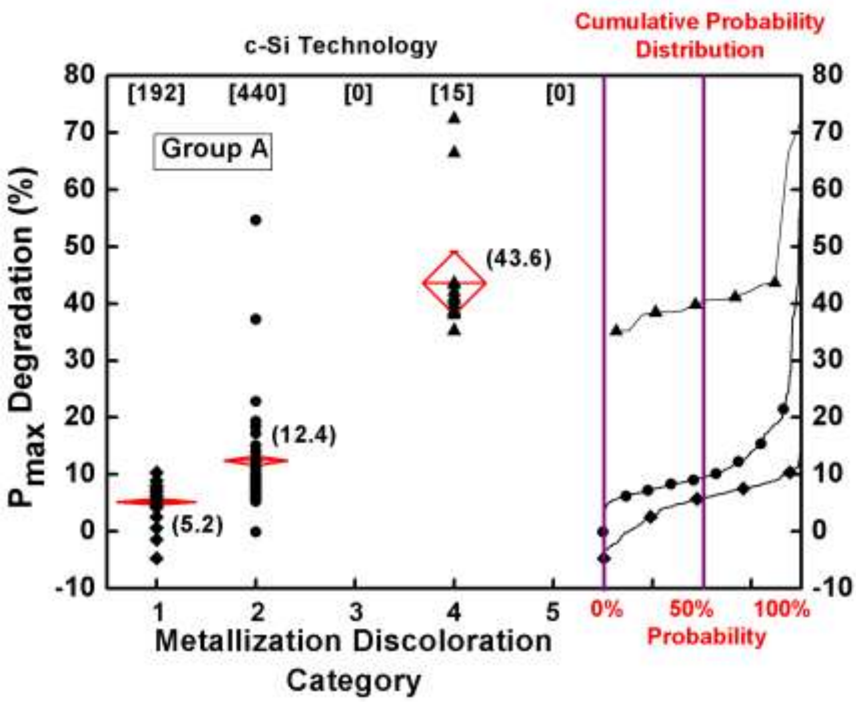

c-Si Technology
Cumulative Probability Distribution
Group A
[192] [440] [0] [15] [0]
(43.6)
(12.4)
(5.2)
P_{max} Degradation (%)
Metallization Discoloration Category
0% 50% 100%
Probability

(a)

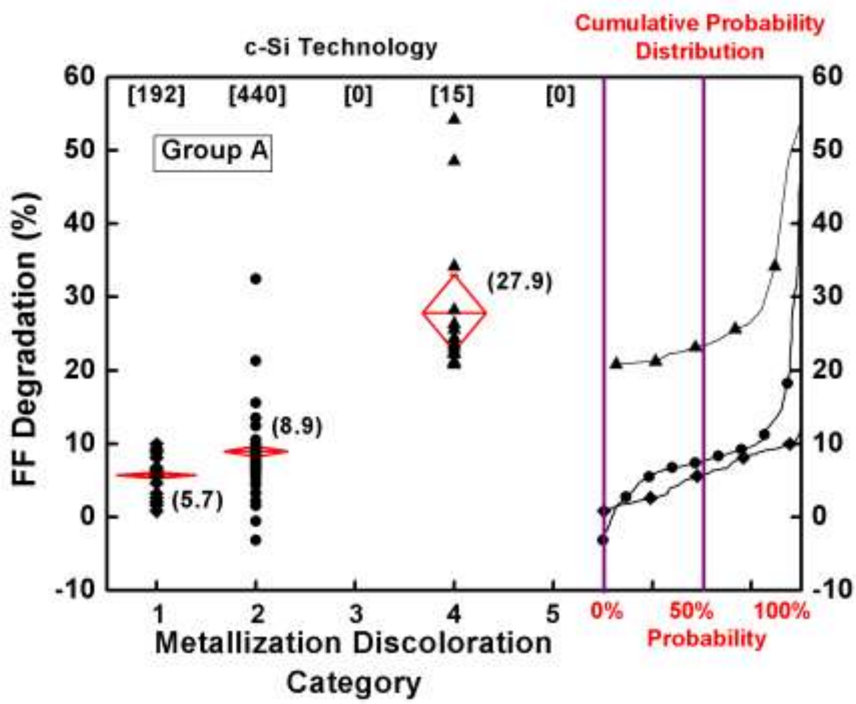

c-Si Technology
Cumulative Probability Distribution
Group A
[192] [440] [0] [15] [0]
(27.9)
(8.9)
(5.7)
FF Degradation (%)
Metallization Discoloration Category
0% 50% 100%
Probability

(b)

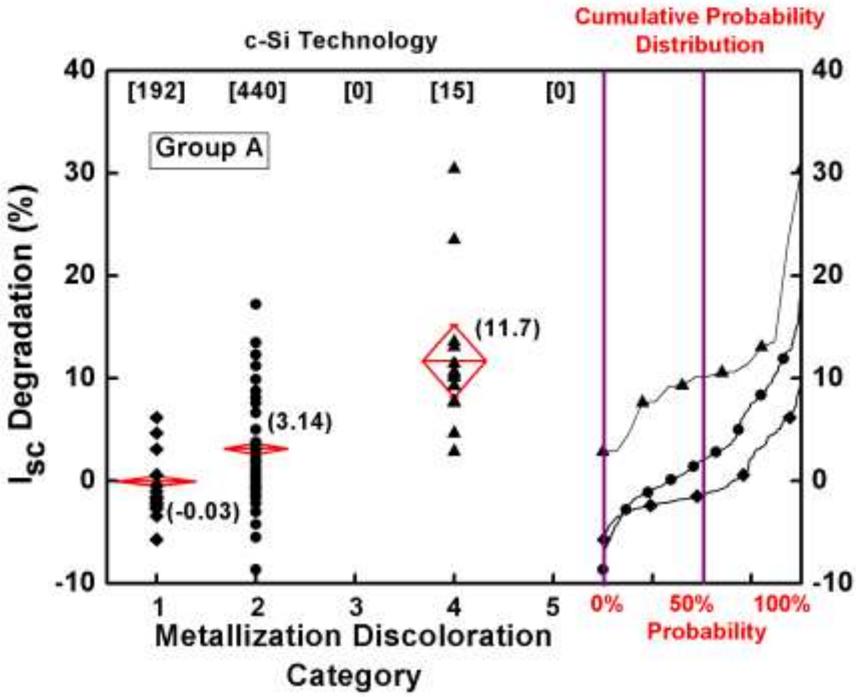

(c)

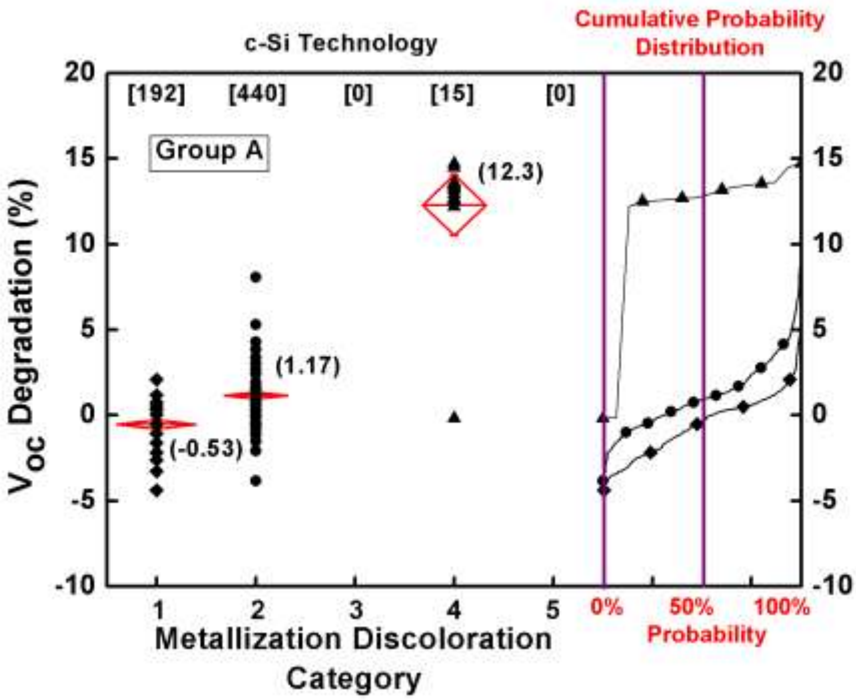

(d)

Fig. 6.15: Plots of electrical degradation versus severity of metallization discoloration (MDI category), for Group X modules: (a) P_{max} degradation (%), (b) *FF* degradation (%), (c) I_{SC} degradation (%), and (d) V_{OC} degradation (%).

c) Visible signs of cell cracks (including Snail Tracks & Photo-bleaching)

Cracks in the solar cells can sometimes cause snail tracks in the young modules, and photo-bleaching in the old discolored modules, which serve as visible indicators of cracks. However, it should also be kept in mind that not all cracks will lead to snail tracks or any other visible signs. The Linear Degradation Rates are plotted for modules with and without the visible signs of cracks (including snail tracks and photo-bleaching) in Fig. 6.16. The average degradation rates are indicated using the red horizontal lines (and the top and bottom edges of the red diamond indicate the 95% confidence interval). The cumulative probability is also shown to the right side of the scatter plot. It is evident from the plot that the average degradation rate of the modules with visible signs of cracks is higher than the modules without the visible cracks. It should be noted here that the "No VC" category includes modules without any cracks and modules with cracks which are not visible to the naked eye and can only be seen through electroluminescence imaging (discussed in Chapter 7). The difference in the average degradation rates has been found to be statistically significant for Group Y (based on the Mann-Whitney-Wilkinson Test). The Fill Factor degradation rate follows a similar trend as shown in Fig. 6.17. However, similar trends are not found for the I_{sc} degradation rate and the V_{oc} degradation rate (as shown in Fig. 6.18 and 6.19 respectively). This indicates that the cracks are causing higher fill factor degradation, leading to increased power loss in the modules.

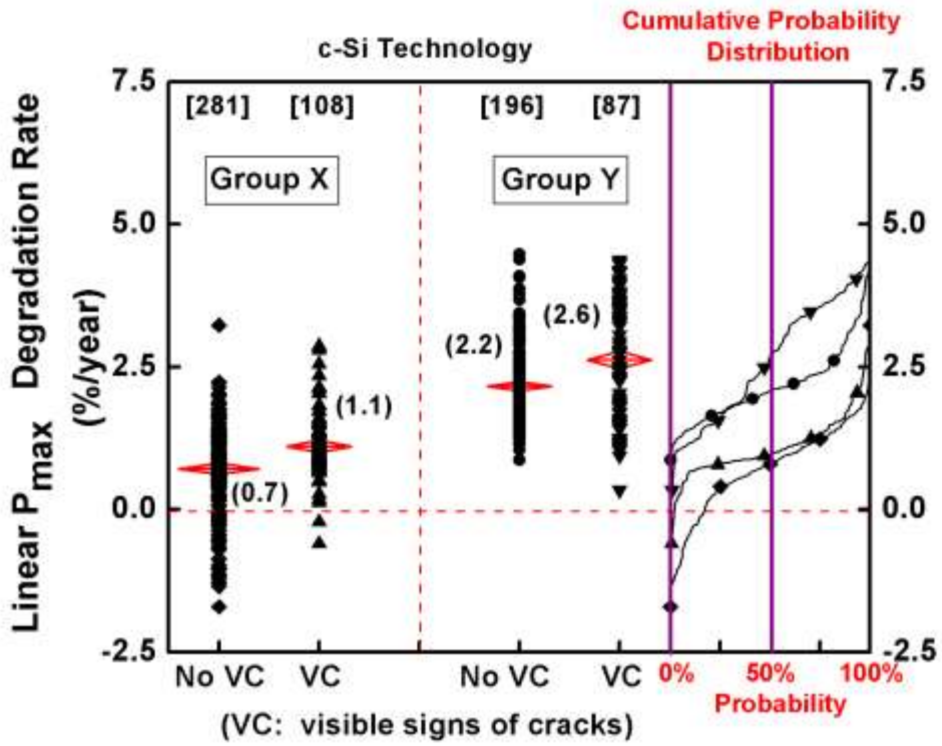

Fig. 6.16: Linear P_{max} Degradation Rate for Group X and Group Y modules with and without visible signs of cracks.

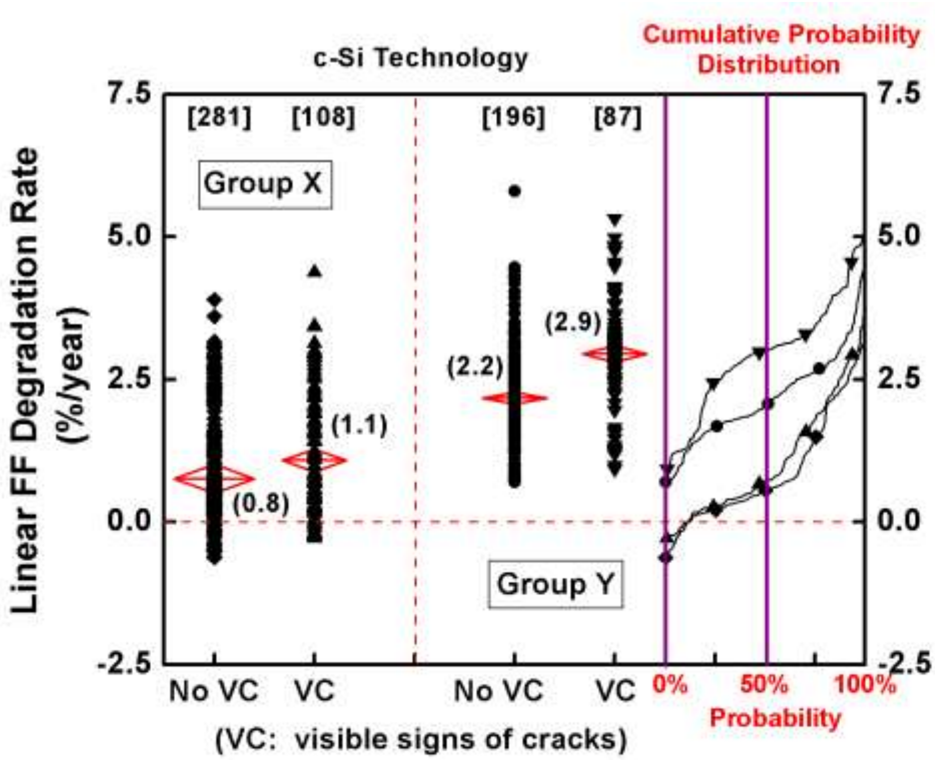

Fig. 6.17: Linear *FF* Degradation Rates for Group X and Group Y modules, with and without visible signs of cell cracks.

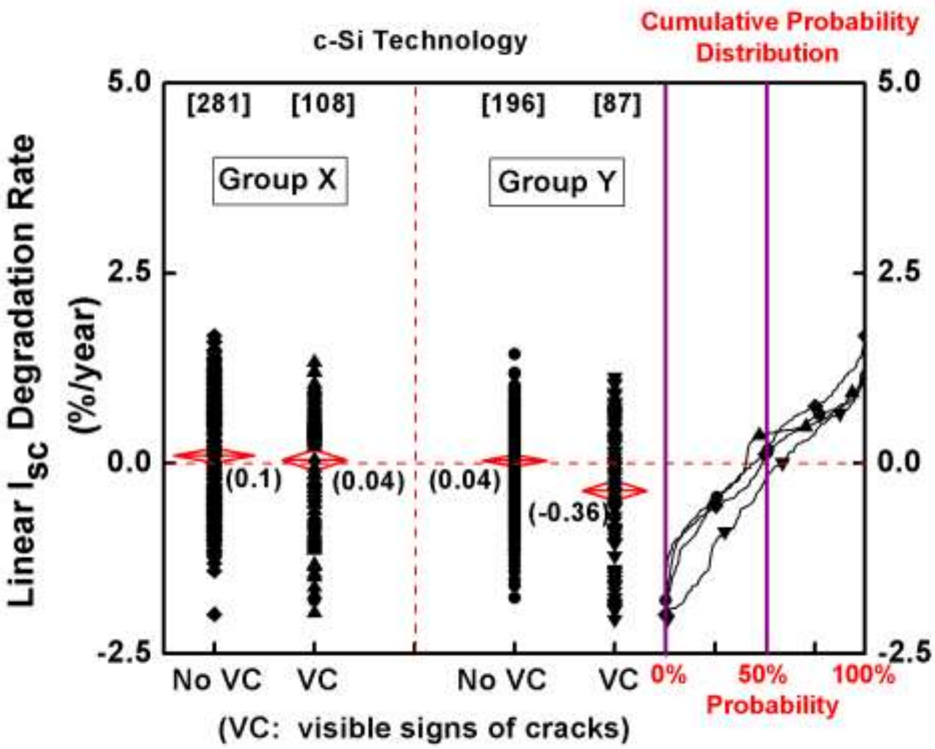

Fig. 6.18: Linear I_{sc} Degradation Rates for Group X and Group Y modules, with and without visible signs of cell cracks.

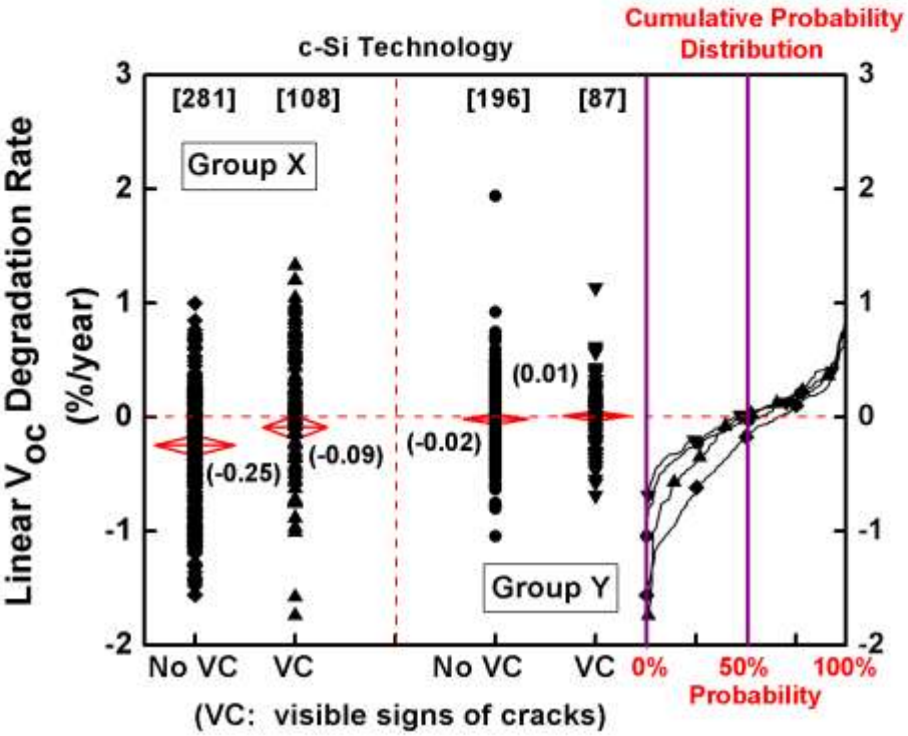

Fig. 6.19: Linear V_{oc} Degradation Rates for Group X and Group Y modules, with and without visible signs of cell cracks.

d) Backsheet Degradation

Degradation of backsheet can lead to safety issues and can affect the performance in the PV modules. The survey data indicates that the power degradation (%) is higher in case of modules with backsheet degradation as shown in Fig. 6.20. It needs to be mentioned here that though there appears to be a correlation, it does not confirm causality and so we cannot say that backsheet degradation is the cause behind the higher degradation in these modules. Fig. 6.21 shows the plots for the degradation in electrical parameters (V_{oc}, I_{sc} and *FF*) with backsheet degradation. It can be seen that the *FF* degradation and I_{sc} degradation are higher for modules with backsheet degradation. The series resistance has also been found to be higher for modules with backsheet degradation, as shown in Fig. 6.22. The average backsheet degradation index increases with increase in encapsulant discoloration category, as shown in Fig. 6.23, which explains the higher I_{sc} degradation for modules with higher backsheet degradation. This is not unreasonable, considering that temperature and UV rays are the primary environmental factors that degrade the polymeric materials – both encapsulant and backsheet.

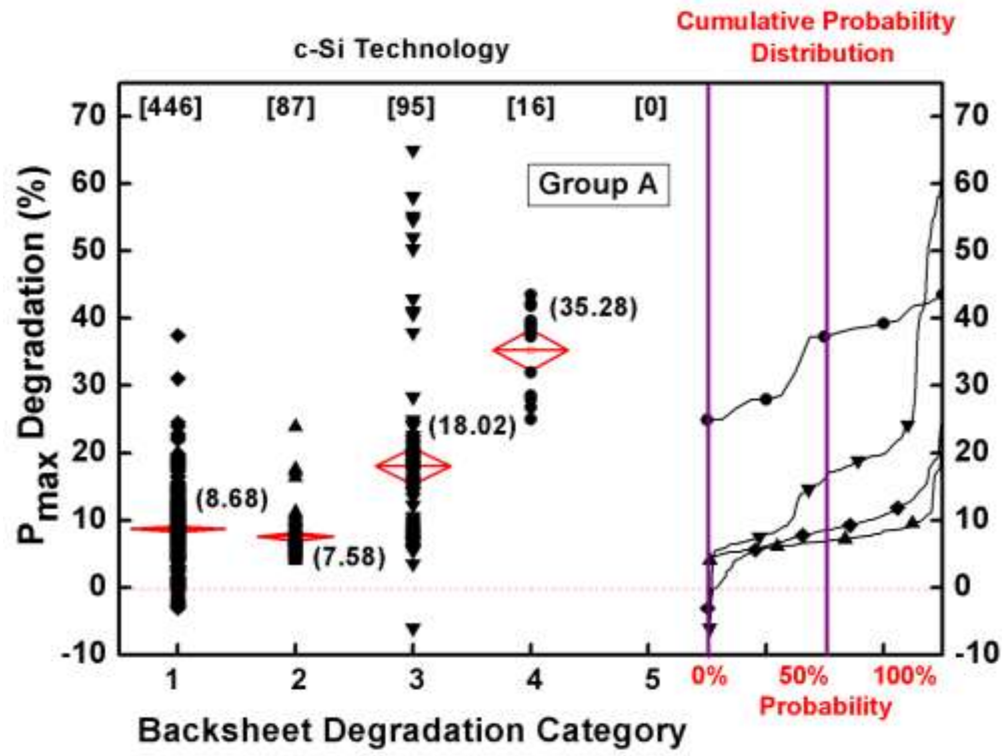

Fig. 6.20: Plot of P_{max} degradation versus extent of backsheet degradation for Group A modules.

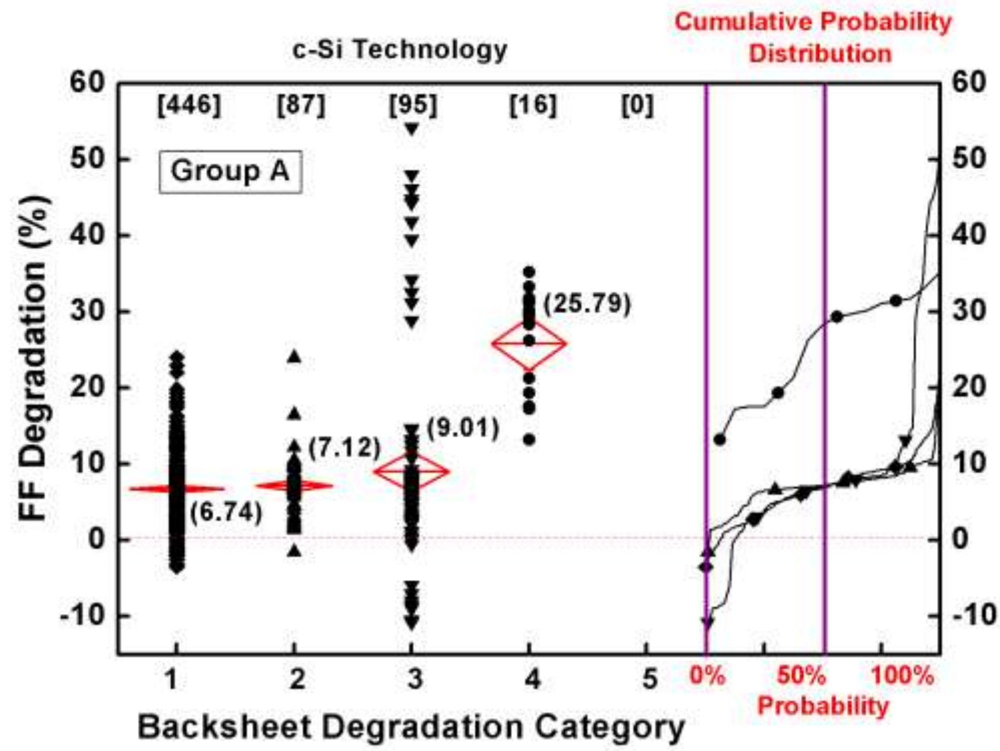

(a)

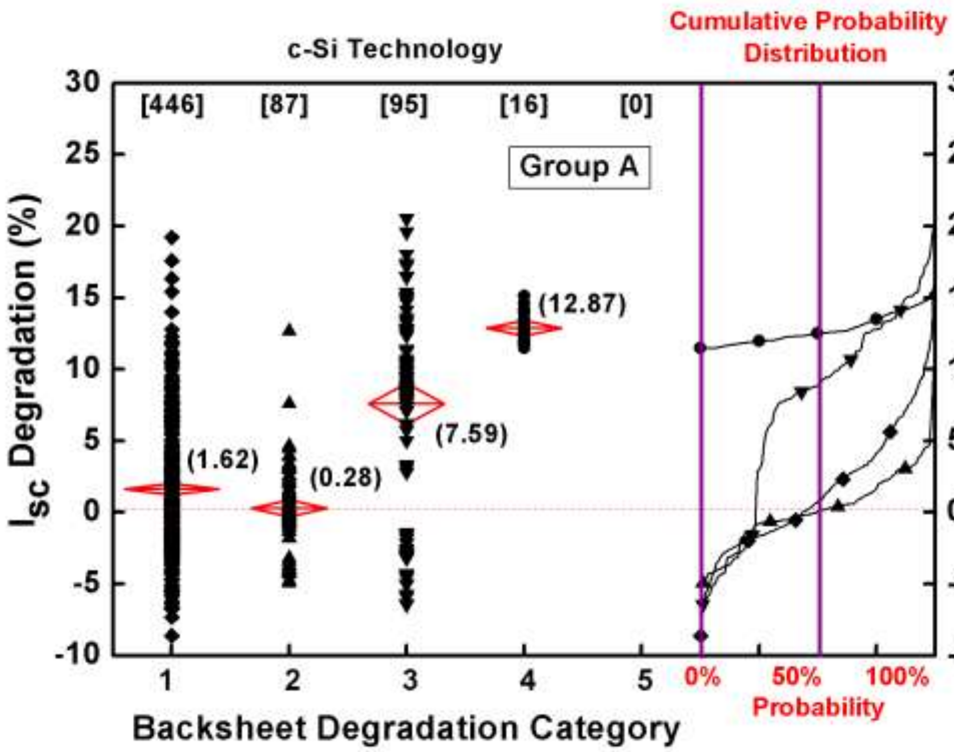

(b)

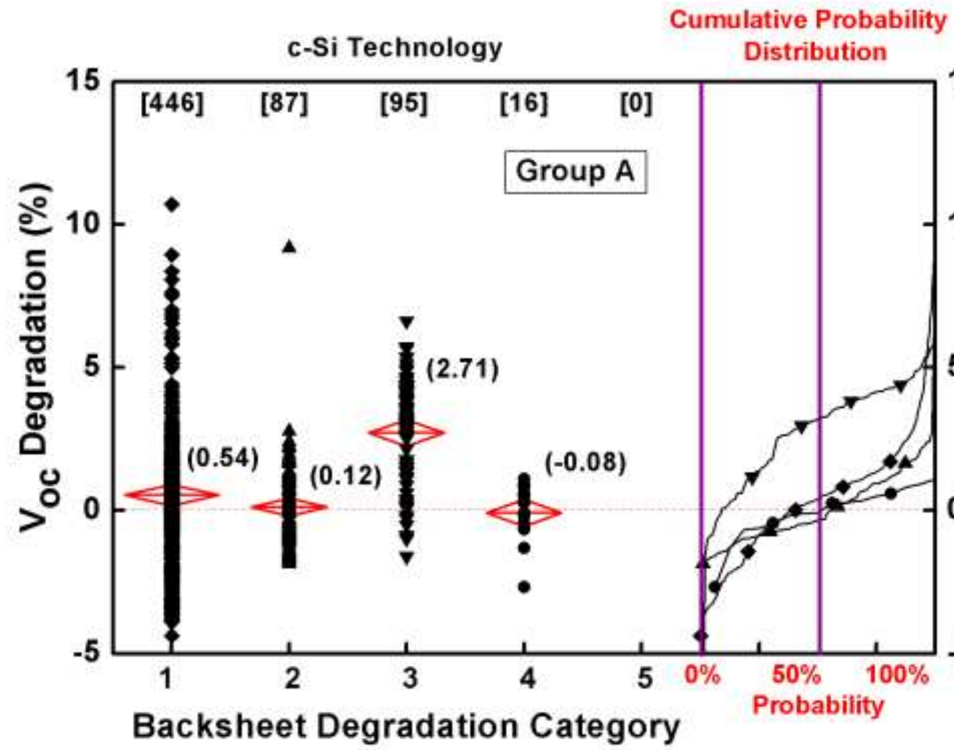

(c)

Fig. 6.21: Plot of electrical degradation versus extent of backsheet degradation for Group A modules - (a) *FF* degradation (%), (b) I_{SC} degradation (%), and (c) V_{OC} degradation (%).

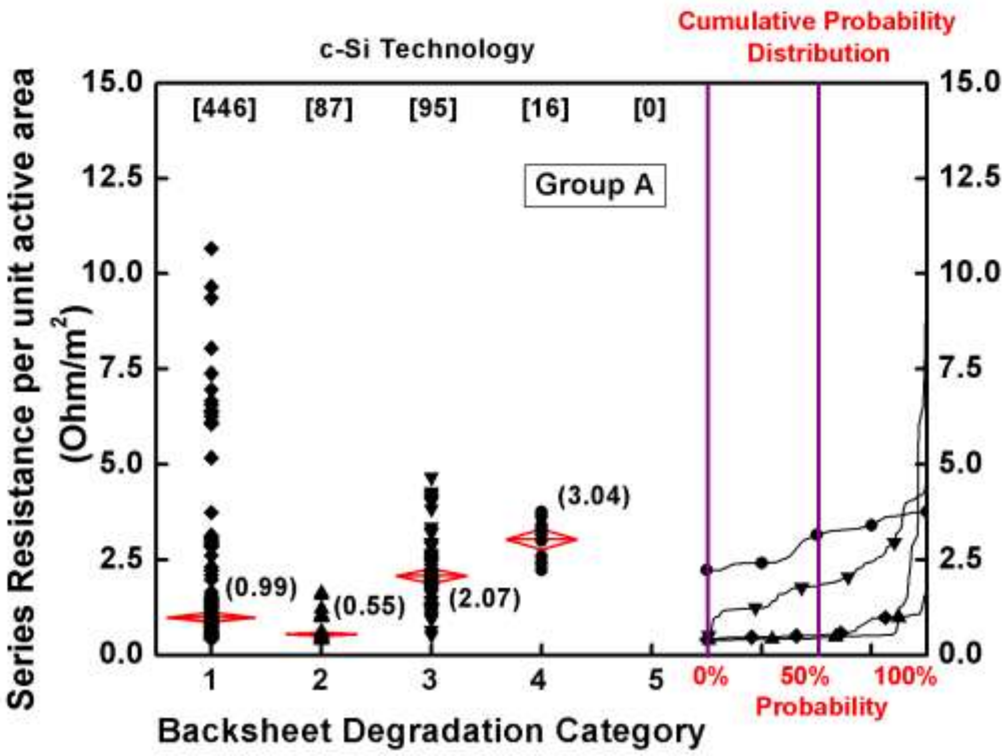

Fig. 6.22: Plot of series resistance (Ohm/m^2) versus the extent of backsheet degradation.

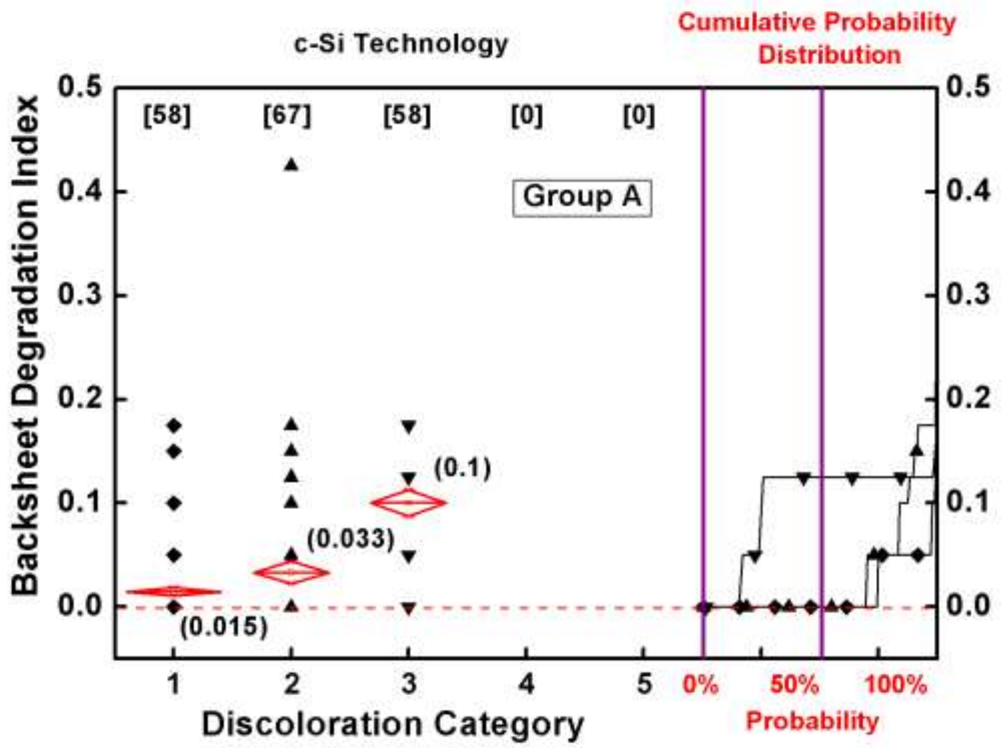

Fig. 6.23: Plot of backsheet degradation index for various encapsulant discoloration categories.

6.2.3 Statistical Analysis

The combined effect of the various degradation modes like encapsulant discoloration, metallization discoloration, snail tracks and photo-bleaching, backsheet degradation etc. on the power degradation rate has been analyzed using statistical techniques. The data has been fitted to a logistic regression model, having the following formulation:

$$\log\frac{\pi(\mathrm{x})}{1-\pi(\mathrm{x})} = \alpha + \beta_1(\mathrm{DI}) + \beta_2(\mathrm{CSI}) + \beta_3(\mathrm{MDI}) + \beta_4(\mathrm{BDI}) \quad \text{.... (6.4)}$$

where,

DI = Discoloration Index (a continuous variable with values ranging from 0 to 1)
CSI = Crack Severity Index (a continuous variable with values ranging from 0 to 1)
MDI = Metallization Discoloration Index (a continuous variable with values ranging from 0 to 1)
BDI = Backsheet Degradation Index (a continuous variable with values ranging from 0 to 1)
$\pi(\underline{x})$ = P[Y=1 for given $\underline{x}$] = P [the P_{max} degradation rate is greater than 1 %/year for given $\underline{x}$]
$\underline{x}$ is a four-dimensional column vector with its elements being the explanatory variables

The parameter estimates from above model are given in Tables 6.45 and 6.46 for young and old modules respectively. For the young modules, CSI and MDI are statistically significant (p-value < 0.05) while the other two explanatory variables i.e. DI and BDI are not significant. The parameter estimates for both CSI and MDI are positive, which means that the odds of the P_{max} degradation rate being more than 1 %/year increases when there are more cracks in the cells, or more discoloration on metallization. Metallization discoloration in the young modules is often a sign of poor quality control in manufacturing, and hence affects the odds of having a higher degradation rate. For the old modules, DI and BDI are statistically significant (refer Table 6.46). BDI has a positive estimator for its coefficient, which means that the odds of having high degradation rate increases when backsheet degradation is high. Interestingly, the estimator for the coefficient for DI is negative, implying that modules with higher discoloration tend to have lower chance of high degradation rates. This perhaps comes from the fact that the PV modules suffer faster degradation initially (due to LID) when there is no discoloration, and as the PV modules age, the degradation rate slows down while the discoloration increases (opposite trends).

Table 6.45: Parameter Estimates and p-values for young crystalline silicon modules

Covariates	Estimates of Parameters	p-value
Intercept	0.55524	0.11190
DI	2.48650	0.72138
CSI	14.32254	0.00492
MDI	31.88149	0.00032
BDI	-0.09736	0.95741

Table 6.46: Parameter Estimates and p-values for old crystalline silicon modules

Covariates	Estimates of Parameters	p-value
Intercept	-0.6109	0.13286
DI	-2.9623	0.02634
CSI	1.4450	0.16130
MDI	2.7346	0.33421
BDI	8.5561	0.00409

Based on the above discussion, it can be said that the manufacturing quality (related to MDI), and the handling of the panels, both during manufacturing and at time of installation (related to CSI), are the critical parameters which influence the odds of having high degradation rates, in the initial years of field exposure. On the other hand, the quality of the backsheet plays a significant role in determining the long term degradation rate of the module.

6.3 Visual Degradation Observed in Thin Film Modules

Thin Film modules are usually glass-glass modules with the active semiconductor material deposited on the top glass substrate. Moisture penetration into the laminate from the edges has for long been one of the most common causes of degradation in thin film modules, which is being countered in the present generation of modules with the help of superior edge seals [47]. As part of the survey, we have inspected a total of 146 thin film modules, the majority of which were CdTe modules. All of the modules were less than 10 years old, and were found only in the Hot climates (Hot & Dry, Warm & Humid, and Composite zones). Figure 6.24 shows some of the most commonly seen degradation modes during our survey and Table 6.45 shows the statistics. White spots are very commonly seen in thin film modules and are reported to be a visual indication of shunts, generated due to operation under partially shaded conditions [39, 48]. Delamination in the edge seal is also very commonly seen, which can lead to TCO corrosion due to ingress of moisture into the module [47].

Table 6.45: Statistics of thin film modules affected by various degradation modes

Technology	Total No. of Modules	Percentage of Modules Affected				
		White Spots	Cracked Glass	Non-Crack Damages	Cell Delamination	Edge Seal Delamination
Amorphous Silicon	44	100%	9%	9%	9%	NA
Cadmium Telluride	75	100%	1%	32%	32%	75%
Micromorph	17*	47%	0%	0%	53%	75%
Copper Indium Gallium Selenide	10	90%	0%	10%	10%	NA
*8 modules were frameless having edge seal, while remaining 9 modules had frame						

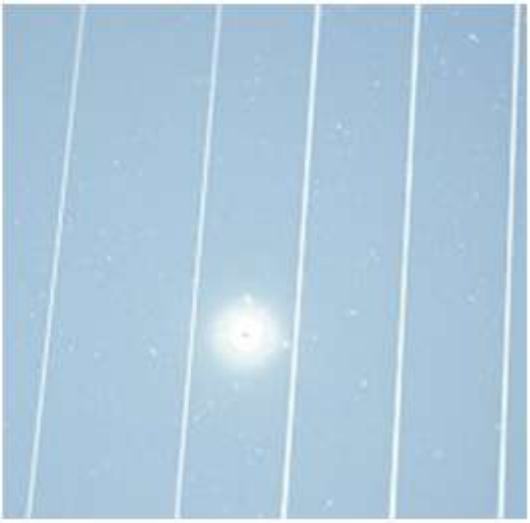

(a)

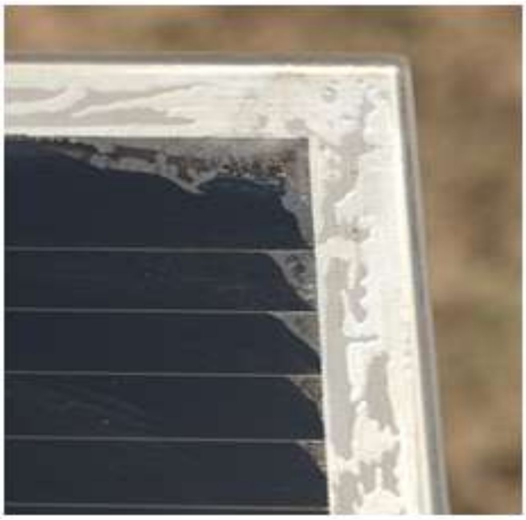

(b)

(c)

(d)

Fig. 6.24: Degradation in Thin Film modules (a) White spot in CdTe module, (b) Delamination of edge seal and inside cells (bar graph corrosion) in CdTe module, (c) haziness in a-Si module, (d) White spots (debonding) in a-Si modules.

6.4 Summary

Visual degradation observed in the surveyed modules provides us valuable information about the degradation modes responsible for the degradation in the electrical performance of the modules. We arrive at the following conclusions based on our analysis:

- Encapsulant discoloration has been observed in many young modules in the Hot & Dry zone, and almost in all old modules (beyond 10 years of field exposure) irrespective of the climate. Hot climates are harsher on the encapsulant as compared to the Non-Hot climates. Higher percentage of modules is affected by discoloration in Group Y as compared to Group X. Severity of discoloration is higher in Group X as compared to Group Y, which indicates that discoloration is not mainly responsible for the higher degradation observed in Group Y modules. The discoloration in the modules has been quantified using in-house developed software, and correlated to the short circuit current degradation and output power degradation.

- Front-side delamination over significant area of the module has been observed only in very old glass-glass modules in Hot & Dry climate. Bubbles have been frequently seen along snail tracks in the young modules, but the area affected is less than 5%. Such bubbles are more frequently observed in Group Y modules than in Group X modules.

- Metallization discoloration is observed in both the young and old modules, but is more severe for the old modules, particularly in the Warm & Humid climate. The Hot zone is harsher for metallization than the Non-Hot zone. Percentage of affected modules is higher in Group Y as compared to Group X. Small/medium installations have a higher average severity as compared to large installations, which implies a difference in material quality used in these installations. Metallization discoloration has been quantified by manually estimating the discoloration in various components like gridlines, busbars and cell interconnects, string interconnects and the output terminals. The extent of metallization discoloration has been found to correlate well with the series resistance of the modules, and their power degradation.

- Visible signs of cracks (which include snail tracks and photo-bleaching effects) are seen more in Group Y modules as compared to Group X modules, and seem to be one of the major factors responsible for the higher degradation rates (of output power and Fill Factor) in the Group Y modules. The percentage of affected modules is higher in the recent installations (less than 10 years old) as compared to the older installations. Highest severity of visible cracks is seen in small/medium installations in the Hot zone, though significant snail track severity is also seen in the large installations, and this calls for improvement in the installation practices in order to prevent crack formation.

- Backsheet degradation is comparable in the young modules in Group X and Group Y, but in the old modules, the degradation severity is higher in Group Y as compared to Group X. There is no difference between the average severities in the small/medium and large installations. Since backsheet degradation is a safety concern, it is important to use proper materials that can resist degradation in outdoor environment, and can provide the necessary levels of safety for the entire service life of the installation.

- Haziness is the most commonly seen degradation mode for the front glass. Scratches on the front glass and the frame have been found in about 10% of the young modules, which points to mishandling of the modules during installation.

- Statistical analysis of the visual degradation data has indicated that the odds of having high P_{max} degradation rate (more than 1 %/year) are increased in case of young modules with cracks and metallization discoloration (which can be taken as an indication of poor quality control during manufacturing). For the old modules, backsheet degradation is associated with a higher chance of P_{max} degradation rate exceeding 1 %/year.

7. Analysis of EL and IR Data

7.1 Introduction

Electroluminescence (EL) and Infra-red (IR) imaging techniques are very commonly used for characterization of PV modules. EL imaging provides insight into the condition and quality of the semiconductor material and helps in the identification of inactive regions and cracks in the solar cells [32]. IR thermography shows the temperature distribution in the PV module, and helps to identify the hot spots.

7.2 Analysis of Electroluminescence Data

EL imaging was performed in the field during the survey using 2 cameras – (a) Silicon CCD based camera available from Sensovation, and (b) modified CMOS based digital camera developed at NCPRE. EL images were taken at current equal to the short circuit current of the PV module under test. At some of the sites, the image difference technique [33] was used, which cancels effects of ambient light enabling us to take EL images in the late afternoon even in the presence of diffused sunlight. In this technique, two images are taken (one at bias and one at open circuit condition) and the difference between the two provides us the actual EL image.

EL images of a total of 202 module were taken during the survey. Figs. 7.1and 7.2 show some of the EL images taken during the survey for both Group X and Group Y site modules. The dark areas in the EL images indicate inactive cell areas. In Fig. 7.1 (a) and (c), we can see dark portions along the edges of some of the cells. This feature appears in wafers taken from the ends of the ingots, and it does not affect the power output significantly [39]. The irregular dark patches are indications of cracks in the module that are affecting the charge collection and hence reducing the output power of the module. In Fig. 7.2 (a)-(c), there are irregular dark patches in the cells which again indicate presence of cracks that are affecting the charge collection. In Fig. 7.2(d), an entire string of cells is dark, which happens when the bypass diode is short-circuited (damaged). In this same module, in two cells in the top-most row, one half of the cells is bright while the other half is dark. This indicates interconnect breakage in these cells, which is forcing current crowding along the intact busbars. A general observation is that the modules in Group Y sites have a much greater number of cracks in modules as compared to the modules in Group X sites. The higher number of cracks may be due to poor manufacturing, transportation or installation practices. This is discussed in more detail later.

7.2.1 Classification of Cracks

Cracks can be classified into 3 categories based on the area affected by the crack as visible in the EL image [49]:

a) Mode A cracks which are basically hair-line cracks, not associated with any dark area
b) Mode B cracks which are associated with a grey (not very dark) area in the cell
c) Mode C cracks which are associated with a dark area in the cell

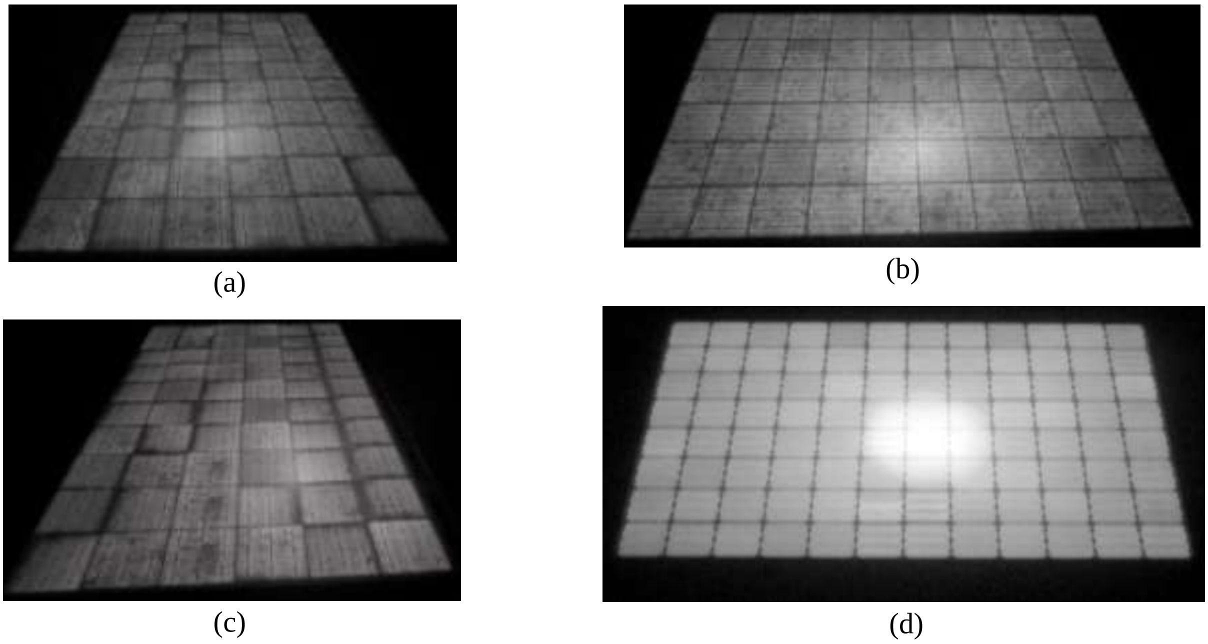

Fig. 7.1: EL images of some Group X modules taken in the field.

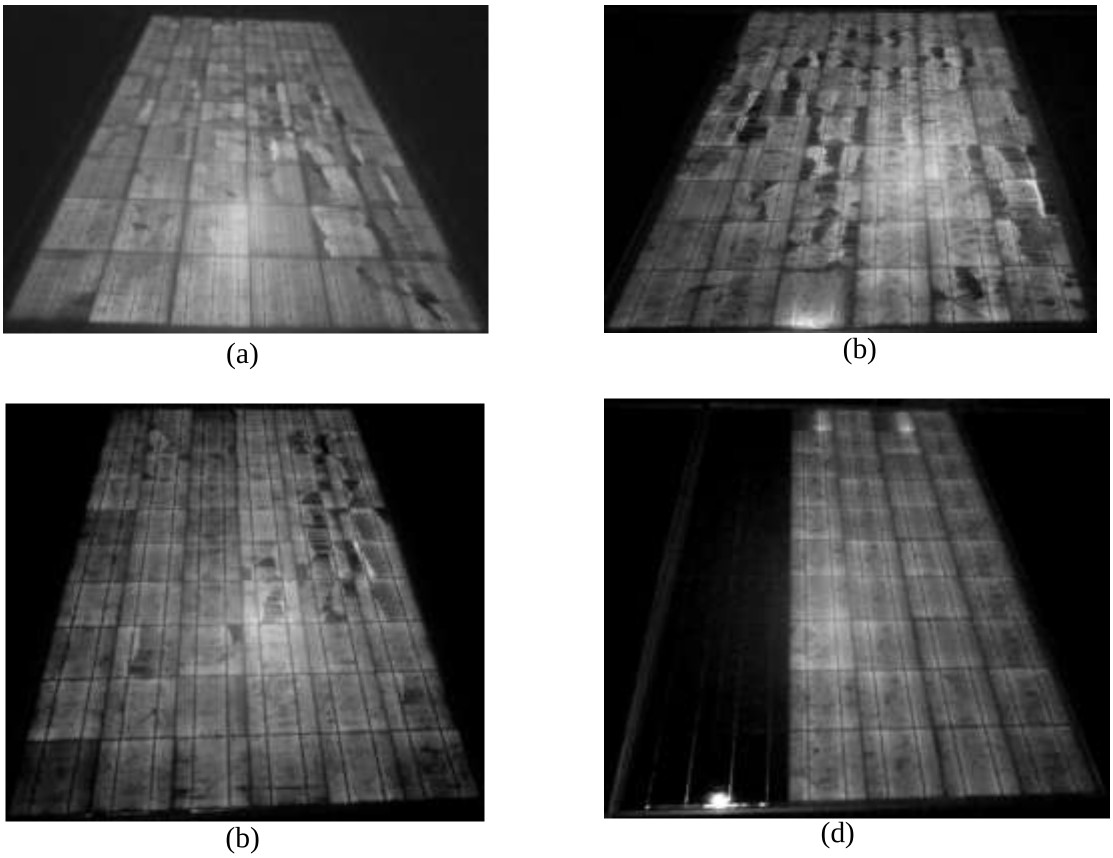

Fig. 7.2: EL images of some Group Y modules taken in the field.

Examples of the 3 types of cracks can be found in Fig. 7.3 [2]. Mode A cracks do not lead to any loss in power output, but Mode B and Mode C cracks can lead to power loss since the dark areas mean that electrical connection to the affected area has been broken. The number of cracks of different categories has been counted from the EL images taken during the survey and the statistics are given in Table 7.1. It is clear that modules in Group Y have a larger number of cracks (of all 3 types) as compared to Group X modules. The statistics for young and old modules are shown in Table 7.2, which shows that the percentage of cracks is higher in young modules as compared to old modules. This suggests that the transportation and/or installation practices for young modules are hasty or improper, and perhaps the starting quality of the modules also. Rooftop installations have higher cracks as compared to ground mounted installations as shown in Table 7.3, and small installations suffer from more cracks than large installations (refer Table 7.4). The number of cracks seen in EL, which can give rise to power loss (as shown in Section 7.2.5), is one reason why Group Y sites, young sites, rooftop sites and small sites show higher degradation.

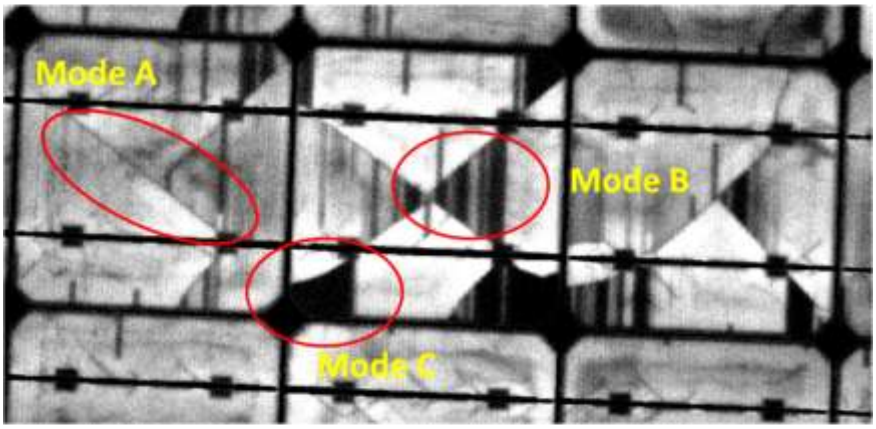

Fig. 7.3: Different types of cracks as visible in EL images [2].

Table 7.1: Percentage of cells affected by different types of cracks in Group X and Group Y modules

	Percentage of cells affected by different types of cracks			Total no. of cells checked
	Mode A cracks	Mode B cracks	Mode C cracks	
Group X	1.23	1.46	0.83	9464
Group Y	7.58	9.48	3.39	3300

Table 7.2: Percentage of cells affected by different types of cracks in young and old modules

	Percentage of cells affected by different types of cracks			Total no. of cells checked
	Mode A cracks	Mode B cracks	Mode C cracks	
Young	3.19	4.14	1.62	8952
Old	2.10	2.10	1.21	3812

Table 7.3: Percentage of cells affected by different types of cracks in Roof top and Ground mounted

	Percentage of cells affected by different types of cracks			Total no. of cells checked
	Mode A cracks	Mode B cracks	Mode C cracks	
Roof-top	3.07	3.97	2.22	4860
Ground Mounted	2.75	3.26	1.05	7904

Table 7.4: Percentage of cells affected by different types of cracks in Large and Small size systems

	Percentage of cells affected by different types of cracks			Total no. of cells checked
	Mode A cracks	**Mode B cracks**	**Mode C cracks**	
Small Size Systems	3.01	3.58	1.85	6920
Large Size Systems	2.70	3.47	1.08	5844

7.2.2 Correlation of Snail Trails with Electroluminescence Images

Snail tracks have been observed in many of the young modules during the survey, which has been described in detail in Chapter 6. The snail trails appear as black or brown curved lines running across the solar cells, and sometimes bordering them (like a frame). Usually the EL images of the cells affected by snail tracks show cracks, as shown in Fig. 7.4. The cracks allow the moisture to reach the top side of the solar cells, where it aids the migration of the silver ions from the gridlines to the encapsulant layer. The silver ions then react with various chemicals from the encapsulant and backsheet producing various compounds of silver [50].

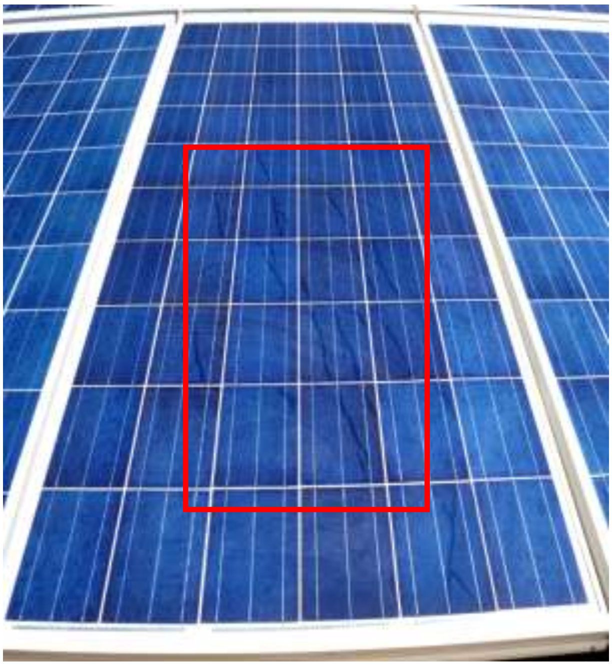

(a)

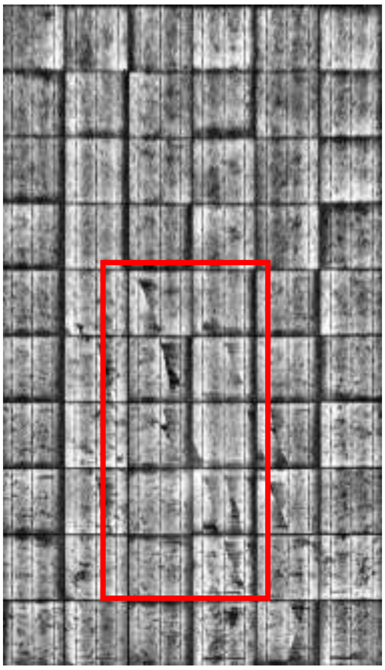

(b)

Fig. 7.4: (a) Snail trails observed in a PV module in Hot & Dry climate, (b) EL image of the same module showing the cell cracks.

7.2.3 Correlation of Interconnect Breakage with Electroluminescence Images

Interconnects provide electrical connection between the cells and conduct the electrical current to the external load from the cells in the PV module. The modules of the yesteryears usually contained 2 – 3 interconnects per cell, but nowadays 4 interconnects is the standard and many module manufacturers are also offering 5 interconnects per cell, which provides greater redundancy, and reduces the resistive losses thereby improving the fill factor of the PV module. In the event of breakage of one of the interconnects the current flow shifts to the remaining intact interconnects, and this leads to darkening of the area corresponding to the broken interconnect, while a current crowding effect is observed at the intact interconnect(s). The series resistance increases in the case of interconnect failure, which causes decrease in output power.

The Togami Cell Line Checker has been used in the survey for detecting interconnect breakage, which has also been verified in some cases using EL imaging. In Fig. 7.6(a), interconnect breakage has been observed in the busbar of the cell (marked in red) using the Cell Line Checker. Fig. 7.6(b) shows the EL image of the same module and the effect of the breakage can be clearly seen in the EL image. These interconnect breakages increase the series resistance of the module which eventually reduces the power output of the module.

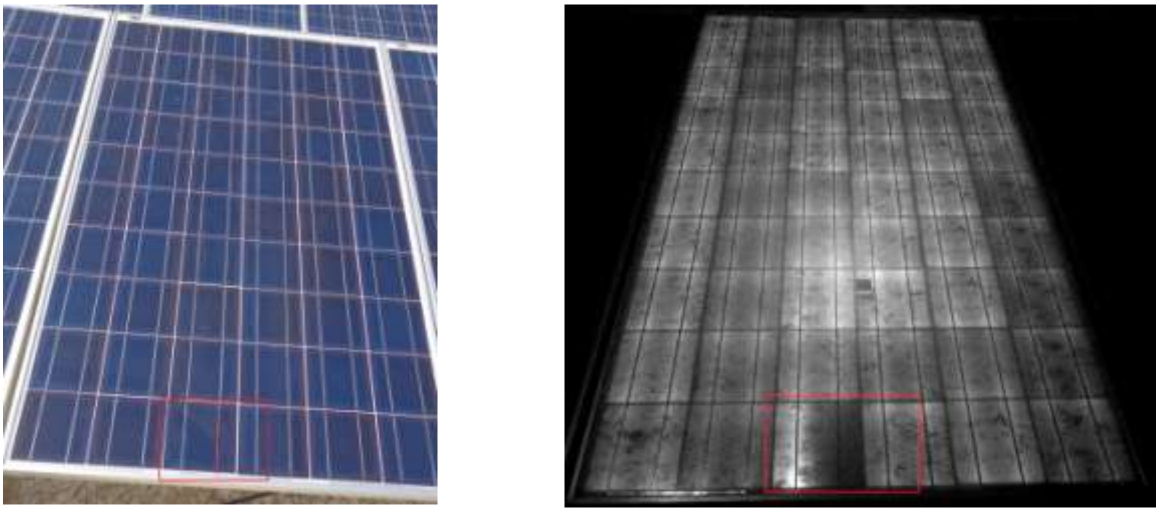

(a) (b)

Fig. 7.5: (a) Interconnect breakage in a PV module, detected using Togami Cell Line checker (marked red on the cell interconnect), and (b) the EL image of the corresponding section.

7.2.4 Correlation of Cracks with Location

The location of the cracks in the PV module can provide us information regarding the possible causes of such cracks. For this analysis, each module is divided into three regions – the central zone, the intermediate zone, and the periphery, as shown in Fig. 7.6. The percentage of cells cracked in the respective region is calculated for each module and the values are plotted for the three regions in Fig. 7.7. The average value for Region 2 is highest followed by the Regions 1 and 3. Mann-Whitney-Wilcoxon test results indicate that the data distribution for Region 3 is significantly different from Regions 1 and 2, so it can be concluded that the cracks are found more in the outer regions as compared to the central region of the PV modules.

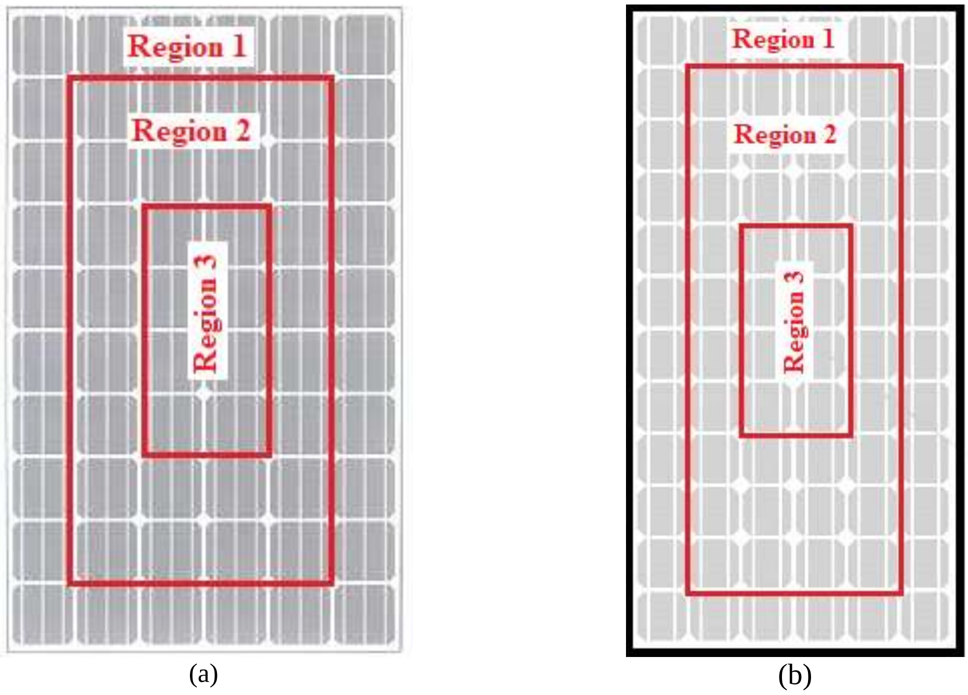

Fig. 7.6: Definition of the three region in (a) 60 cell module, (b) 72 cell module.

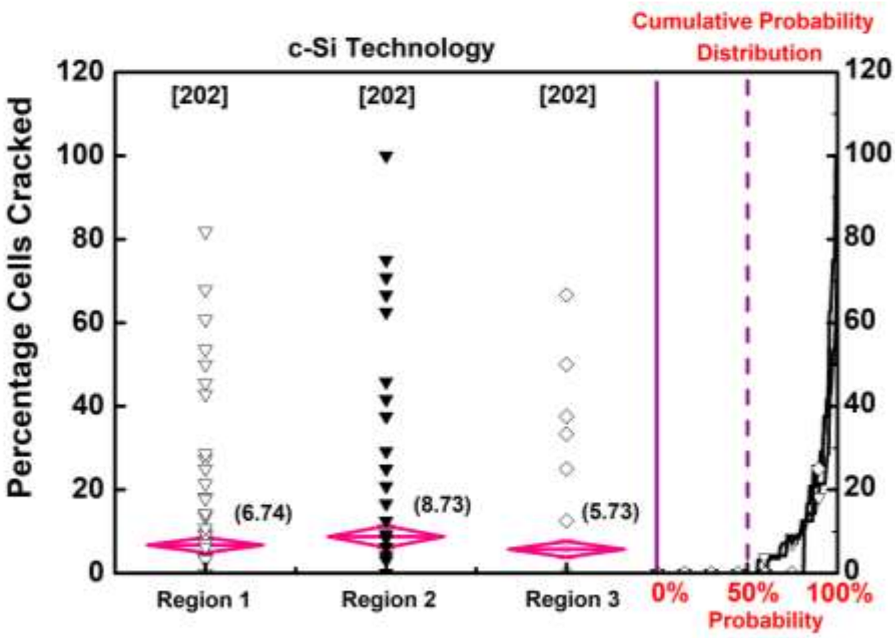

Fig. 7.7: Percentage cells cracked with position on PV module.

7.2.5 Correlation of P_{max} Degradation with Number of Cracks

Figure 7.8 shows the plot of the average Linear P_{max} Degradation Rate (% per year) versus the total number of cracks in the module. It can be seen that the degradation rate increases with increase in the number of cracks. In this figure, the red and green vertical bars indicate the instrument/STC translation error and the nameplate error respectively. As mentioned earlier, this indicates that cracks and microcracks are definitely one of the causes for increased degradation seen in the poor-performing sites.

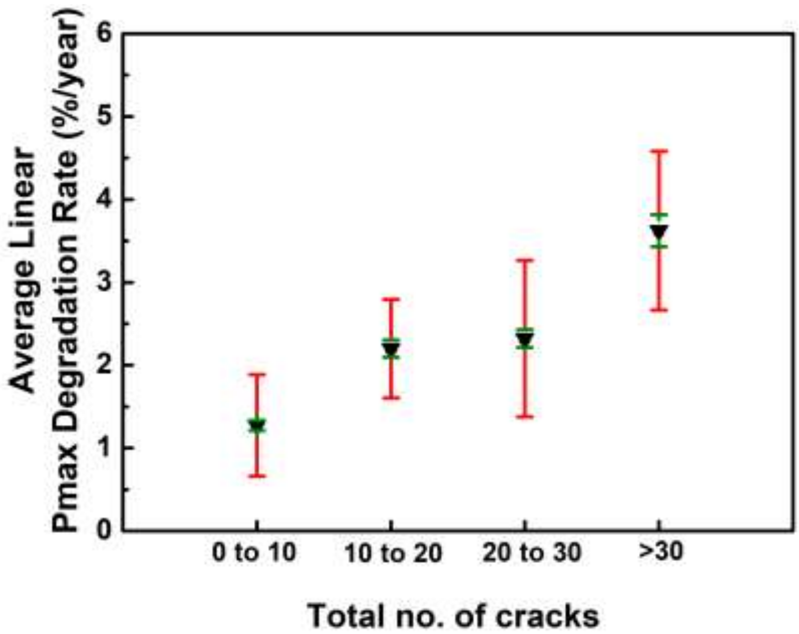

Fig. 7.8: P_{max} degradation rate (%/year) versus the total number of cracks in the module. The green and red bars indicate the instrument/STC translation error and nameplate error respectively.

7.2.7 <u>Correlation of Dark IR images with Electroluminescence images</u>

Dark IR thermography of a selected set of PV modules was performed in the survey, with the module forward biased using a DC power supply at its rated short circuit current. The module is covered from the front using an opaque cover, and the IR image is taken from the backside, with the current flowing through the module. Figure 7.9 shows the EL image of a module with a badly damaged solar cell (left image), highlighted with the red box. On the right, the dark IR image is shown which shows a hot spot in the affected cell. The inactive area is dark in both the EL image and the dark IR image. Note that the IR image has been taken from the backside, while the EL image has been taken from the front so the features are mirrored.

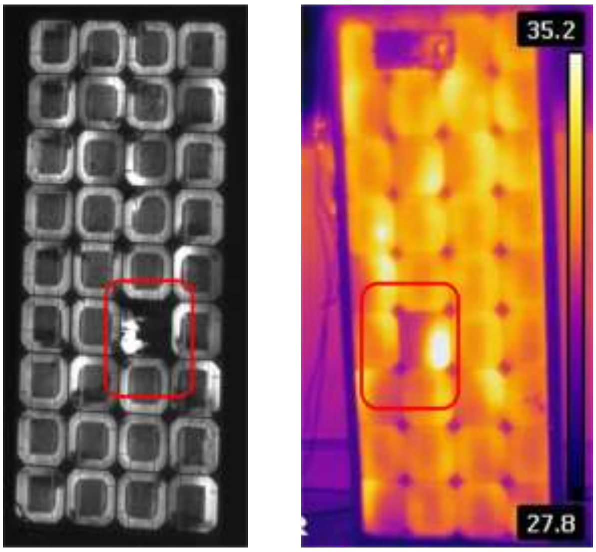

Fig. 7.9: Comparison of the EL image with the Dark IR image of an old module.

7.3 Analysis of Illuminated IR Data

Illuminated IR thermography is a commonly used technique for detection of thermal anomalies in PV modules. Many of the defects in the solar cells and laminate like cell cracks, delamination, shunts etc. lead to thermal signatures that can help in identification of these problems. Hence, IR thermography was also performed during the survey, with the modules under both load (Maximum Power Point Tracking done by string inverter) and short circuit conditions, using a FLIR E60 IR camera. It was ensured that the POA irradiance was above 700 W/m^2 while taking the IR images. For the short circuit IR images, the module was shorted for at least 5 minutes before taking the image. The hot spots obtained in short-circuited condition can be considered as the worst case scenario, since the total input solar energy is dissipated as heat in short circuit condition, whereas in the MPPT condition, the hot spots are expected to be less severe, but more representative of actual operating conditions. Figure 7.10 shows representative IR images of PV modules taken at a PV power plant, under MPPT and short circuit conditions. In this figure, the vertical bar on the right side of each IR image indicates the temperature range of the objects present in that image. The temperature at the top left side of the images indicates the temperature at the pointer present in the centre of the IR images. Areas shown in white are at a higher temperature than areas in red and blue. We can clearly see that the maximum cell temperatures are much higher in the case of the short circuit image as compared to the MPPT image.

As evident from Fig. 7.10, the surrounding structures are also present in the IR image. In order to analyze the IR image, we have developed software which enables us to remove the surrounding objects and select only the object (module) of interest (refer Fig. 7.11). Fig. 7.11(a) shows the thermal map (temperature data) extracted from an IR image of a PV module taken at a power plant site. There are lots of surrounding objects like PV modules and support structures in this image. Using the software, we select the module of interest from this thermal map, and the rest of the surrounding objects are removed by the software as shown in Fig 7.11(b). The temperature histogram of the module of interest is shown in the Fig. 7.11 (c), where we can see that the highest temperature is 46.5 °C for this PV module. The modal value of the histogram is taken as the representative temperature for the PV module, since it is the most frequently occurring temperature in the module IR image. The modal value (43.5 °C) is found to be close to the median of the histogram but very different from the average since the average temperature (obtained from the histogram) is influenced by the temperature of the frame, support structure and other surrounding objects which inevitably appear in the IR images. The highest temperature in the histogram is considered as the maximum cell temperature, which is noted down for further analysis.

Figure 7.12(a) shows the histogram of the representative (modal) module temperature for Group A c-Si modules, under MPPT condition. These temperatures are presented as recorded at site by the IR camera during the survey, without applying any correction for irradiance or ambient temperature. The lowest module temperature recorded under MPPT condition was 25 °C (in Ladakh) while the highest was 66.5 °C (in Rajasthan). All these readings were taken in the summer season, with variable irradiance and ambient temperatures. The histogram of the maximum cell temperatures is shown in Fig. 7.12(b). The highest cell temperature recorded for any module in the survey under MPPT condition was 89 °C (under POA irradiance of 815 W/m^2 and 37 °C ambient temperature). The histogram of the c-Si module temperature and maximum cell temperature observed under short circuit condition are given in Fig. 7.13. The module temperatures under short circuit condition range between 49 °C to 69 °C, and the maximum cell temperature observed under short circuit condition is 110 °C. This shows that the cell temperatures are much higher under short circuit condition as compared to MPPT condition. It should be noted that in some of the sites, IR images were not taken due to site-specific constraints, so the total number of modules reported in this Section is lower than the numbers reported in Chapter 4.

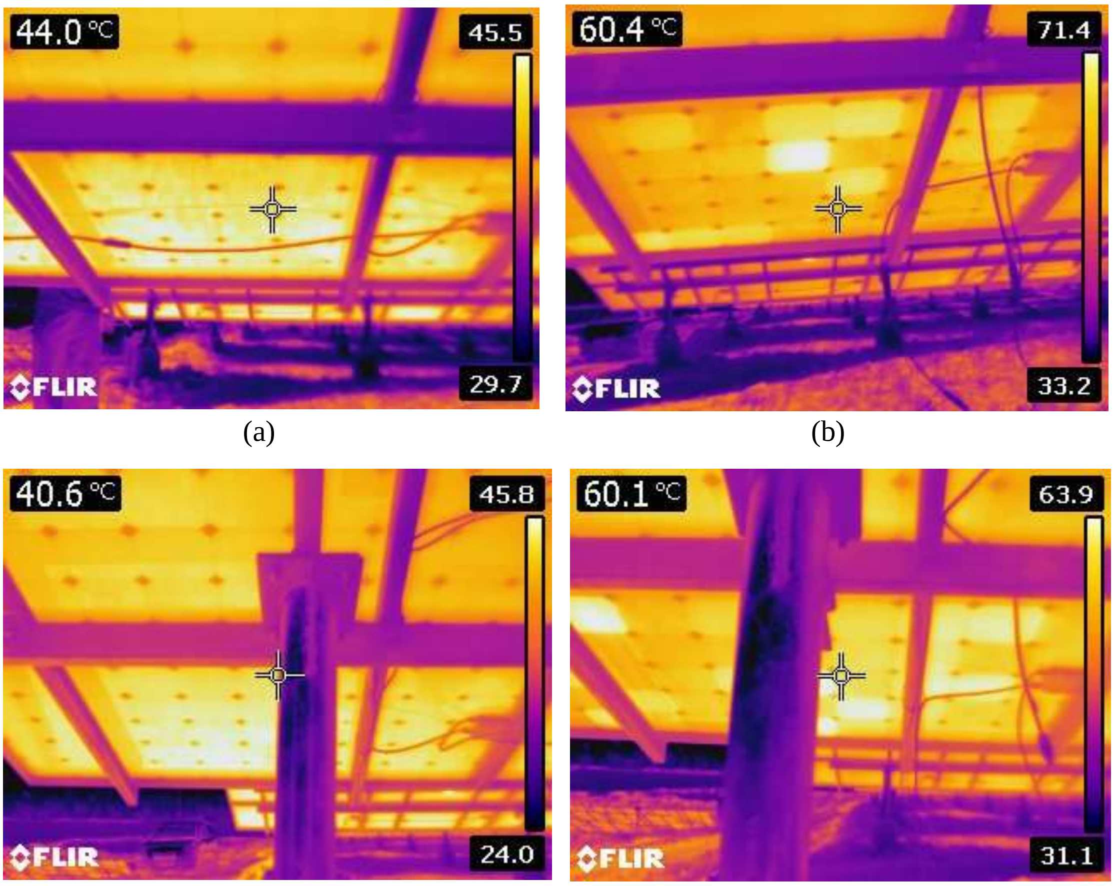

(a) (b) (c) (d)

Fig. 7.10: IR images of PV modules in a PV power plant – (a) Module 1 under MPPT condition, (b) Module 1 under short circuit condition, (c) Module 2 under MPPT condition, and (d) Module 2 under short circuit condition.

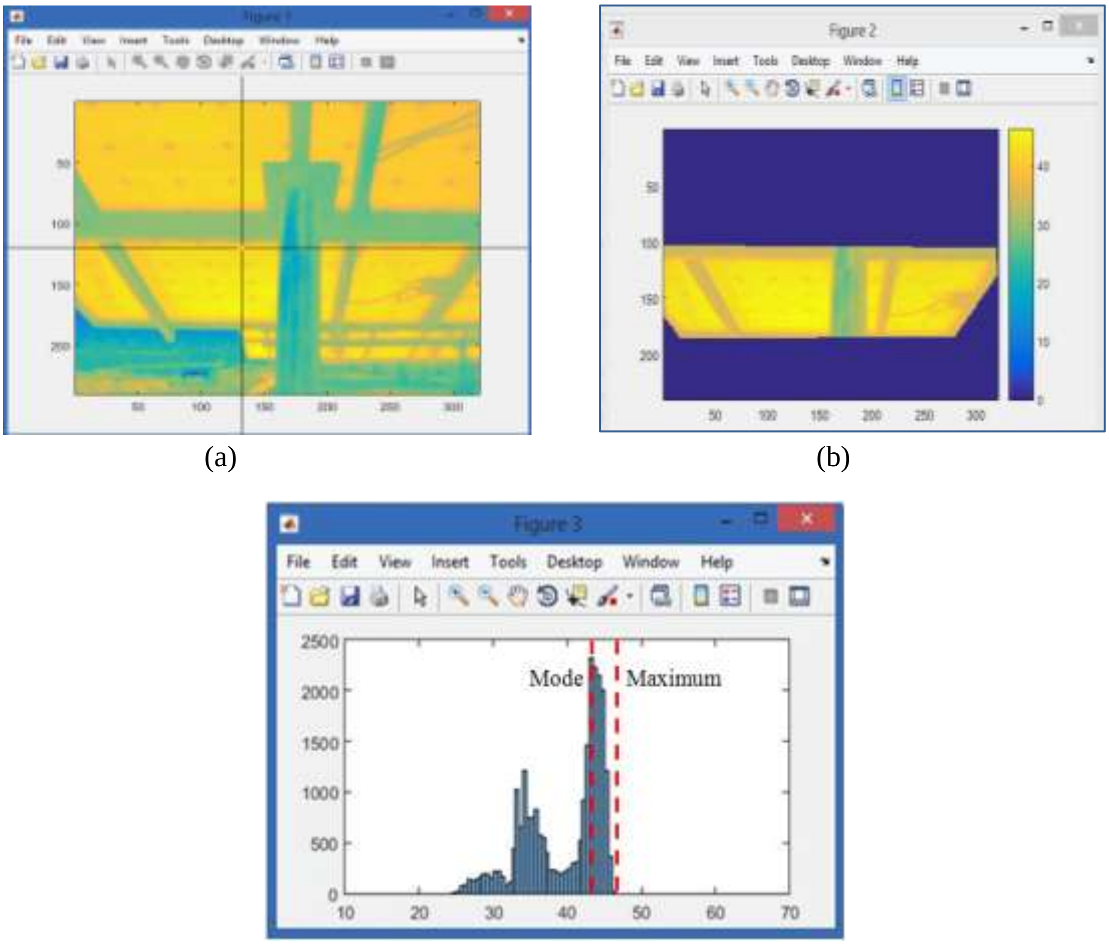

(a) (b)

(c)

Fig. 7.11: (a) Thermal map extracted from the IR image of a PV module (b) Region of interest cropped from the thermal map, and (c) Temperature histogram of the module. The highest temperature in this module is 46.5 °C. The modal temperature of 43.5 °C is taken as the module's representative temperature. The ambient temperature was 29 °C with irradiance of 724 W/m^2 when the IR image was captured.

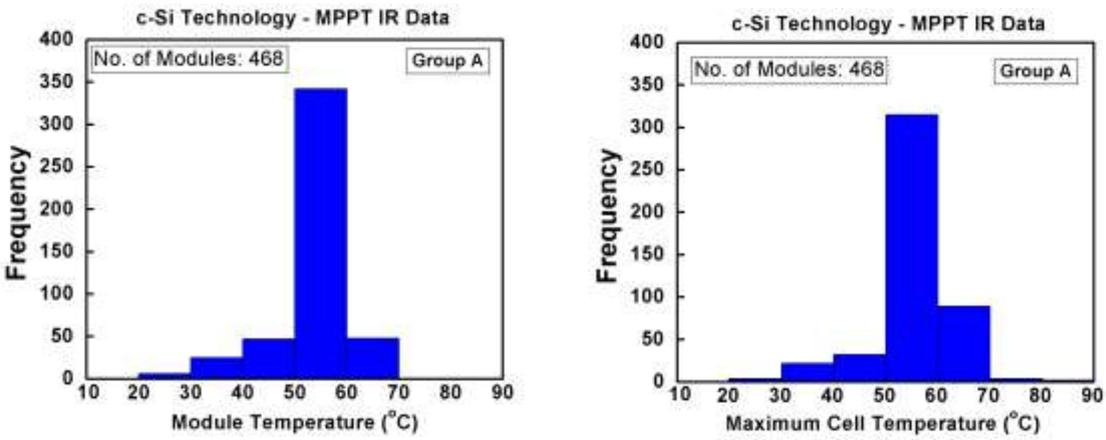

(a) (b)

Fig. 7.12: Histogram of module temperature (a), and maximum cell temperature (b), of c-Si modules inspected in the survey, under MPPT condition.

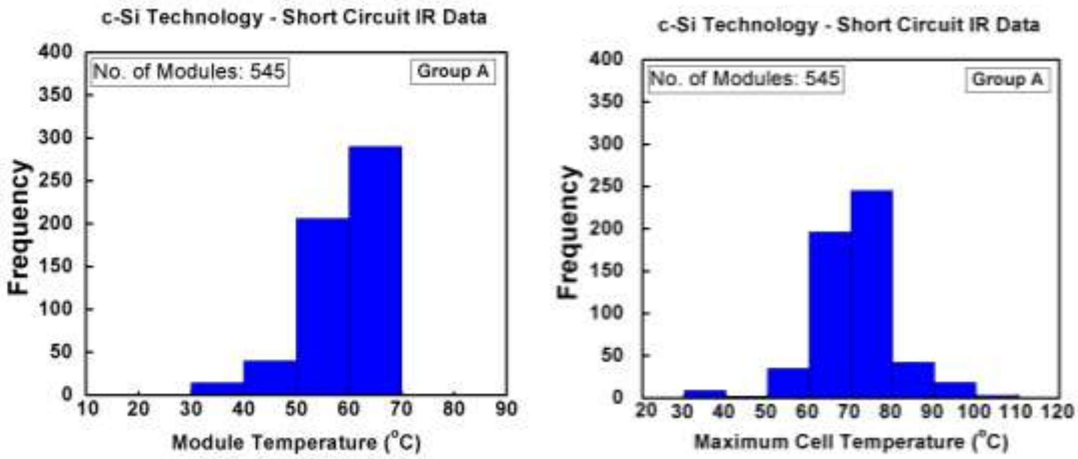

(a) (b)

Fig. 7.13: Histogram of module temperature (a), and maximum cell temperature (b), of c-Si modules inspected in the survey, under short circuit condition.

7.3.1 Normalization of IR data

The temperature of a module depends on the ambient conditions like incident irradiance, ambient temperature and wind speed. In order to compare the temperatures of the modules taken under different ambient conditions (as in our Survey), it is necessary to first translate the module temperature to reference conditions. Based on the work of Moreton *et al.* [51] and Oh *et al.* [52], the temperatures were translated to the reference condition of 1000 W/m^2 and 40°C, using the relation:

$$T_{translated} = 40 + \frac{(T_{measured} - T_{ambient}) \text{ x } 1000}{\text{Irradiance}} \qquad \dots (7.1)$$

where,

$T_{translated}$ = translated temperature of module under reference condition

$T_{measured}$ = measured temperature of module (obtained from IR image)

$T_{ambient}$ = ambient temperature measured at site

The thermal or temperature mismatch between the cells in a module can be quantified in terms of the Module ΔT, which is defined as follows:

$$Module\ \Delta T = T_{maxcell,\ translated} - T_{module,\ translated} \qquad \dots (7.2)$$

where,

$T_{maxcell,\ translated}$ = Translated maximum cell temperature of the module

$T_{module,\ translated}$ = Translated modal temperature of the module

Theoretical calculations show that the power loss in a solar cell (in Watts), due to formation of a defect, is proportional to the temperature rise of the solar cell [53]. Based on the energy balance in a PV module, equating the incoming solar energy with the summation of the electrical power output and the thermal power dissipation, it is possible to derive a relation of the form:

$$\%\ \text{Power loss in a PV module} = \frac{U}{10 \text{x} N \text{x} \eta} \text{ x} \sum_{N\ cells} (T_{cell} - T_{module}) \qquad \dots (7.3)$$

Where,

U = Overall heat transfer coefficient

T_{cell} = Cell Temperature
T_{module} = Module's representative temperature (modal temperature)
η = Initial efficiency of the PV module
N = No. of cells in the PV module

Most of the IR images taken in the 2016 survey have parts of the support structure blocking some of the solar cells of the module, and also the images have an irregular shape (close to trapezoidal). So, it is difficult to apply equation 7.3 directly to the IR data from the 2016 survey, and is prone to errors (owing to obstruction by support structures). Hence, we have used a simplifying assumption and defined a Thermal Mismatch Index (TMI) for the module as follows:

$$\text{TMI} = \frac{Module\ \Delta T}{\eta \text{ x } N} \quad \dots (7.4)$$

Where,
η = Initial efficiency of the PV module
N = No. of cells in the PV module

The value of the denominator for standard 60-cell modules of 17% efficiency is 10.2 which means that a TMI value of 1 implies a *Module ΔT* of 10.2 ^{o}C. However, for modules with different efficiency, the values will change accordingly. A higher TMI indicates the possibility of hot cells. The modules have been grouped into 4 categories based on the TMI values and the electrical parameter degradation has been analyzed in the following sections.

7.3.2 Analysis of Normalized IR data

a) Effect of Thermal Mismatch on Electrical Degradation

In order to analyze the effect of temperature mismatch on the electrical parameters, the modules have been grouped into various categories based on the TMI values for both short circuit and MPPT conditions. Table 7.5 gives TMI values for IR data collected under short circuit condition, hereafter referred to as TMI_{SC}. The P_{max} degradation (%) of the modules in different categories is shown in Fig. 7.14 and the increase in the average degradation rate with increase in TMI_{SC} category is evident. Statistical analysis shows that the categories 1 and 2 are not significantly different, but there is significant difference between categories 1, 3 and 4 (p-value of null hypothesis in Mann Whitney U test is less than 0.05). Fill Factor degradation also follows a similar trend as P_{max} degradation as shown in Fig. 7.15(a). However, no trend can be seen for short circuit current and open circuit voltage degradation, as seen in Figs. 7.15(b) and (c). In Fig. 7.15(b) for I_{sc} degradation, all categories (1 through 4) come out to be statistically similar (p-values greater than 0.05 in Mann Whitney U test). It is clear from these figures that fill factor degradation is the primary reason behind the power degradation for the short circuit temperature mismatch categories.

Table 7.5: Temperature mismatch category based on TMI values at short circuit condition (TMI_{SC})

TMI_{SC}	0 – 1	1 – 2	2 – 3	> 3
Category	1	2	3	4

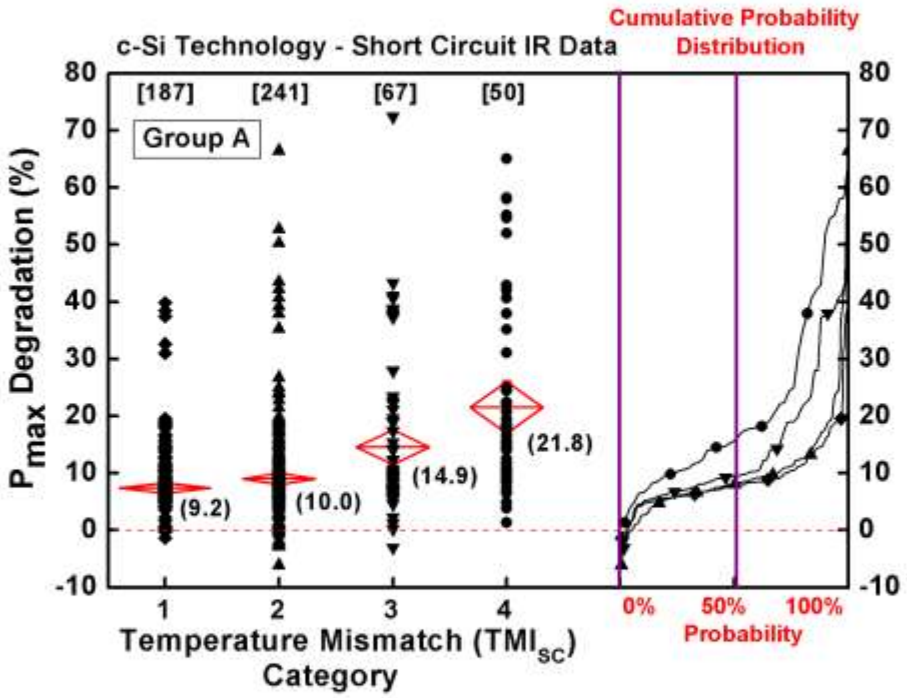

Fig. 7.14: P_{max} degradation (%) for different thermal mismatch categories under short circuit condition.

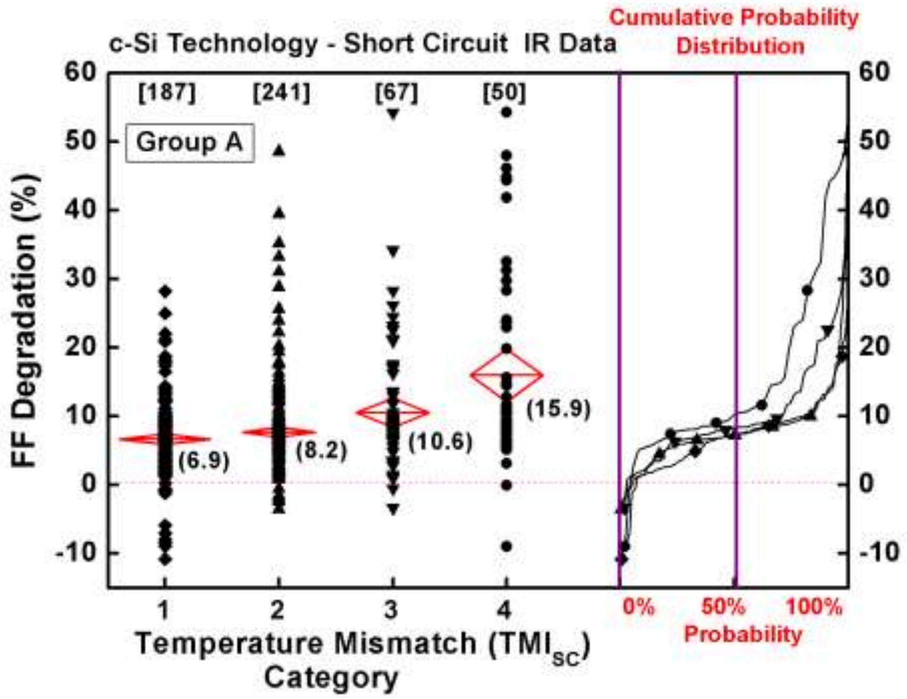

(a)

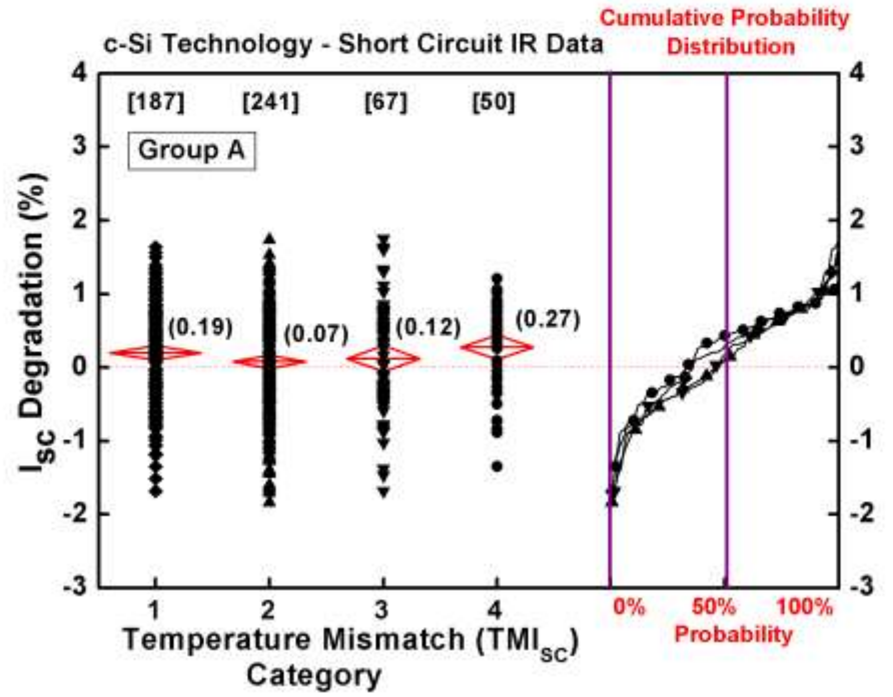

(b)

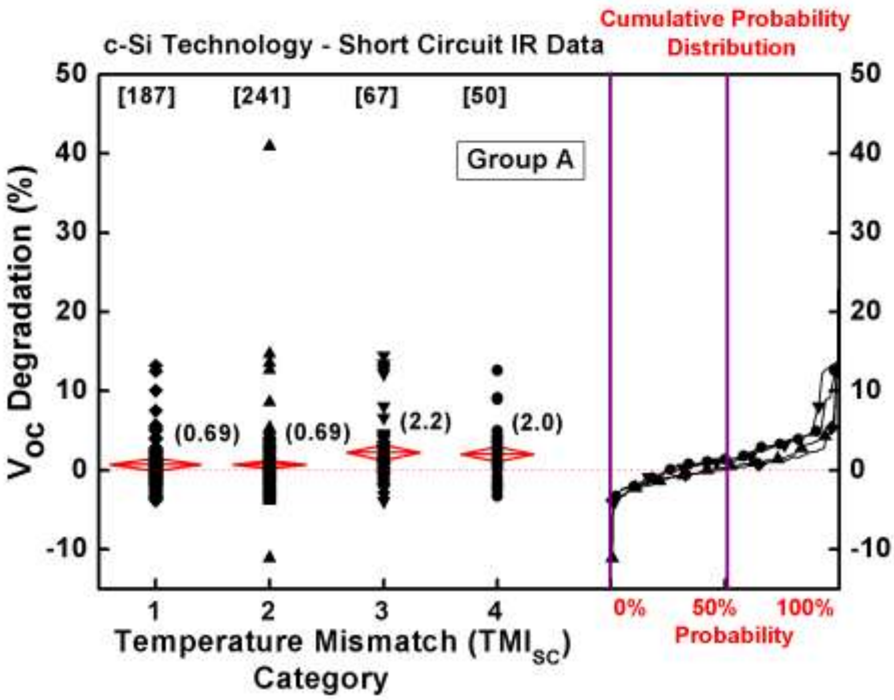

(c)

Fig. 7.15: Degradation of electrical parameters for different Thermal Mismatch categories under short circuit condition – (a) FF degradation (%), (b) I_{sc} degradation (%), and (c) V_{oc} degradation (%).

For analyzing the effect of module temperature mismatch at MPPT condition, the TMI_{MPP} ranges for the various temperature mismatch categories are chosen differently (as shown in Table 7.6), keeping in mind that the module temperatures are much lower when operated at MPPT condition as compared to short circuit condition. Fig. 7.16 shows the variation of the P_{max} degradation with the temperature mismatch categories, and the data for FF, I_{sc} and V_{oc} degradation are shown in Fig. 7.17. Again, we find that the average P_{max}

degradation is higher for higher temperature mismatch. In Fig 7.16, the categories 1, 2 and 3 are statistically different but categories 3 and 4 have similar data distribution (based on Mann Whitney U test statistics). There is good correlation of the fill factor and the short circuit current degradation with the temperature mismatch category. V_{oc} degradation is also higher for categories 3 & 4 as compared to categories 1 and 2, though the actual values are low. It should be noted that these correlations are for the total degradation in the electrical parameter (in percentage) and not with the degradation rate (in %/year).

Table 7.6: Temperature mismatch category based on TMI values at MPPT condition (TMI_{MPP})

TMI_{MPP}	0 – 0.25	0.25 – 0.5	0.5 – 1	> 1
Category	1	2	3	4

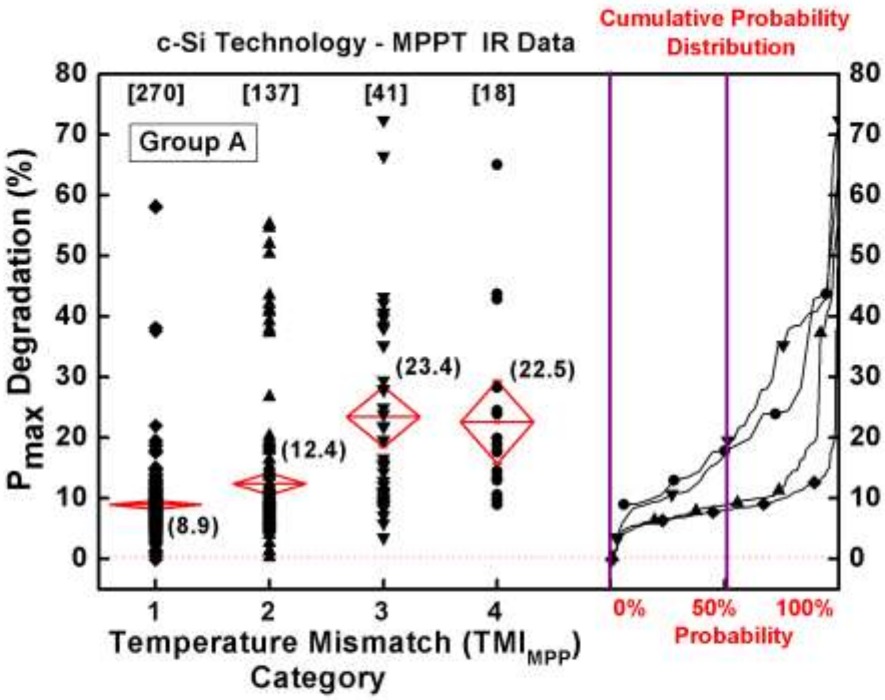

Fig. 7.16: P_{max} degradation (%) for different thermal mismatch categories at MPPT condition.

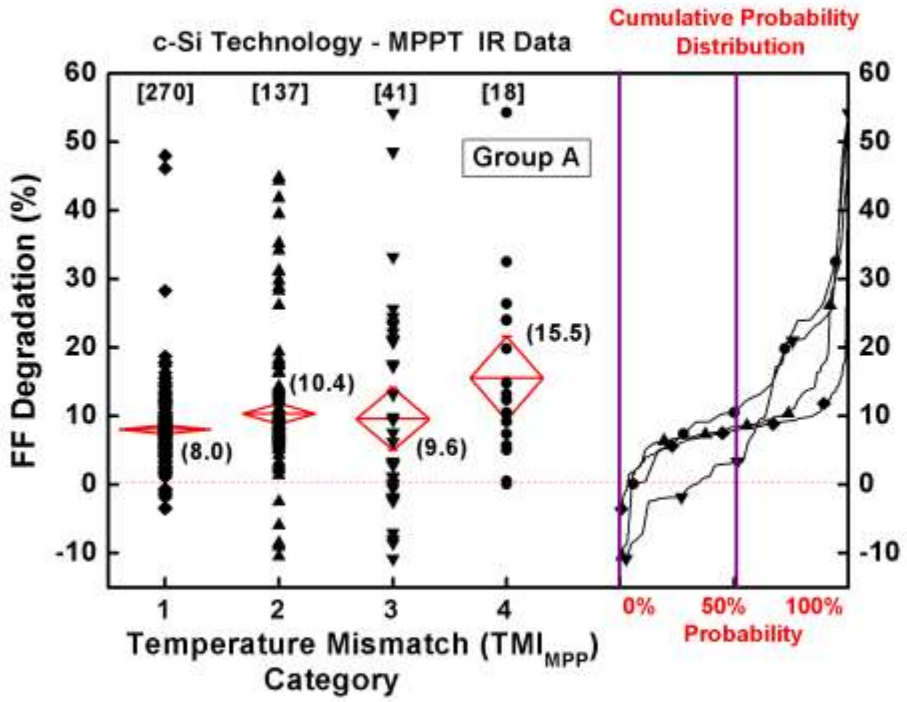
c-Si Technology - MPPT IR Data
Cumulative Probability Distribution
[270]
[137]
[41]
[18]
Group A
(8.0)
(10.4)
(9.6)
(15.5)
FF Degradation (%)
Temperature Mismatch (TMI_{MPP}) Category
0%
50%
100%
Probability

(a)

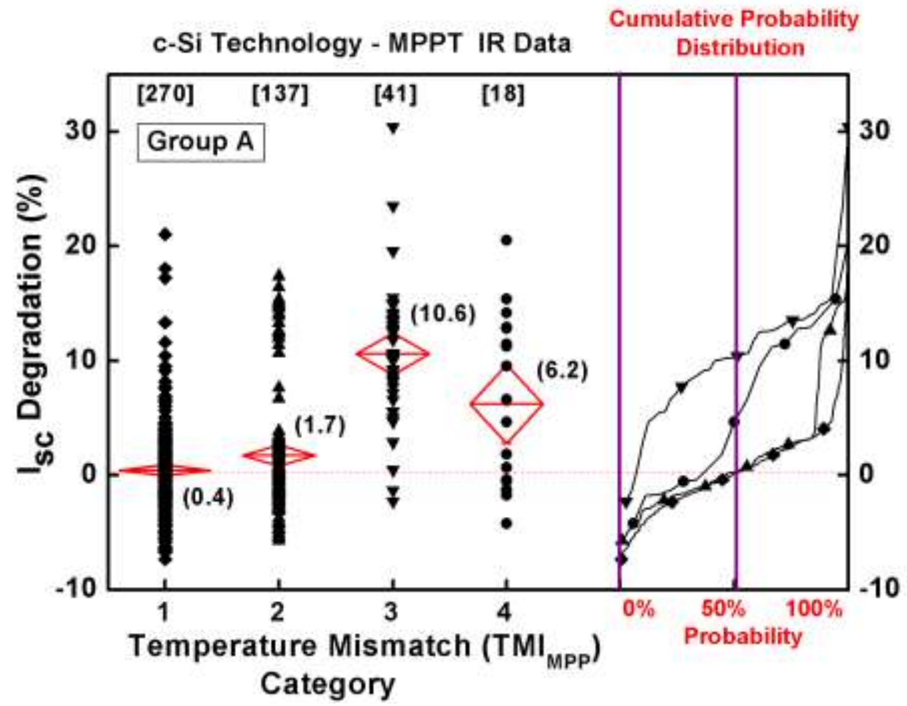
c-Si Technology - MPPT IR Data
Cumulative Probability Distribution
[270]
[137]
[41]
[18]
Group A
(0.4)
(1.7)
(10.6)
(6.2)
I_{SC} Degradation (%)
Temperature Mismatch (TMI_{MPP}) Category
0%
50%
100%
Probability

(b)

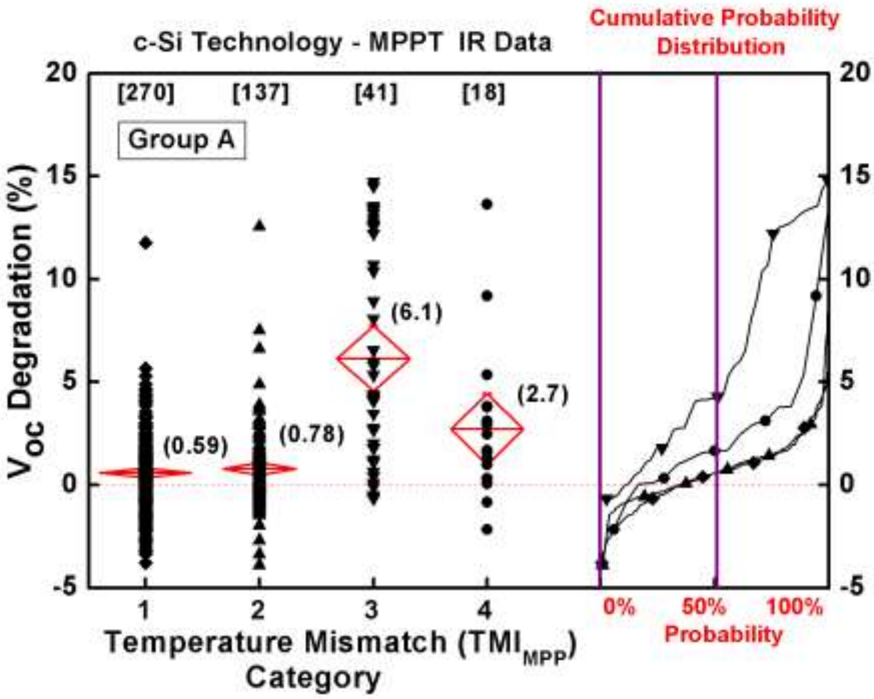

(c)

Fig. 7.17: Degradation of electrical parameters for different Thermal Mismatch categories at MPPT condition – (a) *FF* degradation (%), (b) I_{SC} degradation (%), and (c) V_{OC} degradation (%).

Since the distribution of the P_{max} degradation (%) for temperature mismatch category 3 and category 4 are statistically similar, we can consider modules in these two categories (i.e. $TMI_{MPP} > 0.5$) as modules with hot cells (which corresponds to a temperature difference of >5 °C in standard 60-cell 17% efficient modules under MPPT condition). Fig. 7.18 (a) shows the P_{max} degradation (%) for modules in Hot and Non-Hot zones, for modules with and without hot cells. It is evident that the modules with hot cells are showing higher degradation as compared to modules without hot cells, in both types of climates. Mann Whitney U test results show that difference between HC and NHC categories in both Hot zone and Non-Hot zone are statistically significant (p value < 0.05). There is also significant difference between the average degradation rates of modules with hot cells in Hot zone and Non-Hot zone (p value = 0.039). The module TMI values are similarly plotted in Fig. 7.18(b) and we can see that the TMI values are higher for modules with hot cells (trend similar to the P_{max} degradation plot).

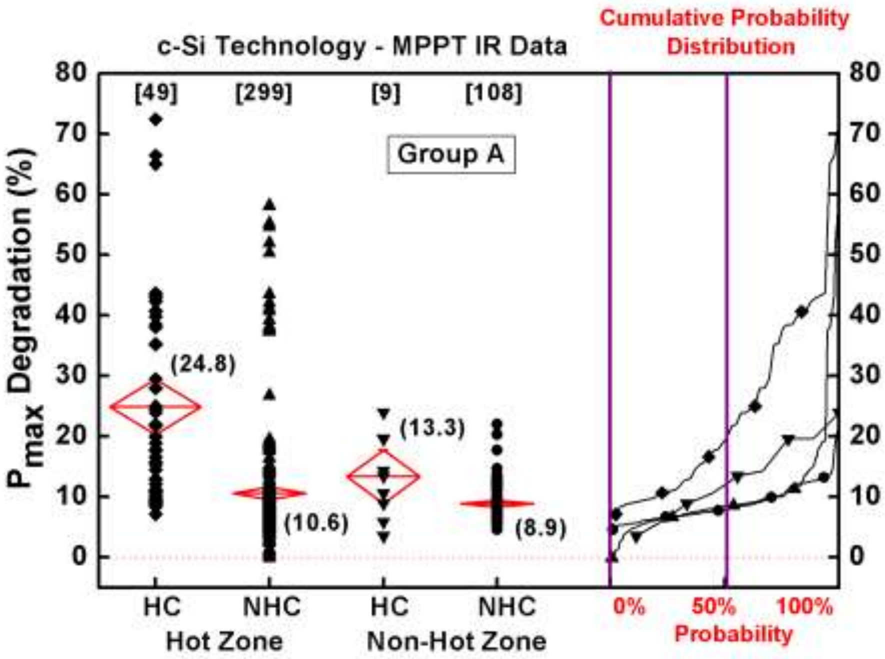

(a)

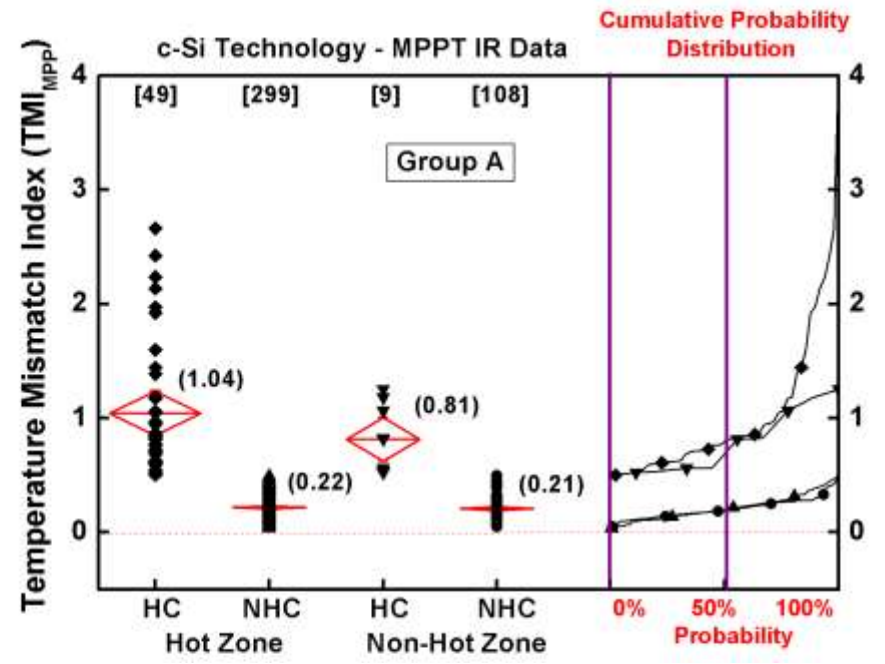

(b)

Fig. 7.18: Effect of Hot Cells on module performance in Hot and Non-Hot zones in terms of (a) P_{max} degradation (%), and (b) Temperature Mismatch Index.

Based on the above discussion, we conclude that the modules with hot cells suffer a higher degradation in power output. The power degradation is mainly being caused by the degradation in fill factor and short circuit current. Modules in the Hot zone show higher average P_{max} degradation due to hot cells as compared to modules in Non-Hot zone (though the number of samples is small so we cannot reach a definitive conclusion). This conclusion highlights the deleterious impact of Hot climates, and is likely to be one of the causes for the observed higher degradation rates in Hot zones as recorded in Chapter 4.

b) Effect of Mounting Location on Module Temperature

The translated module temperature (referenced to 1000 W/m^2 and 40 ^{o}C ambient conditions), for different mounting locations (roof or ground) is shown in Fig. 7.19 for Group X and Group Y separately. It is evident (though surprising) that there is not much difference in the translated module temperature between the different types of installations. Statistical analysis also shows that there is no statistically significant difference between the distributions of ground and rooftop systems in Group X and also ground mounted systems in Group Y, but Rooftop systems in Group Y have a statistically significant difference in the data distribution. It should be emphasized however, that during our Survey, almost all the 'rooftop' systems are actually roof rack-mounted systems, and we see that these do not run any hotter than ground rack-mounted systems. We have seen in Chapter 4 that the rooftop systems show higher degradation that ground systems, but the current analysis indicates that higher operating temperature is *not* a cause for this.

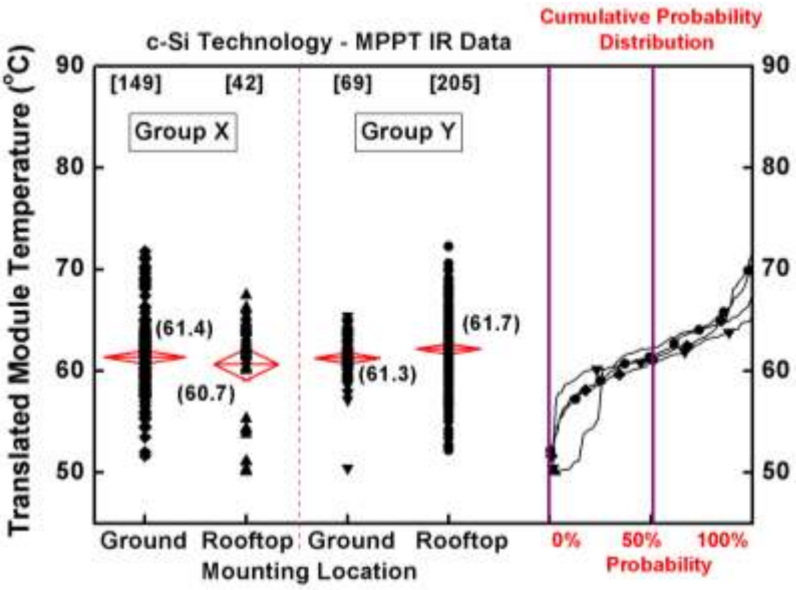

(a)

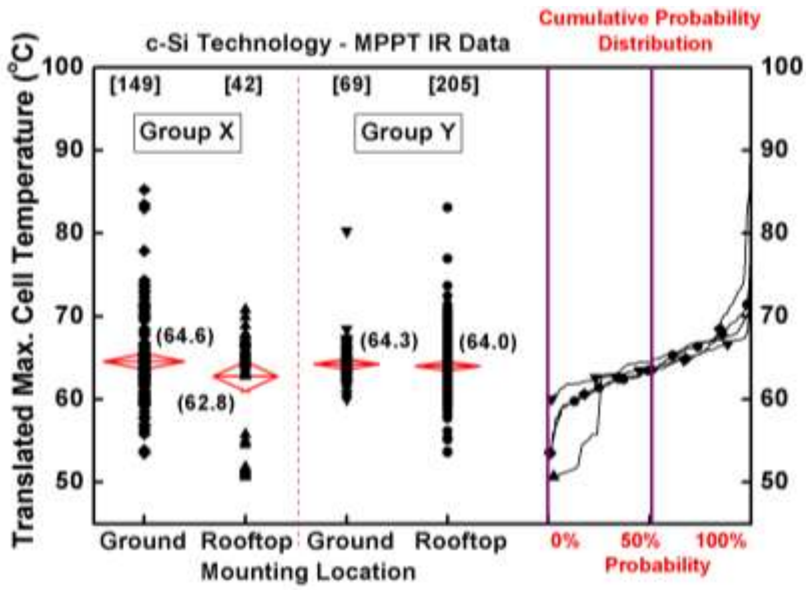

(b)

Fig. 7.19: Effect of mounting location on the translated module temperature (a), and maximum cell temperature (b), for Group X and Group Y sites.

Based on the above data, it can be concluded that modules with hot cells in the Hot zone suffer higher degradation. The power degradation seems to correlate well with the extent of mismatch between the cell temperatures in a module. 13% of the surveyed modules have shown hot cells (14% in the Hot zone sites and 8.5% in the Non-Hot sites), which is not a small number and hence the hot cell issue is a matter of concern. These factors should be considered while designing module reliability test standards for hot climates.

7.4 Summary

From the analysis of the electroluminescence and IR images, we can reach the following conclusions:

- Percentage of cracked cells is higher in modules from Group Y sites as compared to Group X sites, which indicates poor handling of the modules during manufacturing, transportation and/or installation for Group Y sites.

- Rooftop sites show more cracked cells than ground-mounted sites, as also young sites compared to old sites. This again indicates poor handling of the modules during manufacturing, transportation and/or installation for rooftop and young sites

- There is a good correlation between the total number of cracks in the module and the power degradation of the module.

- EL images are helpful in detecting cracked cells and broken interconnects in the module. Modules with snail trails have been found to have cracks in the corresponding cells.

- Modules with hot cells show higher power degradation than other modules, and this gets worse in Hot climates. Both fill factor and short circuit current degradation has been found to be contributors to the higher power degradation. Almost 13% of the surveyed modules fall in the hot cell category.

- No difference in module temperature has been found in ground installations versus rooftop (rack mounted) installations.

8. Quantification of Reliability of PV Modules in India

8.1 Introduction

Quantification of the reliability of PV modules is necessary for choosing reliable products as per the operating environment. The reliability of a PV module can be quantified using Risk Priority Number (RPN) analysis. PV modules have different failure modes or defects based on the materials used for construction of the module and the operating conditions. In this survey, the team has found different failure modes in different climatic zones.

Among the identified failure modes and its effects of a system on the basis of priority ranking, a criticality analysis has been done by using a quantitative index, known as Risk Priority Number (RPN). This analysis is done based on Failure Modes, Effects and Criticality Analysis (FMECA) as per IEC 60812. RPN is calculated as per the following equation:

$$RPN = S \times O \times D \qquad \text{... (8.1)}$$

where S is the severity, representing the impact of failure mode or defects; O is the occurrence, representing the probability of occurrence of failure mode based on the field data; and D is the detection, representing the recognizing or spotting and removing or preventing of failure modes of the analysed system.

The failure modes/defects are observed in PV modules after long term exposure in the field conditions. In this analysis, there are 86 defects of PV modules which are used, and the details are given in the Table 8.1 and Table 8.2. Table 8.1 shows 25 defects related to safety failures of PV modules. Table 8.2 shows 61 defects related to performance failure modes of PV modules.

Table 8.1: Defects of PV module related to safety failures

Glass	Frame	Junction box
Front glass crack Front glass shattered Rear glass crack Rear glass shattered	Frame grounding severe corrosion Frame grounding minor corrosion Frame joint separation Frame cracking	Junction box crack Junction box burn Junction box loose Junction box lid fell off Junction box lid crack Junction box sealing will leak
Backsheet	**Wire**	**Cell**
Backsheet peeling Backsheet delamination Backsheet burn Backsheet crack/cut under cell Backsheet crack/cut between cell	Wires burnt Wires animal bite/marks Wire insulation cracked	Hotspot above 20 ^{0}C String interconnect arc tracks

Table 8.2: Defects of PV module related to performance failure

Glass	Frame	Junction box
Front glass lightly soiled Front glass heavily soiled Front glass crazing Front glass chip Front glass milky discoloration Rear glass crazing Rear glass chip	Major corrosion of frame Minor corrosion of frame Frame bent Frame degraded Frame oozed Frame adhesive missing	Junction box lid loose Junction box warped Junction box weathered Junction box adhesive loose Junction box adhesive fell off Junction box wire attachments loose Junction box wire attachments fell off Junction box wire attachments arced
Cell	**Encapsulant**	**Backsheet**
Cell discoloration Cell burn Mark Cell crack Cell moisture penetration Cell worm mark Cell foreign particle embedded Cell Interconnect discoloration Gridline discoloration Gridline blossoming Busbar discoloration Busbar corrosion Busbar burn marks Busbar misaligned Cell Interconnect ribbon discoloration Cell Interconnect ribbon corrosion Cell Interconnect ribbon burn mark Cell Interconnect ribbon break String Interconnect discoloration String Interconnect corrosion String Interconnect burn mark String Interconnect break Hotspot less than 20˚C	Encapsulant delamination over the cell Encapsulant delamination under the cell Encapsulant delamination over the junction box Encapsulant delamination near interconnect or fingers Encapsulant discoloration -- (yellowing/browning)	Backsheet wavy Backsheet discoloration Backsheet bubble
Edge Seal	**Wires**	**Others**
Edge seal delamination Edge seal moisture penentration Edge seal discoloration Edge seal squeezed / pinched out	Wires pliable degraded Wires embrittled Wires corroded Wires soiled	Solder bond fatigue/failure Module mismatch

8.2 Methodology

8.2.1 Severity

Severity ranking of defects in a PV module is analyzed based on the performance of PV module in terms of power, short circuit current, fill factor and open circuit voltage. Severity was determined by ranking the failure mode of degradation from 1 to 10, where 1 indicates that the observed degradation mode has no effect on performance, and 10 indicates a major effect on both power and safety. The severity ranking is done by performance analysis with different defects for individual PV power plant. Defects are divided into two categories: safety failure mode, and performance failure mode as shown in Tables 8.1 and 8.2. The degradation rate of PV module in terms of P_{max}, I_{sc}, V_{oc} and FF are analyzed for performance defects. The average degradation rate for each defect is arranged and grouped into different categories. The scale is discrete and not continuous because correlating specific degradation modes to certain power losses varies with operating conditions. For each defect observed in a power plant, a ranking is given for a group of average degradation values. For safety failure mode, the ranking is done based on the severity of safety and average degradation rate for the particular defect. However, it is very necessary to provide high ranking for a defect with the risk of electric shock.

8.2.2 Occurrence

Occurrence ranking is done on the basis of defects observed in a power plant. The frequency of occurrence of each failure mode has been calculated by plotting the histogram of number of modules for a particular defect. This ranking corresponds to the observed number of failures that is occurring for a cause over the operational life of the PV power plant. Failure modes are identified in terms of probability of occurrence, grouped into discrete levels. The cumulative number of module failures for each defect per thousand per year (CNF) is calculated by using the following formula:

$$\mathrm{CNF}/1000 = \frac{(\text{cumulative \% defects})/10}{\text{cumulative operating time}} = \frac{\sum_{\text{systems}}(\text{\% defects})/10}{\sum_{\text{system}}(\text{operating time})} \qquad \text{... (8.2)}$$

The ranking is done by making a group of CNF/1000 for different defects and ranking them from 1 to 10. The ranking is high with high occurrence.

8.2.3 Detection

Ranking of detection D of each failure mode is done based on the criteria of detection with monitoring system/procedure used during the survey. The inspection of power plant is done through visual inspection and with sophisticated tools such as EL camera, *I-V* tracer, IR camera, insulation tester, Cell Line Checker, digital camera etc. The ranking 1 of a defect is given if the defect is easily detected by scheduled/regular maintenance or event-triggered inspections. In this study, lower ranking is given for the detection of defects with visual inspection, middle ranking is given for the detection of defects which can be identified only with indirect calculation procedure, and high ranking is given for the defects identified only by using sophisticated tools. However from reliability perspective, the ranking of detection procedure should be normalized.

8.2.4 Performance and Safety RPN

In this study, modules are separated into two categories: modules with less than 5 years of exposure (‘young’ modules) and module greater or equal to 5 year of exposure in the field condition (‘old’ modules). RPN analysis of failure modes/defects is divided into two categories: performance RPN and safety RPN. The risk priority number is analyzed for failure defects related to performance defects (referred to as Performance RPN) and for failure defects of PV module related to safety issues (referred to as Safety RPN). The RPN is calculated using two different ways:

$$\text{RPN} = S \times O \times D \qquad \text{... (8.3)}$$

and

$$\text{RPN\_SO} = S \times O \qquad \text{... (8.4)}$$

A comparison was done between RPN and RPN_SO for each defect to find out the influence of detection in order to estimate dominant defects with high value. It has been observed that some defects which are not easily detectable are also not very severe. But due to the high value of *D* (detection), the RPN is estimated to be high for such defects. This may lead the PV community to a wrong conclusion, and hence RPN_SO is also estimated. The RPN analysis is done for each power plant individually and the total result is combined for a climatic zone. The distributions of ranking of different defects are plotted with the maximum value observed in the respective climatic zone.

8.3 Results and Discussion

All the modules are analysed as per safety, reliability and durability failure definitions stated by Shrestha *et al.* [54]. Shrestha *et al.* have mentioned that defects with safety issues can be termed as safety failure, modules with degradation rate more than 1 %/year excluding the module with safety issues are termed as modules with reliability failure; and modules with degradation rate less than 1 %/year excluding the module with safety issues but having other defects are termed as module with durability failure. In Fig. 8.1, a pie chart of durability loss, safety failure, and reliability failures of the studied modules for the different climatic zones are plotted. This analysis is done for the entire module data collected during the survey, segregating in terms of climatic zones only. It has been observed that more than 70% of the surveyed modules have reliability and safety failure defects.

8.3.1 <u>RPN Analysis for Six Climate Classification</u>

a) Cold & Cloudy climatic zone

In Cold & Cloudy climatic zone, we have studied modules with less than 5 years of exposure only. Figure 8.2 shows the average ranking of severity, occurrence and detection of different failure modes/defects for this zone. In this zone, we have not found any defects which leads to safety issues. Gridline discoloration is the most severe defect in this climatic zone in terms of performance. The maximum average degradation rate of 0.65%/year is observed for module with inter-circuitry discoloration and highest severity ranking is given. In terms of performance RPN, gridline discoloration is the most severe defect as compared to other defects (refer Fig. 8.3). By normalizing the detection of all the defects, RPN_SO is also estimated for all the failure modes observed for the various climatic zones. There is not very much variation in the failure modes in terms of RPN_SO and RPN.

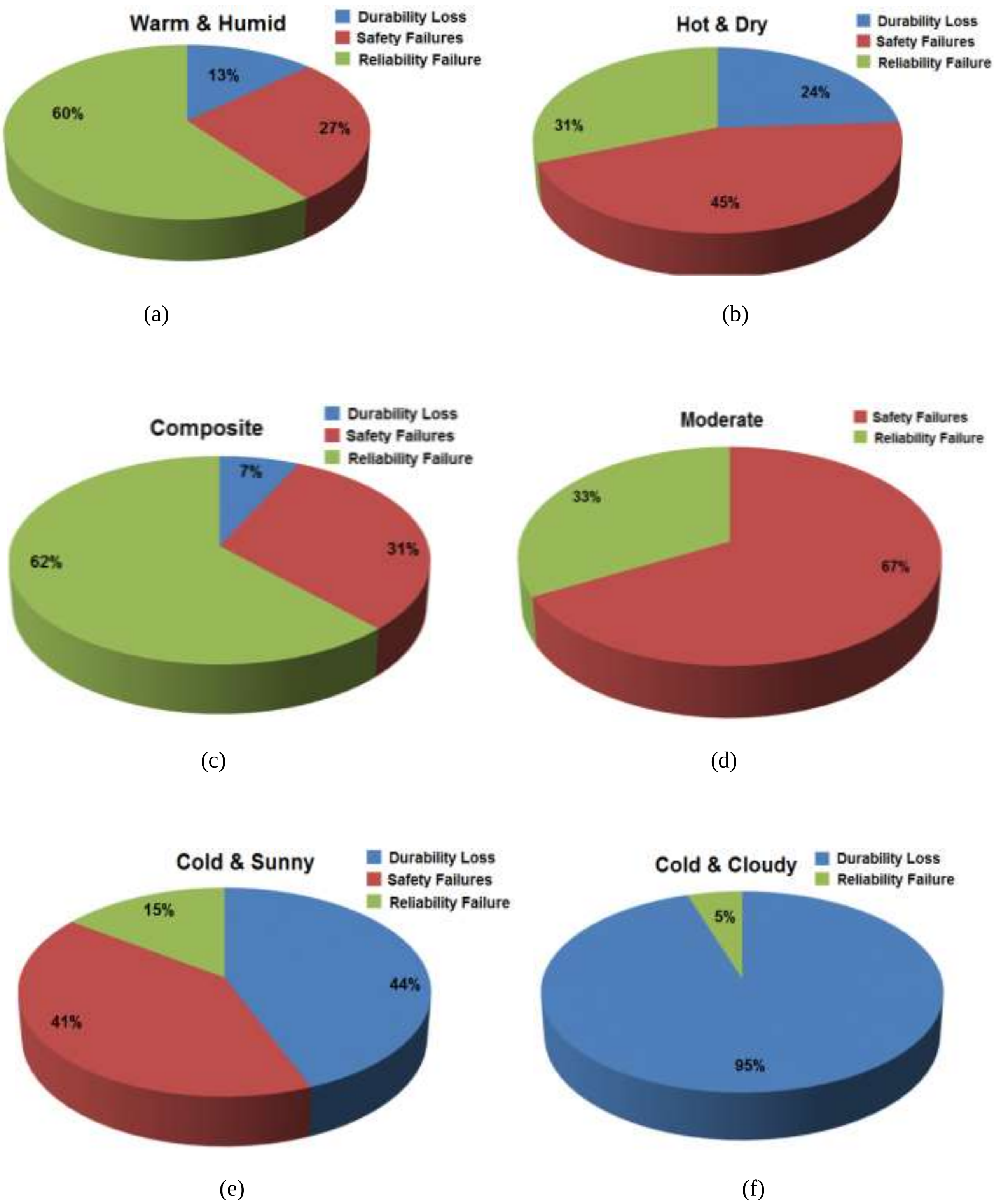

Fig. 8.1: Safety failure, Reliability failure and durability loss of modules for different climatic zones.

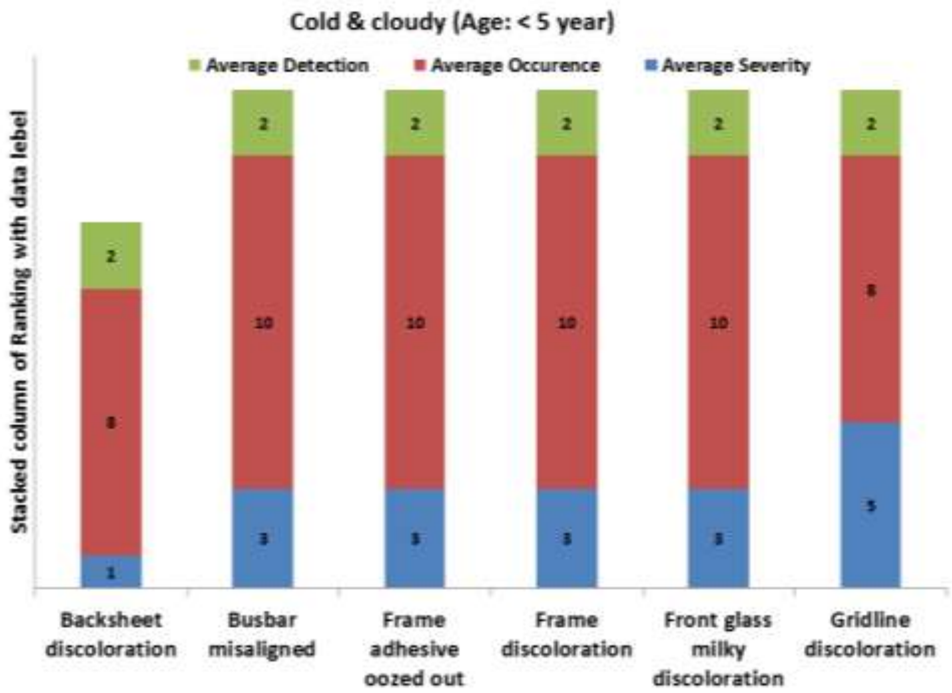

Fig. 8.2: Distribution of average ranking of different defects for Cold & Cloudy zone.

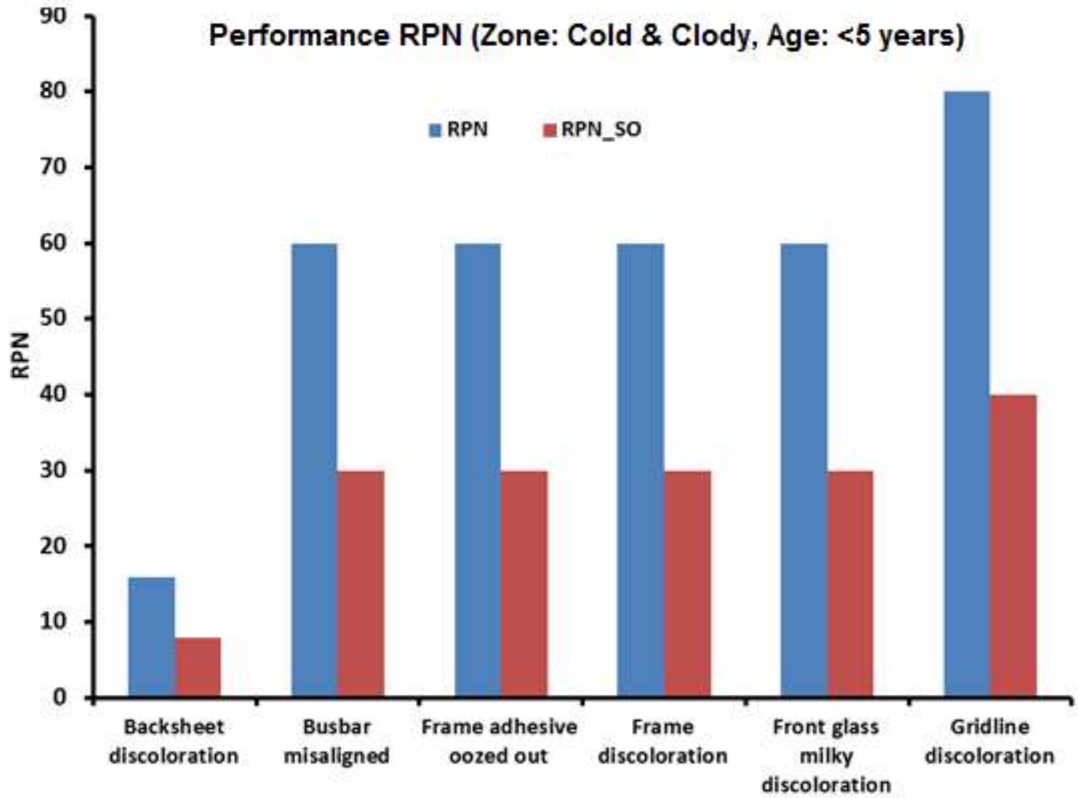

Fig. 8.3: Performance RPN of different defects for Cold & Cloudy zone.

b) Cold & Sunny climatic zone

In this climatic zone, the modules are separated into two groups based on their age viz. less than 5 years of exposure and more than 5 years of exposure. The average ranking of different failure defects in terms of severity, occurrence and detection is shown in Fig. 8.4. For modules with less than 5 years of exposure, the maximum overall average degradation was observed in modules with backsheet peeling and backsheet burn marks. The highest performance RPN is only 20 in this condition. In case of safety failure defects backsheet burn marks and backsheet peeling are the most dominant defects with highest ranking for this condition as shown in Fig. 8.5. In terms of safety RPN, backsheet peeling is the most severe defects with highest RPN and RPN_SO (refer Fig. 8.5).

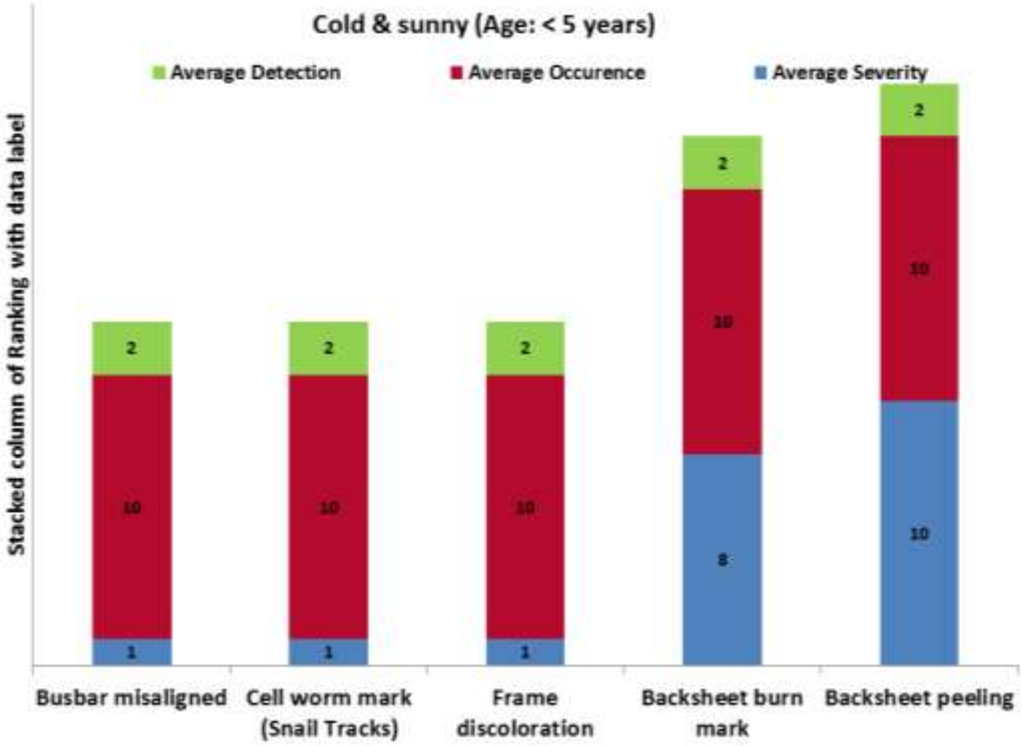

Fig. 8.4: Distribution of average ranking of different defects for Cold & Sunny zone for modules with less than 5 years of exposure.

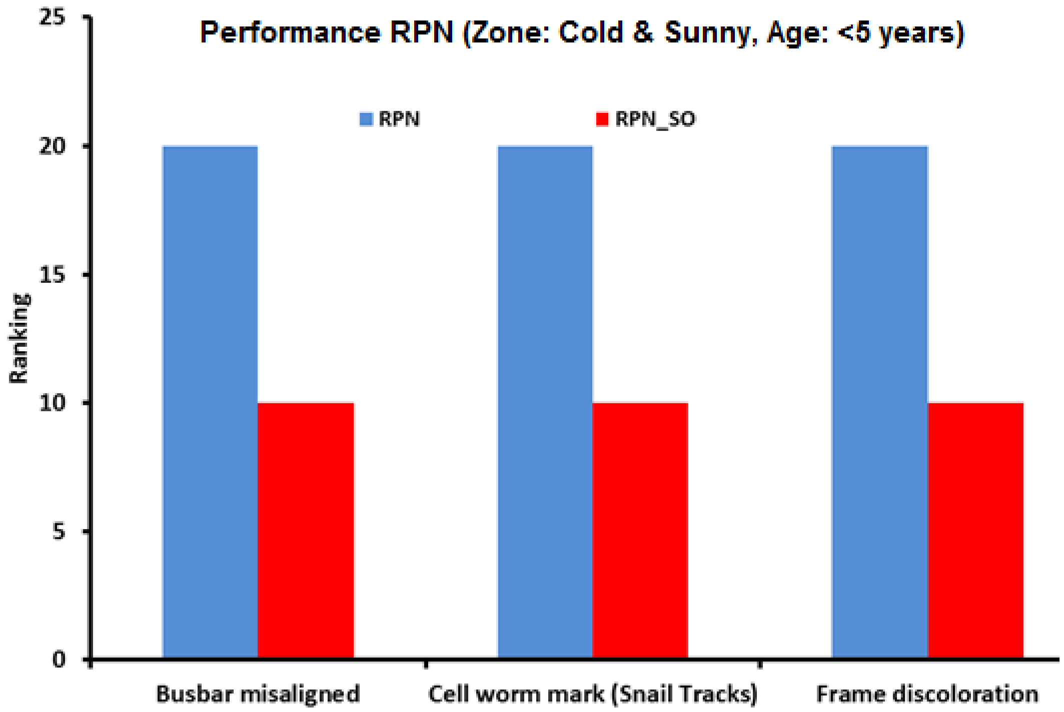

(a)

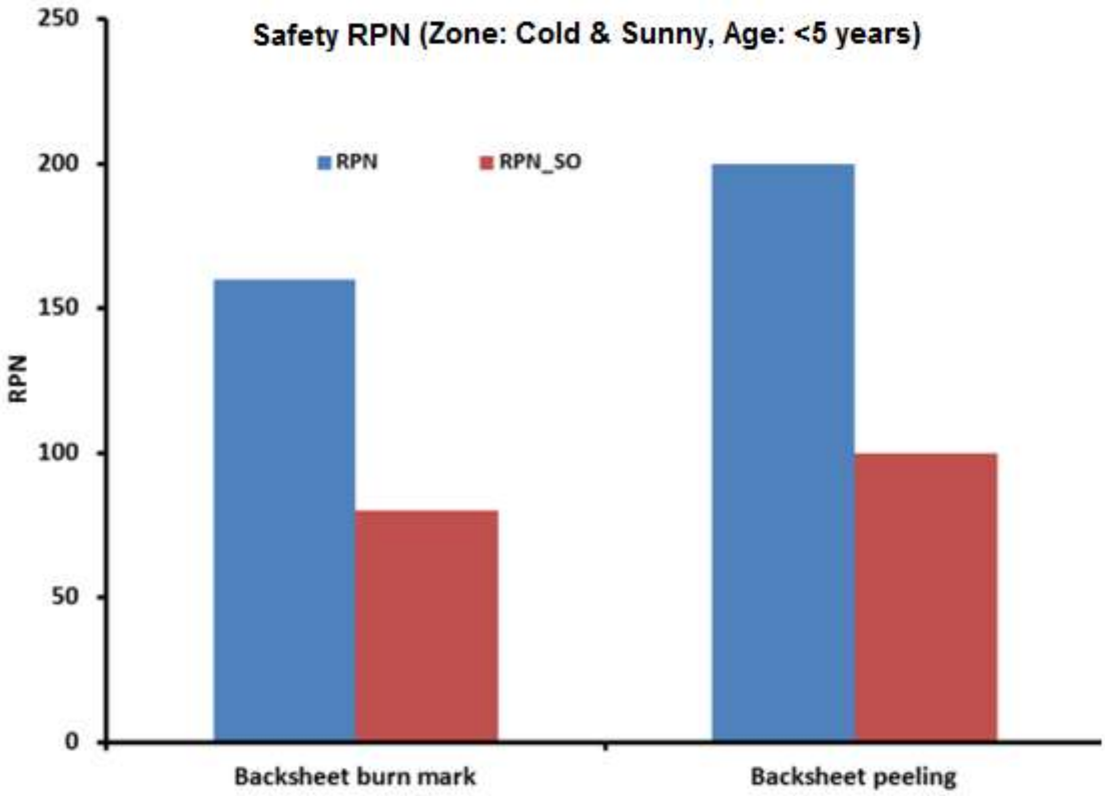

(b)

Fig. 8.5: RPN of different defects for Cold & Sunny zone for modules with less than 5 years of exposure – (a) Performance RPN, and (b) Safety RPN.

For modules with more than 5 years of exposure in Cold & Sunny zone, the distribution of average ranking for different defects is shown in Fig. 8.6. Most of the defects are related to performance of the module only. The maximum average degradation rate of 1.3 %/year is observed in module with string interconnect break. There is a difference of 70% in average degradation rate in best and worst modules with defects. It has been observed that the performance RPN of solder bond fatigue/failure is high, followed by cell discoloration, encapsulant discoloration, problems in frame and gridline discoloration (refer Fig. 8.7). As per RPN_SO, the risk is high for cell discoloration, encapsulant discoloration, problems in frame and gridline discoloration. The highest value of RPN_SO is 70. In case of safety RPN, hot spot over 20 ^{0}C is showing the highest value as compared to other safety failure observed in this climatic zone. The 'wires insulation cracked/disintegrated' is also one of the severe defects in this zone. In terms of RPN_SO, the wires insulation cracked/disintegrated is the highest severe defects as shown in the Fig. 8.7.

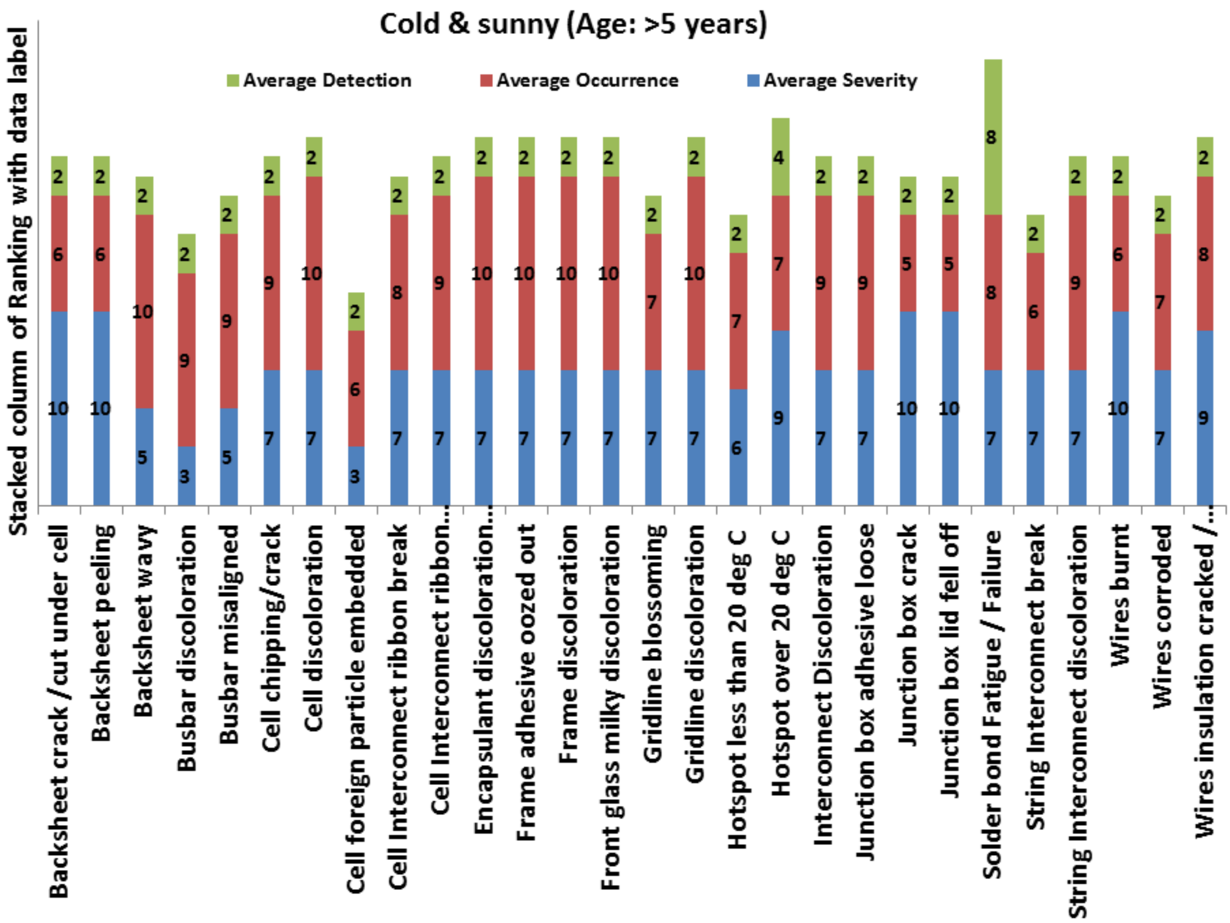

Fig. 8.6: Distribution of average ranking of different defects for Cold & Sunny zone for modules with more than 5 years of exposure.

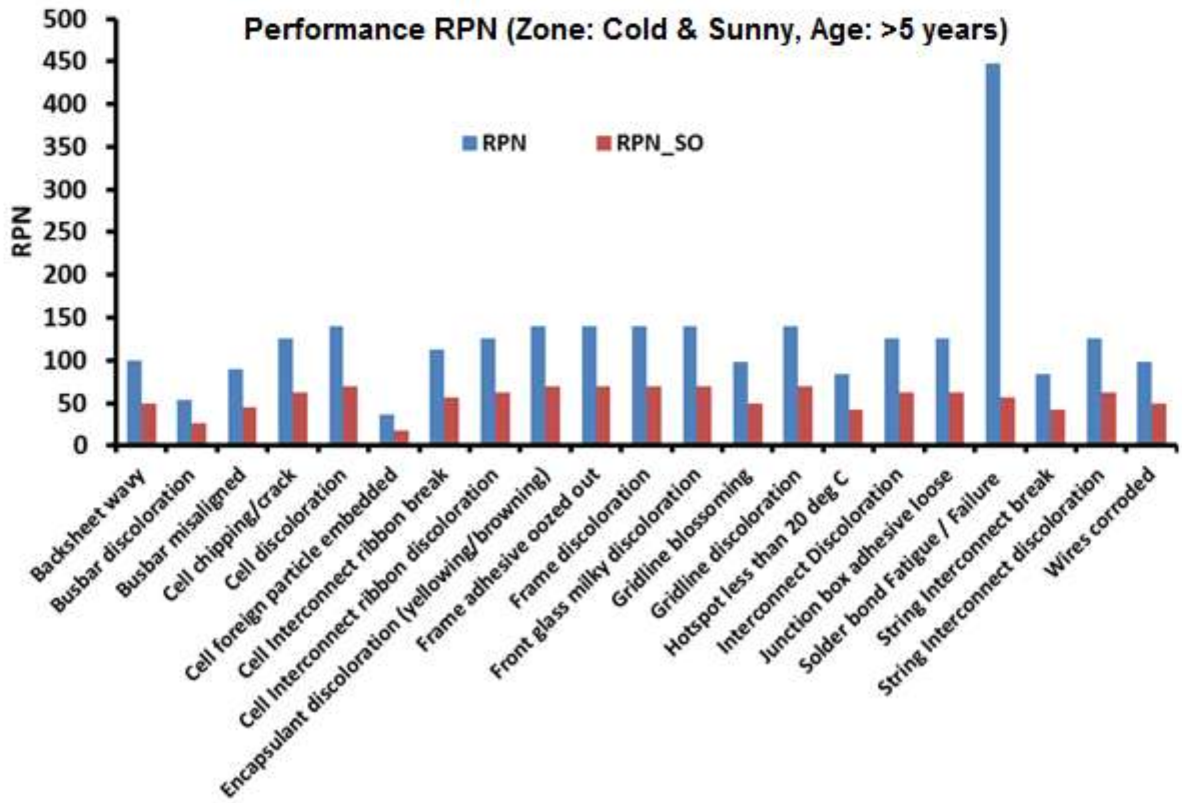

(a)

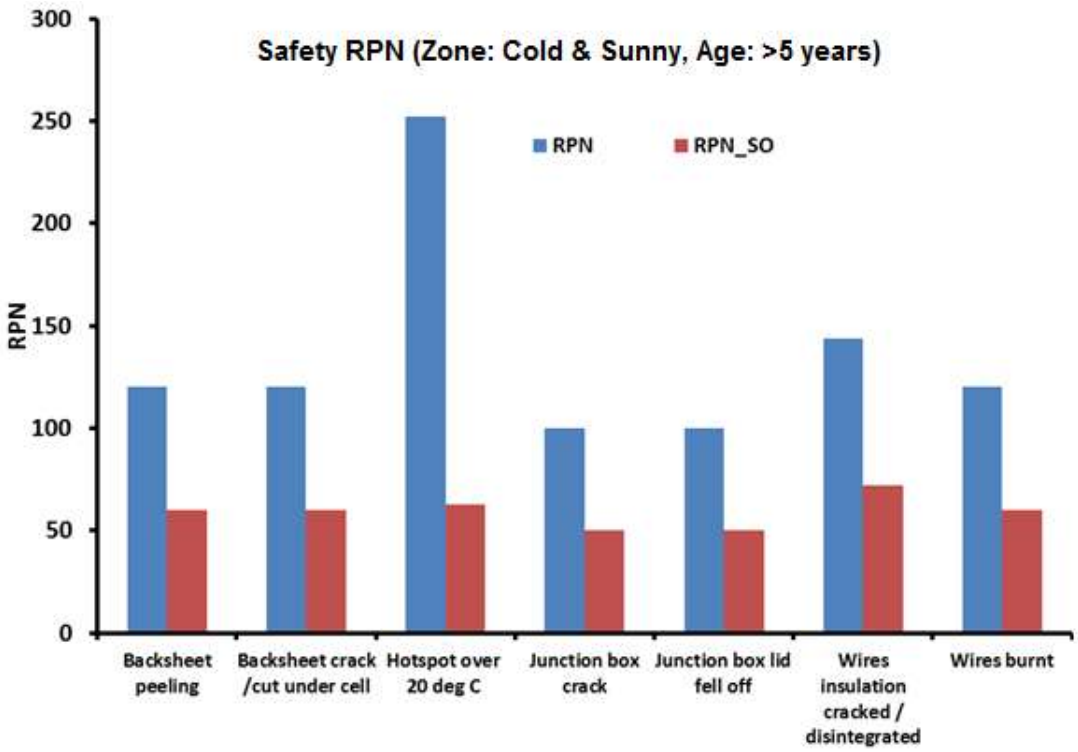

(b)

Fig. 8.7: RPN ranking of different defects for Cold & Sunny zone for modules with more than 5 years of exposure – (a) Performance RPN, and (b) Safety RPN.

c) Hot & Dry climatic zone

In this climatic zone, the performance related defects have high ranking of severity for module with less than 5 years of exposure. The maximum average degradation rate of 4.9 %/year is observed in module with cell chipping/crack and hotspot. Lower degradation rate of 1.2 %/year is found in the module with backsheet bubbles. The occurrence ranking is also found to be high for the defects observed in less than 5 years of exposure (refer Fig. 8.8). The solder bond fatigue is the dominant performance RPN in this climatic zone. In terms of performance RPN_SO for less than 5 years of exposure, the dominant defects are busbar misaligned, cell chipping, gridline and interconnect discoloration. Backsheet burn mark and frame grounding corrosion are the dominant safety failure for this zone with high RPN (refer Fig. 8.9).

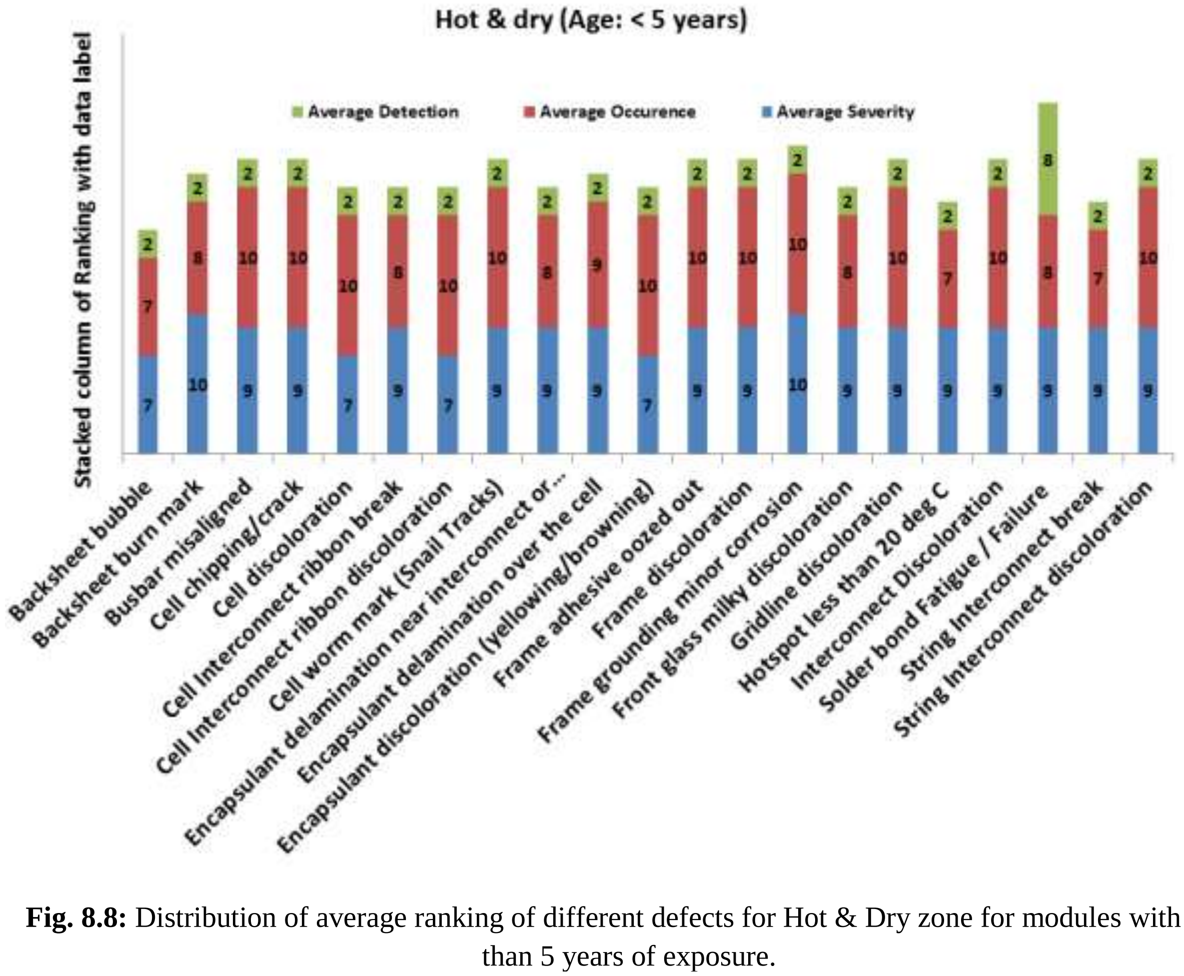

Fig. 8.8: Distribution of average ranking of different defects for Hot & Dry zone for modules with less than 5 years of exposure.

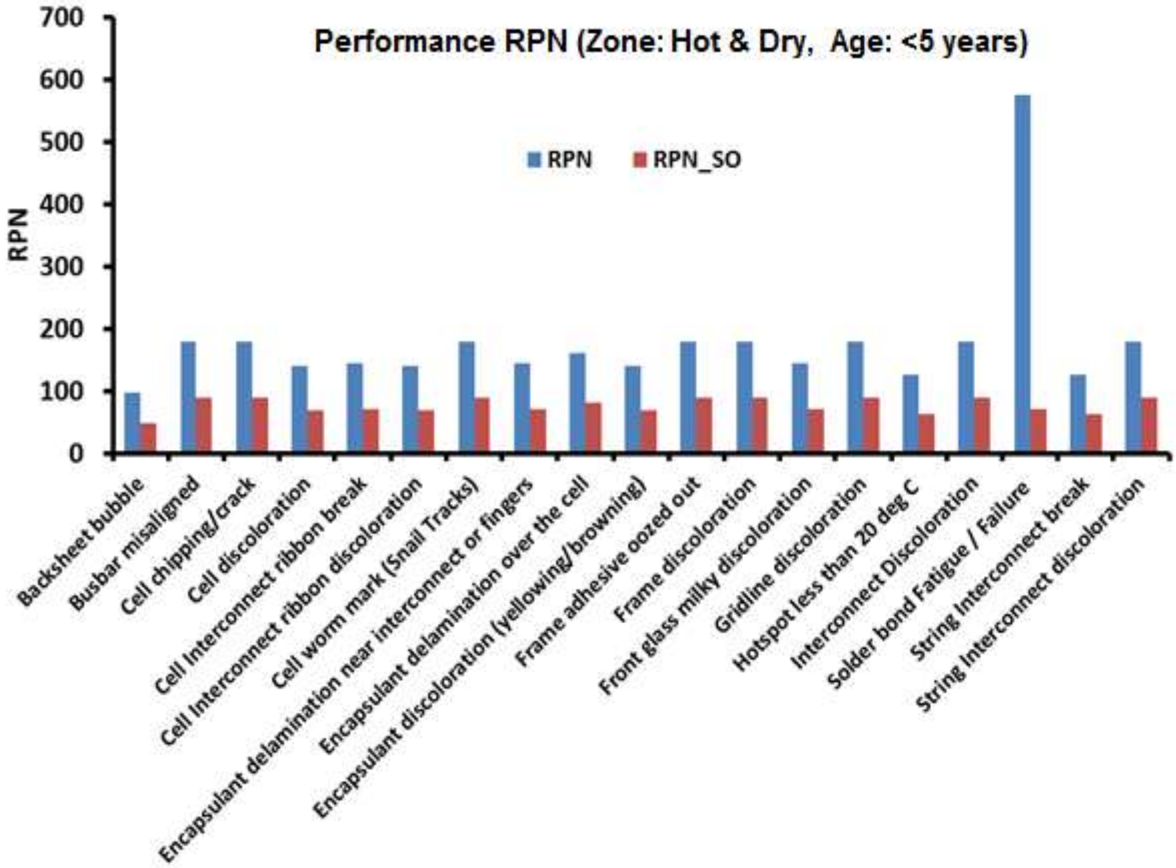

(a)

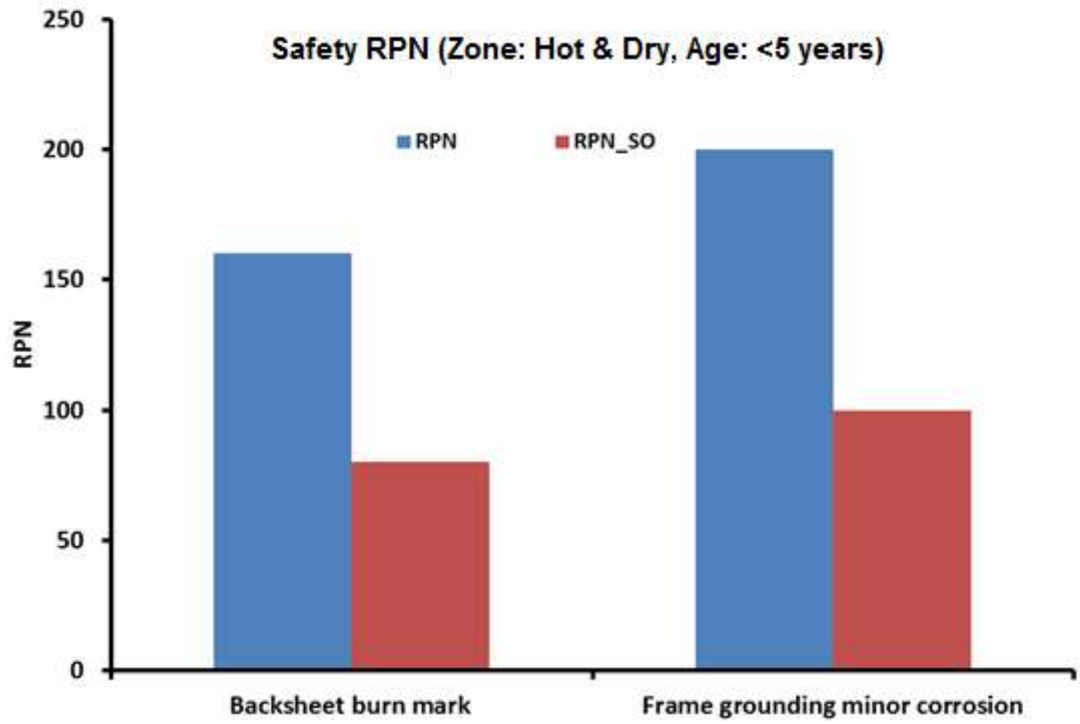

(b)

Fig. 8.9: RPN of different defects for Hot & Dry zone for modules with less than 5 year of exposure – (a) Performance RPN, and (b) Safety RPN.

For installations with greater than 5 year of exposure in Hot & Dry climatic zone, the distribution of average ranking for different failure modes are shown in Fig. 8.10. The severity ranking of all failure modes observed in this zone related to performance defects is more than 6. Average degradation rates of module is high, around 3 %/year, in the case of module with defects viz. hot spot, string interconnect break. There is a difference of 70% in the average degradation rate in best and worst modules with defects. Solder bond fatigue is the defects with highest value of performance RPN followed by hotspot (refer Fig. 8.11). But in terms of performance RPN_SO, dominant defects with high risk are bubbles in the backsheet, encapsulant discoloration. In case of safety RPN, hotspot and frame grounding corrosion are the main defects. However in terms of safety RPN_SO, backsheet crack/cut under cell and frame grounding corrosion are the main defects as shown in the Fig. 8.11.

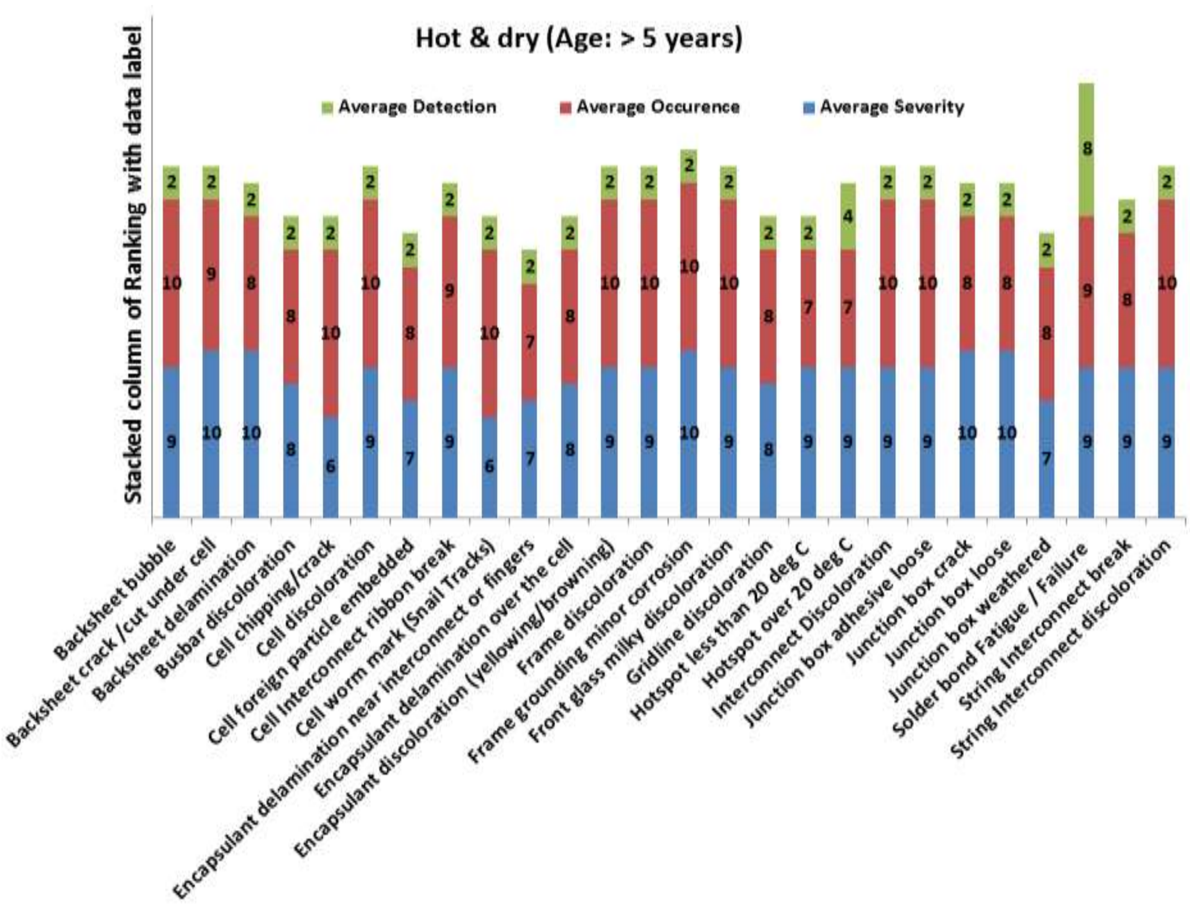

Fig. 8.10: Distribution of average ranking of different defects for Hot & Dry zone for modules with more than 5 years of exposure.

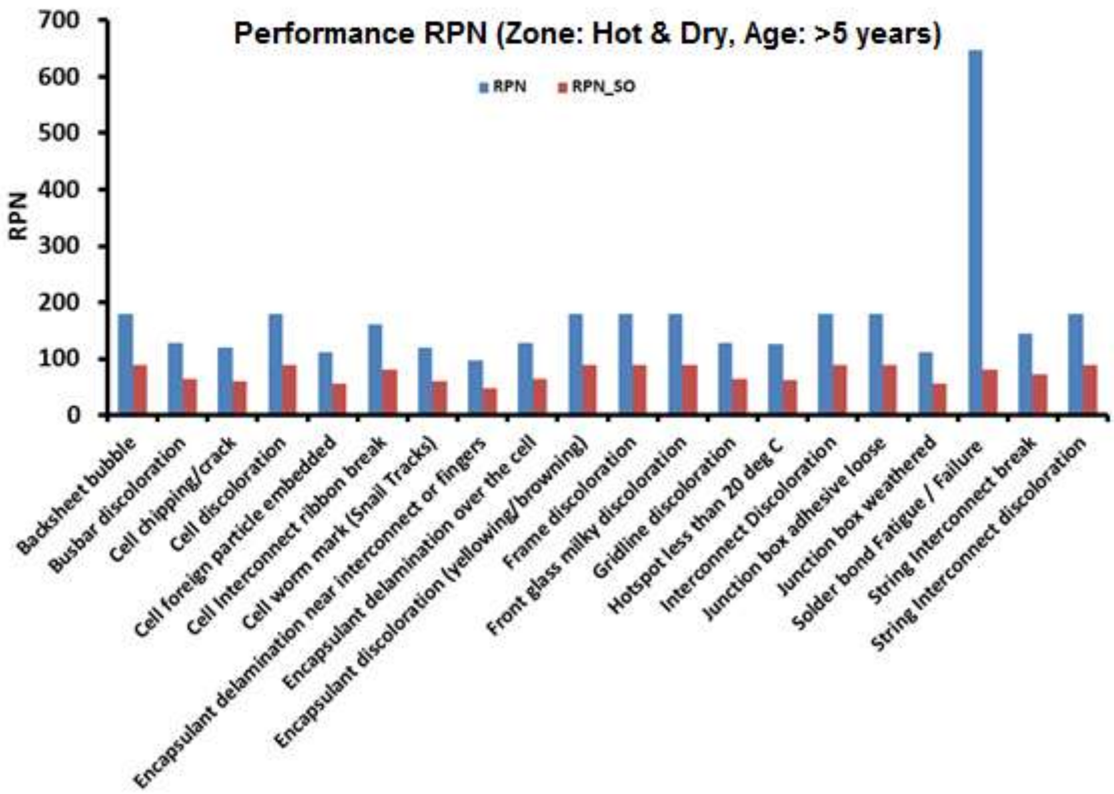

(a)

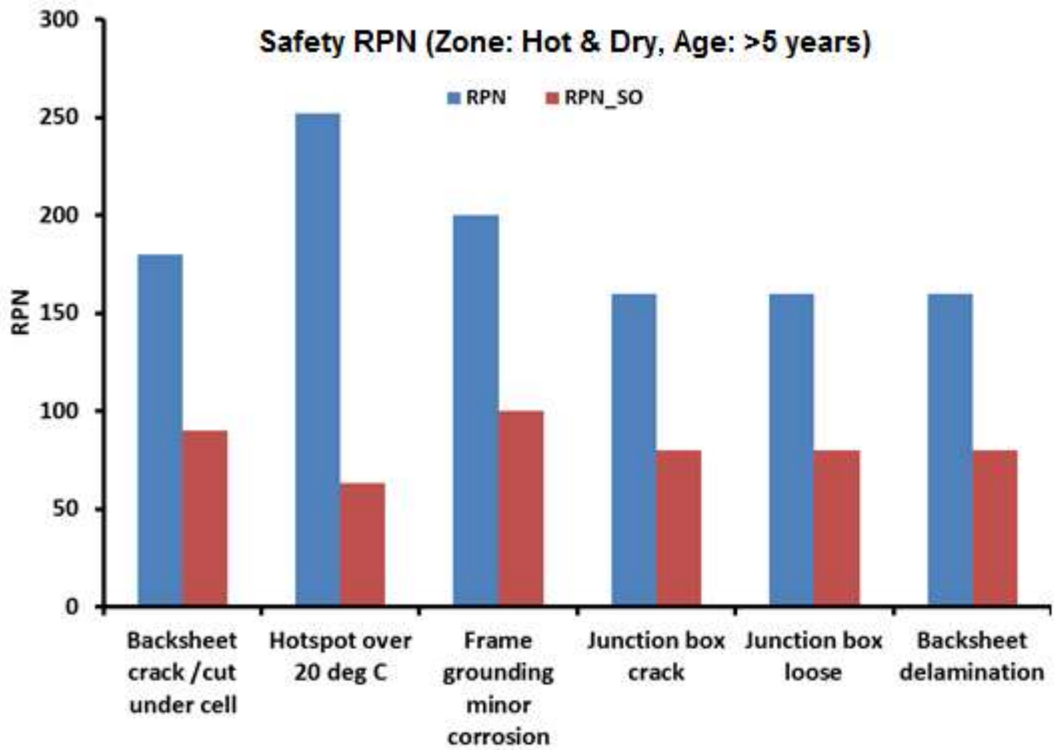

(b)

Fig. 8.11: RPN of different defects for Hot & Dry zone for modules with more than 5 years of exposure – (a) Performance RPN, and (b) Safety RPN.

In this climatic zone, average degradation rate of modules is high around 3.9 %/year in the case of modules with defects (like cell worm marks (Snail Tracks), gridline blossoming and grid line discoloration). The severity rankings of these defects are highest in case of modules with less than 5 years of exposure in moderate climatic zone (refer Fig. 8.12). The lowest mean degradation rate is 0.3 %/year in the case of cell interconnect ribbon discoloration. Based on the ranking and the performance RPN for modules with less than 5 year of exposure, Cell worm mark (Snail Tracks), gridline blossoming and grid line discoloration are the dominant failure modes (refer Fig. 8.13). Frame grounding corrosion is one of the dominant degradation/failure modes in terms of safety for this site. However the mean degradation rate for other safety failure modes (backsheet crack and backsheet peeling) is high around 4.8 %/ year.

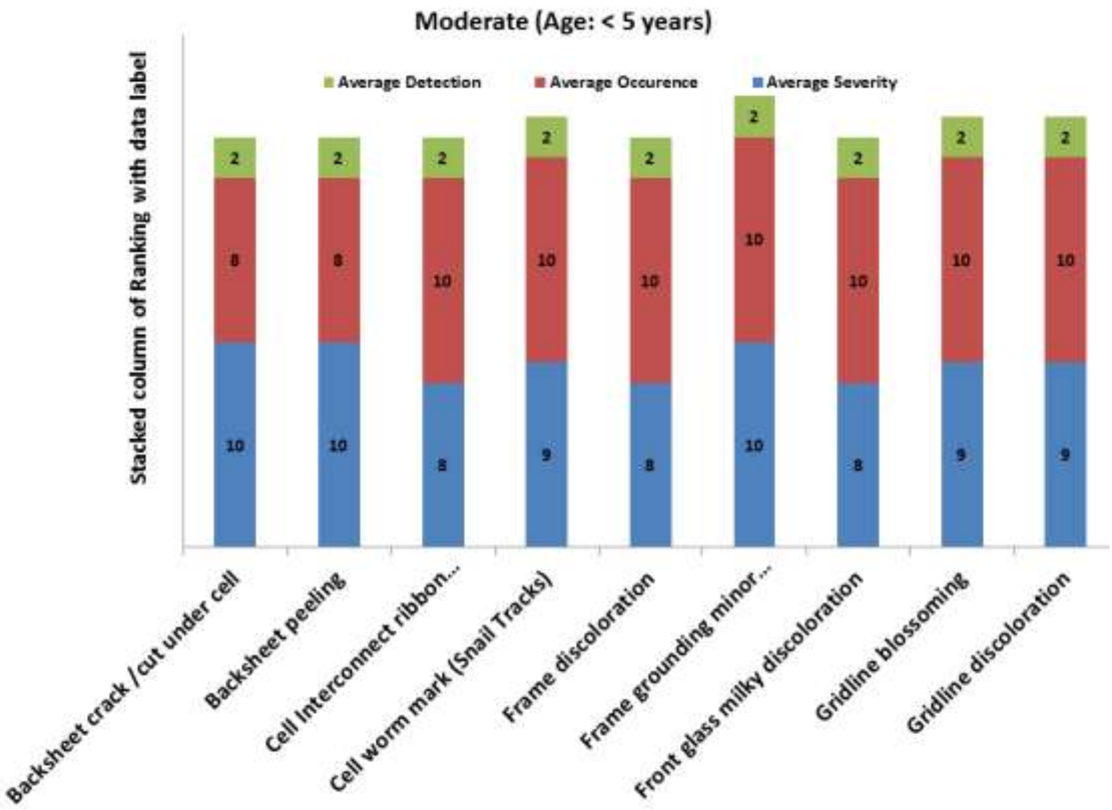

Fig. 8.12: Distribution of average ranking of different defects for Moderate zone for modules with less than 5 years of exposure.

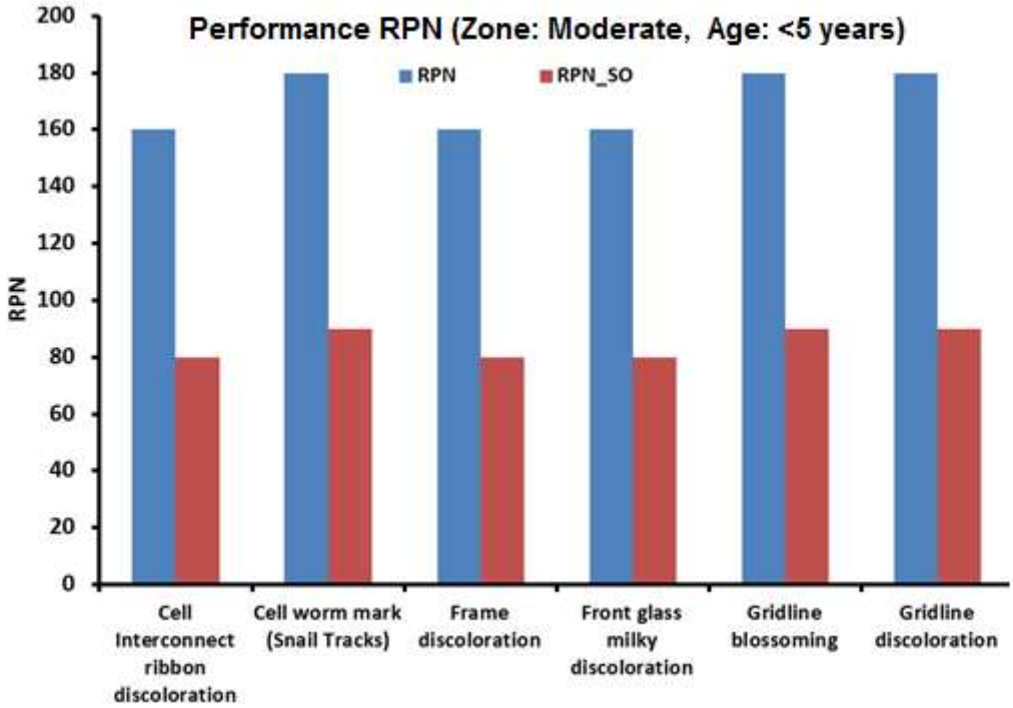

(a)

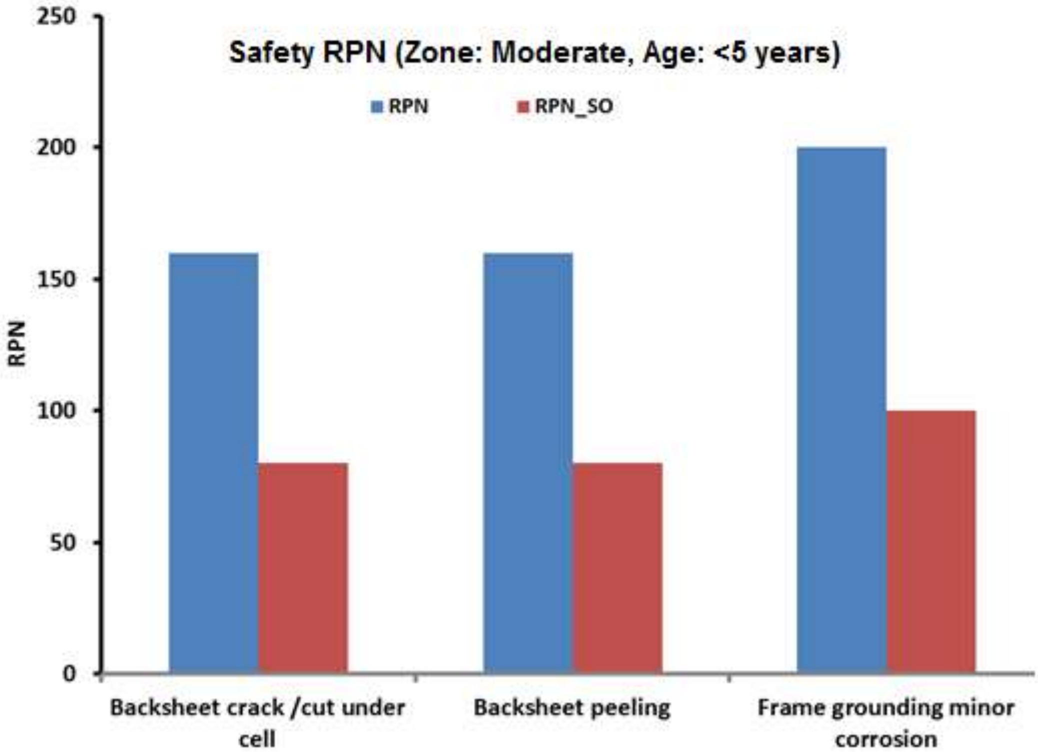

(b)

Fig. 8.13: RPN of different defects for Moderate zone for modules with less than 5 years of exposure – (a) Performance RPN, and (b) Safety RPN.

e) Warm & Humid climatic zone

In this climatic zone, the highest mean degradation rate of 4.2% is observed in the modules with backsheet discoloration and front glass milky discoloration. There is more than 70% change in degradation value between the best and worst modules with performance defects. The occurrence of defects in backsheet and metallization are high for module with less than 5 years of exposure in this climatic zone (refer Fig. 8.14). The solder bond fatigue/failure can be seen as the dominant degradation/failure mode for this site, as it has the highest RPN of 648. In terms of RPN_SO, backsheet discoloration, interconnect discoloration, frame discoloration and milky discoloration of glass are the dominant failure modes (refer Fig. 8.15).

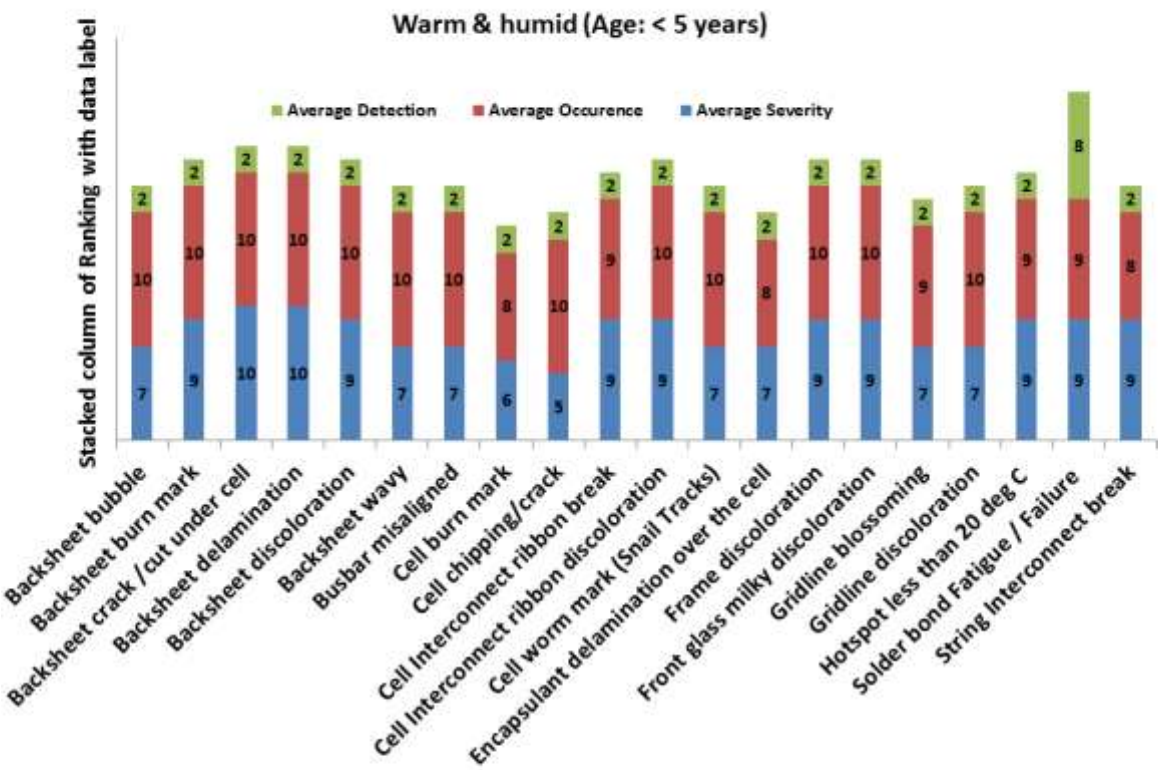

Fig. 8.14: Distribution of average ranking of different defects for Warm & Humid zone for modules with less than 5 years of exposure.

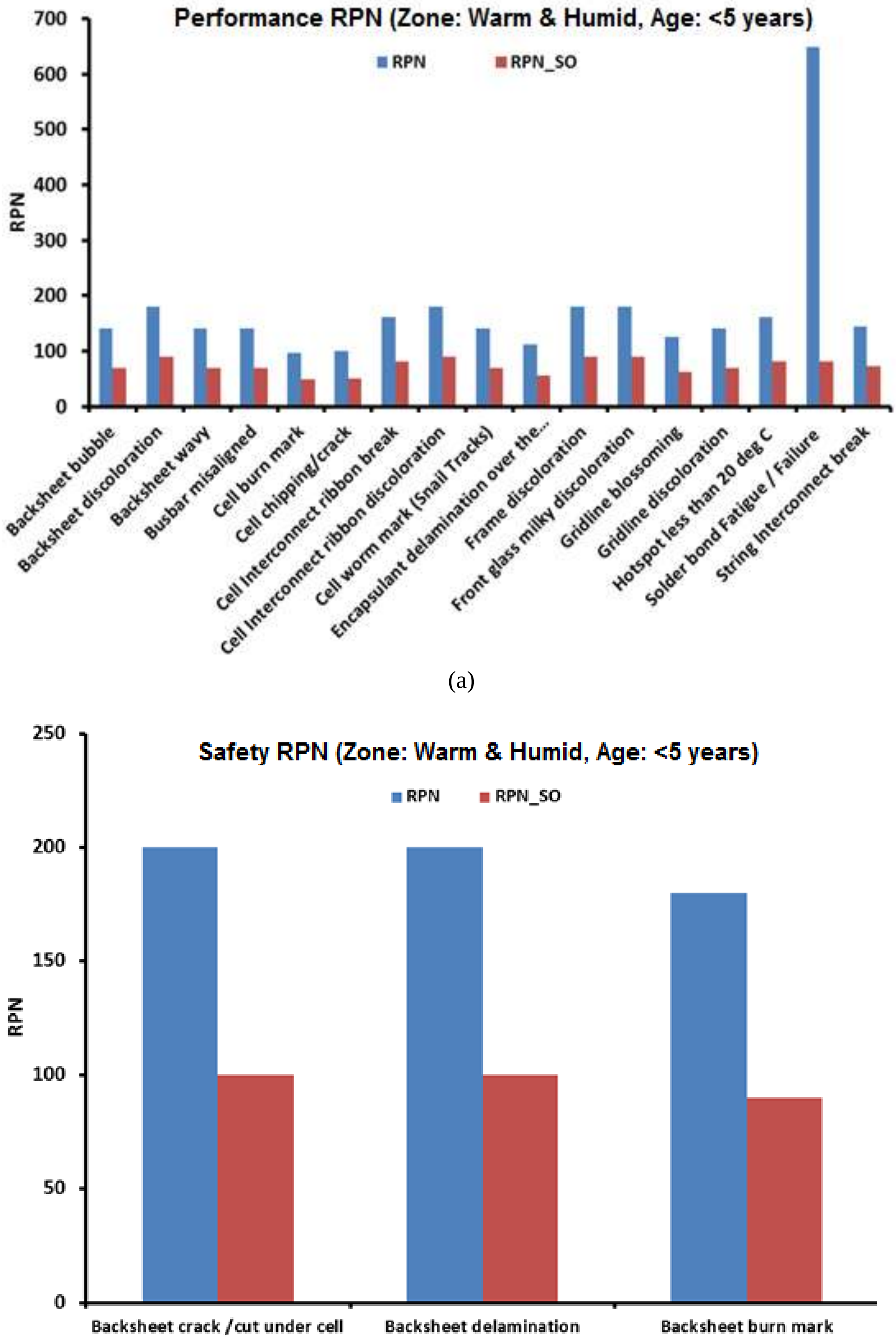

(a)

(b)

Fig. 8.15: RPN of different defects for Warm & Humid zone for modules with less than 5 years of exposure – (a) Performance RPN, and (b) Safety RPN.

In the case of module with more than 5 years of exposure, the highest average degradation rate for modules with encapsulant delamination and interconnect ribbon burn mark is around 2.7 %/year. There is more than 75% change in degradation value between the best and worst modules with performance defects, for modules with more than 5 years of exposure. The occurrences of most of the defects are observed with ranking in the range of 10 only (refer Fig. 8.16). Solder bond fatigue/failure can be seen as the dominant degradation/failure mode for this site, as it has the highest RPN of 504. Figure 8.17 shows that problems in busbar; cell, interconnect & encapsulant discoloration; problems in frame and metallization are the main failure modes as per RPN_SO. In case of safety RPN, hotspot is the dominant degradation mode. However as per safety RPN_SO, backsheet crack/cut is the dominant degradation mode for modules with greater than 5 years of exposure.

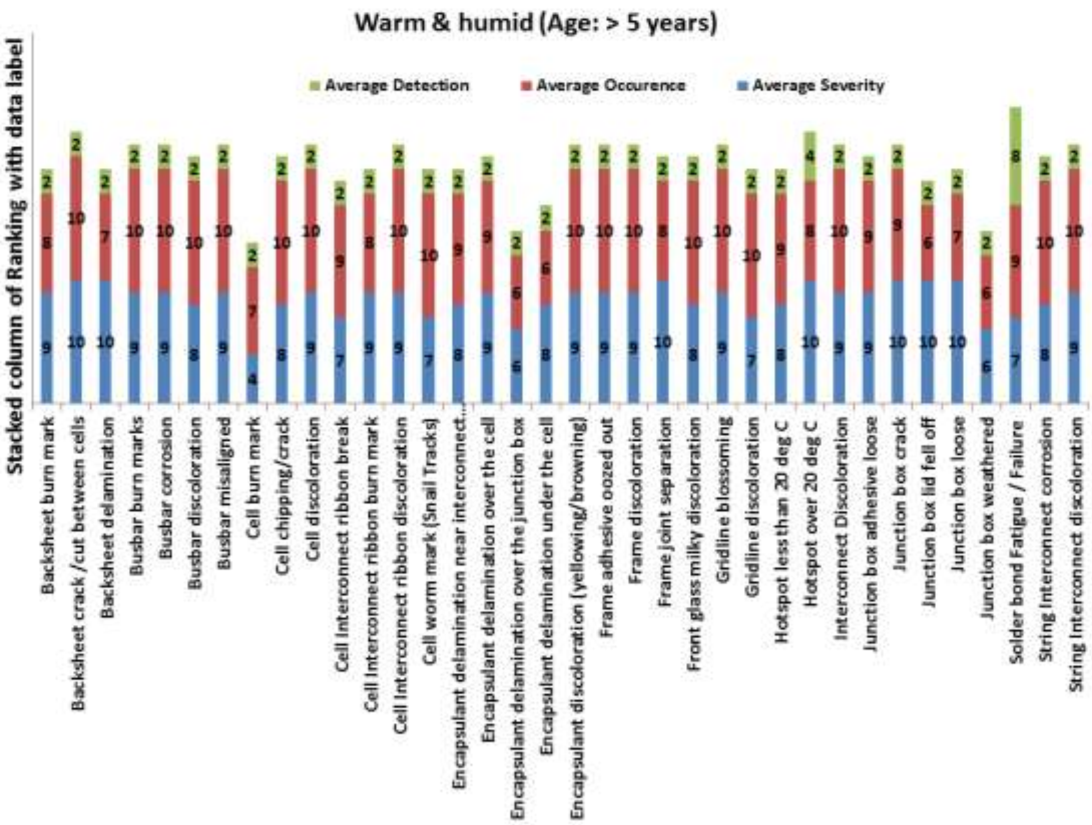

Fig. 8.16: Distribution of average ranking of different defects for Warm & Humid zone for modules with less than 5 years of exposure.

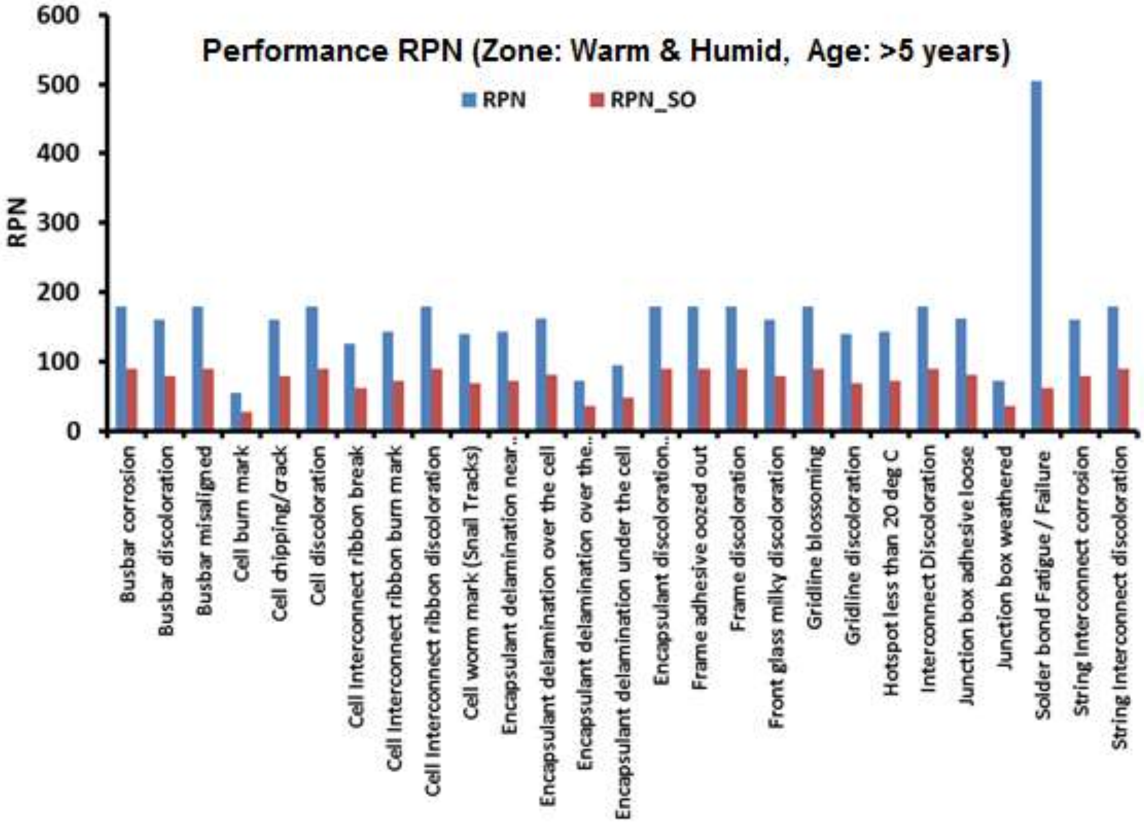

(a)

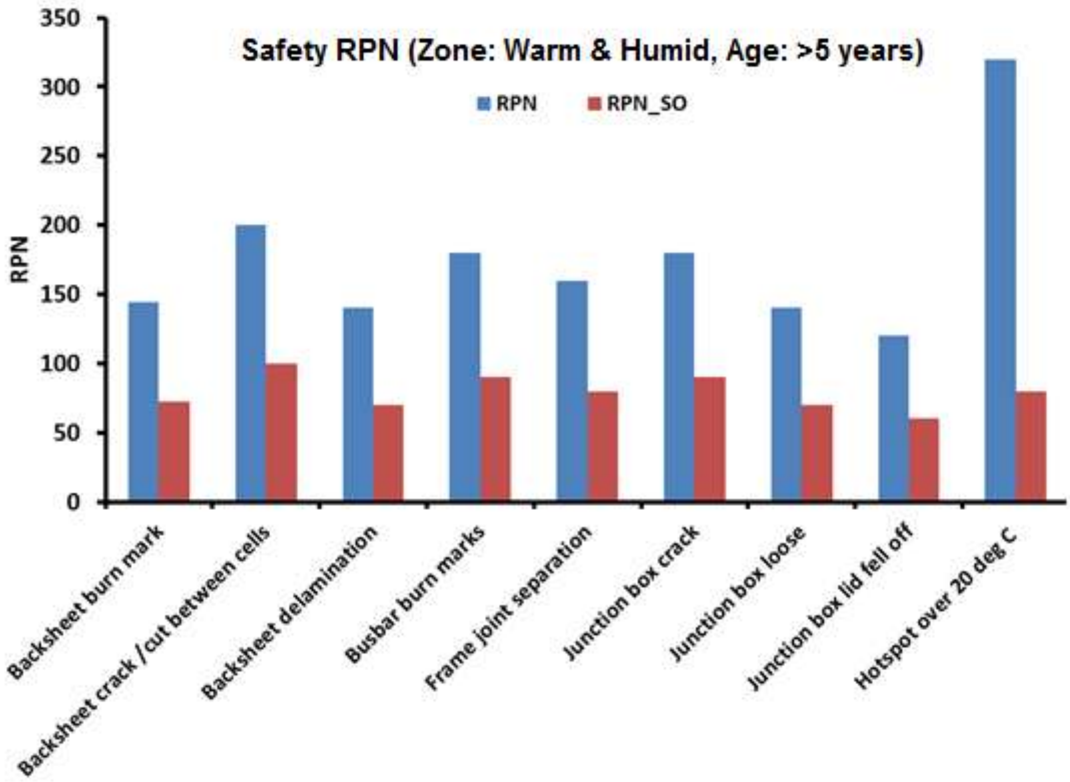

(b)

Fig. 8.17: RPN of different defects for Warm & Humid zone for modules with more than 5 years of exposure – (a) Performance RPN, and (b) Safety RPN.

In this climatic zone, the highest mean degradation rate of more than 3 %/year was observed in the module with backsheet discoloration and cell chipping. There is more than 60% difference in degradation value of the best and worst modules with performance defects for modules with less than 5 years of exposure. The severity and occurrence ranking is very high in most of the performance defects (refer Fig. 8.18). The main performance failure modes for less than 5 years of exposure are problems in backsheet, busbar misalignment, metallization, problems in frame and discoloration of glass. In terms of RPN_SO also, the same defects are in top priority list. There are only two safety issues observed in the module with less than 5 year of exposure viz. frame grounding corrosion and hot spot. Hot spot can be seen as the dominant safety failure mode for this site, as it has the highest RPN of 320 (refer Fig. 8.19).

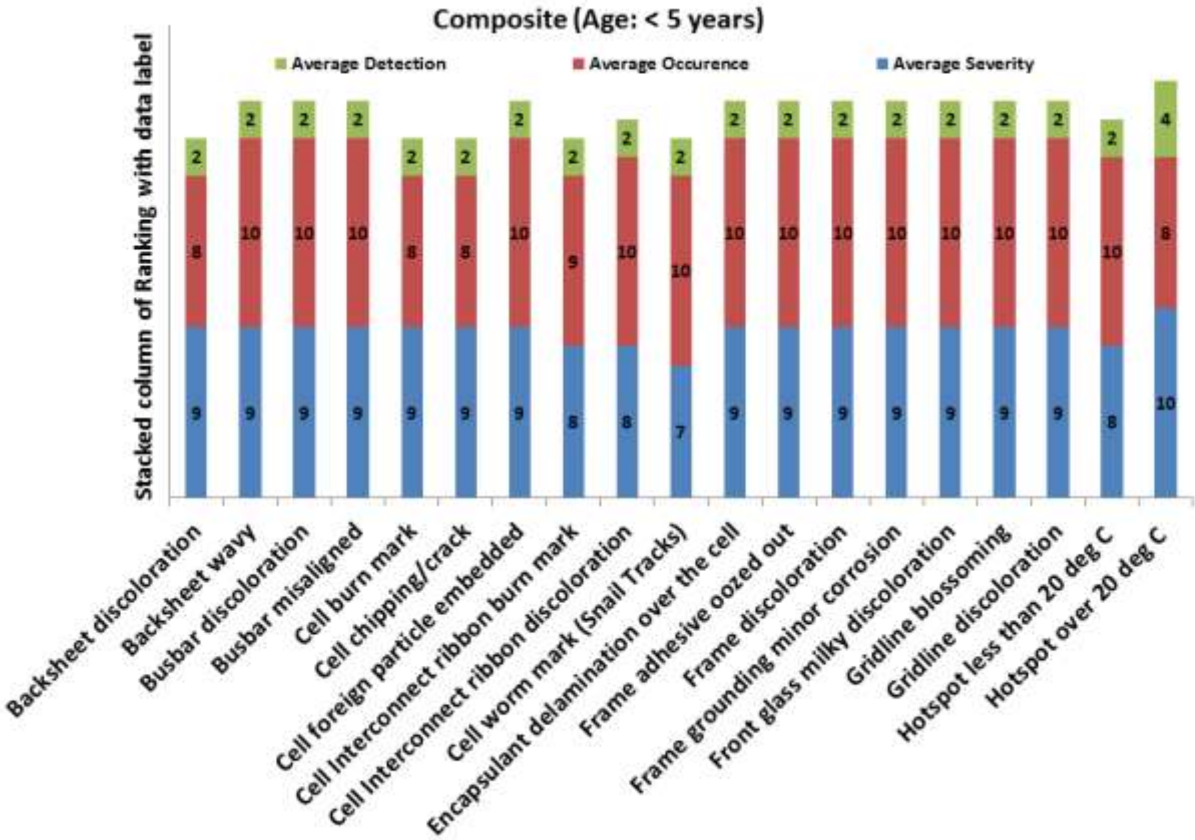

Fig. 8.18: Distribution of average ranking of different defects for Composite zone for modules with less than 5 years of exposure.

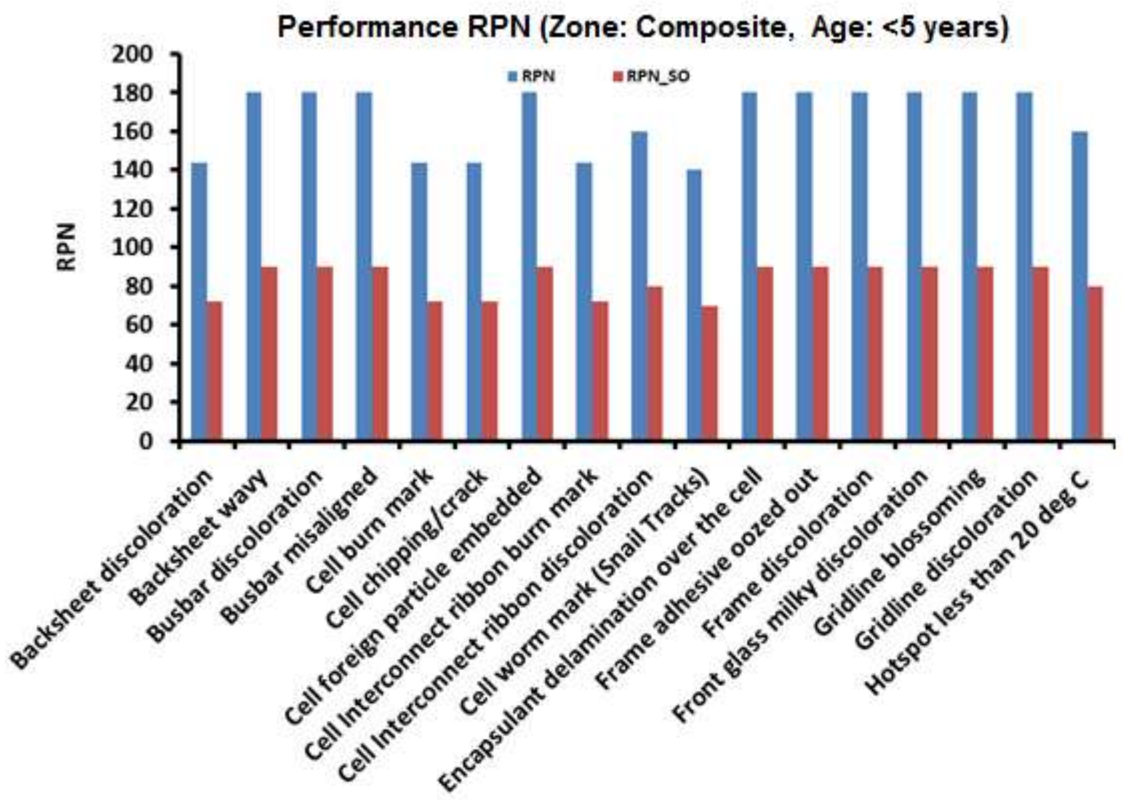

(a)

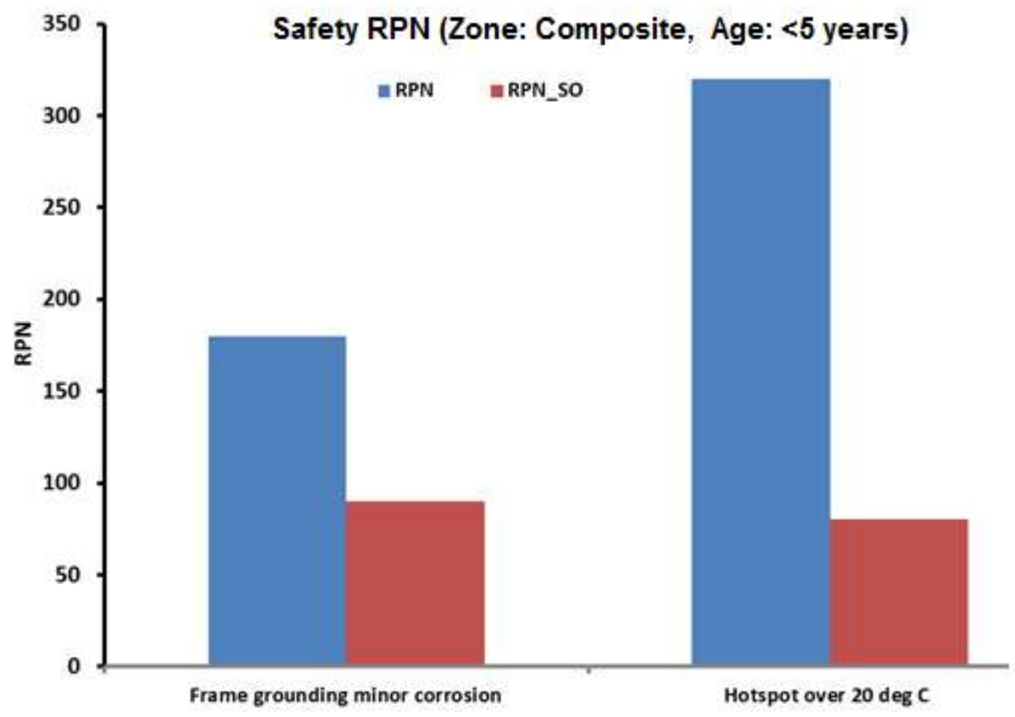

(b)

Fig. 8.19: RPN of different defects for Composite zone for modules with less than 5 years of exposure – (a) Performance RPN, and (b) Safety RPN.

In this climatic zone, the highest mean degradation rate of more than 2 %/year was observed in the module with more than 5 years of exposure with interconnects breakage. There is more than 70% difference in degradation value between the best and worst modules for more than 5 years of exposure with performance defects. The distribution ranking of different failure modes are shown in the Fig. 8.20. The solder bond fatigue/failure can be seen as the dominant performance degradation/failure mode for module with more than 5 years of exposure for this zone, as it has the highest RPN of 320. In terms of RPN_SO, discoloration in frame, glass, gridline and interconnect are the main performance failure defects for module with more than 5 years of exposure. In case of safety RPN, hotspot over 20 ^{0}C temperature is the most significant mode with highest RPN of 252. In terms of safety RPN_SO, frame grounding corrosion, backsheet crack, problems in junction box are the dominant safety failure modes for modules with more than 5 years of exposure (refer Fig. 8.21).

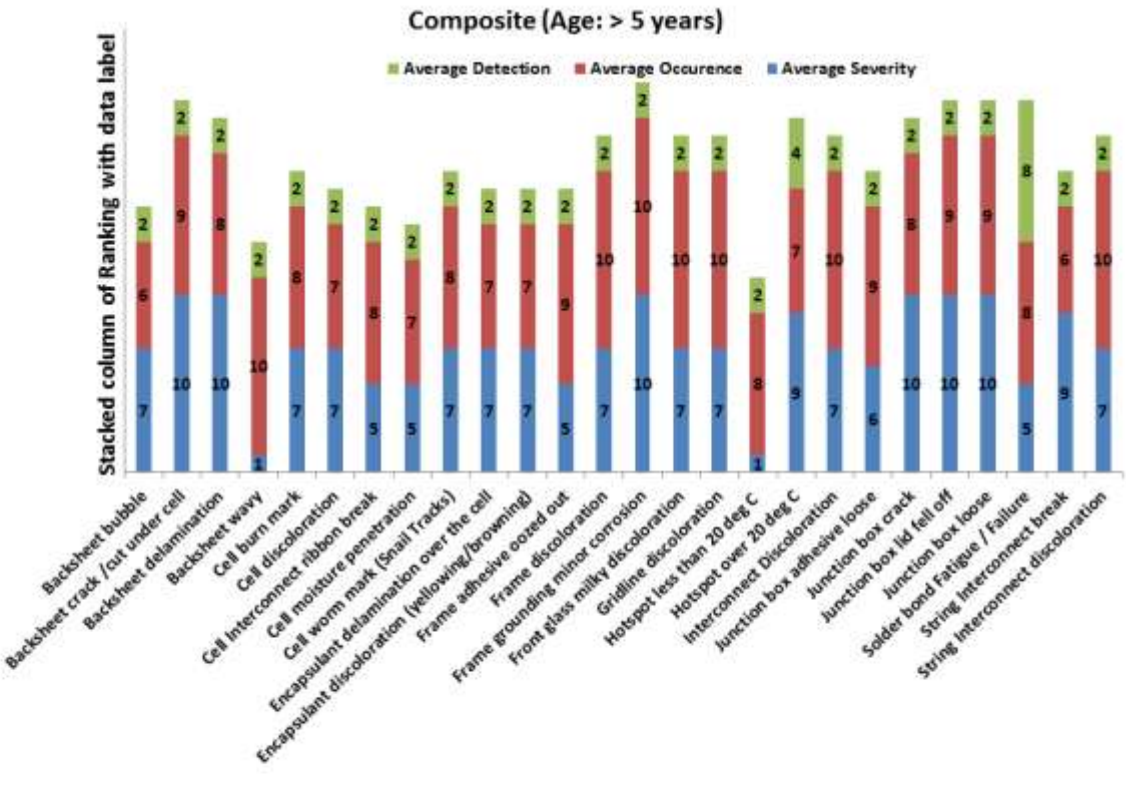

Fig. 8.20: Distribution of ranking of different defects for Composite zone for modules with more than 5 years of exposure.

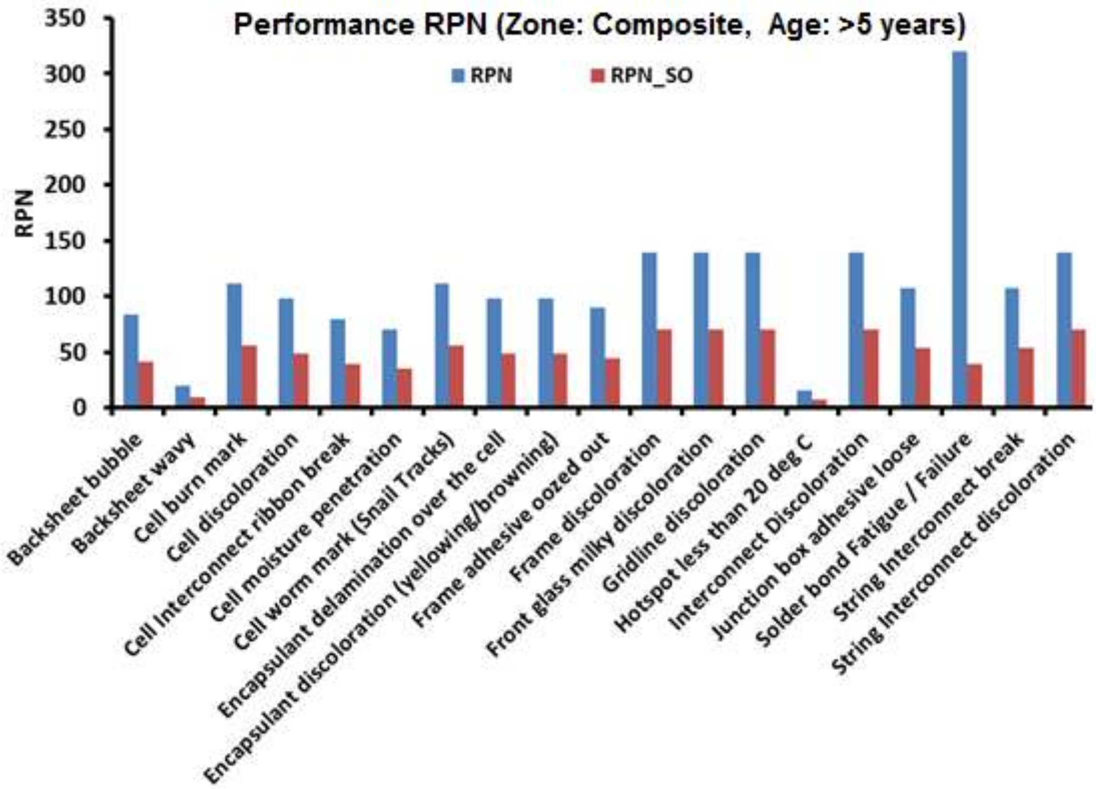

(a)

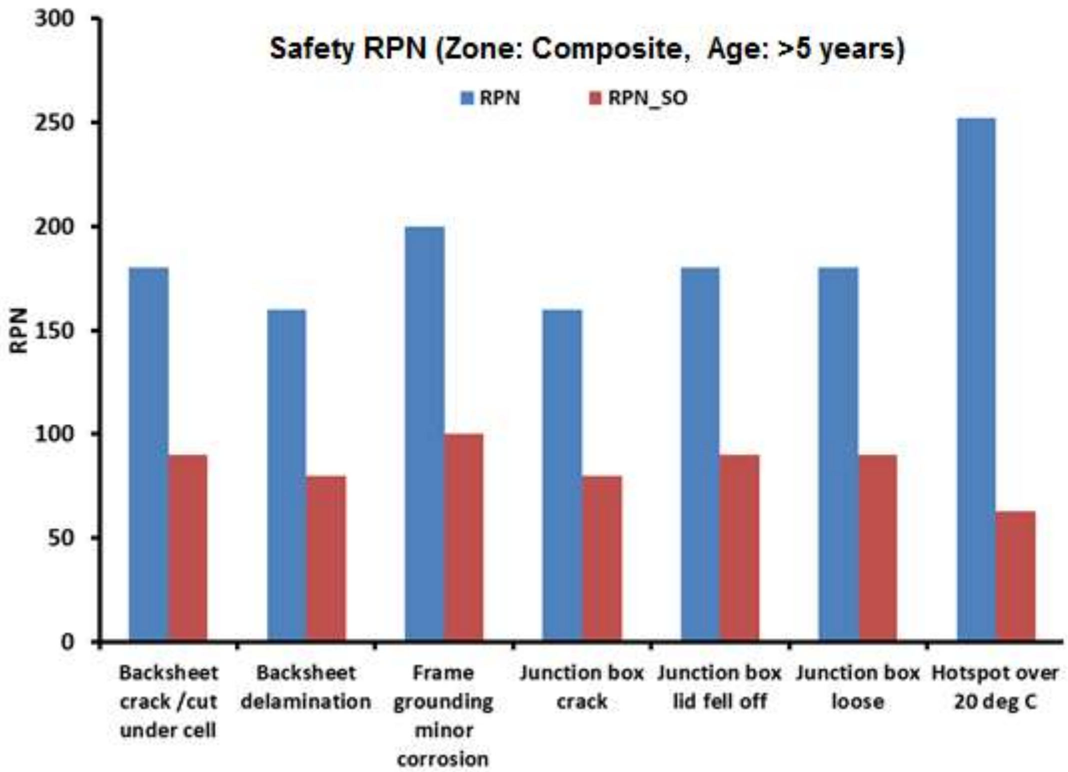

(b)

Fig. 8.21: RPN ranking of different defects for Composite zone for modules with more than 5 years of exposure – (a) Performance RPN, and (b) Safety RPN.

8.3.2 RPN analysis for Hot and Non-Hot climatic zones

As discussed in Chapter 4, climatic zones of India is divided into two zones by clubbing the Warm & Humid, Hot & Dry and Composite zones into one category (Hot zone) and Cold & Sunny, Cold & Cloudy and Moderate zones into the second category (Non-Hot zone) to highlight the effect of hot climates.

a) *Hot zone*

In this climatic zone, the highest mean degradation rate of more than 6 %/year was observed in the module with Backsheet burn mark and Front glass milky discoloration. There is more than 80% difference in degradation value between the best module and worst module with performance defects for modules with less than 5 years of exposure. The severity and occurrence ranking is very high in most of the performance defects (refer Fig. 8.22). The main performance failure modes for less than 5 years of exposure are problems in solder bond, backsheet, busbar misalignment, metallization, problems in frame, snail tracks and discoloration of glass. In terms of RPN_SO also, the same defects are in top priority list. There are five safety issues observed in the module with less than 5 year of exposure viz. frame grounding corrosion, problem in backsheet and hot spot. Hot spot can be seen as the dominant safety failure mode for this site, as it has the highest RPN of 320 (refer Fig. 8.23).

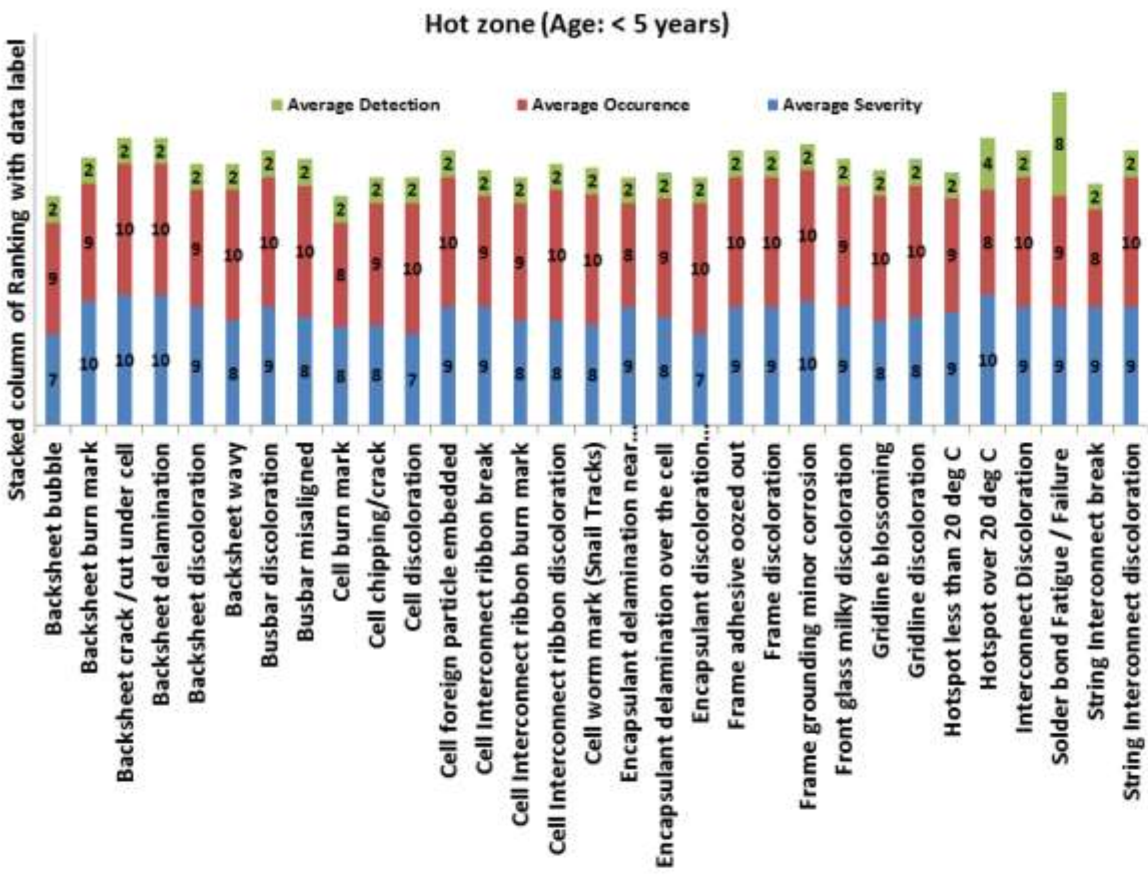

Fig. 8.22: Distribution of average ranking of different defects for Hot zone for modules with less than 5 years of exposure.

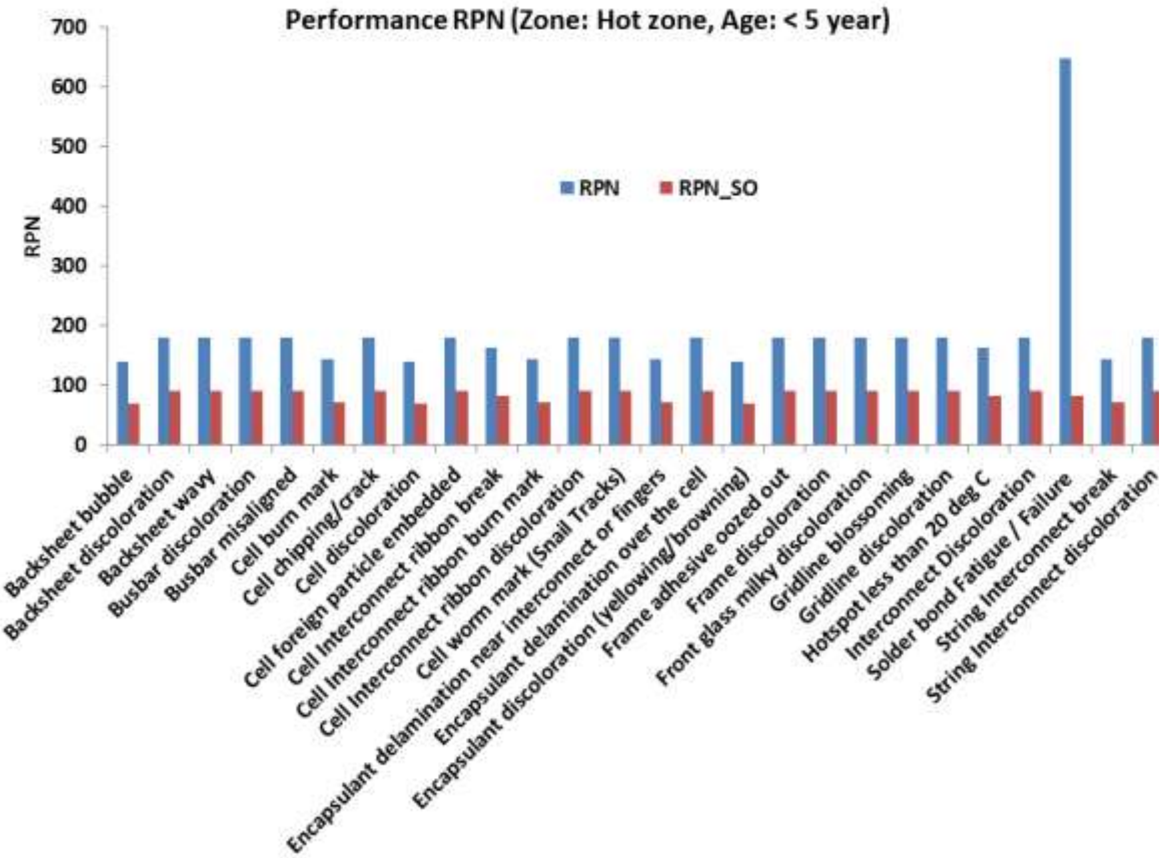

(a)

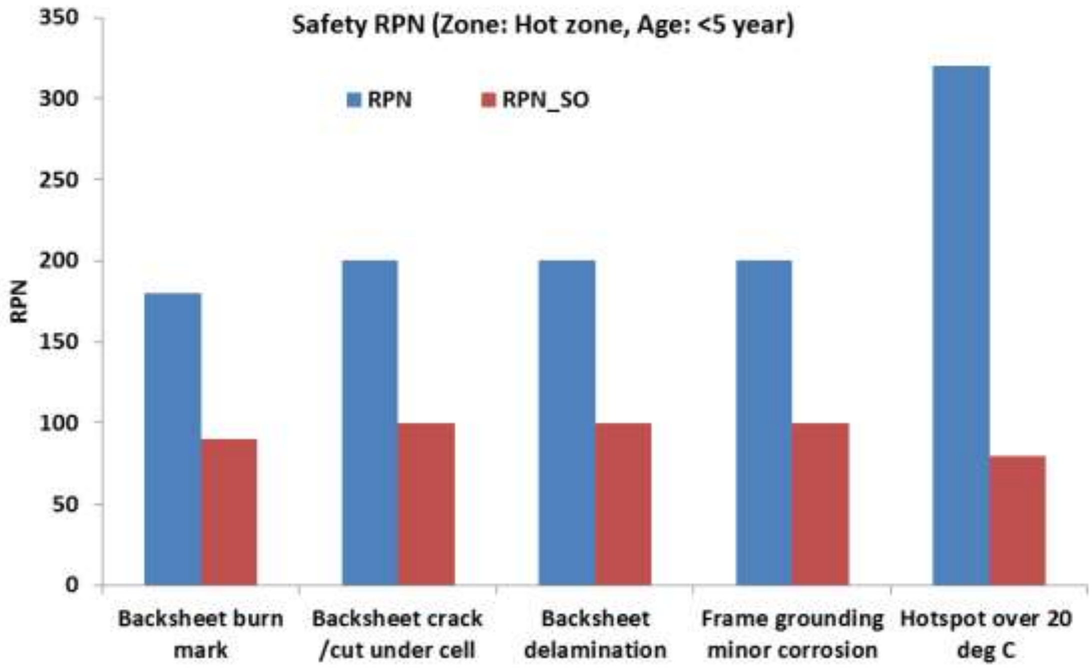

(b)

Fig. 8.23: RPN of different defects for Hot zone for modules with less than 5 years of exposure – (a) Performance RPN, and (b) Safety RPN.

In this Hot climatic zone with more than 5 years of exposure, the highest mean degradation rate of more than 2 %/year was observed in the module with interconnect breakage and other inter-circuitry problems. There is more than 70% difference in degradation value between the best module and worst module for more than 5 years of exposure with performance defects. The distribution of average ranking of different failure modes are shown in the Fig. 8.24. The solder bond fatigue/failure can be seen as the dominant performance degradation/failure mode for module with more than 5 years of exposure for this zone, as it has the highest RPN of 648. In terms of RPN_SO, problems in inter-circuit, discoloration in frame, glass, gridline and interconnect are the main performance failure defects for module with more than 5 years of exposure. In case of safety RPN, hotspot over 20 ^{0}C temperature is the most significant mode with highest RPN of 252. In terms of RPN_SO, frame grounding corrosion, backsheet crack, problems in junction box are the dominant safety failure modes for modules with more than 5 years of exposure (refer Fig. 8.25).

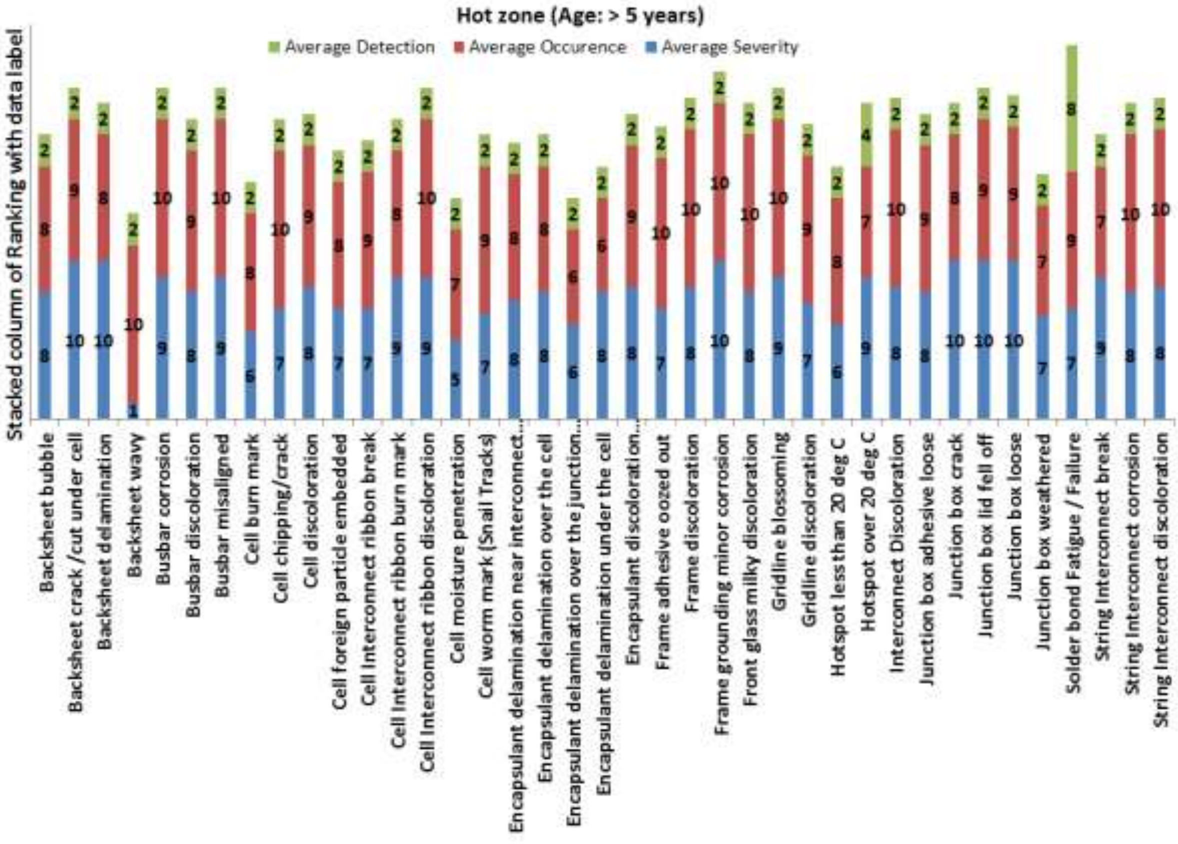

Fig. 8.24: Distribution of average ranking of different defects for Hot zone for modules with more than 5 years of exposure.

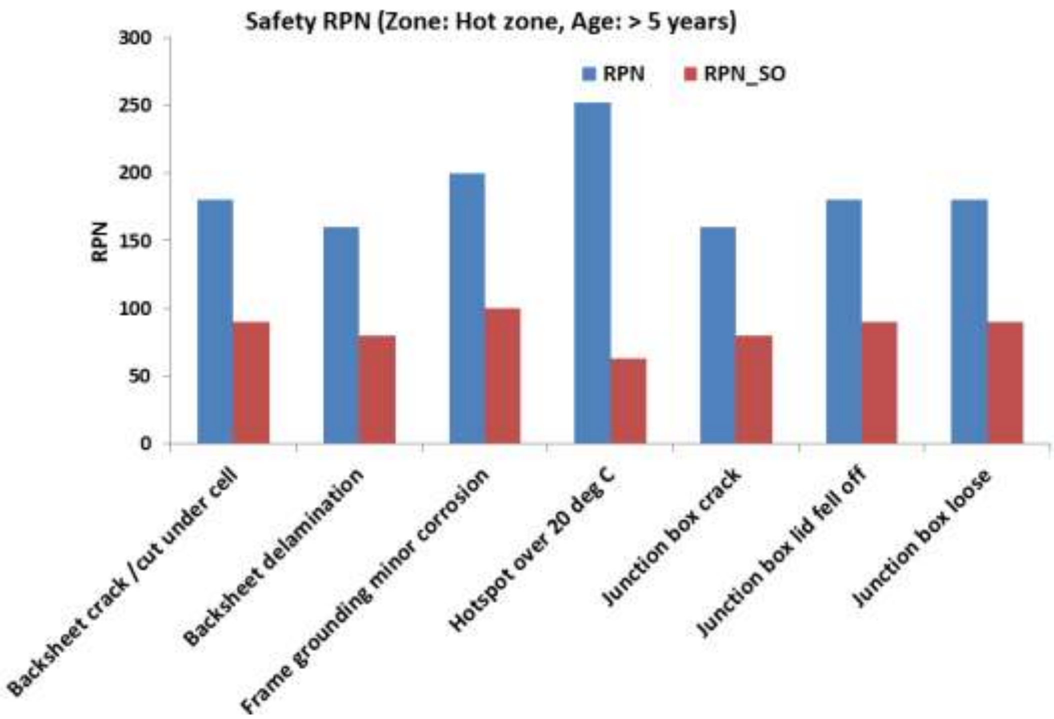

(a)

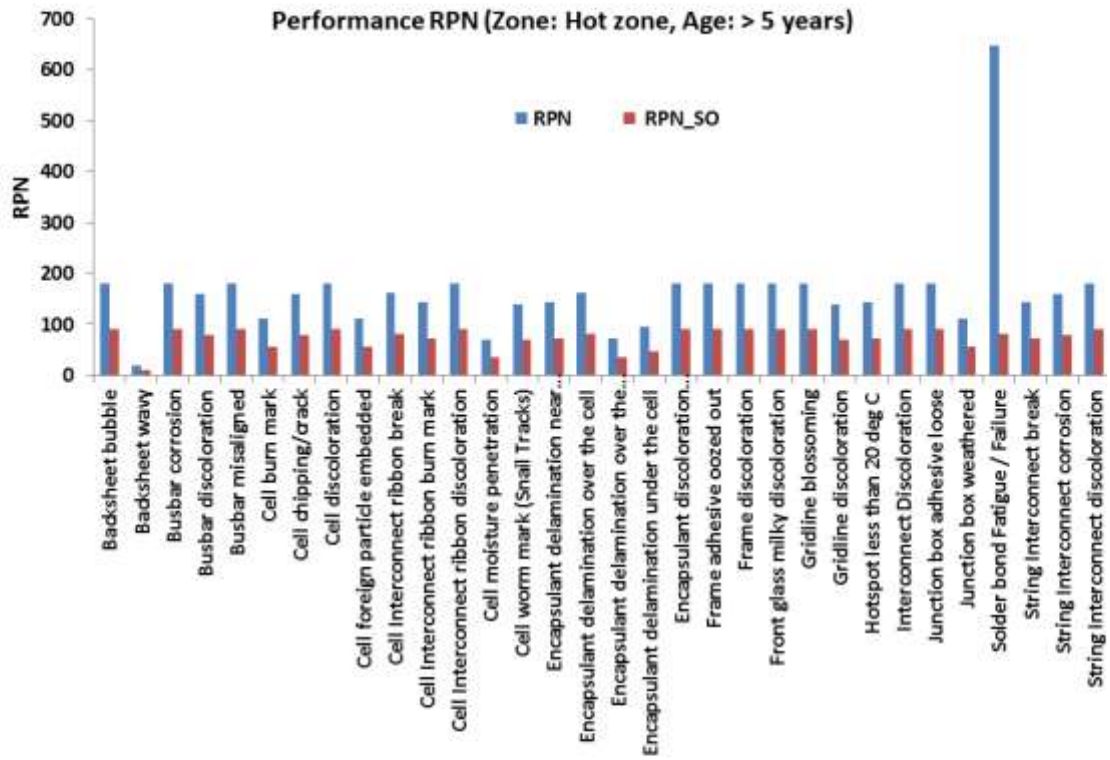

(b)

Fig. 8.25: RPN of different defects for Hot zone for modules with more than 5 years of exposure – (a) Performance RPN, and (b) Safety RPN.

b) Non-Hot zone

In Non-Hot climatic zone, for modules with less than 5 years of exposure, the maximum average degradation 4.8 %/year was observed in modules with backsheet crack /cut under cell. The ranking of different failure defects in terms of severity, occurrence and detection is shown in Fig. 8.26. The highest performance RPN is observed in module with defects snail tracks, problem in gridline & cell interconnect ribbon. In terms of RPN_SO also, the same defects are with high priority of risk. In case of safety failure backsheet burn marks, backsheet peeling, backsheet cut and grounding corrosion are the dominant defects as shown in Fig. 8.27. Backsheet peeling and grounding corrosion is the most severe defects with highest RPN and RPN_SO value in terms of safety RPN (refer Fig. 8.27).

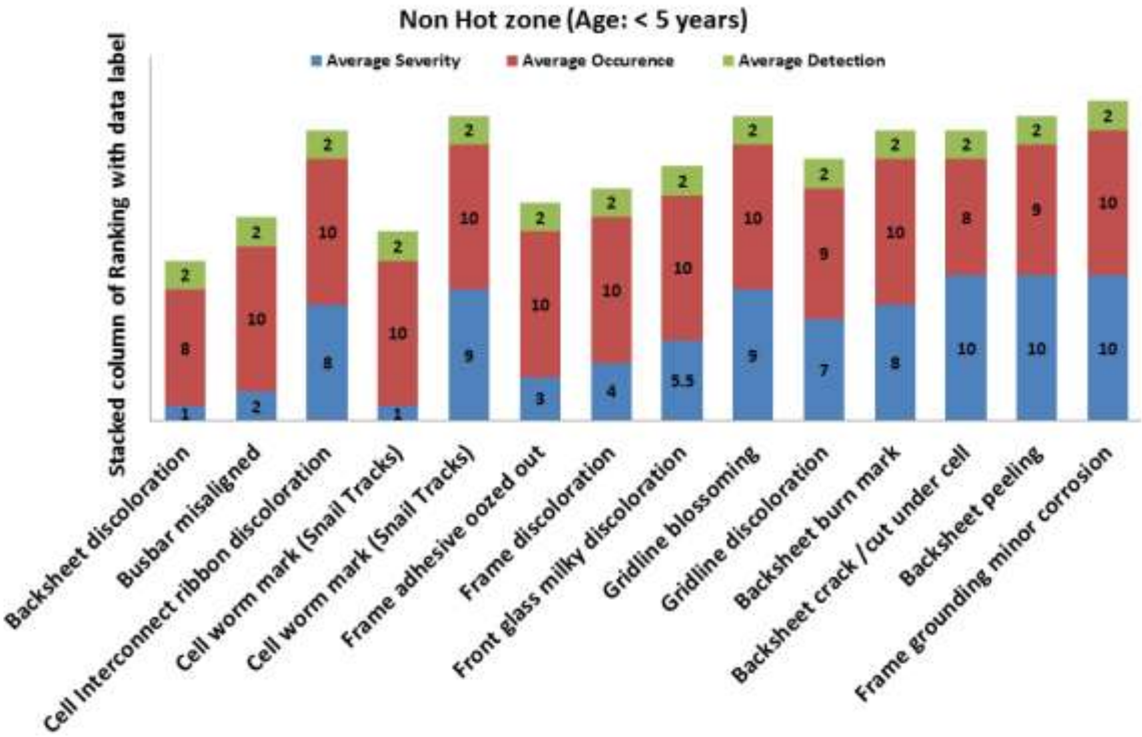

Fig. 8.26: Distribution of ranking of different defects for Non Hot zone for modules with less than 5 years of exposure.

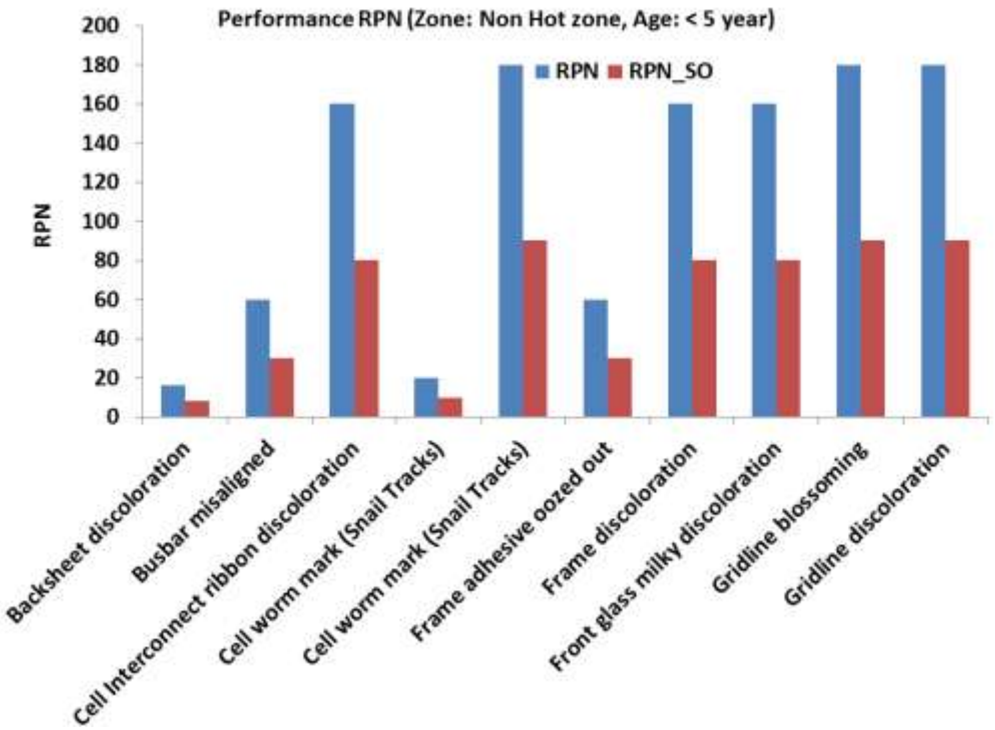

(a)

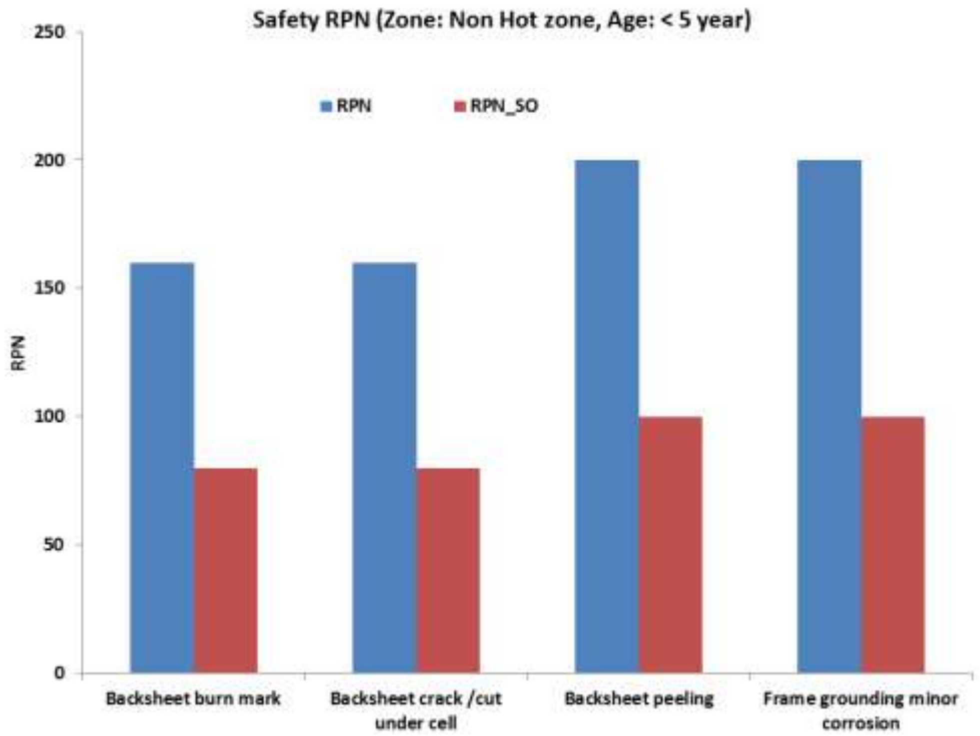

(b)

Fig. 8.27: RPN of different defects for Non-Hot zone for modules with less than 5 years of exposure – (a) Performance RPN, and (b) Safety RPN.

For modules with more than 5 years of exposure in Non-Hot zone, the distribution of average ranking for different defects is shown in Fig. 8.28. Most of the defects are related to performance of the module only. The maximum average degradation rate of 1.3 %/year is observed in module with string interconnect break, problem in backsheet and hot spot. There is a difference of 70% in average degradation rate in best and worst modules with defects. The performance RPN of solder bond fatigue/failure is high in module with more than 5 years of exposure, followed by cell discoloration, encapsulant discoloration, problems in frame and gridline discoloration (refer Fig. 8.29).

As per RPN_SO, the risk is high for cell discoloration, encapsulant discoloration, problems in frame and gridline discoloration, the highest value of RPN_SO is 70 for all these defects. In case of safety RPN, hot spot over 20 ^{0}C is showing the highest value as compared to other safety failure observed in this climatic zone. The 'wires insulation cracked/disintegrated' is also one of the severe defects in this zone. In terms of RPN_SO, the wires insulation cracked/disintegrated is the highest severe defects as shown in the Fig. 8.29.

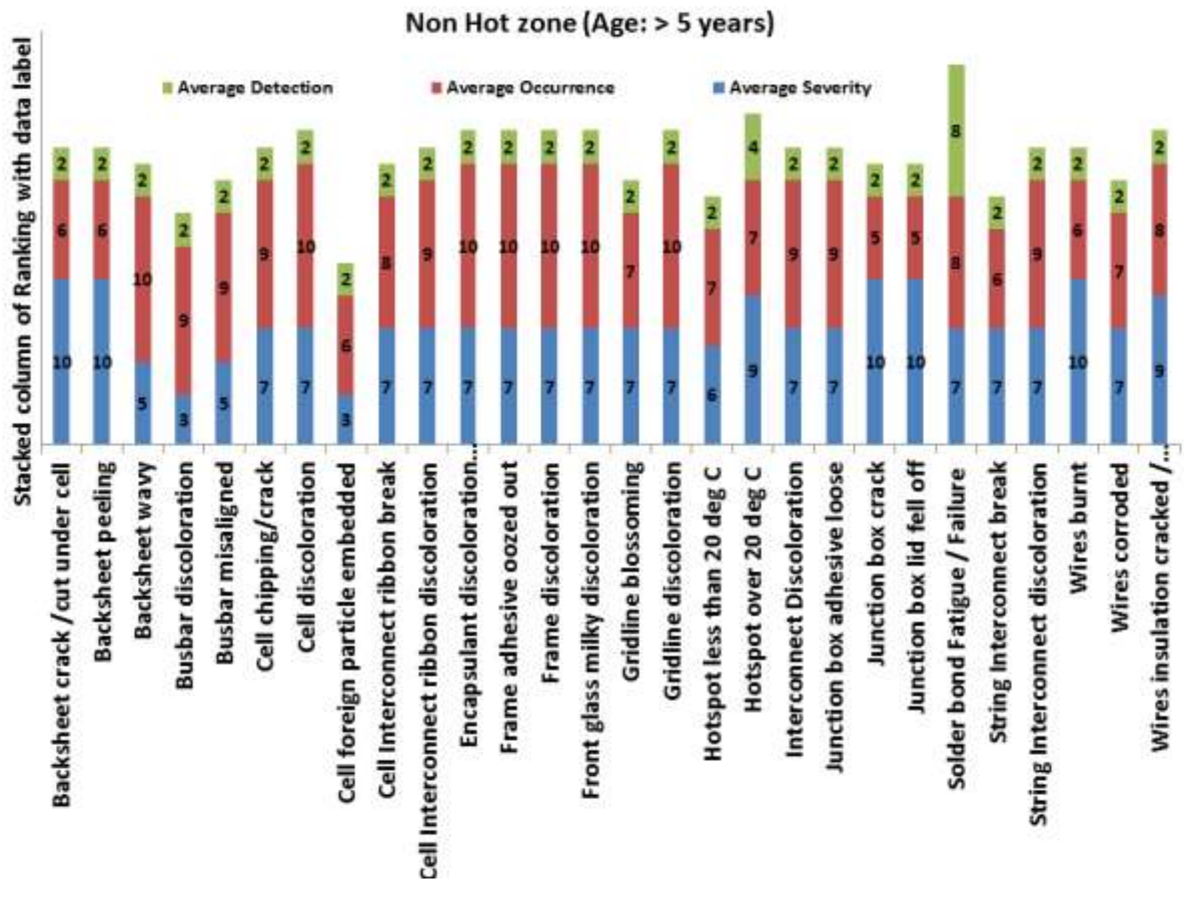

Fig. 8.28: Distribution of average ranking of different defects for Non Hot zone for modules with greater than 5 years of exposure.

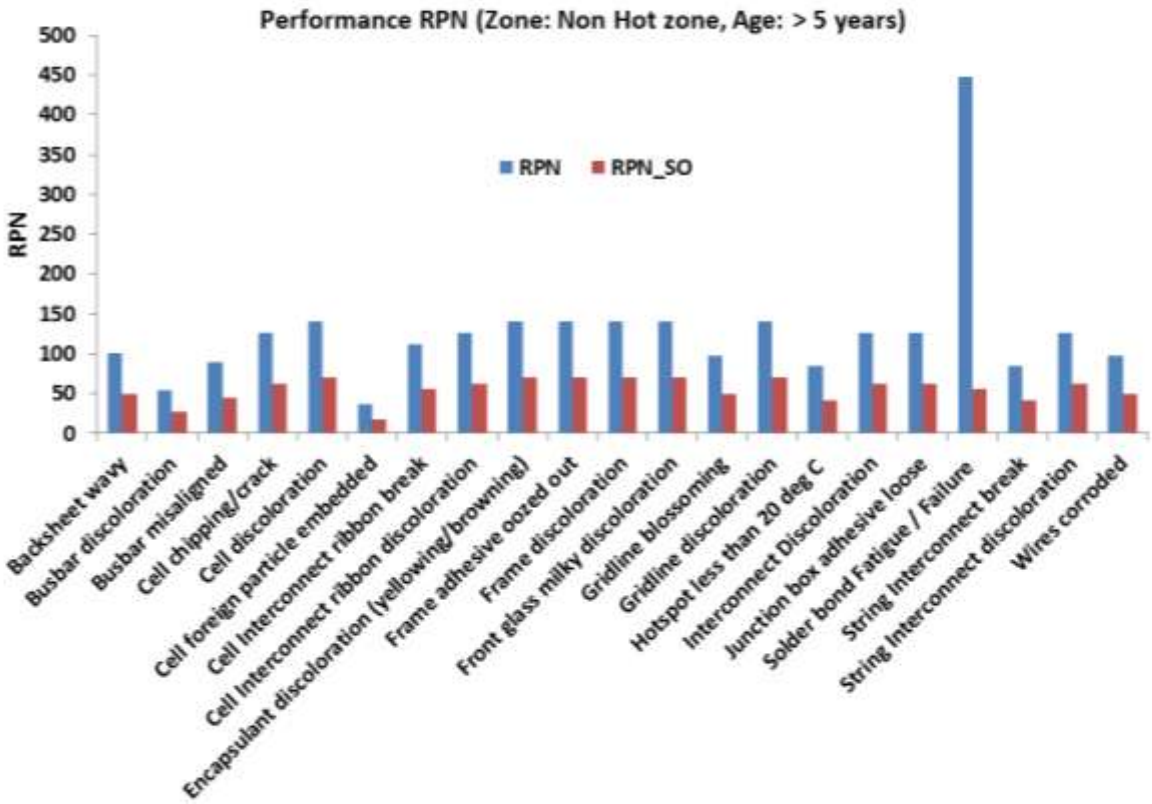

(a)

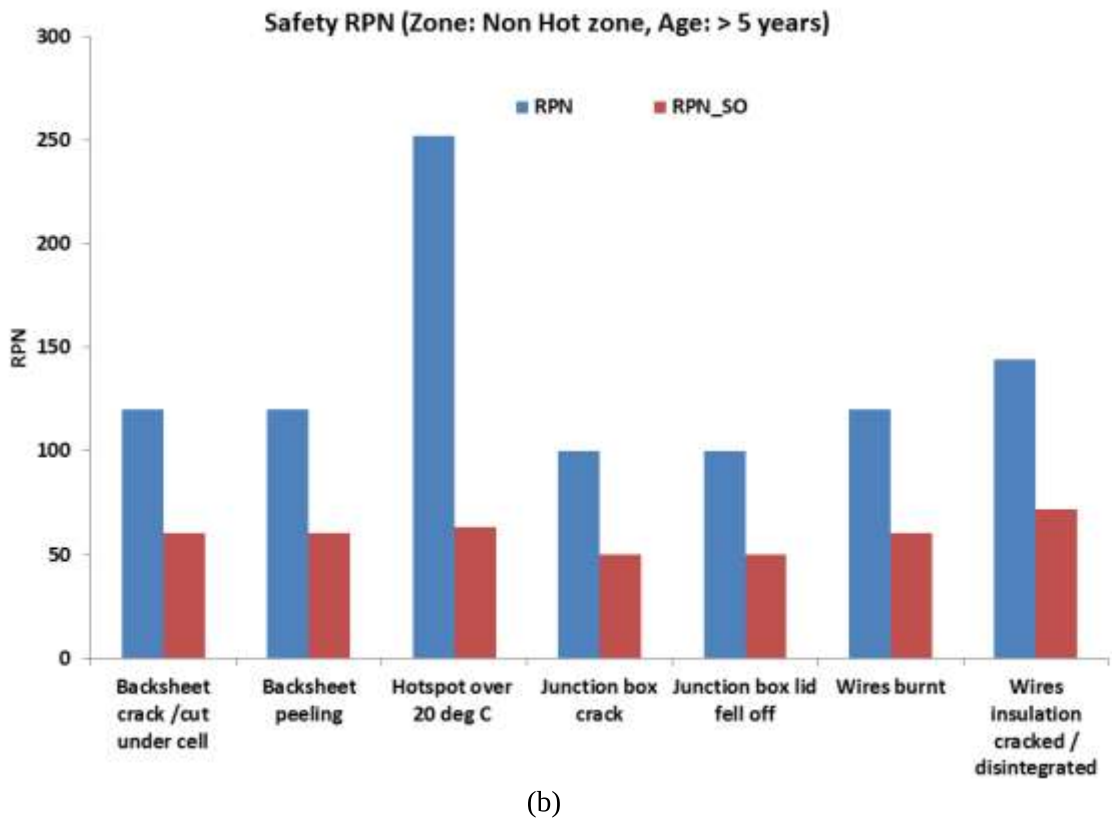

(b)

Fig. 8.29: RPN of different defects for Non Hot zone for modules with greater than 5 years of exposure – (a) Performance RPN, and (b) Safety RPN.

8.4 Conclusion

The quantification of reliability of PV modules inspected during the survey has been analyzed as per IEC 60812 standard. The failure rates of PV modules are higher in old modules (age > 5 years) as compared to young modules (age < 5 years). However the degradation rates of young modules are more as compared to old module in some cases. Modules deployed in Cold & Cloudy climate had a considerably low variety of failure modes of degradation for the studied modules, but the number of studied modules in this zone is not sufficient to come to any conclusion. Modules deployed in Cold & Sunny, Hot & Dry, Warm & Humid and Composite climates were found to have a wider variety of degradation modes than those in Cold & Cloudy and Moderate climates. Solder bond fatigue/failure is one of the common defects in all climatic zones except Cold & Cloudy zone for old modules with more than 5 years of exposure. Delamination and junction box issues are more prevalent in Hot & Dry, Warm & Humid and Composite climates than in other climates. The highest concerns of systems installed 5 years ago appear to be hot spots, internal circuitry discoloration, problems in backsheet and corrosion in grounding wire. An analysis about the causes of these failure modes could help alleviate the problem for future module generations. For all the climates (except Cold & Cloudy), encapsulant discoloration was the most common degradation mode, particularly in old installations. In young installations, it appears in Hot zone, but the degree of occurrence is less. Snail tracks are common in both young and old modules in all the climates except Cold & Cloudy zone and old modules in Cold & Sunny zone. In terms of climatic classifications as Hot and Non-Hot zone, solder bond fatigue/failure is the most common defect with highest concern. In the young modules of Hot zone, problem in backsheet, busbar misalignment, metallization, problems in frame, snail tracks and discoloration of glass are the major defects and hot spot is the severe safety issue. In old modules of Hot zone, problems in inter-circuit, discoloration in frame, glass, gridline and interconnect are the main performance failure defects and in case of safety RPN, hotspot over 20 $^{\circ}$C temperature is the most severe. In young modules of Non-Hot zones, performance defects are less as compared to Hot zone. Highest performance RPN in young modules of Non-Hot zone is observed with defects of snail tracks, problem in gridline & cell interconnect ribbon. In case of old modules in Non-Hot zone solder bond fatigue, cell discoloration, encapsulant discoloration, problems in frame and gridline discoloration are the main severe performance defects. In case of safety RPN, hot spot over 20 $^{\circ}$C and wires insulation cracked/disintegrated are the most severe defects for the old module in Non-Hot zone.

9. Conclusions and Recommendations

9.1 Conclusions

We present below the major conclusions of the 2016 All-India Survey of Photovoltaic Module Reliability conducted during March - May 2016. The survey covered 925 modules in 37 sites in all six climatic zones of India. The age of the modules ranged from 1 year to more than 25 years, and included 6 technologies, though the majority was crystalline silicon. Of the 37 sites, 11 were large installations with installed capacity more than 100 kW.

The main conclusions of the study are summarized below.

- The performance of PV modules surveyed is found to vary widely. The Annual Linear Degradation Rates for crystalline silicon modules vary from less than 0.6 %/year to more than 5 %/year, even after discounting 2% degradation in initial power output due to LID. Observations made by visual, IR, EL and other means also show significant variation in the degradation of PV modules.
- In order to analyze the performance critically, we have separated the crystalline silicon sites into two groups – Group X and Group Y. Group X sites have *average* value of Overall Power Degradation Rate less than 2 %/year, and are the so-called 'good' sites. Group Y sites have *average* value of Overall Power Degradation Rate more than 2 %/year, and are the so-called 'problematic' sites. The average Linear Degradation Rate for Group X modules is 0.89 %/year, which compares reasonably well with the internationally reported degradation rates. Average Linear Degradation Rate for Group Y sites, however, is 2.21 %/year, which is quite high and is a cause of concern.
- When sites are separated based on their size, the large installations (>100 kW) show a good average Linear Degradation Rate of 0.99 %/year compared to the small/medium sites (<100 kW) which show a much higher average Linear Degradation Rate of 1.68 %/year. All large sites fall in the Group X category. However, the average Linear Degradation Rate for large sites in only the Hot zone is higher at 1.18 %/year. When we look at a further subset of young modules large installations in Hot climates, the average rate is 1.5 %/year (almost double of the linear warranty limit of 0.8 %/year). This number is important as it represents the performance of recent and perhaps future utility-scale installations. Hence, the installers of both small and large installations need to be cautious about the quality of the materials and the installation procedures. Deliberate over-rating of modules in recent years also cannot be ruled out.
- A detailed climatic zone analysis for Group X modules was performed. This shows that modules in the 'Hot' climates (Hot & Dry, Warm & Humid, Composite) degrade at a faster rate of 1.18 %/year (on the average) as compared to modules in 'Non-Hot' climates (Moderate, Cold & Sunny, Cold & Cloudy), which degrade at 0.39 %/year. This is likely to be partly because of the higher percentage of interconnect failures and faster encapsulant discoloration observed in the 'Hot' climates.
- Overall, young modules (<5 years) show a higher degradation rate than old modules (>5 years old). However, taken together with the fact that for only Group X modules, young modules degrade slower than old modules, the results also suggest that newer installations have poorer quality of modules and/or installation practices, and also possibly over-rating of modules supplied in recent years. For the young modules, the main, indeed only, contributor for P_{max} degradation is the fill factor (*FF*), which also suggests the possibility of over-rating. For the old modules in Group X, short circuit current (I_{sc}) degradation and *FF* degradation both are equally responsible, while for the old modules in Group Y, *FF* degradation is the main factor.

- Roof-(rack)-mounted modules suffer from a higher degradation rate as compared to ground-mounted modules. Similarly, the small/medium systems (which are mostly rack-mounted systems on rooftop) show higher degradation rate than the large systems (which are mostly ground mounted). This means special attention is needed for the 40 GW rooftop target of India's National Solar Mission.
- Statistical analysis of the survey data has shown that module degradation rates in the different climates falling in Hot category are similar, and hence it is recommended that for analysis of photovoltaic degradation, only two climatic zones be considered – Hot and Non-Hot. The power degradation rate for the surveyed c-Si modules does not follow any known statistical distribution, but the maximum degradation rates at the sites follow the Gumbel distribution.
- Modules in Group Y sites have higher percentage of cracked cells than modules in Group X sites as seen by visual checking (evident from snail tracks and photo-bleaching effect) and electroluminescence (EL) imaging. This indicates poor handling of the modules during manufacturing, transportation and/or installation for Group Y sites, many of which fall into the young category. Higher percentage of mode A, B and C cracks have been observed in the young modules as compared to the old modules. There is a good correlation between the total number of cracks in the module and the power degradation of the module.
- Hot cells (cells with hot spots) have been detected in 13% of the surveyed modules using IR thermography (under MPPT condition). Modules which contain hot cells have higher power degradation than rest of the modules. This problem gets worse in 'Hot' climates, where the modules containing hot cells show a much higher average thermal mismatch index, and degrade faster than their counterparts in 'Non-Hot' climates. High degree of mismatch in cell temperatures can lead to higher degradation in module's output power. Both fill factor and short circuit current degradation are responsible for the higher power degradation. No difference in module temperature has been found in ground installations versus rooftop (rack mounted) installations.
- The quality of encapsulant appears to be another differentiating factor between modules of Groups X and Group Y sites. Higher percentage of modules from Group Y sites are affected by discoloration as compared to Group X sites. These observations, together with that of cracks in Group Y modules as mentioned above, point to poorer quality of materials used and improper or hasty installation practices for Group Y sites.
- Snail tracks have been observed mostly in the young modules. Modules with non-framing type snail tracks have been found to have cracks in the corresponding cells. The average Linear Degradation Rate of the modules with non-framing type snail tracks is higher as compared to the modules without snail tracks. The percentage of modules affected by snail tracks is higher in Group Y sites as compared to Group X sites. Highest severity of visible cracks (detected through snail tracks and photo-bleaching) is seen in the small/medium installations in Hot zones, though significant severity is also seen in large installations, which calls for improvement in the material selection and installation practices.
- Metallization discoloration is observed not only in the old modules, but even in some young modules, which again hints at poor material quality and manufacturing processes. Metallization discoloration is observed in all climatic zones but its severity is highest in the Warm & Humid zone. It has been found to correlate well with the series resistance of the modules and their power loss. Small/medium installations have a higher average severity as compared to large installations, which implies a difference in material quality used in these installations.
- Scratches in backsheet, front glass and frame have been found in the young modules, again indicating improper handling during installation. Backsheet degradation is comparable in the young modules in Group X and Group Y, but in the old modules, the degradation severity is higher in Group Y as compared to Group X. Since backsheet degradation is a safety concern, it is important to use proper

materials that can resist degradation in outdoor environment, and can provide the necessary levels of safety for the entire service life of the installation.

- Statistical analysis of the visual degradation data has indicated that the odds of having high P_{max} degradation rate (more than 1 %/year) are increased in case of young modules with cracks and metallization discoloration (which can be taken as an indication of poor quality control during manufacturing). For the old modules, backsheet degradation is associated with a higher chance of P_{max} degradation rate exceeding 1 %/year, so ensuring the quality of the backsheet is important.
- 99% of the surveyed modules have passed the dry insulation test, with 100% passing in the large installations.
- For thin-film modules V_{oc} is the main contributor to the P_{max} degradation, whereas for crystalline silicon modules, *FF* degradation is the main contributor. In the thin-film modules, white spots and edge seal delamination are the most prevalent visible degradation modes.
- Risk Priority Number (RPN) analysis has shown that in the young modules of Hot zone, problem in backsheet, busbar misalignment, metallization, problems in frame, snail tracks and discoloration of glass are the major defects and hot spot is the severe safety issue. In old modules of Hot zone, problems in inter-circuit, discoloration in frame, glass, gridline and interconnect are the main performance failure defects and in case of safety RPN, hotspot over 20 °C temperature is the most severe. In young modules of Non-Hot zones, performance defects are less as compared to Hot zone. Highest performance RPN in young modules of Non-Hot zone is observed with defects of snail tracks, problem in gridline & cell interconnect ribbon. In case of old modules in Non-Hot zone, solder bond fatigue, cell discoloration, encapsulant discoloration, problems in frame and gridline discoloration are the main severe performance defects.
- The ‘Hot’ climatic zones of India – ‘Hot & Dry’, ‘Warm & Humid’ and ‘Composite’, where most of the installations are likely to take place, present a challenging environment for PV modules. Problems encountered in these zones include higher annual degradation rates, greater incidence of hot cells, more encapsulant discoloration, higher metal corrosion, and more interconnect breakage.
- The higher annual degradation rates seen in the ‘Hot’ climatic zones appear to be most likely due to the following mechanisms: enhanced discoloration (which reduces I_{sc}), enhanced metal corrosion (which increases series resistance and hence reduces *FF*), and enhanced interconnect breakage, possibly due to thermal cycling (which again increases series resistance and reduces *FF*).

It is worthwhile comparing the results obtained during the 2016 Survey with the results of the 2014 Survey. By and large, very similar conclusions emerge from both the Surveys. Modules at some installations perform reasonably well, while those at other installations do not. This wide variability in performance indicates significant differences in the quality of modules being procured, and in installation practices being followed. There also appears to be evidence of under-rating of modules by conservative manufacturers and over-rating by unethical ones. In both Surveys, we have seen that modules in Hot climates degrade faster than those in Non-Hot climates; modules on rooftops degrade faster than those which are ground-mounted; modules in small- and medium-sized installations degrade faster than those in large installations; and young modules are degrading faster than old ones. Furthermore, many of the defects seen by visible inspection, IR imaging and EL imaging also show similar trends in the two Surveys: encapsulant discoloration is prevalent in Hot climates, especially in older modules; hot spots occur more frequently in Hot climates; cell cracks are seen more in rooftop installations than ground-mounted.

Some key differences between the 2016 and 2014 Surveys are the following: the average value of Overall Degradation Rate for all modules is 1.55 %/year in 2016 compared to 2.07 %/year in 2014. The corresponding numbers if we look at only c-Si modules are 1.90 %/year in 2016 and 2.26 %/year in 2014.

The lower values seen in 2016 are mainly due to the inclusion of more 'large' installations in the 2016 Survey. In the 2016 study, we have introduced the Linear Degradation Rate, which discounts an initial 2% LID loss for c-Si modules, thereby attempting to put young and old modules on the same footing for a fair comparison. Further, in the 2016 Survey, we have focused more on c-Si modules as these constitute the majority of modules surveyed, and are not affected by light-soaking and spectral mismatch effects of thin film modules.

9.2 Recommendations

Based on, and arising out of, the above conclusions, our recommendations for the photovoltaic community are as follows:

- Quality of modules can vary significantly, so due diligence should be exercised while selecting and procuring modules. This may include verifying the antecedents of the manufacturer, and independent checks on the quality of the module(s). Although most modules available in the market carry the IEC certification, it should be noted that the IEC certification is really a certification of the module design, and does not guarantee that the module will perform adequately through its intended life. This is especially important for the installation of small/medium sites, where this problem is seen to be most prevalent during this survey.
- Materials used in modules are important. EVA and backsheet particularly can be of different qualities, and should be specified by the manufacturer in the datasheet, and also in the tender for procurement.
- Some cases of 'over-rating' of modules cannot be ruled out. This may be one of the reasons for high calculated degradation rates, especially for young modules. Owners and installers should be vigilant about this malpractice.
- An independent audit of modules and installations by third party is recommended. This may include detailed testing of randomly selected modules before as well as after shipment.
- Module manufacturers and installers should place more emphasis on proper packaging and handling of the modules during transportation since improper handling can induce cracks in the solar cells and lead to long-term degradation.
- Installation procedures and protocols are important, and standard procedures as recommended should be diligently followed. This calls for a well-trained workforce, and the need for a good certification programme.
- It is recommended that a field-based electroluminescence (EL) study be performed after receiving the modules at site and after installation to reveal micro-cracks which may have been caused during the transport and installation phases. Though this may not feasible at the smaller sites, it would be possible for the large sites.
- It has been noted that the 'Hot' climates present a harsh operating environment for PV modules. An intensive study of degradation phenomena in hot climates, which has not been emphasized sufficiently by the PV community so far, is needed. This is particularly important for India, since much of the 100 GW is expected to come up in the 'Hot' zones of the country.
- The IEC certification protocols (eg. 61215), and other standards, which are currently being updated, need to take into account the hot climate phenomena, and develop more aggressive test protocols going to higher temperatures. Indian R&D and industry involvement in PVQAT (International PV Quality Assurance Task Force) is highly recommended.
- Modules and sites perform very well in the 'Cold & Sunny' climate of Ladakh. Power plants set up in this region will enjoy not only low degradation rates, but also excellent irradiance.

- It is felt that some of the quality issues seen especially in the young modules are the result of aggressive pricing and timelines and improper handling/installation.

References

[1] R. Dubey, S. Chattopadhyay, V. Kuthanazhi, J. John, C. S. Solanki, A. Kottantharayil, B. M. Arora, K. Narsimhan, J. Vasi, B. Bora, Y. Singh and O.S. Sastry, *All India Survey of Photovoltaic Module Degradation: 2013*, [Online] Available at: http://www.ncpre.iitb.ac.in/research/pdf/All_India_Survey_of_Photovoltaic_Module_Degradation_2013.pdf

[2] R. Dubey, S. Chattopadhyay, V. Kuthanazhi, J. John, F. Ansari, S. Rambabu, B. M. Arora, A. Kottantharayil, K. L. Narasimhan, J. Vasi, B. Bora, Y. K. Singh, K. Yadav, M. Banger, R. Singh and O. S. Sastry *et al.*, *All India Survey of Photovoltaic Module Reliability: 2014*, available at http://www.ncpre.iitb.ac.in/research/pdf/All_India_Survey_of_Photovoltaic_Module_Reliability_2014.pdf

[3] S. Chattopadhyay, R. Dubey, V. Kuthanazhi, J. J. John, C. S. Solanki, A. Kottantharayil, B. M. Arora, K.L. Narasimhan, V. Kuber, J. Vasi, A. Kumar, O.S. Sastry, "Visual Degradation in Field-aged Crystalline Silicon PV Modules in India and Correlation with Electrical Degradation," *IEEE Journal of Photovoltaics* vol. 4, p. 1470, 2014.

[4] R. Dubey, S. Chattopadhyay, V. Kuthanazhi, J. J. John, J. Vasi, A. Kottantharayil, B. M. Arora, K.L. Narsimhan, C.S. Solanki, A. Kumar, O.S. Sastry, "Performance Degradation in Field-aged Crystalline Silicon PV Modules in Different Indian Climatic Conditions," *40th IEEE Photovoltaic Specialists Conference*, Denver, USA, 2014.

[5] S. Chattopadhyay, R. Dubey, V. Kuthanazhi, J. J.John, C. S. Solanki, A. Kottantharayil, B. M. Arora, K.L. Narasimhan, J. Vasi, B. Bora, Y. K. Singh and O.S. Sastry, "All India Survey of Photovoltaic Module Degradation 2014: Survey Methodology and Statistics," *42nd IEEE Photovoltaic Specialists Conference*, New Orleans, USA, 2015.

[6] R. Dubey, S. Chattopadhyay, V. Kuthanazhi, J. J. John, C. S. Solanki, A. Kottantharayil, B. M. Arora, K.L. Narasimhan, J. Vasi, B. Bora, Y. K. Singh and O.S. Sastry, "Correlation of Electrical and Visual Degradation seen in Field Survey in India," *43rd IEEE Photovoltaic Specialists Conference*, Portland, USA, 2016.

[7] R. Dubey, S. Chattopadhyay, V. Kuthanazhi, A. Kottantharayil, C. S. Solanki, B. M. Arora, K.L. Narasimhan, J. Vasi, B. Bora, Y. K. Singh and O.S. Sastry, "Comprehensive study of performance degradation of field-mounted PV modules in India," *Energy Science and Engineering* vol. 5, p. 51, 2017.

[8] R. Dubey, S. Zachariah, S. Chattopadhyay, V. Kuthanazhi, S. Rambabu, S. Bhaduri, H. K. Singh, A. Sinha, C. S. Solanki, A. Kottantharayil, B. M. Arora, K. L. Narasimhan, J. Vasi, B. Bora, R. Kumar, and O. S. Sastry, "Performance of Field-Aged PV Modules in India: Results from 2016 All India Survey of PV Module Reliability," *44th IEEE Photovoltaic Specialists Conference*, Washington DC, USA, 2017.

[9] R. Dubey, P. Batra, S. Chattopadhyay, A. Kottantharayil, B. M. Arora, K. L. Narasimhan, and J. Vasi, "Measurement of temperature coefficient of photovoltaic modules in field and comparison with laboratory measurements" *42nd IEEE Photovoltaic Specialists Conference*, New Orleans, USA, 2015.

[10] D. C. Jordan, S. R. Kurtz, K. VanSant and J. Newmiller, "Compendium of photovoltaic degradation rates", *Progress in Photovoltaics: Research and Applications*, vol. 24, pp. 978–989, 2016. DOI: 10.1002/pip.2744

[11] D. C. Jordan, T. J. Silverman., J. Wohlgemuth, S. R. Kurtz, and K. T. VanSant, "Photovoltaic failure and degradation modes," *Progress in Photovoltaics: Research and Applications*, vol. 25, pp. 318–326, 2016. DOI: 10.1002/pip.2866

[12] D. C. Jordan, T. J. Silverman, B. Sekulic and S. R. Kurtz, “PV degradation curves: non-linearities and failure modes”, *Progress in Photovoltaics: Research and Applications*, vol. 25, pp. 583–591, 2017. DOI: 10.1002/pip.2835

[13] D. L. Staebler, C.R. Wronski, “Reversible conductivity changes in discharge-produced amorphous Silicon“, *Applied Physics Letters*, vol. 31, p. 292, 1977. DOI: http://dx.doi.org/10.1063/1.89674

[14] R. Rüther, J. Livingstone, “Seasonal variations in amorphous silicon solar module outputs and thin film characteristics”, *Solar Energy Materials and Solar Cells*, vol. 36, no. 1, pp. 29-43, 1995. DOI: 10.1016/0927-0248(94)00165-O

[15] S. Demtsu, S. Bansal, and D. Albin, "Intrinsic stability of thin-film CdS/CdTe modules," *35th IEEE Photovoltaic Specialists Conference*, Hawaii, 2010, pp. 1161-1165. DOI: 10.1109/PVSC.2010.5614753

[16] J. A. del Cueto and B. von Roedern, "Long-term transient and metastable effects in cadmium telluride photovoltaic modules," *Progress in Photovoltaics: Research and Applications*, vol. 14, no. 7, pp. 615-628, 2006. DOI: 10.1002/pip.687

[17] T. J. Silverman, U. Jahn, G. Friesen, M. Pravettoni, M. Apolioni, A. Louwen, W van Sark, M. Schweiger, G. Belluardo, J. Wagner, A. Tetzlaff, P. Ingenhoven, D. Moser, “Characterization of Performance of Thin Film Photovoltaic Technologies”, International Energy Agency Report No. IEA-PVPS T13-02:2014, May 2014.

[18] Vikram Solar, “Limited and Linear Warranty for PV Modules”, [Online] Available: https://www.vikramsolar.com/wp-content/uploads/2016/03/Warranty-Certificate_Dec16.pdf

[19] Jinko Solar, “Limited Warranty”, [Online] Available: https://www.jinkosolar.com/download.html?downid=223

[20] JA Solar, “Limited Warranty”, [Online] Available: http://en.jasolar.com/site/pdf/594

[21] S. Pingel, D. Koshnicharov, O. Frank, T. Geipel, Y. Zemen, B. Striner and J. Berghold, “Initial Degradation of Industrial Silicon Solar Cells in Solar Panels”, *25th European PV Solar Energy Conference and Exhibition*, Valencia, Spain, 2010. DOI: 10.4229/25thEUPVSEC2010-4AV.3.20

[22] PVSyst, “LID (Light Induced Degradation) Loss”, [Online] Available: http://files.pvsyst.com/help/lid_loss.htm

[23] J. H. Reiss, R. R. King, and K. W. Mitchell,”Characterization of diffusion length degradation in Czochralski silicon solar cells”, *Applied Physics Letters*, vol. 68, pp. 3302, 1996. DOI: 10.1063/1.116581

[24] K. Peter, P. Preis, P. E. Díaz-Pérez, J. Theobald, E. Enebakk, Anne-Karin Soiland, A. Savtchouk, M. Wilson and J. Lagowski, ”Light Induced Degradation in Multicrystalline Solar Grade Silicon Solar Cells Evaluated using Accelerated LID”, 26th *European PV Solar Energy Conference and Exhibition*, 2011. DOI: 10.4229/26thEUPVSEC2011-2BV.4.21

[25] B. Sopori, P. Basnyat, S. Shet, V. Mehta, Jeff Binns and Jesse Appel, “Understanding Light-Induced Degradation of c-Si Solar Cells”, *38th IEEE Photovoltaic Specialists Conference,* Austin, 2012. DOI: 10.1109/PVSC.2012.6317798

[26] K. M. Broek, I. J. Bennett, M. J. Jansen, N.J.C.M. van der Borg and W. Eerenstein, “Light and current induced degradation in p-type multi-crystalline cells and development of an inspection method and a stabilisation method”, in proceedings of the *27th European PV Solar Energy Conference and Exhibition*, Frankfurt, 2012. DOI: 10.4229/27thEUPVSEC2012-4DO.6.5

[27] C. Packard, J. H. Wohlgemuth and S. R. Kurtz, “Development of a visual inspection data collection tool for evaluation of fielded PV Module condition,” NREL, Technical Report no. NREL/TP-5200-56154, Golden, Colorado, 2012.

[28] S. V. Spataru, D. Sera, P. Hecke, T. Kerekes and R. Teodorescu, “Fault identification in crystalline silicon PV modules by complementary analysis of the light and dark current–voltage characteristics,” *Progress in Photovoltaics: Research and Applications*, 2015.

[29] G. A. Gueymard, “SMARTS2: A Simple Model of the Atmospheric Radiative Transfer of Sunshine: Algorithms and Performance Assessment”, Florida Solar Energy Center Technical Report No. FSEC-PF-270-95, 1995, Florida.

[30] C. Buerhop, D. Schlegel, M. Niess, C. Vodermayer, R. Weißmann and C. Brabec, “Reliability of IR Imaging of PV Plants under operating conditions,” *Solar Energy Materials and Solar Cells*, vol. 107, pp. 154-164, 2012.

[31] M. Kempe, M. Reese, A. Dameron and T. Moricone, “Types of Encapsulant Materials and Physical Differences Between Them,” *NREL Photovoltaic Module Reliability Workshop*, Denver, USA, 2010.

[32] A. Mansouri, M. Zettl, O. Mayer, M. Lynass, M. Bucher, O. Stern and R. Burhenne, “Defect detection in photovoltaic modules using electroluminescence imaging,” *27th European PV Solar Energy Conference and Exhibition*, Frankfurt, Germany, 2012, pp. 3374-3378.

[33] R. Dubey, S. Chattopadhyay, V. Kuthanazhi, J. John, C. S. Solanki, A. K., B. M. Arora, K. Narsimhan and J. Vasi, “Daylight Electroluminiscence Imaging of Photovoltaic Modules by Image Difference Technique,” *6th World Conference on Photovoltaic Energy Conversion*, Kyoto, 2014.

[34] G. Tamizhmani and J. Kuitche, “Failure and Degradation Modes of PV Modules in a Hot Dry Climate: Results after 12 to 26 years of field exposure,” *NREL PV Module Reliability Workshop*, 2013.

[35] N. G. Dhere, N. S. Shiradkar and E. Schneller, “Cell Line Checker Correlated to Infrared Thermography,” *US PVMC Infrared Thermography Workshop*, 2013.

[36] Bureau of Indian Standards, *National Building Code of India*, SP 7:2005, 2005.

[37] N. K. Bansal and G. Minke, *Climatic Zones and Rural Housing in India*, Julich: Forschungszentrum Julich GmbH, 1995.

[38] *Photovoltaic devices - Procedures for temperature and irradiance corrections to measured I-V characteristics*, IEC 60891, 2009

[39] M. Kontges, C. Packard, S. Kurtz, U. Jahn, K. A. Berger, K. Kato, T. Friesen, H. Liu, "Review of Failures of Photovoltaic Modules," International Energy Agency, Technical Report no. IEA-PVPS T13-01,2014.

[40] K. Bouzidi, M. Chegaar and M. Aillerie, "Solar cells parameters evaluation from dark I–V characteristics," *Energy Procedia*, vol. 18, pp. 1601-1610, 2012

[41] O. Breitenstein, P. Altermatt, K. Ramspeck, M. Green, J. Zhao and A. Schenk, "Interpretation of the commonly observed I–V characteristics of C-Si cells having ideality factor larger than two," in *IV World Conference on Photovoltaic Energy Conversion*, Waikaloa, Hawaii, 2006, pp. 879-884.

[42] *Crystalline Silicon Terrestrial Photovoltaic Modules - Design Qualification and Type Approval*, IEC 61215 Ed. 2, 2005.

[43] A. W. Czanderna and F. Pern, "Encapsulation of PV Modules using ethylene vinyl Acetate Co-polymer as a pottant : A Critical review," *Solar Energy Materials & Solar Cells*, vol. 43, pp. 101-181, 1996.

[44] S. Chattopadhyay, S. Tatapudi, C. S. Solanki, A. Kottantharayil, K.L. Narasimhan, J. Vasi, G. TamizhMani, “Quantification of PV Module Discoloration using Visual Image Analysis”, 44th *IEEE Photovoltaic Specialist Conference*, Washington DC, 2017

[45] M. Kontges, I. Kunze, V. Naumann, S. Richter, C. Hagendorf, J. Berghold and M. Roericht, "Snail Tracks (Schneckenspuren), Worm marks & Cell Cracks," [Online]. Available: http://iea-pvps.org/index.php?id=223&eID=dam_frontend_push&docID=1272. [Accessed 3/12/2017].

[46] S. Meyer , S. Richter , S. Timmel , M. Gläser , M. Werner , S. Swatek , C. Hagendorf , “Snail trails: root cause analysis and test procedures”, *Energy Procedia*, vol. 38, pp. 498-505, 2013.

[47] M. D. Kempe, A. A. Dameron, T. J. Moricone, and M. O. Reese, “Evaluation and Modeling of Edge-Seal Materials for Photovoltaic Applications”, *35th IEEE Photovoltaic Specialist Conference*, Honolulu, 2010

[48] Sharp Corporation, "SHARP Installation Manual" [Online]. Available: http://www.beck-solar.de/fileadmin/user_upload/Datenblaetter/Sharp/InstallationManual_SHARP_NA_FxxxGK_KTA10007_Ver3-11.pdf

[49] M. Kontges, I. Kunze, S. Kajari-Schroder, X. Breitenmoser and B. Bjorneklett, "The risk of power loss in crystalline silicon based photovoltaic modules due to micro-cracks," *Solar Energy Materials & Solar Cells,* vol. 95, pp. 1131-1137, 2011.

[50] S. Meyer, S. Timmel, S. Richter, M. Werner, M. Gläser, S. Swatek, U. Braun and C. Hagendorf, "Silver nanoparticles cause snail trails in photovoltaic modules," Solar Energy Materials and Solar Cells, vol. 121, pp. 171-175, 2014.

[51] R. Moreton, E. Lorenzo, J. Leloux and J.M.Carrillo, "Dealing in Practice with Hot Spots," in *29th European Photovoltaic Solar Energy Conference and Exhibition*, Amsterdam, 2014, pp. 2722-2727.

[52] J. Oh and G. TamizhMani, "Temperature Testing and Analysis of PV modules per ANSI/UL 1703 and IEC 61730 standards," in *35th IEEE Photovoltaic Specialist Conference*, Honolulu, 2010, pp. 984-988.

[53] I. A. Tsanakas, E. Pilat, L. D. Ha, F. A. Shakarchi, "Early Reliability Issues and Symptoms Evaluated in Four Large PV Plants in Southern France", *NREL PV Module Reliability Workshop*, Denver, 2017

[54] S. M. Shrestha, J. K. Mallineni, K. R. Yedidi, B. Knisely, S. Tatapudi, J. Kuitche, & G. Tamizhmani, "Determination of dominant failure modes using FMECA on the field deployed c-Si modules under hot-dry desert climate," *IEEE Journal of Photovoltaics*, vol. 5(1), pp. 174-182, 2015.

[55] "Koppen Climate Classification", [Online] Available: http://www.thesustainabilitycouncil.org/resources/the-koppen-climate-classification-system/

[56] M.c. Peel, B. L. Finlayson, B. L. and T. A. McMahon, "Updated world map of the Köppen-Geiger climate classification", *Hydrology and Earth System Sciences*, vol. 11, pp. 1633-1644, 2007.

Appendix A
Survey Checklist

Site No.: ELECTRICAL CHECKLIST (GROUP – A)

A1. Module & System Information

Manufacturer _______________ Model # ________________ Serial # ________________

Year of Installation_________________________________

Module Nameplate Data: ☐ Available ☐ Missing

P_{max} ______________ V_{oc} ____________ I_{sc} ____________________

Sys Volt_________ V_{max} ___________ I_{max} ______________________

Bypass diode, I_f _____________ Series fuse ______________________________

Temperature Coefficients:

Voltage: _______________ Current: ________________ Power: ______________

System design: ☐ single module ☐ multiple modules (a) ☐ unknown

(a.) Multiple module system:
Module location/number in a series string (from negative) _____________
No of modules in series (string) _______ No of strings in parallel (array) _________
No of bypass diodes___________ Rating & Model No. of Bypass Diodes: ______________
No of modules per blocking diode _________ Rating & Model No. of Bypass Diodes: ___________

System Bias: ☐ open circuit ☐ resistive load ☐ max. power tracked ☐ short circuit ☐ unknown

Frame Grounding: ☐ grounded ☐ not grounded

System Grounding – DC Side: ☐ grounded (a.) ☐ not grounded ☐ unknown

(a.) ☐ negative ☐ positive ☐ center of string ☐ unknown

System Grounding – AC Side: ☐ grounded ☐ not grounded ☐ unknown

Comments: ____
____

Filed by: Page 1 Date:

Site No.:

ELECTRICAL CHECKLIST (GROUP – A)

A2. I-V Characteristics (☐ Not applicable ☐ Applicable)

Tracer used ☐ Solmetric 1 ☐ Solmetric 2
☐ PVPM I-V curve tracer ☐ Meco System Analyzer

I-V Curve File number/name & Time: ____

Relative Humidity (%) ________________ Ambient Temperature (° C) _______________

Comments on I-V curve: ____

____

A3. Bypass Diode Test (☐ Not applicable ☐ Applicable)

No. of Bypass Diodes: _____________

No. of solar cells per Bypass Diode: ________________

Diode position from (+) terminal	**1**	**2**	**3**	**4**	**5**
Status (√, X, NA)					
If not working (open/short)					

No. of Diodes functioning properly: ________________

A4. Interconnect Failure Test (☐ Not applicable ☐ Applicable)

Interconnect Failure Present: ☐ Yes (a) ☐ No (b)

(a) No. of interconnect failure sites: ________________

(a) Visual Image File No. : ______________________

(b) Max signal strength (No. of LED glowing 1 to 10) _______

Min signal strength (No. of LED glowing 1 to 10) _______

Comments: ____

____

Filed by: Page 2 Date:

Site No.:

SOCIO-ECONOMIC & SYSTEM LEVEL CHECKLIST (GROUP – B)

1. **Year and month of** Procurement: _____________ Installation_____________ Commissioning: ______________
2. **System Ownership**

☐ Private Individual ☐ Private Institution ☐ Community Ownership ☐ Govt/Semi-Govt Institutions

3. **Implementation Model**

☐ EPC Company /System Integrators ☐ Supervised by NGOs ☐ Supervised by MNRE Nodal Agency ☐ Self (local electrician)

4. **Financial Model: Capital Investment:** Rs ___________

Did you avail any loans from banks? ☐ Yes ☐ No Bank: __________________

Loan Amount: Rs __________________ Interest rate =__%

☐ Availed capital subsidy from MNRE
☐ Pending
Percentage/Amount: ________________
Year Received: ____

☐ Availed capital subsidy from State Govt
☐ Pending
Percentage/Amount: _________________
Year Received: ____

☐ Received funds from Govt/CSRs/Foreign Aids/NGOs
Amount: ______________
Year Received: ____

5. **O&M Expenses**

☐ Self
☐ Generated by pay for service model
☐ Can be met from the savings in electricity bills
☐ Can be met from the replacement cost of previous power source (kerosene etc.)

☐ Receive funds from Govt/Foreign Aids

6. **System Maintenance**

☐ **Preventive**

☐ Daily ☐ Monthly ☐ Half Yearly ☐ Yearly Other__________

Basic Trouble Shooting and Maintenance done by:

☐ Self ☐ Trained Technician Next Technician Visit Due on: ____________ After _________days/months/

☐ From same locality ☐ Comes from nearest town (___km away)

Comes from nearest town (___km away)

☐ **Responsive**

No of times the system failed in a year: _____

Repair works when system is down done by

☐ Self (Owner is trained) ☐ Trained Technician

☐ From same locality Response Time:_______________Mean repair time: __________

☐ Comes from nearest town (___km away), Response time: _____Mean repair time: _______

Average Expenses on operation and Maintenance: ___________Rs/ Year

7. **Skill Level of Technician**

☐ High School ☐ Diploma ☐ Graduate ☐ Engineering Graduate ☐ Other: _______

Years of Experience: ___________

☐ Taken PV training at technical Institutes/ NGOs /Companies etc.

8. **What all maintenance services are done in a technician visit?**

Visual Inspection, Module Cleaning ☐ Checking the Junction boxes for tight wiring/ corrosion ☐ Check battery terminal
☐ Check for shading issues ☐ Remove debris ☐ Adjust tilt ☐ Inspect mounting system ☐ Inspect Battery Enclosure
☐ Watering of battery ☐ Specific Gravity Measurement of electrolyte ☐ Charge Equalization ☐ Load Testing
☐ Capacity Testing ☐ Thermal inspection of Electrical equipment ☐ Disconnects, Fuses, Circuit breakers
☐ Strains in Wiring, Insulation damage

Comments: ____

____

Filled By: Page: 1 Date:

Site No.: SOCIO-ECONOMIC & SYSTEM LEVEL CHECKLIST (GROUP – B)

List of Equipment: ____

____

____

____

Level of trouble shooting: ☐ System Level ☐ Subsystem Level ☐ Component level ☐ Element level

Most frequently replaced part of the system: ____

9. Motivation for installation of the system

☐ **Necessity:** ☐ **Optional power back up** __

☐ ***Home Lighting System*** ☐ Grid is available, but high interruption rates

Impact of SHS: No of additional hours added to daily activities____ ☐ Grid available, but with low interruption rates

☐ Entertainment and Information form TV/Radio

☐ Extra income generation through small artisanal activities

☐ Reduced indoor pollution (kerosene fumes)

☐ Communication facility (Mobile phone charging)

☐ **PV for community**

☐ Provision of potable water

☐ Powering Health centers

☐ Powering of educational/community center

☐ Street lights

☐ Telecommunication (Towers/ Repeaters etc.)

☐ **Promotion of green energy**

☐ Even though the economies are not attractive, invested on PV for proving pro-green.

☐ Demonstrate the viability and scope (publicity)

Others________________________________

____

☐ **Income generation/saving**

☐ ***Non-Agricultural productive Enterprises***

☐ Cottage industry (by powering small tools)

☐ Commercial Sector (Telephone Shops, Restaurant, Cinema etc.)

☐ Service Sector (Charging station, hiring of lamps, Power supplier, Communication services etc.)

☐ ***Agricultural and Animal Husbandry***

☐ Irrigation

☐ Aeration for Aquaculture/Fishing

☐ Electric Fencing

☐ ***Saving from electricity bill***/Previous electricity source, pay back in ____years

Cost of 1 unit of replaced electricity:______Rs/unit. LCOE of 1 unit of PV electricity: _____Rs/unit

☐ ***Income generation through sale of electricity***

☐ To Grid Rate: _____Rs/unit REC mechanism utilized: ☐ Yes ☐ No Years of PPA:____

☐ Microgrid Rate: _____Rs/unit REC mechanism utilized: ☐ Yes ☐ No Years of agreement:__

☐ **Tax Savings**: Accelerated depreciation of assets and associated tax savings, etc.

☐ **Research**

Comments: ____

____

Filled By: Page: 2 Date:

Site No.: SOCIO-ECONOMIC & SYSTEM LEVEL CHECKLIST (GROUP – B)

10. Constrains faced while installation/ What delayed you getting into solar?

☐ High capital investment and Lack of Financial Model (Credit/ Soft loans/ EMIs/ FITs, PPAs)
☐ Lack of knowledge about technology (didn't get information about the possibilities of application of PV)
☐ Poor market infrastructure and supply chain (Didn't know where to buy and what to buy, quality assurance etc.)
☐ Lack of legal and regulatory framework, administrative delays
☐ Lack of standards, codes and certification for quality control
☐ Lack of trained man power/consultants ☐
Lack of infrastructure and grid connectivity

Inverter and Battery Bank

1. **Type of system:** ☐ Off Grid ☐ Grid tied, export ☐ Grid sharing (captive) ☐ Grid dependent (Battery+Grid)
2. **Inverter Details** **ϕ:☐ 1☐ 3 Rated kVA ______**
   Max.Load:____ _ Tripped at ______kVA
   ☐ Connected ☐ Indoor ☐ Adequate ventilation ☐ Outdoor ☐ Vibration and Noise ☐ Properly Earthed
   MPPT available: ☐ Yes ☐ No
   MMPT Range: _______________V ___________________A
   IP Protection: ☐ 65 ☐ 64 ☐ Not Available
3. **Operation at maximum load: DC Side:** _____V, _____A , ____W
   AC Side: ____V, ____A, _____W Efficiency: ___%
   P.F=_____ T.H.D: ____% Operation Temperature:_____ Nominal Temperature:_____ Array Grounding:______
4. **Condition of Battery**
   ☐ Connected Manufacturer:________ Single Unit: ____V, ____Ah Price per unit: _______ Parallel:___, Series:____
   Terminals Corroded: ☐ Yes ☐ No Terminal Lugs: ☐ Tight ☐ Loose ☐ Sulphation Observed
   Electrolyte levels above critical: ☐ Yes ☐ No ☐ NA
   Electrolyte levels equal in all cells: ☐ Yes ☐ No ☐ NA
   Difference in specific gravity of electrolyte among different cells >±0.004: ☐ Yes ☐ No ☐ NA
   How often batteries are changed:___________________
5. Module Transportation related issues
   What are the precautions done during transportation of modules?

____

____

Mode of transport: ____________________
Place from where the modules were shipped in: ____

Comments: ____
____

Filled By: Page: 3 Date:

Site No.: SOCIO-ECONOMIC & SYSTEM LEVEL CHECKLIST (GROUP – B)

System Layout Diagram

Comments: ____
____

Filled By: Page: 4 Date:

Site No. :

SOILING & IR CHECKLIST (GROUP – C)

C1. Surroundings:

Soiling

Appearance of Glass: ☐ clean ☐ lightly soiled ☐ heavily soiled

Location of soiling: ☐ locally soiled near frame:

☐ left ☐ right ☐ top ☐ bottom ☐ all sides

☐ locally soiled on glass /bird droppings

Soiling sample taken on glass slides ☐ yes ☐ no

Cleaning interval: ☐ daily ☐ weekly ☐ monthly ☐ never

Last cleaned on (date) ____

Shading

Kind of shading: ☐ Building ☐ Trees

Any reflecting surface nearby ☐ Yes ☐ No

Debris ☐ Yes ☐ No

Solar Path Finder Details Camera used:

Corner 1	Corner 2	Corner 3	Corner 4
Image No:	Image No:	Image No:	Image No:

Surrounding objects that may affect module performance

☐ AC outdoor unit ☐ Chimney ☐ Other: ____________________

IR Images of system

IR Image before cleaning:

IR image after cleaning:

Filed By: Page 1 Date:

Site No. : SOILING & IR CHECKLIST (GROUP – C)

C2. IR Images

IR Camera used:

Mod. Id.	IR Image No. & Condition
1	Backside IR Images:

Image No.	Module operating condition			Irradiance (W/m^2)	Ambient Temp. ($^\circ C$)	Remarks
	MPPT	O/C	S/C			

Hot Spot (Y/N):

Mod. Id.	IR Image No. & Condition
2	Backside IR Images:

Image No.	Module operating condition			Irradiance (W/m^2)	Ambient Temp. ($^\circ C$)	Remarks
	MPPT	O/C	S/C			

Hot Spot (Y/N):

Mod. Id.	IR Image No. & Condition
3	Backside IR Images:

Image No.	Module operating condition			Irradiance (W/m^2)	Ambient Temp. ($^\circ C$)	Remarks
	MPPT	O/C	S/C			

Filed By: Page 2 Date:

Site No.:

VISUAL CHECKLIST (GROUP – D)

Location: ……………………………………………… Lat/Long: ……………………… Altitude: …………………

Module Details:
Manufacturer: ……………………………………
Type of Module: *Mono-cSi / Multi-cSi / Thin Film (…………..)*
No. of Cells: …… Dimension of Cells (cm): …….. x …….
Dimension of Module (cm): …………… x ……………

Module Name Plate Available: Y/N
Name Plate Condition: *Like New / Discolored / Torn*
Certification: *IEC61215 / IEC61646 / IEC61730 / UL1703*
Estimated deployment date: …………………………………

Crystalline Silicon Module : Y/N
Cells in each string x strings in parallel: ……… x ……….
Spacing: Cell to Cell = …….. mm
Frame to Cell (mm) = …….. (top), …….. (bottom), ………(left), ……..(right)
Module Discoloration: *None / Light / Dark, (……% area)*
No. of cells discoloured: ……
Discoloration Location : *Overall / Module centre / Module edges / Cell Center / Cell edges / over fingers / over busbars / over tabbing / between cells / individual cells darker than others / partial cell discoloration / others (………………………)*
Effect in JB area: *Same as elsewhere / more / less*
Effect in Name Plate area: *Same as elsewhere / more / less*
Damage : *Burn marks / Cracks / Moisture /Snail tracks / foreign particles embedded*
Burn marks (nos.): …… Cells w/ Snail Tracks (nos.): …..
Cells cracked (nos.): …… Cells with Framing (nos.): ……
Area Delaminated: *Nil /Over cells (…%), Between cells (…%), uniform / from edges / at corners / near JB / near Interconnects (cell or string)*

Backsheet Applicable: Y/N
Texture: *Like New / Wavy (Delam / No Delam.) / Dented*
Damage: *None / Small Localized / Extensive*
Discoloration: *Like New / Major / Minor*
Chalking: *None / Slight / Significant*
Delaminated area (%) : *<5 / 5-25 / 25-50 / 50-75 />75%*
Bubbles (nos., dimension): … , *<5mm / 5-30mm />30mm*
Fraction of area with bubbles > 5mm:
<5% / 5-25% / 25-50% / 50-75% />75%
Cracks/scratches (nos. & location): …… *,random/over cells / between cells*
Cracks location: *Only Near JB / Only near Nameplate / Other (………………………………………)*
Fraction of cracks/scratches that exposes the circuit:
<5% / 5-25% / 25-50% / 50-75% />75%
Burn Marks (nos. & area): ……, *<5% / 5-25% / 25-50% / 50-75% />75%*

Front Cover : Glass / Polymer / Others
Features: *Smooth / slightly textured / pyramid texture / ARC*
Damage: *None / Small Localized / Extensive*
Shattered (tempered/non-tempered): ……
Cracks: nos. : *1 / 2 / 3 / 4-10 / >10*
Cracks start from: *mod. corner / mod. edge / cell / JB*
Chips: nos. : *1 / 2 / 3 / 4-10 / >10*
Chipping location: *module corner / module edge*
Damaged Area : *<5% / 5-25% / 25-50% / 50-75% />75%*
Fraction of area affected by Haziness / milky discoloration:
NA / <5% / 5-25% / 25-50% / 50-75% />75%

Metallization :
A1: < 5%, A2: 5-25%, A3: 25-50%, A4:50-75%, A5:>75%
Fingers: *NA / Like New / Discolored (Light / Dark, ……%)*
Busbars: *NA / Like New / Discolored (Light / Dark, ……%)/ Obvious Corrosion / Diffuse Burn Marks / Misalignment*
Cell Interconnect Ribbon: *NA / Like New / Discolored (Light / Dark, ……%)/ Obvious Corrosion / Burn Marks / Breakage*
String Interconnect: *NA / Like New / Discolored (Light / Dark, ……%) / Obvious Corrosion / Burn Marks / Breakage / Arc tracks (thin burns)*

Colorimeter Readings:

Cell Centre	Brown Ring (if any)	Cell Edge	Non-Cell area

Filed by: Page 1 Date:

Site No.:

VISUAL CHECKLIST (GROUP – D)

Colorimeter Readings:

Busbar :

Backsheet :

Cell Interconnect:

String Interconnect :

Frame Applicable: Y/N

Appearance: *Like New / damaged / Missing*

Damage: *Corrosion (major or minor) / Bent/ Joints separated/ Cracking*

Frame Adhesive : *Not visible / Like New / Degraded / oozed out / missing in some areas*

Frame Grounding Present: Y/N

Original State : *No ground / Wired / Resistive/ Unknown*

Corrosion : *Nil / Minor / Major*

Functionality: *Well Grounded / No Connection*

Wires:

NA / Like New / pliable but degraded / embrittled / Cracked or disintegrated insulation / burnt / corroded / animal bites /soiled

Connectors: Y/N

Type: *MC3 or MC4 / Tyco / Others*

Condition: *Like New / pliable but degraded / embrittled / Cracked or disintegrated insulation / burnt / corroded / animal bites / soiled*

Junction Box (JB) Applicable: Y/N

Physical state : *Intact / unsound / weathered / cracked / burnt/ warped/ output terminals corroded*

Lid : *Intact(potted) / loose / fell off / cracked*

Attachment : *Well attached / loose / fallen off*

Wire attached in JB : *Well attached / Loose / Fell off/ arced / caused fire*

Seal : *Good sealing / will Leak*

Mounting Structure Details:

Material: ......

Condition of structure: *Good / rusted / bent / broken*

Installation Site : Roof top / Ground

Tilt Angle: .... Direction of PV Panels: ......

Height of lowest part of module from floor (cm): ....

Type of floor: ....

Rear-Side Glass Applicable: Y/N

Damage: *None/ Small Localized / Extensive*

Crazing (or other non-crack damage): ......

Shattered (tempered/non-tempered): ......

Cracks: nos. : *1 / 2 / 3 / 4-10 / >10*

Cracks start from: *mod. corner / mod. edge / cell / JB / foreign object impact spot*

Chips: nos. : *1 / 2 / 3 / 4-10 / >10*

Chipping location: *module corner / module edge*

Frameless Edge Seal Applicable: Y/N

Appearance: *Like New / discolored / Visibly degraded*

Discoloration area : *<5% / 5-25% / 25-50% / 50-75% / >75%*

Material Problems : *Squeezed Out / signs of moisture penetration*

Delamination : *Localized / widespread*

Delaminated area (%) : *<5 / 5-25 / 25-50 / 50-75 />75%*

Thin Film Module : Y/N

Cells in each string (nos.): ......,

Strings in parallel (nos.): ......

Distance between frame and cell : .... mm

Module Discoloration: *None / Light / Dark, (...... % area)*

Discoloration Type : *White Spots/Haze /Pin holes/Other*

Discoloration Location : *overall / Module centre / Module edges / Cell Center / Cell edges / near cracks*

Damage : *No / Small Localized / Extensive*

Damage Type : Burn Marks / Cracking / Moisture / Foreign particles embedded

Delamination : *None / Small Localized / Extensive*

Delamination Location: *From edges / uniform / corners/ near junction box / near busbar / along scribe lines*

Delamination Type : *Absorber delamination/ AR Coating delamination/ Other*

Filed by: Page 2 Date:

Site No.:

Dark I-V, IR & EL CHECKLIST

<table>
<tr><td rowspan="3">1</td><td colspan="3">Module Id No. : ____________________</td></tr>
<tr><td>Module Dark I-V File Nos.:
a) Data : __________________
b) Graph: __________________

Diode I-V File Nos.:
a) Data : __________________
b) Graph: __________________</td><td>Dark IR Image:
a) No Bias Image No.: ________
a) Bias Voltage : __________
b) Bias Current: ______________
c) IR Image File Nos.:___________</td><td>EL Image:
a) No-bias Image Name.:
____
b) Bias Voltage :
____
b) Bias Current:
____
c) EL Image File Name.:
____________________</td></tr>
<tr><td colspan="3">Remarks:</td></tr>
</table>

<table>
<tr><td rowspan="3">2</td><td colspan="3">Module Id No. : ____________________</td></tr>
<tr><td>Module Dark I-V File Nos.:
a) Data : __________________
b) Graph: __________________

Diode I-V File Nos.:
a) Data : __________________
b) Graph: __________________</td><td>Dark IR Image:
a) No Bias Image No.: ________
a) Bias Voltage : __________
b) Bias Current: ______________
c) IR Image File Nos.:___________</td><td>EL Image:
a) No-bias Image Name.:
____
b) Bias Voltage :
____
b) Bias Current:
____
c) EL Image File Name.:
____________________</td></tr>
<tr><td colspan="3">Remarks:</td></tr>
</table>

Comments: ____
____

Filed by:

Appendix B
Koppen-Geiger Climate Classification

While the six-climate classification of Bansal *et al.* [37] is being used throughout this report for the analysis of the survey data (as discussed in Chapter 1), we have presented some of the important climate-dependent analysis in Chapter 4 also in terms of internationally accepted Koppen-Geiger climate classification system. This Appendix briefly describes the Koppen-Geiger system, and also lists the climatic zone of all sites visited as per this classification.

Unlike the six-climate classification system of Bansal *et al.*, which uses temperature and relative humidity as the classification criteria, the Koppen-Geiger system uses temperature and precipitation [36]. The Koppen-Geiger classification system has 5 main groups – Tropical (type A), Arid (type B), Warm Temperate (type C), Continental (type D) and Polar (type E), out of which India has the first four climates. The criteria for determining these main groups are shown in Fig. B.1. Each of these groups is further sub-divided based on temperature and annual precipitation ranges. The climatic zone map of India as per the Koppen-Geiger classification system is shown in Fig. B.2. The Koppen-Geiger system uses 2 or 3 letters to designate the climatic zone of any location, which have been described in Tables B.1 and B.2.

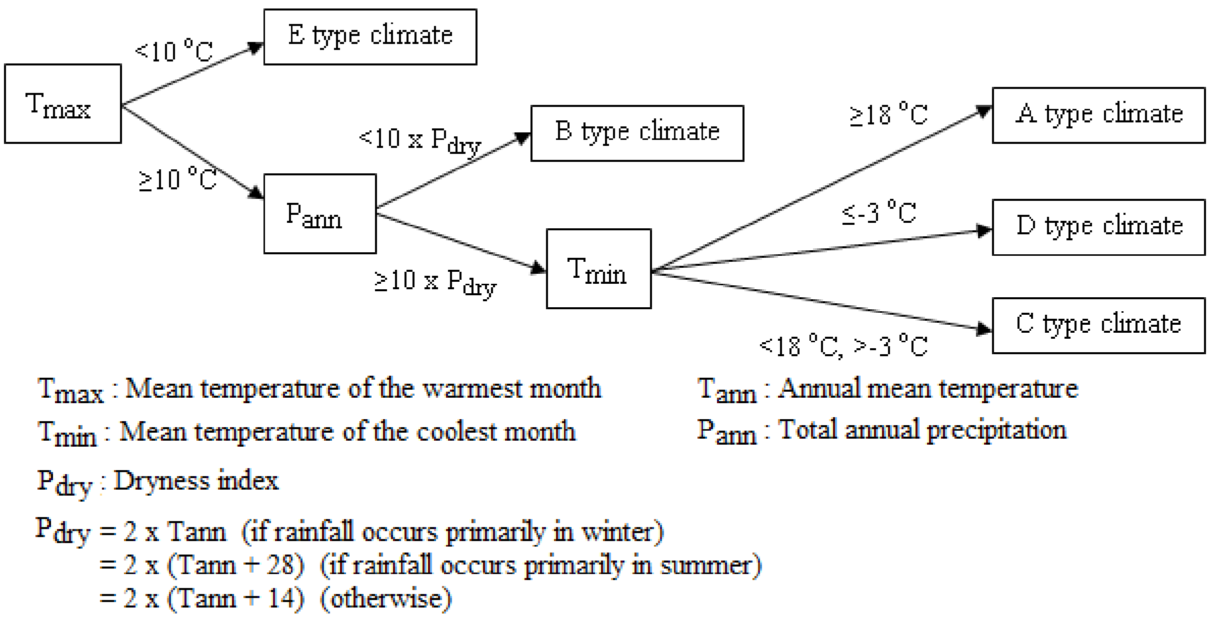

Fig. B.1: Criteria for determining the main climate types in Koppen-Geiger Climate classification system [55].

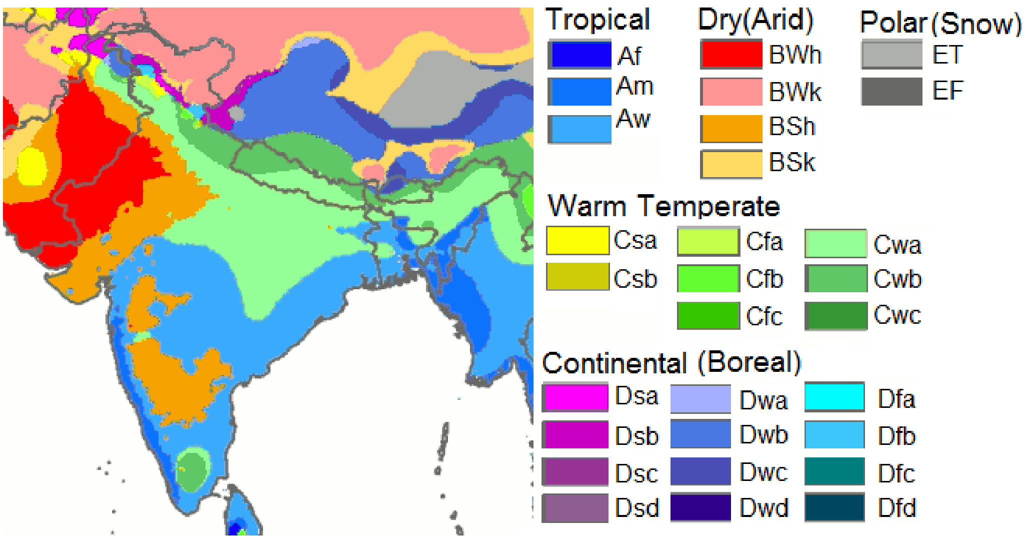

Fig. B.2: Koppen-Geiger Climate classification Map of India (based on [56]).

Table B.1: Meaning of 2nd Letter in Koppen-Geiger classification [55]

Main Classes (1st Letter)	2nd Letter	Meaning
A,C,D	f	Missing dry period
	s	Dry period in summer
	w	Dry period in winter
B	S	Steppe
	W	Desert
E	T	Tundra
	F	Frost

Table B.2: Meaning of 3rd Letter in Koppen-Geiger classification [55]

Main Classes (1st Letter)	3rd Letter	Meaning
B	h	Hot
	k	Cold
C, D	a	Hot summer
	b	Warm summer
	c	Cool summer, cold winter
	d	Extremely continental

Table B.3 shows the climate classification of the survey sites as per the six-zone classification and also the Koppen-Geiger classification. As per the Koppen-Geiger classification, the survey sites can be grouped into the following categories: - (a) Tropical with dry winters, (b) Arid – hot steppe, (c) Arid – cold desert, (d) Warm temperate with hot & dry summer, (e) Warm temperate with dry winter and warm summer.

Table B.3: Climate classification of the survey sites

Survey Site	**Classification as per Bansal *et al.***	**Koppen-Geiger Classification**
Belgaum	Warm & Humid	Tropical Savanna Wet – dry winter (Aw)
Bangalore	Moderate	Tropical Savanna Wet – dry winter (Aw)
Mysore	Moderate	Arid – hot steppe (BSh)
Kochi	Warm & Humid	Tropical Monsoon (Am)
Kayamkulam	Warm & Humid	Tropical Monsoon (Am)
Trivandrum	Warm & Humid	Tropical Savanna Wet – dry winter (Aw)
Madurai	Warm & Humid	Tropical Savanna Wet – dry winter (Aw)
Pondicherry	Warm & Humid	Tropical Savanna Wet – dry winter (Aw)
Chennai	Warm & Humid	Tropical Savanna Wet – dry winter (Aw)
Sricity	Warm & Humid	Tropical Savanna Wet – dry winter (Aw)
Hyderabad	Warm & Humid	Arid – hot steppe (BWh)
Ramagundam	Composite	Tropical Savanna Wet – dry winter (Aw)
Rajgarh	Composite	Temperate – dry winter warm summer (Cwb)
Dhule	Composite	Arid – hot steppe (BSh)
Gandhinagar	Hot & Dry	Arid – hot steppe (BSh)
Bap	Hot & Dry	Arid – hot steppe (BSh)
Jodhpur	Hot & Dry	Arid – hot steppe (BWh)
Tilonia	Hot & Dry	Arid – hot steppe (BSh)
Jaipur	Hot & Dry	Arid – hot steppe (BSh)
Gurgaon	Composite	Arid – hot steppe (BSh)
Dadri	Composite	Temperate – hot & dry summer (Csa)
Srinagar	Cold & Cloudy	Temperate – without dry season – hot summer (Cfa)
Hanle	Cold & Sunny	Arid – cold desert (BWk)
Leh	Cold & Sunny	Arid – cold desert (BWk)

Appendix C
Analysis of Correction Procedure 1a

In order to understand the level of accuracy of Correction Procedure 1a, we performed the following experiment. We measured the characteristics of a crystalline silicon module at STC condition on the Spire Solar Simulator Model 5600 SPL Blue at IIT Bombay. First this module was then taken outdoors and allowed to heat up in the sun. When the temperature of the module stabilized at around 60 °C, it was quickly brought back inside the laboratory. Since the laboratory temperature was set at 25 °C, the module temperature started decreasing, and its *I-V* was taken at regular intervals on the Spire till the module reached room temperature. The simulator was set such that it could take *I-V* data at three different irradiance levels (1000 W/m^2, 800 W/m^2 and 600 W/m^2) in a single flash. The temperature coefficients of current (α) and voltage (β) were calculated by taking the slope of I_{sc} with temperature and V_{oc} with temperature respectively. The values of R_s and k were calculated as per the procedure described in IEC 60891 (since we had available three *I-V* curves at constant temperature but different irradiances and three *I-V* curves at constant irradiance but different temperatures). Then an *I-V* data set measured at 800 W/m^{2}and 47 °Cwas translated to STC using four different parameter combinations: (a) using only α and β measured experimentally (R_s and k set to 0), (b) using only α and β obtained from literature (R_s and k set to 0), (c) using α, β and R_s measured experimentally (k set to 0) and (d) using α, β, R_s and k measured experimentally. Different *I-V* parameters such as P_{max}, V_{oc}, I_{sc} and *FF* were calculated. These data for one module are compared in Table C.1. It can be seen that not much error – about1.5% in P_{max}– is made by using only α and β obtained from literature (i.e., Correction Procedure 1a).

Table C.1: Comparison of P_{max}, V_{oc}, I_{sc} and *FF* translated to STC using different parameters

Parameter	STC Values measured directly on Spire	Translated from 800 W/m^2 and 47 °C to STC using			
		α,β (measured)	α,β (from literature)	α,β&R (measured)	α,β, R&k (measured)
V_{oc} (Volts)	44.2	44.6	44.94	43.96	44.05
I_{sc} (Amp)	5.2	5.17	5.19	5.18	5.17
P_{max} (Watts)	170.1	171.2	172.7	167.6	169.6
FF (%)	74.0	73.9	74.02	73.6	74.3

Similar data were taken on four other modules, and the full *I-V* curves are shown in Fig. C.1 for all 5 modules. From the figure we can see that the Spire-measured STC *I-V* data and the translated *I-V* data (measured at 800 W/m^2 and 47 °C) using only α and β obtained from literature (i.e., using Procedure 1a) match very well, and the RMS error is between 1.4% and 5.4%.

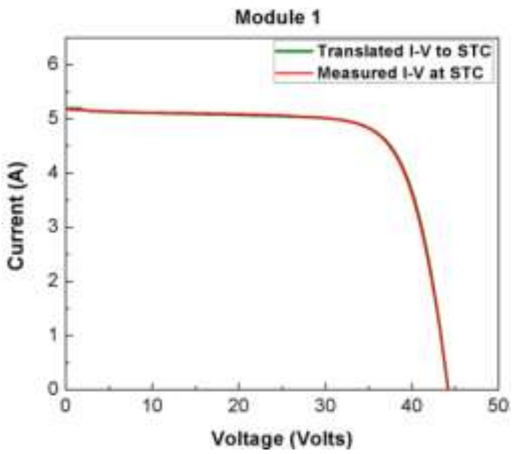

Error: 1.4%

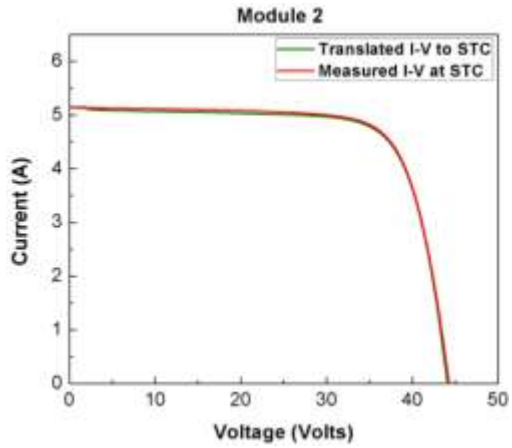

Error: 3.1%

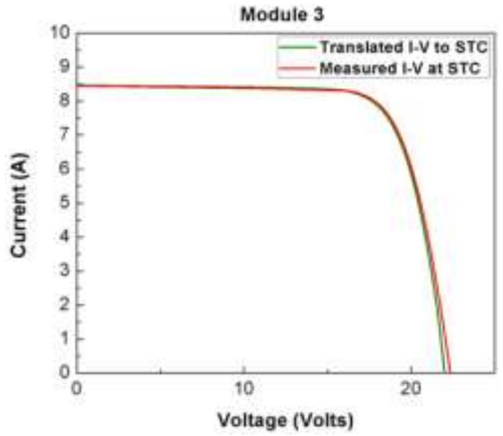

Error: 5.4%

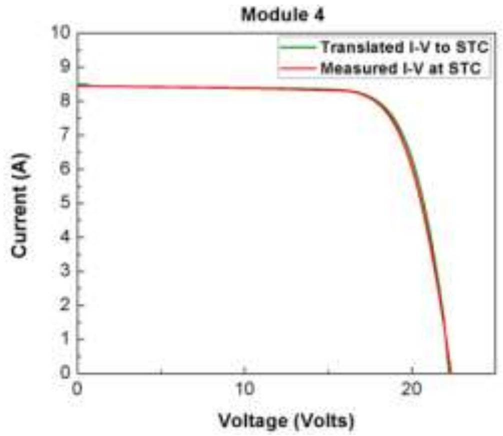

Error: 3.6%

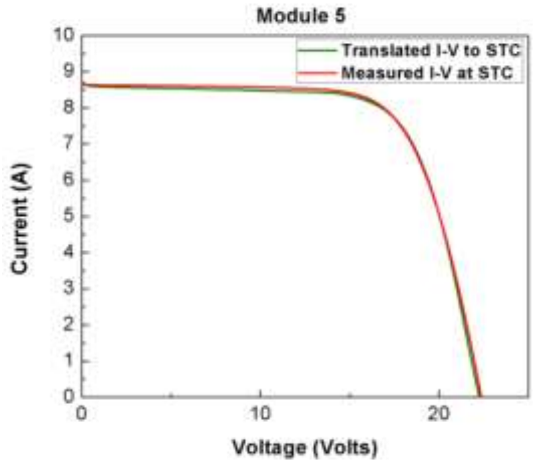

Error: 3.8%

Fig. C.1: Comparison of R.M.S error for the measured *I-V* data at STC and translated *I-V* using only α, β obtained from literature.

Appendix D
Error Analysis for Low Irradiance Correction

In order to estimate the error in translating *I-V* data measured down to 500 W/m^2 to STC using Correction Procedure 1a, we measured the *I-V* data of a crystalline silicon module at different values of irradiance (ranging from 500 to 1000 W/m^2) and temperature (ranging from 25 ^{o}C to 70 ^{o}C). These *I-V* data were then corrected to STC by using Correction Procedure 1a. Table D.1 shows the P_{max} value when translated to STC from the given set of irradiance and temperature for a crystalline silicon module. Table D.2 shows the percent error associated with P_{max} (error is estimated with respect to the P_{max} at STC) when translated to STC from the given set of irradiance and temperature. Table D.3 shows the number of surveyed modules which fall in different categories of irradiance and temperature. Using Table D.2 and Table D.3 we obtained a modified error Table D.4. The shaded region in this Table means that we do not have any *I-V* data in these categories. Hence from Table D.4 we can conclude that the error in translation (using Procedure 1a) from irradiance of 500 W/m^2 or above is within 5% for crystalline silicon modules. This experiment was further repeated for 4 more modules and similar results were obtained. This important experiment and conclusion allows us to use data obtained at irradiance levels above 500 W/m^2 with reasonable accuracy. However, the errors in translation of the actual field data may be marginally higher than the 5% value mentioned above, since the spectral changes associated with overcast (low irradiance) conditions could not be simulated in our controlled laboratory experiment.

Table D.1: P_{max} value at STC obtained by translating using Procedure 1a

P_{max} (Watts)	Temperature (^{o}C)									
Irradiance (W/m^2)	**25.00**	**30.00**	**35.00**	**40.00**	**45.00**	**50.00**	**55.00**	**60.00**	**65.00**	**70.00**
500	150.43	149.74	149.64	149.72	150.11	150.42	150.86	151.12	151.59	152.32
550	149.70	148.97	148.83	148.87	149.20	149.47	149.89	150.11	150.56	151.25
600	149.12	148.37	148.18	148.24	148.49	148.67	149.06	149.25	149.67	150.31
650	148.25	147.58	146.38	146.08	145.81	145.68	145.55	145.36	145.17	145.03
700	147.59	146.92	145.69	145.32	144.99	144.86	144.67	144.45	144.21	144.05
750	147.01	146.29	144.99	144.56	144.22	144.01	143.80	143.54	143.26	143.08
800	146.27	145.51	145.21	145.16	145.30	145.53	145.62	145.71	145.26	145.66
850	145.62	144.86	144.45	144.38	144.53	144.68	144.73	144.77	144.32	144.39
900	145.06	144.24	143.81	143.71	143.77	143.91	143.92	143.92	143.40	143.41
950	144.35	143.28	142.46	142.03	141.57	141.41	140.94	140.27	139.89	139.65
1000	143.82	142.96	141.80	141.30	140.80	140.59	140.09	139.38	138.99	138.67

Table D.2: Percent error in P_{max} value at STC obtained by translating using Procedure 1a

ΔP_{max} (%)	Temperature (°C)									
Irradiance (W/m²)	**25.00**	**30.00**	**35.00**	**40.00**	**45.00**	**50.00**	**55.00**	**60.00**	**65.00**	**70.00**
500	4.59	4.12	4.05	4.10	4.37	4.59	4.90	5.08	5.41	5.91
550	4.09	3.58	3.48	3.51	3.74	3.93	4.22	4.37	4.69	5.17
600	3.69	3.17	3.03	3.07	3.25	3.37	3.65	3.78	4.07	4.51
650	3.08	2.61	1.78	1.57	1.38	1.29	1.20	1.07	0.94	0.84
700	2.62	2.16	1.30	1.04	0.82	0.72	0.60	0.44	0.27	0.16
750	2.22	1.72	0.82	0.52	0.28	0.13	-0.01	-0.19	-0.39	-0.51
800	1.70	1.18	0.96	0.94	1.03	1.19	1.25	1.32	1.00	1.28
850	1.25	0.72	0.44	0.39	0.49	0.60	0.63	0.66	0.35	0.40
900	0.86	0.29	0.00	-0.07	-0.03	0.07	0.07	0.07	-0.29	-0.28
950	0.37	-0.37	-0.94	-1.24	-1.56	-1.67	-2.00	-2.47	-2.73	-2.90
1000	0.00	-0.60	-1.40	-1.75	-2.10	-2.24	-2.59	-3.08	-3.36	-3.58

Table D.3: Number of surveyed modules in different categories of irradiance and temperature.

# of Modules	Temperature (°C)								
Irradiance (W/m²)	**25 – 30**	**30 – 35**	**35 – 40**	**40 – 45**	**45 – 50**	**50 – 55**	**55 – 60**	**60 – 65**	**65 – 70**
500 – 550	0	0	0	0	0	0	0	0	0
550 – 600	0	0	0	0	0	0	0	0	0
600 – 650	0	0	0	0	0	0	0	0	0
650 – 700	0	0	0	0	0	0	0	0	0
700 – 750	0	0	0	0	0	0	0	0	0
750 – 800	0	0	0	0	0	0	0	0	0
800 – 850	0	0	1	9	7	11	51	13	9
850 – 900	0	0	0	3	12	29	43	70	30
900 – 950	0	0	0	16	22	52	66	101	29
950 – 1000	0	0	7	8	8	20	38	76	59

Table D.4: Modified error in P_{max} value at STC obtained by translating using Procedure 1a

ΔP_{max} (%)	**Temperature (^oC)**									
Irradiance (W/m^2)	**25.00**	**30.00**	**35.00**	**40.00**	**45.00**	**50.00**	**55.00**	**60.00**	**65.00**	**70.00**
500	4.59	4.12	4.05	4.10	4.37	4.59	4.90	5.08	5.41	5.91
550	4.09	3.58	3.48	3.51	3.74	3.93	4.22	4.37	4.69	5.17
600	3.69	3.17	3.03	3.07	3.25	3.37	3.65	3.78	4.07	4.51
650	3.08	2.61	1.78	1.57	1.38	1.29	1.20	1.07	0.94	0.84
700	2.62	2.16	1.30	1.04	0.82	0.72	0.60	0.44	0.27	0.16
750	2.22	1.72	0.82	0.52	0.28	0.13	-0.01	-0.19	-0.39	-0.51
800	1.70	1.18	0.96	0.94	1.03	1.19	1.25	1.32	1.00	1.28
850	1.25	0.72	0.44	0.39	0.49	0.60	0.63	0.66	0.35	0.40
900	0.86	0.29	0.00	-0.07	-0.03	0.07	0.07	0.07	-0.29	-0.28
950	0.37	-0.37	-0.94	-1.24	-1.56	-1.67	-2.00	-2.47	-2.73	-2.90
1000	0.00	-0.60	-1.40	-1.75	-2.10	-2.24	-2.59	-3.08	-3.36	-3.58

Appendix E
Instrument Error Analysis

In order to calculate the errors caused by the instrument on the *I-V* parameters at STC we did the following analysis. From the equations used for Correction Procedure 1a (reproduced below as Eqs. (E.1) and (E.2)), we can conclude that the maximum positive deviation in the translated current at STC (I_2) is obtained if there is maximum positive deviation in current measurement (I_1, I_{sc}), maximum negative deviation in irradiance measurement (G_1) and maximum negative deviation in temperature (T_1) measurement.

$$I_2 = I_1 + I_{sc} * \left(\frac{1000}{G_1} - 1\right) + \propto * (25 - T_1) \quad \text{.... (E.1)}$$

Similarly, maximum positive deviation in voltage at STC (V_2) occurs if there is maximum positive deviation in voltage measurement (V_1) and maximum positive deviation in temperature (T_1) measurement (refer equation F.2).

$$V_2 = V_1 + \beta * 25 - \beta * T_1 \quad \text{.... (E.2)}$$

The instrument error for temperature measurement is ±2 °C. If we consider the maximum negative deviation of temperature (–2°C), then the maximum P_{max} error will be 2.81% but if we consider the maximum positive deviation of temperature (+2°C), then the maximum P_{max} error will be 3.81%. Considering all possible combinations of measurement error in voltage, current, irradiance, and temperature, the maximum possible error caused by the instrument in the P_{max} value at STC is shown in Table E.1 for different combinations of irradiance and temperature. The shaded region in the table again means that we do not have any *I-V* data in these categories (refer Appendix D). Hence the maximum error caused by the instrument is 4.05%.

Table E.1: P_{max} Error caused by the instrument on P_{max} at STC

Error (%)	Temperature (°C)									
Irradiance (W/m²)	25	30	35	40	45	50	55	60	65	70
500	4.05	4.05	4.04	4.03	4.01	4.00	3.99	3.97	3.96	3.93
550	4.05	4.05	4.03	4.03	3.97	3.95	3.94	3.91	3.90	3.88
600	4.05	4.05	4.04	4.03	3.97	3.95	3.94	3.92	3.91	3.88
650	4.05	4.05	4.01	3.99	3.97	3.95	3.93	3.92	3.90	3.89
700	4.04	4.04	4.01	3.99	3.97	3.95	3.93	3.92	3.91	3.89
750	4.04	4.05	4.00	3.99	3.97	3.95	3.93	3.92	3.90	3.89
800	4.04	4.04	3.99	3.97	3.96	3.94	3.92	3.91	3.89	3.88
850	4.04	4.04	4.00	3.98	3.96	3.94	3.93	3.91	3.90	3.89
900	4.03	4.03	4.00	3.98	3.97	3.95	3.93	3.92	3.91	3.89
950	4.03	4.03	4.01	3.99	3.98	3.96	3.95	3.94	3.93	3.88
1000	4.03	4.03	4.00	3.99	3.98	3.96	3.95	3.94	3.93	3.92

Appendix F
Outliers

F.1 Introduction

Out of the 925 PV modules inspected in the 2016 survey, 34 modules had Overall P_{max} Degradation Rate greater than 5.12 %/year, and hence were separated out as "outliers" (this criteria is based on statistical analysis, as mentioned in Chapter 3). This Appendix deals with these 'outliers'. 79% of the modules in the Outlier category are young modules, which have been in the field for less than 5 years, as evident from Fig. F.1, and most of these modules come from the small/medium rooftop sites. This fact raises concerns regarding the quality and nameplate rating of the modules, and installation practices, in the small/medium sites. A deliberate 'over-rating' of the modules (that is, the actual power rating being significantly less than the nameplate value) is also possible in some cases.

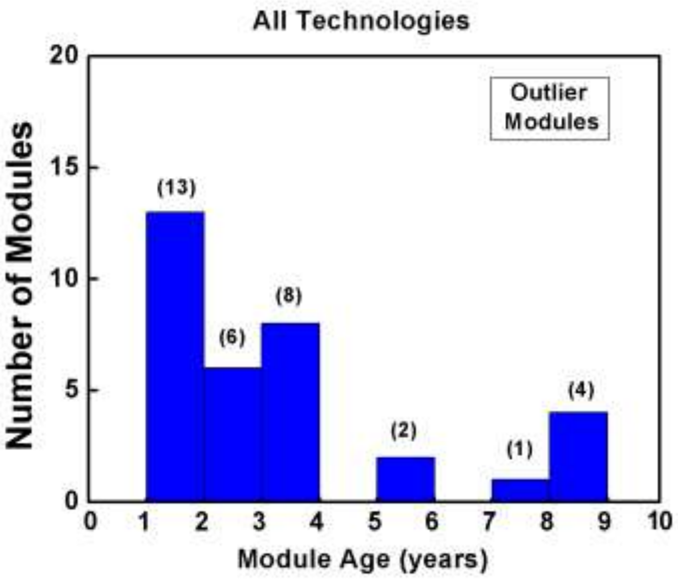

Fig. F.1: Age distribution of the Outlier modules.

F.2 Electrical Degradation

The histogram of the P_{max} degradation rates for the Outlier modules is shown in Fig. F.2 and the degradation rates for Hot and Non-Hot climatic zones are shown in Fig. F.3 The average degradation rate for these modules is 6.62 %/year. The modules in the Hot zone are degrading at a slightly higher rate than modules in the Non-Hot zone, though climatic conditions do not seem to be the primary cause behind the high degradation rates. Fig. F.4 gives the degradation rates of the various electrical parameters (P_{max}, FF, V_{oc} and I_{sc}) for the Outlier modules. It is evident that FF degradation is the major contributing factor to the power degradation in most of the Outlier modules. In some cases, high degradation rate of the open circuit voltage is also observed. Module nos. 33 and 34 are amorphous silicon modules that have suffered extensive cracks in the top glass, and these modules show a high degradation of the short circuit current. Rests of the modules are crystalline silicon modules and in these modules, the short circuit current is not affected significantly. Further analysis of the high *FF* loss in the crystalline silicon modules has indicated that there is not much increment in the series resistance but the shunt resistances of many of the modules have decreased below 100 Ohm (while good crystalline silicon modules usually have shunt resistance of the order of 1000 Ohm). Hence it can be said that shunting in the crystalline silicon modules is one of the reasons behind the very high degradation rates seen in the Outlier modules.

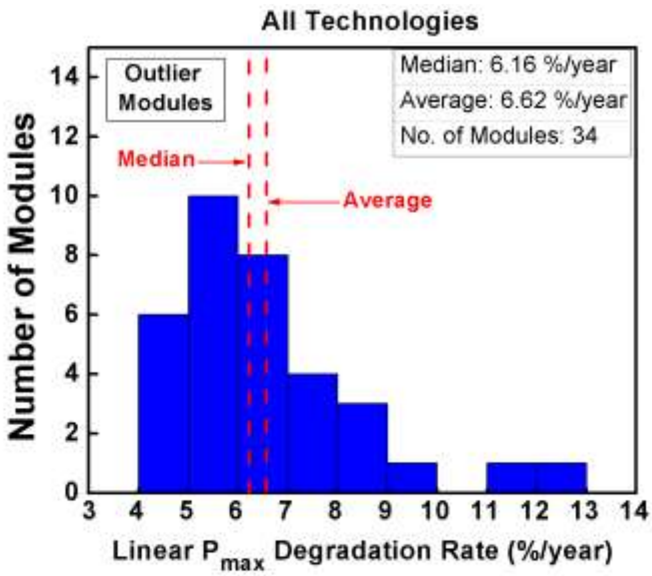

Fig. F.2: Histogram of Linear P_{max} Degradation Rates of the modules in Outlier category.

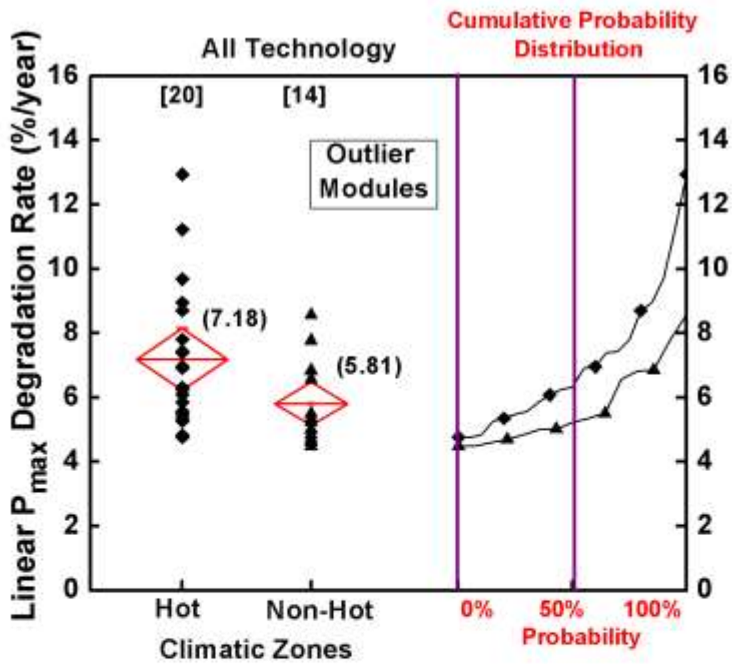

Fig. F.3: Effect of climatic zone on Linear P_{max} Degradation Rate of the Outlier modules.

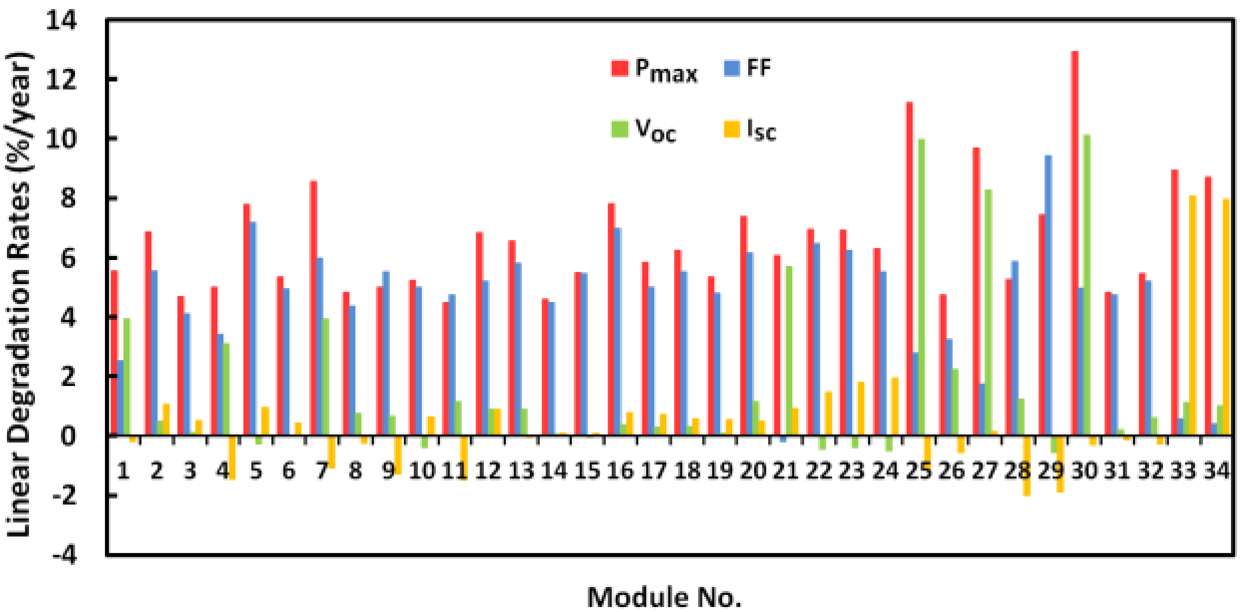

Fig. F.4: Linear Degradation Rates of different electrical parameters of the Outlier modules.

F.3 Visual Degradation and Correlation to Electrical Degradation

The outliers are mostly young modules which have been in the field for less than 5 years, and show very minor visual degradation. Some examples of visual degradation observed in the Outlier modules are shown in Fig. F.5. Table F.1 shows the percentage of the modules in the Outlier category which show some visual degradation. In some of these modules, minor discoloration has occurred within 5 years of outdoor exposure. A vast majority of the modules suffer from metallization discoloration, which points at raw materials and/or manufacturing quality issues. The table also shows the average power degradation rate for modules with and without the specified visual degradation. From the data, it is evident that in most cases the visually unaffected modules have as high as or higher power degradation rate than the affected modules. Hence it is clear that visible degradation is not the underlying cause for the poor performance of these modules. This is in contrast to the modules described in the main body of the report, where we have been able to correlate, in many cases, visual degradation and electrical degradation rates.

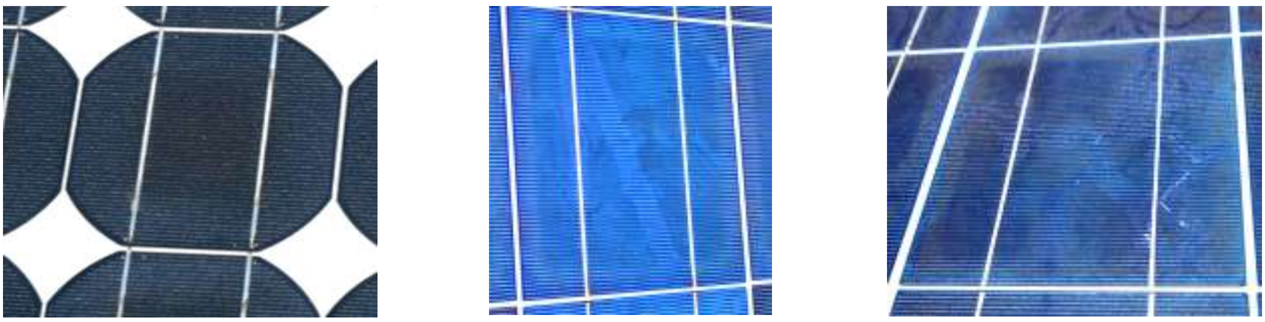

(a) (b) (c)

Fig. F.5: EL images of some crystalline silicon Outlier modules – (a) light discoloration at centre of cells, (b) discoloration and photo-bleaching (indicating cracks), and (c) discoloration, photo-bleaching and bubbles along the photo-bleached areas.

Table F.1: Percentage of Outlier modules affected by various visual degradation modes and correlation to power degradation rate

Type of Visual Degradation	Percentage of outlier modules affected	Power degradation rate for affected Outlier modules (%/year)	Power degradation rate for un-affected Outlier modules (%/year)
Encapsulant Discoloration	25%	6.9	6.3
Visible signs of cracks	38%	6.1	6.7
Metallization Discoloration	88%	6.4	6.9
Backsheet Damage	34%	5.9	6.8

F.4 Electroluminescence Imaging and IR Thermography Results

The EL images of the outlier modules show signatures of different types of defects in the cells, as shown in Fig. F.6. Fig F.6(a) has no EL emission from 1 string of the module, which can occur due to shorting of the bypass diode. In Fig. F.6(b), the bottom row of cells and also 2 cells in the top row have low EL emission, suggesting potential induced degradation (PID) as the degradation mode. There were 5 modules at this site which fell in the outlier category and all showed low EL emission in the bottom row cells. In Fig. F.6(c), cracks can be seen in multiple cells, which has lead to high loss of output power. Due to these defects, the cells run hotter under MPPT condition, as evident from the IR images shown in Fig. F.7.

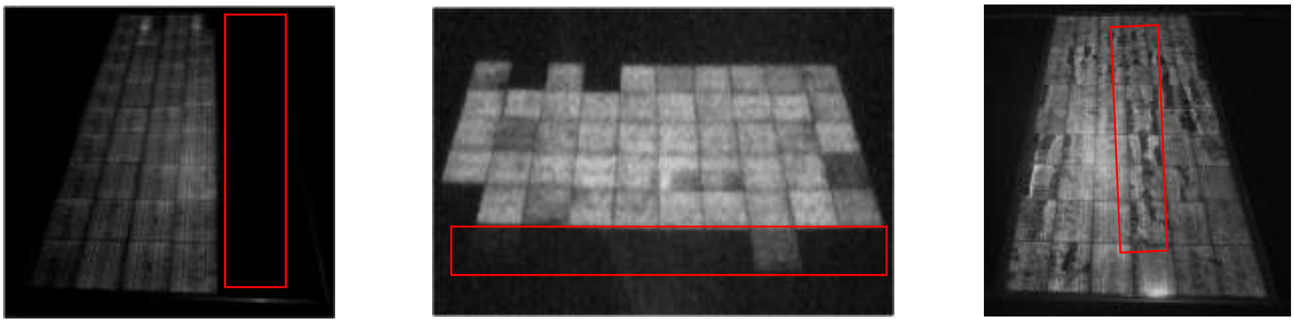

(a) (b) (c)

Fig. F.6: EL images of some crystalline silicon Outlier modules – (a) module with 1 string shorted (probably bypass diode shunting), (b) module with edge cells defective (PID suspected), and (c) module with cracks in multiple cells.

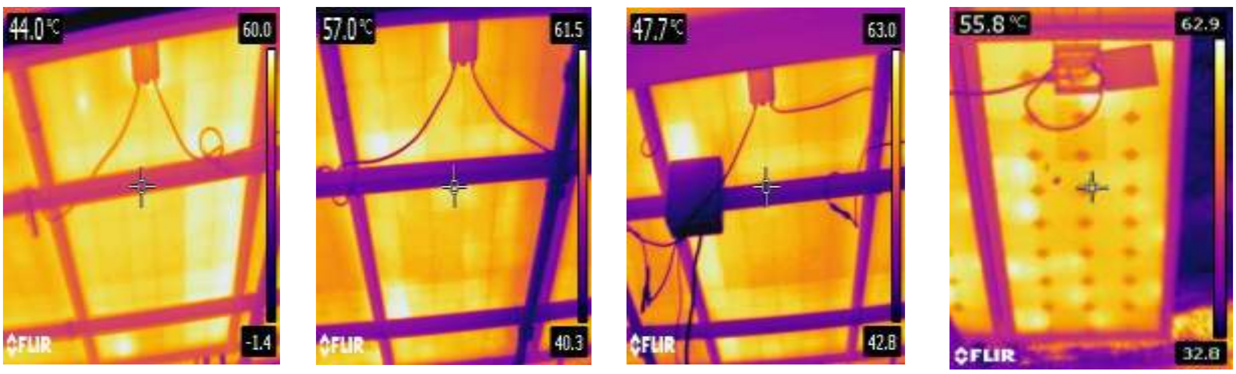

Fig. F.7: IR images of some crystalline silicon Outlier modules with multiple hot spots.

F.5 Summary

A significant number of modules in the small/medium sites have shown very high degradation rates in excess of 5 %/year. Analysis of the electrical data has shown that the primary cause of high power degradation in most of these Outlier modules is high *FF* degradation, coupled with high V_{oc} degradation in a few cases. Electroluminescence images of the Outlier modules point towards cracks as the main culprits, and also PID is suspected to be the reason at one of the sites.

Appendix G
Dark *I-V* Parameter Extraction Methodology

In order to calculate the dark *I-V* parameter of the module we converted the dark *I-V* of the module into the dark *I-V* of an equivalent solar cell by dividing the voltage (at each *I-V* data point) by the number of cells in the module. Figure G.1 graphically demonstrates the concept of dark *I-V* of the equivalent cell. It should be noted that the module's cell-to-cell interconnect resistance gets subsumed into an equivalent solar cell series resistance.

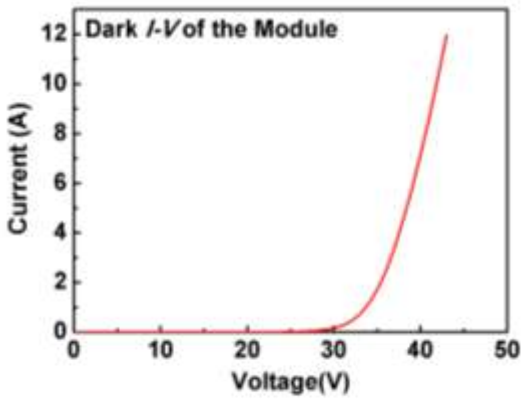

(a)

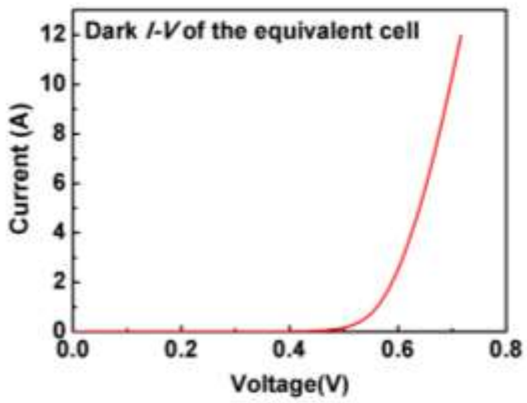

(b)

Fig. G.1: (a) Measured dark *I-V* of the module and, (b) dark *I-V* of an equivalent cell obtained by dividing the module *I-V* voltages by number of cells (here 60).

Ideality factor of the equivalent solar cell diode is calculated from slope obtained by drawing a tangent at the maximum power point voltage V_{mp}, (as shown in Fig. G.2). Figure G.3 shows the procedure to calculate the dark *I-V* parameters from the slope and intercept at V_{mp} point

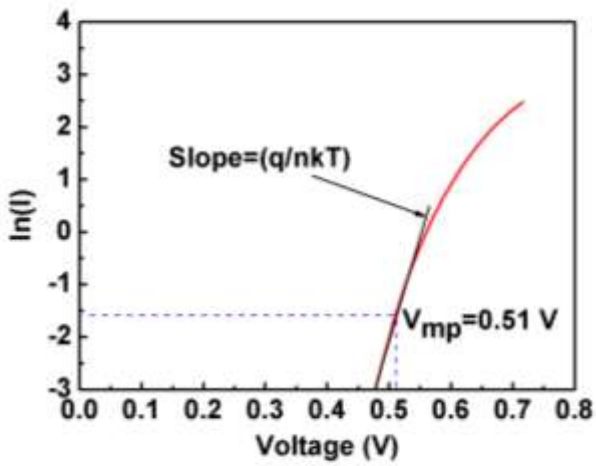

Fig. G.2: ln(I) vs. Voltage plot, showing also the tangent at V_{mp}, from which n can be found.

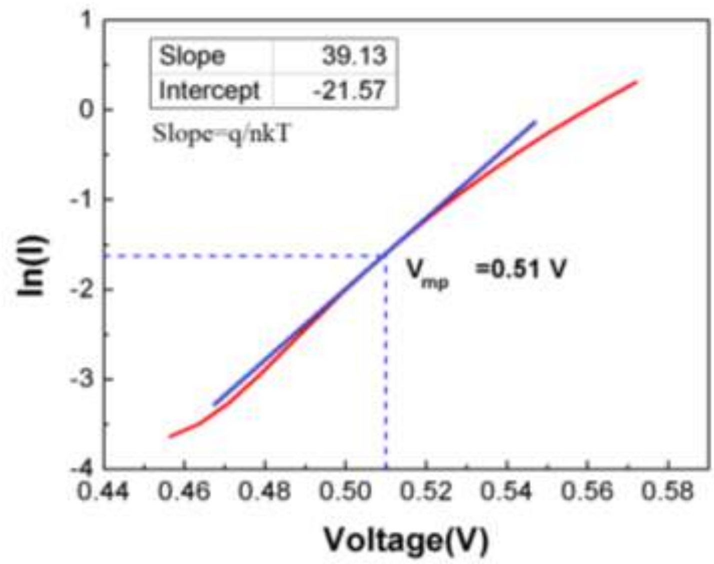

Fig. G.3: Enlarged plot of ln(I) vs. Voltage around V_{mp}, also showing the tangent at V_{mp}, from which n and I_o can be calculated.